

Fluid mechanics, turbulent flow and turbulence modeling

Lars Davidson

Division of Fluid Dynamics
Department of Mechanics and Maritime Sciences
Chalmers University of Technology
SE-412 96 Göteborg, Sweden
<https://www.tfd.chalmers.se/~lada>
lada@chalmers.se

September 6, 2024

Abstract

This course material is used in two courses in the International Master's programme **Applied Mechanics** at Chalmers. The two courses are [TME226 Mechanics of fluids](#) (Chapters 1-10, part of Chapter 11), and [MTF271 Turbulence Modeling](#) (part of Chapter 9 and 10, Chapters 11-27). MSc students who follow these courses are supposed to have taken one basic course in fluid mechanics.

This eBook can be downloaded at
https://www.tfd.chalmers.se/~lada/postscript_files/solids-and-fluids_turbulent-flow_turbulence-modelling.pdf

The Fluid courses in the MSc programme are presented at
<https://www.tfd.chalmers.se/~lada/msc/msc-programme.html>

The MSc programme is presented at
<https://www.chalmers.se/en/education/programmes/masters-info/Pages/Applied-Mechanics.aspx>

Contents

1	Motion, flow	18
1.1	Eulerian, Lagrangian, material derivative	18
1.2	What is the difference between $\frac{dv_2}{dt}$ and $\frac{\partial v_2}{\partial t}$?	19
1.3	Viscous stress, pressure	20
1.4	Strain rate tensor, vorticity	21
1.5	Product of a symmetric and antisymmetric tensor	23
1.6	Deformation, rotation	24
1.7	Irrotational and rotational flow	26
1.7.1	Ideal vortex line	27
1.7.2	Shear flow	29
1.8	Eigenvalues and eigenvectors: physical interpretation	30
2	Governing flow equations	31
2.1	The Navier-Stokes equation	31
2.1.1	The continuity equation	31
2.1.2	The momentum equation	31
2.2	The energy equation	32
2.3	Transformation of energy	34
2.4	Left side of the transport equations	35
2.5	Material particle vs. control volume (Reynolds Transport Theorem)	36
3	Solutions to the Navier-Stokes equation: three examples	38
3.1	The Rayleigh problem	38
3.2	Flow between two plates	41
3.2.1	Curved plates	41
3.2.2	Flat plates	42
3.2.3	Force balance, channel flow	44
3.2.4	Balance equation for the kinetic energy	46
3.3	Two-dimensional boundary layer flow over flat plate	47
3.3.1	Momentum balance, boundary layer	50
4	Vorticity equation and potential flow	52
4.1	Vorticity and rotation	52
4.2	The vorticity transport equation in three dimensions	54
4.3	The vorticity transport equation in two dimensions	57
4.3.1	Boundary layer thickness from the Rayleigh problem	58
4.4	Potential flow	60
4.4.1	The Bernoulli equation	60
4.4.2	Complex variables for potential solutions of plane flows	61
4.4.3	$f \propto z^n$	62
4.4.3.1	Parallel flow	63
4.4.3.2	Stagnation flow	63
4.4.3.3	Flow over a wedge and flow in a concave corner.	64
4.4.4	Analytical solutions for a line source	65
4.4.5	Analytical solutions for a vortex line	66
4.4.6	Analytical solutions for flow around a cylinder	67
4.4.7	Analytical solutions for flow around a cylinder with circulation	70
4.4.7.1	The Magnus effect	72

4.4.8	The flow around an airfoil	74
5	Turbulence	77
5.1	Introduction	77
5.2	Turbulent scales	78
5.3	Energy spectrum	79
5.4	The cascade process created by vorticity	83
6	Turbulent mean flow	88
6.1	Time averaged Navier-Stokes	88
6.1.1	Boundary-layer approximation	90
6.2	Wall region in fully developed channel flow	90
6.3	Reynolds stresses in fully developed channel flow	95
6.4	Boundary layer	97
7	Probability density functions	99
8	Transport equations for turbulent kinetic energy	102
8.1	Rules for time averaging	102
8.1.1	What is the difference between $\overline{v'_1 v'_2}$ and $\overline{v'_1} \overline{v'_2}$?	102
8.1.2	What is the difference between $\overline{v'^2_1}$ and $\overline{v'^2_1}$?	103
8.1.3	Show that $\overline{\bar{v}_1 v'^2_1} = \bar{v}_1 \overline{v'^2_1}$	103
8.1.4	Show that $\overline{\bar{v}_1} = \bar{v}_1$	104
8.2	The Exact k Equation	104
8.2.1	Expressing dissipation with s_{ij} ; non-isotropic dissipation . .	108
8.2.2	Spectral transfer dissipation ε_κ vs. “true” viscous dissipation, ε	109
8.3	The Exact k Equation: 2D Boundary Layers	109
8.4	Spatial vs. spectral energy transfer	110
8.5	The overall effect of the transport terms	111
8.6	The transport equation for $\bar{v}_i \bar{v}_i / 2$	112
9	Transport equations for Reynolds stresses	115
9.1	Source terms	119
9.2	Reynolds shear stress vs. the velocity gradient	120
10	Correlations	124
10.1	Two-point correlations	124
10.2	Auto-correlation	126
10.3	Taylor’s hypothesis of frozen turbulence	127
11	Reynolds stress models and two-equation models	128
11.1	Mean flow equations	128
11.1.1	Flow equations	128
11.1.2	Temperature equation	129
11.2	The exact $\overline{v'_i v'_j}$ equation	129
11.3	The exact $\overline{v'_i \theta'}$ equation	131
11.4	The k equation	133
11.5	The ε equation	134
11.6	The Boussinesq assumption	135
11.7	Modeling assumptions	136

11.7.1	Production terms	136
11.7.2	Diffusion terms	137
11.7.3	Dissipation term, ε_{ij}	138
11.7.4	Slow pressure-strain term	139
11.7.5	Rapid pressure-strain term	142
11.7.6	Wall model of the pressure-strain term	148
11.8	The $k - \varepsilon$ model	149
11.9	The modeled $\overline{v_i'v_j'}$ equation with IP model	151
11.10	Algebraic Reynolds Stress Model (ASM)	151
11.11	Explicit ASM (EASM or EARSM)	152
11.12	Derivation of the Explicit Algebraic Reynolds Stress Model (EARSM)	153
11.13	Boundary layer flow	158
11.14	Wall boundary conditions	158
11.14.1	Wall Functions	159
11.14.2	Low-Re Number Turbulence Models	161
11.14.3	Low-Re $k - \varepsilon$ Models	163
11.14.4	Wall boundary Condition for k	165
11.14.5	Different ways of prescribing ε at or near the wall	165
12	Reynolds stress models vs. eddy-viscosity models	167
12.1	Stable and unstable stratification	167
12.2	Curvature effects	168
12.3	Stagnation flow	171
12.4	RSM/ASM versus $k - \varepsilon$ models	172
13	Realizability	173
13.1	Two-component limit	174
14	Non-linear Eddy-viscosity Models	176
15	The V2F Model	179
15.1	Modified V2F model	182
15.2	Realizable V2F model	183
15.3	To ensure that $v^2 \leq 2k/3$	183
16	The SST Model	184
17	Overview of RANS models	189
18	Large Eddy Simulations	190
18.1	Time averaging and filtering	190
18.2	Differences between time-averaging (RANS) and space filtering (LES)	191
18.3	Resolved & SGS scales	192
18.4	The box-filter and the cut-off filter	193
18.5	Highest resolved wavenumbers	194
18.6	Subgrid model	195
18.7	Smagorinsky model vs. mixing-length model	196
18.8	Energy path	196
18.9	SGS kinetic energy	197
18.10	LES vs. RANS	198
18.11	The dynamic model	198

18.12	The test filter	200
18.12.1	2D filtering	200
18.12.2	3D filtering	200
18.13	Stresses on grid, test and intermediate level	201
18.14	Numerical dissipation	203
18.15	Scale-similarity Models	204
18.16	The Bardina Model	204
18.17	Redefined terms in the Bardina Model	205
18.18	A dissipative scale-similarity model.	205
18.19	Forcing	207
18.20	Numerical method	207
18.20.1	RANS vs. LES	208
18.21	One-equation k_{sgs} model	209
18.22	Smagorinsky model derived from the k_{sgs} equation	209
18.23	A dynamic one-equation model	210
18.24	A Mixed Model Based on a One-Eq. Model	211
18.25	Applied LES	211
18.26	Resolution requirements	212
19	URANS: Unsteady RANS	214
19.1	Turbulence Modeling	215
19.2	Discretization	216
20	DES: Detached-Eddy-Simulations	218
20.1	DES based on two-equation models	219
20.2	DES based on the $k - \omega$ SST model	220
20.3	DDES	221
21	Hybrid LES-RANS	223
21.1	Momentum equations in hybrid LES-RANS	225
21.2	The one-equation hybrid LES-RANS model	225
22	The SAS model	226
22.1	Resolved motions in unsteady	226
22.2	The von Kármán length scale	227
22.3	The SST-SAS model	228
22.4	The second derivative of the velocity	229
22.5	Evaluation of the von Kármán length scale in channel flow	229
23	The PANS Model	232
23.1	PANS as a hybrid LES-RANS model	235
23.1.1	The interface conditions at the RANS-LES interface	235
23.2	Zonal PANS: different treatments of the RANS-LES interface	236
23.2.1	The Interface Condition	237
23.2.2	Modeling the Interface	239
23.2.2.1	Interface Model 1	239
23.2.2.2	Interface Model 2	239
23.2.2.3	Interface Model 3	240
23.2.2.4	Interface Model 4	240
23.3	A new formulation of f_k for the PANS model	241

23.3.1	f_k derived from the equivalence criterion	241
23.4	The IDD-PANS model	243
23.4.1	LES length scale	243
23.4.2	The IDDES model	243
23.4.3	Equivalence between PANS and DES/IDDES	244
23.4.3.1	PANS equations	246
23.4.3.2	IDDES equations	246
23.4.3.3	PITM equations	247
23.4.4	Deriving an expression for f_k for PANS	247
23.4.5	Deriving an expression for f_k for PITM	248
23.4.6	Turbulence with convection	248
23.4.6.1	PANS/PITM equations	248
23.4.6.2	DES equations	249
24	The PITM model	251
24.1	RANS mode	251
24.2	LES mode	251
25	Hybrid LES/RANS for Dummies	255
25.1	Introduction	255
25.1.1	Reynolds-Averaging Navier-Stokes equations: RANS	255
25.1.2	Large Eddy Simulations: LES	255
25.1.3	Zonal LES/RANS	256
25.2	The PANS $k - \varepsilon$ turbulence model	256
25.3	Zonal LES/RANS: wall modeling	257
25.3.1	The interface conditions	257
25.3.2	Results	258
25.4	Zonal LES/RANS: embedded LES	258
25.4.1	The interface conditions	258
25.4.2	Results	260
26	Commutation terms in the k and ω equations	261
27	Inlet boundary conditions	265
27.1	Synthesized turbulence	265
27.2	Random angles	265
27.3	Highest wave number	266
27.4	Smallest wave number	266
27.5	Divide the wave number range	266
27.6	von Kármán spectrum	267
27.7	Computing the fluctuations	267
27.8	Introducing time correlation	267
27.9	Anisotropic Synthetic Turbulent Fluctuations	271
27.9.1	Eigenvalues and eigenvectors	272
27.9.2	Synthetic fluctuations in the principal coordinate system	273
28	Overview of LES, hybrid LES-RANS and URANS models	274
29	Best practice guidelines (BPG)	277
29.1	EU projects	277

29.2	Ercoftac workshops	277
29.3	Ercoftac Classical Database	278
29.4	ERCOFTAC QNET Knowledge Base Wiki	278
A	Introduction to tensor notation	279
A.1	What is a tensor?	280
A.2	Examples of equations using tensor notation	281
A.2.1	Newton's second law	281
A.2.2	Divergence $\nabla \cdot \mathbf{v} = 0$	281
A.2.3	The left-hand side of Navier-Stokes $v_\ell \partial v_m / \partial x_\ell$	282
A.3	Contraction	282
A.4	Two Tensor Rules	282
A.4.1	The summation rule	282
A.4.2	Free Index	282
A.5	Special Tensors	282
A.5.1	Kronecker's δ (identity tensor)	282
A.5.2	Levi-Civita's ε_{ijk} (permutation tensor)	283
A.6	Symmetric and antisymmetric tensors	283
A.7	Vector Product	284
A.8	Derivative Operations	284
A.8.1	The derivative of a vector \mathbf{B} :	284
A.8.2	The gradient of a scalar a :	284
A.8.3	The divergence of a vector \mathbf{B} :	285
A.8.4	The curl of a vector \mathbf{B} :	285
A.8.5	The Laplace operator on a scalar a :	285
A.9	Integral Formulas	285
A.10	Multiplication of tensors	285
B	TME226: $\epsilon - \delta$ identity	287
C	TME226 Assignment 1 in 2024: laminar flow in a channel	288
C.1	Fully developed region	289
C.2	Wall shear stress	289
C.3	Inlet region	290
C.4	Wall-normal velocity in the developing region	290
C.5	Vorticity	290
C.6	Deformation	290
C.7	Dissipation	290
C.8	Eigenvalues	291
C.9	Eigenvectors	291
33	TME226 Assignment 1 in 2023: laminar flow in a boundary layer	292
33.1	Velocity profiles	293
33.2	Boundary layer thickness	294
33.3	Velocity gradients	294
33.4	Skinfriction	295
33.5	Vorticity	295
33.6	Deformation	295
33.7	Dissipation	295
33.8	Eigenvalues	296

33.9	Eigenvectors	296
33.10	Terms in the v_1 equation	296
AH	TME226, Assignment 2: Turbulent flow using STAR-CCM+	298
AH.1	Backward Facing Step Tutorial (Optional)	298
AH.2	2D Hill Flow	298
AH.3	Steady Flow: 2D Hill Flow Tutorial	299
AH.3.1	Pressure	305
AH.3.2	Skinfriction	305
AH.3.3	Vorticity	306
AH.3.4	Turbulent viscosity	306
AH.3.5	Diffusion	307
AH.3.6	Production	307
AH.3.7	Wall boundary conditions for ε	307
AH.3.8	Near-wall behaviour of f_μ	307
AH.3.9	Compare with experiments	308
AI	TME226: Fourier series	309
AI.1	Orthogonal functions	309
AI.2	Trigonometric functions	310
AI.2.1	“Length” of ψ_k	311
AI.2.2	Orthogonality of ϕ_n and ψ_k	311
AI.2.3	Orthogonality of ϕ_n and ϕ_k	311
AI.2.4	“Length” of ϕ_k	311
AI.3	Fourier series of a function	312
AI.4	Derivation of Parseval’s formula	312
AI.5	Complex Fourier series	314
36	TME226: Why does the energy spectrum have such strange dimensions?	315
36.1	Energy spectrum for an ideal vortex	315
36.2	An example	316
36.3	An example: Matlab code	317
37	TME226 Learning outcomes	321
AL	TME226 Discussion seminars	337
39	MTF271: Some properties of the pressure-strain term	361
40	MTF271: Galilean invariance	362
41	MTF271: Computation of wavenumber vector and angles	364
41.1	The wavenumber vector, κ_j^n	364
41.2	Unit vector σ_i^n	365
42	MTF271: 1D and 3D energy spectra	366
42.1	Energy spectra from two-point correlations	367
43	MTF271. Derivations of the IDD-PANS model	369
43.1	DES model	369
43.2	PANS model	370

43.3	PITM model	371
44	MTF271, Assignment 1: Reynolds averaged Navier-Stokes	373
44.1	Part a: Data of Two-dimensional flow	373
44.1.1	Analysis	374
44.1.2	The momentum equations	374
44.1.3	The turbulent kinetic energy equation	375
44.1.4	The Reynolds stress equations	375
44.2	Part b: Machine learning	378
45	MTF271, Assignment: LES, $Re_\tau = 1\,000$	382
45.1	Time history	382
45.2	Time averaging	383
45.3	Auto-correlation	383
45.4	Probability density/histogram	385
45.5	Frequency spectrum	386
45.6	Backstep	387
45.7	Channel flow: resolved stresses	388
45.8	Resolved production and pressure-strain	389
45.9	Filtering	390
45.10	SGS stresses: Smagorinsky model	390
45.11	SGS stresses: WALE model	391
45.12	Dissipations	391
45.13	Test filtering	394
45.14	Near-wall behavior	394
45.15	Two-point correlations	394
45.16	Energy spectra, optional	395
45.17	Something fun	395
46	MTF271: Compute energy spectra from LES/DNS data using Python	396
46.1	Introduction	396
46.2	An example of using FFT	396
46.3	Energy spectrum from the two-point correlation	399
46.4	Energy spectra from the auto-correlation	401
47	MTF271, Assignment 2a: DES, DDES and SAS	402
47.1	Time history	402
47.2	Mean velocity profile	404
47.3	Resolved stresses	404
47.4	Turbulent kinetic energy	405
47.5	The modelled turbulent shear stress	405
47.6	Location of interface in DES and DDES	405
47.7	SAS turbulent length scales	406
47.8	Anisotropic errors (optional)	406
48	MTF271, Assignment 2b, recirculating flow: PANS, DES, DDES and SAS	408
48.1	Discretization schemes	409
48.2	The modeled turbulent shear stress	410
48.3	The turbulent viscosity	410
48.4	Location of interface	411

48.5	Location of interface in DES and DDES	412
48.6	The SAS model (optional)	413
48.7	Different ways to evaluate resolution	413
48.7.1	Anisotropic errors (optional)	414
48.7.2	Two-point correlations	415
49	MTF271, Assignment: Embedded LES with PANS, channel flow	417
49.1	Time history	417
49.2	Resolved stresses	418
49.3	Turbulent viscosity	418
49.4	Modeled stresses	419
49.5	Turbulent SGS dissipation	419
50	MTF271, Assignment 3: Hybrid LES-RANS, channel flow	421
50.1	Time history	421
50.2	Mean velocity profile	422
50.3	Resolved stresses	422
50.4	Turbulent kinetic energy	423
50.5	The modelled turbulent shear stress	423
50.6	Location of interface in DES and DDES	423
50.7	Turbulent length scales	423
51	MTF271, Assignment 4: Synthetic inlet fluctuations	424
51.1	synt_main	424
51.2	angles	424
51.3	rand1.m	424
51.4	rand2.m	424
51.5	Mean values; randomness	424
51.6	RMS and shear stress	425
51.7	Two-point correlations	426
51.8	The integral length scale	427
51.9	Correlation in time	427
51.10	Auto-correlation in time	429
51.11	Spectrum	430
51.12	Anisotropic fluctuations	430
52	MTF271, Assignment 5: synthetic anisotropic fluctuations using EARS	433
52.1	Mean flow	433
52.2	Synthetic fluctuations	433
52.2.1	Chapter 1	434
52.2.2	Chapter 2-3	434
52.3	Exercises	434
53	MTF271: Transformation of tensors	435
53.1	Rotation from $x_{1*} - x_{2*}$ to $x_1 - x_2$	435
53.2	Rotation from $x_1 - x_2$ to $x_{1*} - x_{2*}$	436
53.3	Transformation of a velocity gradient	437
54	MTF271: Green's formulas	438
54.1	Green's first formula	438

54.2	Green's second formula	438
54.3	Green's third formula	438
54.4	Analytical solution to Poisson's equation	441
55	MTF271: the <code>np.correlate</code> command	442
56	MTF271, How to compute derivatives on a curvi-linear mesh	443
56.1	Geometrical quantities	444
57	MTF271: Learning outcomes for 2022	445
58	MTF271: Discussion seminars and Oral Exam	454
58.1	Seminar 1	454
58.2	Seminar 2	456
58.3	Seminar 3	459
58.4	Seminar 4	461
58.5	Seminar 5	462
58.6	Seminar 6	463
59	IMS135, Assignment on Machine Learning for Turbulence Modeling	464
59.1	Machine Learning	464
59.2	The Assignment	465
59.3	DNS Data bases for validating NN model	466
60	MTF271: Derivation of an Explicit Algebraic Stress Model in 2D	467
60.1	Cayley-Hamilton in 2D	471
60.2	The 2nd tensor $T^{(2)}$ can be expressed in the zeroth tensor $T^{(0)}$. . .	471
61	MTF271: How to compute the wall pressure-strain term	473

List of Figures

1.1	A fluid particle described in Lagrangian coordinate	18
1.2	Flow path: Lagrangian and Eulerian coordintes	19
1.3	Stress tensor, volume force and stress vector	21
1.4	Rotation of a fluid particle	25
1.5	Deformation of a fluid particle by shear	25
1.6	Deformation of a fluid particle by elongation during time Δt .	26
1.7	Line integral. The surface, S , is enclosing by the line ℓ	26
1.8	Ideal vortex	28
1.9	Transformation of v_θ into Cartesian components.	29
1.10	A shear flow. A fluid particle with vorticity. $v_1 = cx_2^2$.	29
1.11	Eigenvecors and Eigenvalues of a two-dimensional fluid element	30
3.1	The plate moves to the right with speed V_0 for $t > 0$.	38
3.2	The v_1 velocity at three different times. $t_3 > t_2 > t_1$.	38
3.3	The velocity, $f = v_1/V_0$, given by Eq. 3.11.	40
3.4	The shear stress for water	40
3.5	Flow in a horizontal channel. The inlet part of the channel is shown.	41
3.6	Flow in a channel bend.	42
3.7	Secondary flow in a duct bend.	42
3.8	The velocity profile in fully developed channel flow, Eq. 3.28.	45
3.9	Force balance of the flow between two plates.	46
3.10	Force balance of boundary layer flow along a flat plate.	50
4.1	Surface forces acting on a fluid particle	52
4.2	Vortex stretching of a fluid element	56
4.3	Vortex tilting of a fluid element	57
4.4	Boundary layer and its boundary layer thickness, δ	59
4.5	The complex plane in polar coordinates	62
4.6	Parallel flow.	63
4.7	Potential flow. Stagnation flow.	64
4.8	Potential flow of stagnation flow	64
4.9	Line source. $\dot{m} > 0$	65
4.10	Vortex line.	67
4.11	Flow around a cylinder of radius r_0 .	67
4.12	Flow around a cylinder of radius r_0 . Integration of surface pressure.	68
4.13	Pressure coefficients.	68
4.14	Flow around a cylinder of radius r_0 with additional circulation	70
4.15	Flow around a cylinder of radius r_0 with maximal additional circulation.	71
4.16	Table tennis. The loop uses the Magnus effect. Side view.	72
4.17	Football. A free-kick uses the Magnus effect. Top view	73
4.18	Potential flow. Flettner rotor on a ship	73
4.19	Potential flow around an Airfoil	74
4.20	Airfoil. Streamlines from potential flow	75
4.21	Airfoil. Streamlines from potential flow with added circulation	75
5.1	Laminar and turbulent boundary layer.	77
5.2	Cascade process with a spectrum of eddies	78
5.3	Spectrum for turbulent kinetic energy, k	81
5.4	Family tree of turbulent eddies	84
5.5	A fluid element is stretched by $\frac{\partial v'_1}{\partial x_1} > 0$	86

5.6	The rotation rate of the fluid element	86
6.1	Flow between two infinite parallel plates	90
6.2	The wall region of a turbulent boundary layer	91
6.3	Reynolds shear stress. $Re_\tau = 2000$	93
6.4	Velocity profiles in fully developed channel flow	93
6.5	Symmetry plane of channel flow.	94
6.6	Fully developed channel flow. $Re_\tau = 2000$. Forces in the \bar{v}_1 equation	96
6.7	Forces in a boundary layer	96
6.8	Normal Reynolds stresses and turbulent kinetic energy. $Re_\tau = 2000$	97
6.9	Velocity profiles in a boundary layer along a flat plate	97
7.1	Time history of v' . Horizontal red lines show $\pm v_{rms}$	99
7.2	Probability density functions of time histories	100
8.1	The size of the largest eddies for different velocity profiles.	106
8.2	Zoom of the energy spectrum in Region II or III	107
8.3	Channel flow at $Re_\tau = 2000$. Terms in the k equation	110
8.4	Velocity gradient and shear stress	110
8.5	Channel flow at $Re_\tau = 2000$. Mean and fluctuating dissipation terms	113
8.6	Transfer of energy between K , k and internal energy	114
9.1	Channel flow at $Re_\tau = 2000$. Terms in the $\overline{v_1'^2}$ equation	118
9.2	One-dimensional unsteady heat conduction	119
9.3	Energy spectrum. Transfer of kinetic energy	121
9.4	Channel flow at $Re_\tau = 2000$. Terms in the $\overline{v_2'^2}$ equation	121
9.5	Channel flow at $Re_\tau = 2000$. Terms in the $\overline{v_3'^2}$ equation	122
9.6	Channel flow at $Re_\tau = 2000$. Terms in the $\overline{v_1'v_2'}$ equation	122
9.7	Sign of the Reynolds shear stress $-\rho\overline{v_1'v_2'}$ in a boundary layer.	122
10.1	Two-point correlation.	124
10.2	Schematic relation between the two-point correlation and largest eddies	125
10.3	Two-point correlation and frozen turbulence.	127
11.1	Physical illustration of the pressure-strain term.	139
11.2	Decaying grid turbulence	141
11.3	The exact solution to the Poisson equation	143
11.4	Modeling of wall correction in pressure-strain terms.	148
11.5	Boundary layer flow.	158
11.6	Boundary along a flat plate. Energy balance in k equation	159
11.7	Wall-adjacent cell. Cell-centered finite volume grid.	159
11.8	Turbulent kinetic energy in a boundary layer. LES	160
11.9	Flow in fully developed channel flow. Energy balance in k equation	162
11.10	Flow between two parallel plates. Fluctuations. DNS	163
11.11	Flow between two parallel plates. Energy balance in k equation. DNS	164
12.1	Stable stratification due to positive temperature gradient $\partial\bar{\theta}/\partial x_3 > 0$	167
12.2	Flow in a polar coordinate system illustrating streamline curvature	169
12.3	Streamline curvature occurring near a separation region	169
12.4	The velocity profile for a wall jet.	170
12.5	The flow pattern of stagnation flow.	171
15.1	Illustration of Helmholtz equation in the V2F model	181
16.1	Flow around an airfoil. Pressure contours	184
18.1	Filtering the velocity.	190
18.2	Box filter illustrated for a control volume.	192
18.3	Spectrum of velocity.	193

18.4	The Fourier modes of a fluctuation	195
18.5	Physical space and wavenumber space	195
18.6	Energy spectrum.	197
18.7	Energy spectrum with grid and test filter.	199
18.8	Control volume for grid and test filter.	200
18.9	A 2D test filter control volume.	201
18.10	Numerical dissipation.	203
18.11	Dissipation and production term from DNS data	206
18.12	Time averaging in LES.	208
18.13	Spectrum for k	210
18.14	Energy spectra in fully developed channel flow	212
18.15	Onera bump. Computational domain (not to scale).	213
18.16	Energy spectra $E_{33}(\kappa_3)$ in the recirculation region and shear layer	213
19.1	Decomposition of velocities in URANS	214
19.2	The domain for the flow past a triangular flameholder	216
19.3	2D URANS $k - \varepsilon$ simulations	216
19.4	2D URANS $k - \varepsilon$ simulations compared with experiment	217
19.5	Domain of URANS simulations: a surface-mounted cube	218
19.6	URANS simulations: profiles upstream the cube [1].	218
20.1	Grid and a velocity profile and RANS-LES interface	222
21.1	Illustration of near-wall turbulence (taken from [2]).	224
21.2	Fluctuating streamwise velocity at $x_2^+ = 5$. DNS of channel flow	224
21.3	The LES and URANS region.	224
22.1	The SAS model. Velocity profiles from a DNS of channel flow	226
22.2	The SAS model. Mean and instantaneous velocity profiles	226
22.3	SAS model. Turbulent length scales in fully developed channel flow	230
22.4	SAS model. Turbulent length scales in fully developed channel flow	230
23.1	The URANS and the LES regions.	235
23.2	Control volume, P , in the LES region adjacent to the interface.	235
23.3	The URANS and the LES regions near a wall.	238
23.4	[PANS. Embedded LES. f_k near the interface	238
24.1	Spectral energy balance in PITM. Homogeneous turbulence.	252
25.1	The LES and URANS regions. Fully developed channel flow	257
25.2	Hybrid LES-RANS. Velocities and resolved shear stresses	258
25.3	Turbulent viscosity.	259
25.4	Embedded LES. The LES and RANS regions	259
25.5	Channel flow. Velocities, fluctuations and turbulent viscosity	259
26.1	Channel flow.	262
26.2	Boundary layer flow.	262
27.1	Synthetic fluctuations. The wave-number and velocity unit vector	266
27.2	Modified von Kármán spectrum	268
27.3	Auto-correlation of synthetic fluctuations	269
27.4	Anisotropic synthetic turbulence. Eigenvectors	273
27.5	Anisotropic synthetic turbulence. Eigenvectors and eigenvalues	273
C.1	Flow between two plates (not to scale).	289
33.1	Flow along a flat plate	293
AH.1	flow over two consecutive hills	298
AI.1	Scalar product.	309
36.1	Fourier modes of v'	317
36.2	Energy spectrum of v'	317

41.1	The probability of a randomly direction of a wave in wave-space . . .	364
44.1	The Neural Network: two input variables, $a_1^{(0)} = y^+$ and $a_2^{(0)} = P^+$.	379
45.1	Channel domain.	387
45.2	Backstep domain.	388
45.3	Spectrum with cut-off.	390
45.4	Transfer of kinetic turbulent energy	392
45.5	Energy spectrum. Transfer of kinetic energy	393
46.1	Two-point correlation, $B(\hat{x}_3) = \langle v'_3(x_3 - \hat{x}_3)v'_3(x_3) \rangle$	397
46.2	The u function.	398
46.3	The U/N Fourier coefficients.	399
46.4	Periodic two-point correlation, $B_{33}(\hat{x}_3) = \langle v'_3(x_3)v'_3(x_3 + \hat{x}_3) \rangle$. . .	400
46.5	The energy spectrum of $\overline{v'^2_3}$ versus wavenumber, κ_3	400
48.1	Hump flow. Grid. Every 4 th grid line is shown.	408
49.1	Channel flow. The interface separates the RANS and the LES regions. . . .	417
49.2	Energy spectrum.	419
53.1	Transformation between (x_{1*}, x_{2*}) and (x_1, x_2)	435
54.1	Green's 3 rd formula. A volume V with surface S with normal vector n_i . . .	439
56.1	Control volume. The velocity v_1 is stored at the corners	443
59.1	Grids for DNS simulations. Every 5 th grid lines are shown.	466

List of Tables

3.1	Blasius numerical solution of laminar flow along a flat plate.	49
5.1	Number of eddies of turbulent eddies at each generation	84
11.1	Constants in the LRR and LRR-IP pressure-strain models.	148
12.1	Effect of streamline curvature on turbulence.	170
18.1	Differences between a finite volume RANS and LES code.	208
21.1	Turbulent viscosity and turbulent length scales in the URANS and LES	225
B.1	The components of the $\epsilon - \delta$ identity which are non-zero.	287
41.1	Probability distributions of the random variables.	364
41.2	Examples of value of κ_i^n , σ_i^n and α^n	365
45.1	Backstep. Data points.	388
50.1	Expressions for ℓ and ν_T in the LES and URANS regions	423

TME226 Mechanics of fluids

L. Davidson

Division of Fluid Dynamics
Department of Mechanics and Maritime Sciences
Chalmers University of Technology, Göteborg, Sweden
<https://www.tfd.chalmers.se/~lada>, lada@chalmers.se

This eBook can be downloaded at
<https://www.tfd.chalmers.se/~lada/MoF/>

Recorded lectures are found at https://www.tfd.chalmers.se/~lada/MoF/recorded_lecture.html

1 Motion, flow

1.1 Eulerian, Lagrangian, material derivative

SEE also [3], Chapt. 3.2.

Assume a fluid particle is moving along the line in Fig. 1.1. We can choose to study its motion in two ways: Lagrangian or Eulerian. In the Lagrangian approach we keep track of its original position (X_i) and follow its path which is described by $x_i(X_i, t)$. For example, at time t_1 the temperature of the particle is $T(X_i, t_1)$, and at time t_2 its temperature is $T(X_i, t_2)$, see Fig. 1.1. This approach is not used for fluids because it is very tricky to define and follow a fluid particle. It is however used when simulating movement of particles in fluids (for example soot particles in gasoline-air mixtures in combustion applications). The speed of the particle is then expressed as a function of time and its position at time zero, i.e. $v_i = v_i(X_i, t)$.

In the Eulerian approach we pick a position, e.g. x_i^1 , and watch the particle pass by. This approach is used for fluids. The temperature of the fluid, T , for example, is expressed as a function of the position, i.e. $T = T(x_i)$, see Fig. 1.1. It may be that the temperature at position x_i , for example, varies in time, t , and then $T = T(x_i, t)$.

Now we want to express how the temperature of a fluid particle varies. In the Lagrangian approach we first pick the particle (this gives its starting position, X_i). Once we have chosen a particle its starting position is fixed, and temperature varies only with time, i.e. $T(t)$ and the temperature gradient can be written dT/dt .

In the Eulerian approach it is a little bit more difficult. We are looking for the temperature gradient, dT/dt , but since we are looking at fixed points in space we need to express the temperature as a function of both time and space. From classical mechanics, we know that the velocity of a fluid particle is the time derivative of its space location, i.e. $v_i = dx_i/dt$. The chain-rule now gives

$$\frac{dT}{dt} = \frac{\partial T}{\partial t} + \frac{dx_j}{dt} \frac{\partial T}{\partial x_j} = \frac{\partial T}{\partial t} + v_j \frac{\partial T}{\partial x_j} \quad (1.1)$$

Note that we have to use partial derivative on T since it is a function of more than one (independent) variable. The first term on the right side is the **local rate of change**; by this we mean that it describes the variation of T in time at position x_i . The second term on the right side is called the **convective rate of change**, which means that it describes

**local rate
of change**
**Conv. rate
of change**

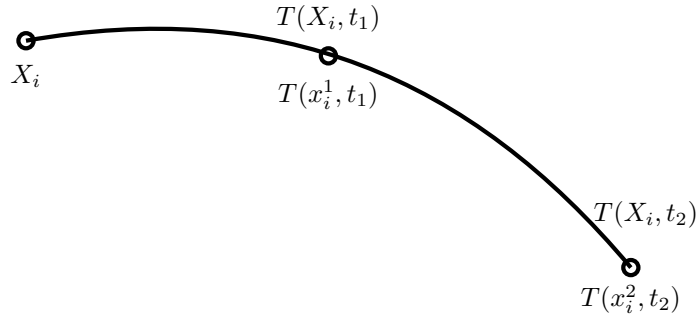


Figure 1.1: The temperature of a fluid particle described in Lagrangian, $T(X_i, t)$, or Eulerian, $T(x_i, t)$, approach.

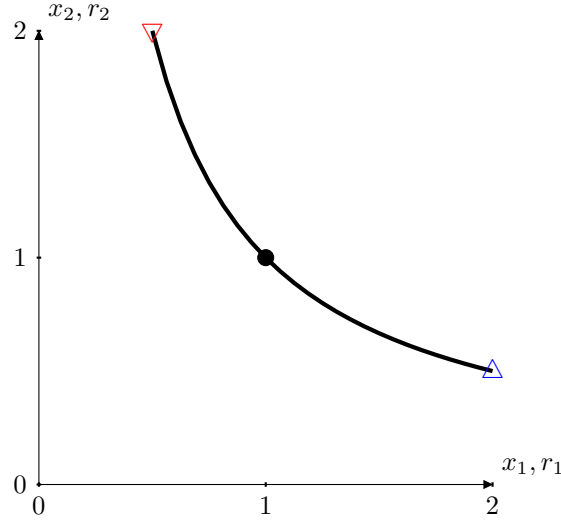


Figure 1.2: Flow path $x_2 = 1/x_1$. The filled circle shows the point $(x_1, x_2) = (1, 1)$. ∇ : start ($t = \ln(0.5)$); \triangle : end ($t = \ln(2)$).

the variation of T in space when it passes the point x_i . The left side in Eq. 1.1 is called the **material derivative** and is in this text denoted by dT/dt .

Exercise 1 Write out Eq. 1.1, term-by-term.

1.2 What is the difference between $\frac{dv_2}{dt}$ and $\frac{\partial v_2}{\partial t}$?

Students sometimes get confused about the difference between $\frac{dv_2}{dt}$ and $\frac{\partial v_2}{\partial t}$. Here we give a simple example. Figure 1.2 shows a flow path of fluid particles which can be expressed in time as

$$r_1 = X_1 \exp(t), \quad r_2 = X_2 \exp(-t) \quad (1.2)$$

where r_i is the location of the particle and X_i is the initial location. For $X_1 = X_2$ we get $r_2 = 1/r_1$. By varying X_1 (and/or X_2) we get different flow paths. The flow path in Fig. 1.2 is steady in time and it starts at $(r_1, r_2) = (X_1, X_2) = (0.5, 2)$ and ends at $(r_1, r_2) = (x_1, x_2) = (2, 0.5)$. The flow path is taken from stagnation flow, see Fig. 4.7. Equation 1.2 gives the velocities

$$v_1^L = \frac{dr_1}{dt} = X_1 \exp(t), \quad v_2^L = \frac{dr_2}{dt} = -X_2 \exp(-t) \quad (1.3)$$

and Eqs. 1.2 and 1.3 give

$$v_1^E = r_1 = x_1, \quad v_2^E = -r_2 = -x_2 \quad (1.4)$$

(cf. Eq. 4.50). The superscripts E and L denote Eulerian and Lagrangian, respectively. Note that $v_1^L = v_1^E$ and $v_2^L = v_2^E$; the only difference is that v_i^E is expressed as

function of (t, x_1, x_2) and v_i^L as function of (t, X_1, X_2) . Now we can compute the time derivatives of the v_2 velocity as

$$\begin{aligned}\frac{dv_2^L}{dt} &= \exp(-t) \\ \frac{dv_2^E}{dt} &= \frac{\partial v_2^E}{\partial t} + v_1^E \frac{\partial v_2^E}{\partial x_1} + v_2^E \frac{\partial v_2^E}{\partial x_2} = 0 + x_1 \cdot 0 - x_2 \cdot (-1) = x_2\end{aligned}\quad (1.5)$$

We find, of course, that $\frac{dv_2}{dt} = \frac{dv_2^E}{dt} = \frac{dv_2^L}{dt} = x_2 = \exp(-t)$.

Consider, for example, the point $(x_1, x_2) = (1, 1)$ in Fig. 1.2. The difference between $\frac{dv_2}{dt}$ and $\frac{\partial v_2}{\partial t}$ is now clearly seen by looking at Eq. 1.5. The velocity at the point $(x_1, x_2) = (1, 1)$ does not change in time and hence $\frac{\partial v_2^E}{\partial t} = 0$. However, if we sit on a particle which passes the location $(x_1, x_2) = (1, 1)$, the velocity, v_2^L , increases by time, $\frac{dv_2^L}{dt} = \frac{dv_2}{dt} = 1$ (the velocity, v_2 , gets less negative). Actually it increases all the time from the starting point where $\frac{dv_2}{dt} = 2$ and $v_2 = -2$ until the end point where $\frac{dv_2}{dt} = 0.5$ and $v_2 = -0.5$.

1.3 Viscous stress, pressure

See also [3], Chaps. 6.3 and 8.1.

We have in Part I [4] derived the balance equation for linear momentum which reads

$$\boxed{\rho \dot{v}_i - \sigma_{ji,j} - \rho f_i = 0} \quad (1.6)$$

Switch notation for the material derivative and derivatives so that

$$\rho \frac{dv_i}{dt} = \frac{\partial \sigma_{ji}}{\partial x_j} + \rho f_i \quad (1.7)$$

where the first and the second term on the right side represents, respectively, the net force due to surface and volume forces (σ_{ij} denotes the stress tensor). Stress is force per unit area. The first term on the right side includes the viscous stress tensor, τ_{ij} . As you have learnt earlier, the first index relates to the surface at which the stress acts and the second index is related to the stress component. For example, on a surface whose normal is $n_i = (1, 0, 0)$ act the three stress components σ_{11} , σ_{12} and σ_{13} , see Fig. 1.3a; the volume force acts in the middle of the fluid element, see Fig. 1.3b.

In the present notation we denote the velocity vector by $\mathbf{v} = v_i = (v_1, v_2, v_3)$ and the coordinate by $\mathbf{x} = x_i = (x_1, x_2, x_3)$. In the literature, you may find other notations of the velocity vector such as $u_i = (u_1, u_2, u_3)$. If no tensor notation is used the velocity vector is usually denoted as (u, v, w) and the coordinates as (x, y, z) .

The diagonal components of σ_{ij} represent the normal stresses and the off-diagonal components of σ_{ij} represent the shear stresses. In Part I [4] you learned that the pressure is defined as minus the sum of the normal stress, i.e.

$$P = -\sigma_{kk}/3 \quad (1.8)$$

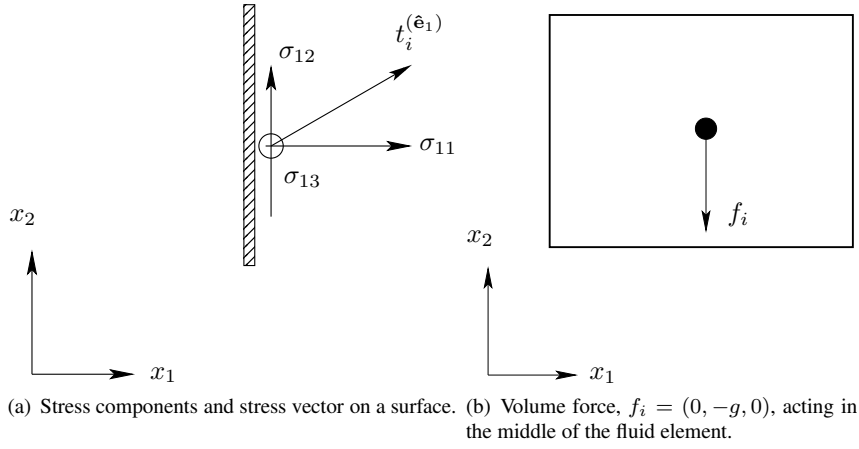


Figure 1.3: Stress tensor, volume (gravitation) force and stress vector, $t_i^{(\hat{e}_1)}$, see Eq. C.2.

The pressure, P , acts as a normal stress. In general, pressure is a thermodynamic property, p_t , which can be obtained – for example – from the ideal gas law. In that case the thermodynamics pressure, p_t , and the mechanical pressure, P , may not be the same but Eq. 1.8 is nevertheless used. The *viscous* stress tensor, τ_{ij} , is obtained by subtracting the trace, $\sigma_{kk}/3 = -P$, from σ_{ij} ; the stress tensor can then be written as

$$\sigma_{ij} = -P\delta_{ij} + \tau_{ij} \quad (1.9)$$

τ_{ij} is the deviator of σ_{ij} . The expression for the viscous stress tensor is found in Eq. 2.4 at p. 31. The minus-sign in front of P appears because the pressure acts *into* the surface. When there is no movement, the viscous stresses are zero and then of course the normal stresses are the same as the pressure. In general, however, the normal stresses are the sum of the pressure and the viscous stresses, i.e.

$$\sigma_{11} = -P + \tau_{11}, \quad \sigma_{22} = -P + \tau_{22}, \quad \sigma_{33} = -P + \tau_{33}, \quad (1.10)$$

Exercise 2 Consider Fig. 1.3. Show how $\sigma_{21}, \sigma_{22}, \sigma_{23}$ act on a surface with normal vector $n_i = (0, 1, 0)$. Show also how $\sigma_{31}, \sigma_{32}, \sigma_{33}$ act on a surface with normal vector $n_i = (0, 0, 1)$.

Exercise 3 Write out Eq. 1.9 on matrix form.

1.4 Strain rate tensor, vorticity

See also [3], Chapt. 3.5.3, 3.6.

We need an expression for the viscous stresses, τ_{ij} . They are needed in the momentum equations, Eq. 1.7 (see also Eq. 1.9). They will be expressed in the velocity gradients, $\frac{\partial v_i}{\partial x_j}$. Hence we will now discuss the velocity gradients.

The velocity gradient tensor can be split into two parts as

$$\begin{aligned}\frac{\partial v_i}{\partial x_j} &= \frac{1}{2} \left(\underbrace{\frac{\partial v_i}{\partial x_j} + \frac{\partial v_j}{\partial x_i}}_{2\partial v_i/\partial x_j} + \underbrace{\frac{\partial v_j}{\partial x_i} - \frac{\partial v_i}{\partial x_j}}_{=0} \right) \\ &= \frac{1}{2} \left(\frac{\partial v_i}{\partial x_j} + \frac{\partial v_j}{\partial x_i} \right) + \frac{1}{2} \left(\frac{\partial v_i}{\partial x_j} - \frac{\partial v_j}{\partial x_i} \right) = S_{ij} + \Omega_{ij}\end{aligned}\quad (1.11)$$

where

S_{ij} is a *symmetric* tensor called the **strain-rate tensor**

Ω_{ij} is a *anti-symmetric* tensor called the **vorticity tensor**

**Strain-rate
tensor
vorticity tensor**

The vorticity tensor is related to the familiar **vorticity vector** which is the curl of the velocity vector, i.e. $\boldsymbol{\omega} = \nabla \times \mathbf{v}$, or in tensor notation

$$\omega_i = \epsilon_{ijk} \frac{\partial v_k}{\partial x_j} \quad (1.12)$$

where ϵ_{ijk} is the permutation tensor, see lecture notes of Ekh [4] and Table B.1 in Appendix B. If we set, for example, $i = 3$ we get

$$\omega_3 = \partial v_2 / \partial x_1 - \partial v_1 / \partial x_2. \quad (1.13)$$

The vorticity represents rotation of a fluid particle. Inserting Eq. 1.11 into Eq. 1.12 gives

$$\omega_i = \epsilon_{ijk} (S_{kj} + \Omega_{kj}) = \epsilon_{ijk} \Omega_{kj} \quad (1.14)$$

since $\epsilon_{ijk} S_{kj} = 0$ because the product of a symmetric tensor (S_{kj}) and an anti-symmetric tensor (ϵ_{ijk}) is zero. Let us show this for $i = 1$ by writing out the full equation. Recall that $S_{ij} = S_{ji}$ (i.e. $S_{12} = S_{21}$, $S_{13} = S_{31}$, $S_{23} = S_{32}$) and $\epsilon_{ijk} = -\epsilon_{ikj} = \epsilon_{jki}$ etc (i.e. $\epsilon_{123} = -\epsilon_{132} = \epsilon_{231} \dots$, $\epsilon_{113} = \epsilon_{221} = \dots \epsilon_{331} = 0$)

$$\begin{aligned}\epsilon_{1jk} S_{kj} &= \epsilon_{111} S_{11} + \epsilon_{112} S_{21} + \epsilon_{113} S_{31} \\ &\quad + \epsilon_{121} S_{12} + \epsilon_{122} S_{22} + \epsilon_{123} S_{32} \\ &\quad + \epsilon_{131} S_{13} + \epsilon_{132} S_{23} + \epsilon_{133} S_{33} \\ &= 0 \cdot S_{11} + 0 \cdot S_{21} + 0 \cdot S_{31} \\ &\quad + 0 \cdot S_{12} + 0 \cdot S_{22} + 1 \cdot S_{32} \\ &\quad + 0 \cdot S_{13} - 1 \cdot S_{23} + 0 \cdot S_{33} \\ &= S_{32} - S_{23} = 0\end{aligned}\quad (1.15)$$

Now let us invert Eq. 1.14. We start by multiplying it with ϵ_{ilm} so that

$$\epsilon_{ilm} \omega_i = \epsilon_{ilm} \epsilon_{ijk} \Omega_{kj} \quad (1.16)$$

The ϵ - δ -identity gives (see Table B.1 at p. 287)

$$\epsilon_{ilm} \epsilon_{ijk} \Omega_{kj} = (\delta_{lj} \delta_{mk} - \delta_{lk} \delta_{mj}) \Omega_{kj} = \Omega_{ml} - \Omega_{\ell m} = 2\Omega_{m\ell} \quad (1.17)$$

This can easily be proved by writing out all the components, see Table B.1 at p. 287. Now Eqs. 1.16 and 1.17 give

$$\Omega_{m\ell} = \frac{1}{2}\varepsilon_{i\ell m}\omega_i = \frac{1}{2}\varepsilon_{\ell m i}\omega_i = -\frac{1}{2}\varepsilon_{m\ell i}\omega_i \quad (1.18)$$

or, switching indices

$$\Omega_{ij} = -\frac{1}{2}\varepsilon_{ijk}\omega_k \quad (1.19)$$

It turns out that is is much easier to go from Eq. 1.14 to Eq. 1.19 by writing out the components of Eq. 1.14 (here we do it for $i = 1$)

$$\omega_1 = \varepsilon_{123}\Omega_{32} + \varepsilon_{132}\Omega_{23} = \Omega_{32} - \Omega_{23} = -2\Omega_{23} \quad (1.20)$$

and we get

$$\Omega_{23} = -\frac{1}{2}\omega_1 \quad (1.21)$$

which indeed is identical to Eq. 1.19.

Exercise 4 Write out the second and third component of the vorticity vector given in Eq. 1.12 (i.e. ω_2 and ω_3).

Exercise 5 Complete the proof of Eq. 1.15 for $i = 2$ and $i = 3$.

Exercise 6 Write out Eq. 1.20 also for $i = 2$ and $i = 3$ and find an expression for Ω_{12} and Ω_{13} (cf. Eq. 1.21). Show that you get the same result as in Eq. 1.19.

Exercise 7 In Eq. 1.21 we proved the relation between Ω_{ij} and ω_i for the off-diagonal components. What about the diagonal components of Ω_{ij} ? What do you get from Eq. 1.11?

Exercise 8 From your course in linear algebra, you should remember how to compute a vector product using Sarrus' rule. Use it to compute the vector product

$$\boldsymbol{\omega} = \nabla \times \mathbf{v} = \begin{bmatrix} \hat{\mathbf{e}}_1 & \hat{\mathbf{e}}_2 & \hat{\mathbf{e}}_3 \\ \frac{\partial}{\partial x_1} & \frac{\partial}{\partial x_2} & \frac{\partial}{\partial x_3} \\ v_1 & v_2 & v_3 \end{bmatrix}$$

Verify that this agrees with the expression in tensor notation in Eq. 1.12.

1.5 Product of a symmetric and antisymmetric tensor

In this section we show the proof that the product of a symmetric and antisymmetric tensor is zero. First, we have the definitions:

- A tensor a_{ij} is symmetric if $a_{ij} = a_{ji}$;
- A tensor b_{ij} is antisymmetric if $b_{ij} = -b_{ji}$.

It follows that for an antisymmetric tensor all diagonal components must be zero; for example, $b_{11} = -b_{11}$ can only be satisfied if $b_{11} = 0$.

The (inner) product of a symmetric and antisymmetric tensor is always zero. This can be shown as follows

$$a_{ij}b_{ij} = a_{ji}b_{ij} = -a_{ji}b_{ji},$$

where we first used the fact that $a_{ij} = a_{ji}$ (symmetric), and then that $b_{ij} = -b_{ji}$ (antisymmetric). Since the indices i and j are both dummy indices we can interchange them in the last expression ($-a_{ji}b_{ji} = -a_{ij}b_{ij}$), which gives

$$a_{ij}b_{ij} = -a_{ij}b_{ij}$$

This expression says that $A = -A$ which can be only true if $A = 0$ and hence $a_{ij}b_{ij} = 0$.

This can of course also be shown by writing out $a_{ij}b_{ij}$ on component form, i.e.

$$\begin{aligned} a_{ij}b_{ij} &= \underbrace{a_{11}b_{11}}_I + \underbrace{a_{12}b_{12}}_{II} + \underbrace{a_{13}b_{13}}_{III} \\ &\quad + \underbrace{a_{21}b_{21}}_I + \underbrace{a_{22}b_{22}}_{II} + \underbrace{a_{23}b_{23}}_{III} \\ &\quad + \underbrace{a_{31}b_{31}}_{II} + \underbrace{a_{32}b_{32}}_{III} + \underbrace{a_{33}b_{33}}_{III} = 0 \end{aligned}$$

The underlined terms are zero ($b_{11} = b_{22} = b_{33} = 0$); terms I cancel each other ($a_{12} = a_{21}$, $b_{12} = -b_{21}$) as do terms II and III.

1.6 Deformation, rotation

See also [3], Chapt. 3.3.

The velocity gradient can, as shown above, be divided into two parts: S_{ij} and Ω_{ij} . We have shown that the latter is connected to *rotation* of a fluid particle. During rotation the fluid particle is not deformed. This movement can be illustrated by Fig. 1.4. The vertical movement (v_2) of the right end of the horizontal edge ($x_1 + \Delta x_1$) of the particle in Fig. 1.4 is estimated as follows. The velocity at the left edge is $v_2(x_1)$. Now we need the velocity at the right edge which is located at $x_1 + \Delta x_1$. It is computed using the first term in the Taylor series as¹

rotation

$$v_2(x_1 + \Delta x_1) = v_2(x_1) + \Delta x_1 \frac{\partial v_2}{\partial x_1}$$

It is assumed that the fluid particle in Fig. 1.4 is rotated the angle $\Delta\alpha$ during the time Δt . The angle rotation per unit time can be estimated as $\Delta\alpha/\Delta t \simeq d\alpha/dt = -\partial v_1/\partial x_2 = \partial v_2/\partial x_1$; if the fluid element does not rotate as a solid body, the rotation is computed as the average, i.e. $d\alpha/dt = (\partial v_2/\partial x_1 - \partial v_1/\partial x_2)/2$. The vorticity is computed as $\omega_3 = \partial v_2/\partial x_1 - \partial v_1/\partial x_2 = -2\Omega_{12} = 2d\alpha/dt$, see Eq. 1.13 and Exercise 4. Hence, the vorticity ω_3 can be interpreted as twice the average rotation per unit time of the horizontal edge ($\partial v_2/\partial x_1$) and vertical edge ($-\partial v_1/\partial x_2$).

Next let us have a look at the deformation caused by S_{ij} . It can be divided into two parts, namely shear and elongation (also called extension or dilatation). The deformation due to shear is caused by the off-diagonal terms of S_{ij} . In Fig. 1.5, a pure shear deformation by $S_{12} = (\partial v_1/\partial x_2 + \partial v_2/\partial x_1)/2$ is shown. The deformation due to elongation is caused by the diagonal terms of S_{ij} . Elongation caused by $S_{11} = \partial v_1/\partial x_1$ is illustrated in Fig. 1.6.

In general, a fluid particle experiences a combination of rotation, deformation and elongation as indeed is given by Eq. 1.11.

¹this corresponds to the equation for a straight line $y = kx + \ell$ where k is the slope which is equal to the derivative of y , i.e. dy/dx , and $\ell = v_2(x_1)$

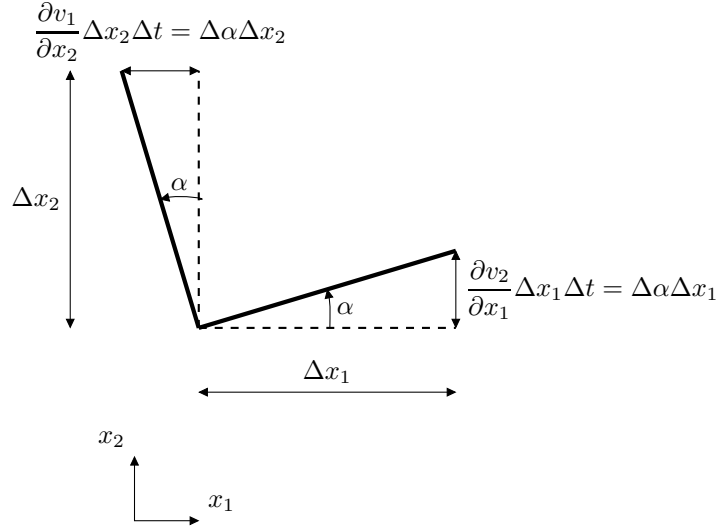


Figure 1.4: Rotation of a fluid particle during time Δt . Here $\partial v_1/\partial x_2 = -\partial v_2/\partial x_1$ so that $-\Omega_{12} = \omega_3/2 = \partial v_2/\partial x_1 > 0$. The distance the upper part of the left edge is negative because it has moved with a negative v_1 velocity.

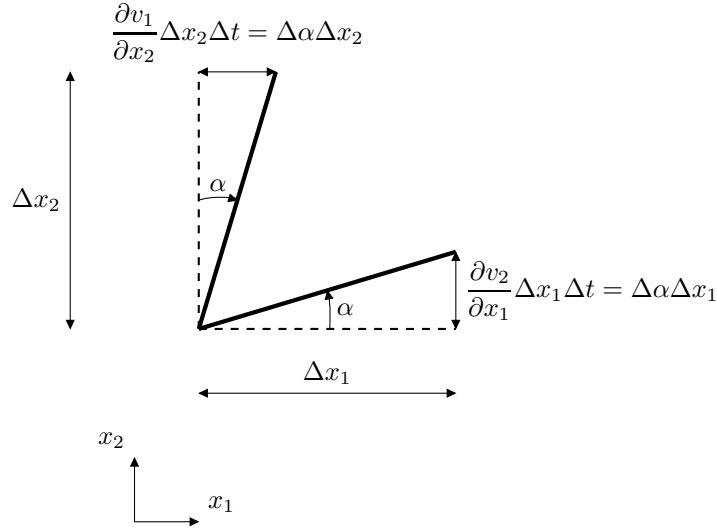


Figure 1.5: Deformation of a fluid particle by shear during time Δt . Here $\partial v_1/\partial x_2 = \partial v_2/\partial x_1$ so that $S_{12} = \partial v_1/\partial x_2 > 0$.

Exercise 9 Consider Fig. 1.4. Show and formulate the rotation by ω_1 .

Exercise 10 Consider Fig. 1.5. Show and formulate the deformation by S_{23} .

Exercise 11 Consider Fig. 1.6. Show and formulate the elongation by S_{22} .

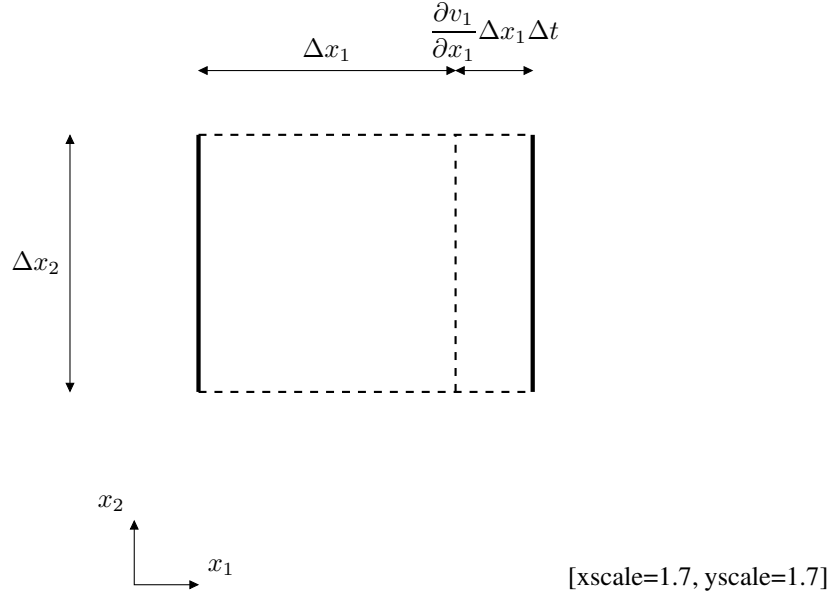


Figure 1.6: Deformation of a fluid particle by elongation during time Δt .

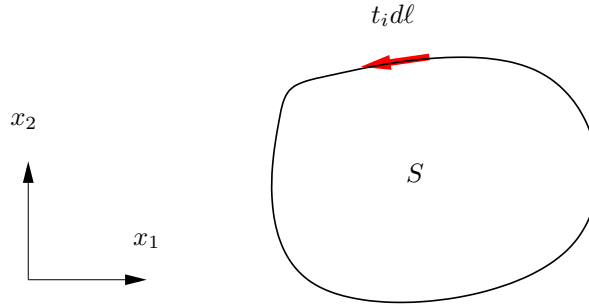


Figure 1.7: The surface, S , is enclosed by the line ℓ . The vector, t_i , denotes the unit tangential vector of the enclosing line, ℓ .

1.7 Irrotational and rotational flow

In the previous subsection we introduced different types of movement of a fluid particle. One type of movement was rotation, see Fig. 1.4. Flows are often classified based on rotation: they are *rotational* ($\omega_i \neq 0$) or *irrotational* ($\omega_i = 0$); the latter type is also called inviscid flow or potential flow. We will talk more about that later on, see Section 4.4. In this subsection we will give examples of one irrotational and one rotational flow. In potential flow, there exists a potential, Φ , from which the velocity components can be obtained as

$$v_k = \frac{\partial \Phi}{\partial x_k} \quad (1.22)$$

Before we talk about the ideal vortex line in the next section, we need to introduce the concept **circulation**. Consider a closed line on a surface in the $x_1 - x_2$ plane, see Fig. 1.7. When the velocity is integrated along this line and projected onto the line we

obtain the circulation

$$\Gamma = \oint v_m t_m d\ell \quad (1.23)$$

Using Stokes's theorem we can relate the circulation to the vorticity as

$$\Gamma = \oint v_m t_m d\ell = \int_S \varepsilon_{ijk} \frac{\partial v_k}{\partial x_j} n_i dS = \int_S \omega_i n_i dS = \int_S \omega_3 dS \quad (1.24)$$

where $n_i = (0, 0, 1)$ is the unit normal vector of the surface S . Equation 1.24 reads in vector notation

$$\Gamma = \oint \mathbf{v} \cdot \mathbf{t} d\ell = \int_S (\nabla \times \mathbf{v}) \cdot \mathbf{n} dS = \int_S \boldsymbol{\omega} \cdot \mathbf{n} dS = \int_S \omega_3 dS \quad (1.25)$$

The circulation is useful in, for example, aeronautics and windpower engineering where the lift of a 2D section of an airfoil or a rotorblade is expressed in the circulation for that 2D section. The lift force is computed as (see Eqs. 4.84 and 4.85)

$$L = \rho V \Gamma \quad (1.26)$$

where V is the velocity around the airfoil (for a rotorblade it is the relative velocity, since the rotorblade is rotating). In an PhD project, an inviscid simulation method (based on the circulation and vorticity sources) is used to compute the aerodynamic loads for windturbine rotorblades [5].

Exercise 12 In potential flow $\omega_i = \varepsilon_{ijk} \partial v_k / \partial x_j = 0$. Multiply Eq. 1.22 by ε_{ijk} and derivate with respect to x_k (i.e. take the curl of) and show that the right side becomes zero as it should, i.e. $\varepsilon_{ijk} \partial^2 \Phi / (\partial x_k \partial x_j) = 0$.

1.7.1 Ideal vortex line

The two-dimensional ideal vortex line is an irrotational (potential) flow where the fluid moves along circular paths, see Fig. 1.8. The governing equations are derived in Section 4.4.5. The velocity field in polar coordinates reads

$$v_\theta = \frac{\Gamma}{2\pi r}, \quad v_r = 0 \quad (1.27)$$

where Γ is the circulation. Its potential reads

$$\Phi = \frac{\Gamma \theta}{2\pi} \quad (1.28)$$

The velocity, v_θ , is then obtained as

$$v_\theta = \frac{1}{r} \frac{\partial \Phi}{\partial \theta} = \frac{\Gamma}{2\pi r} \quad (1.29)$$

To transform Eq. 1.27 into Cartesian velocity components, consider Fig. 1.9. The Cartesian velocity vectors are expressed as

$$\begin{aligned} v_1 &= -v_\theta \sin(\theta) = -v_\theta \frac{x_2}{r} = -v_\theta \frac{x_2}{(x_1^2 + x_2^2)^{1/2}} = -\frac{\Gamma x_2}{2\pi(x_1^2 + x_2^2)} \\ v_2 &= v_\theta \cos(\theta) = v_\theta \frac{x_1}{r} = v_\theta \frac{x_1}{(x_1^2 + x_2^2)^{1/2}} = \frac{\Gamma x_1}{2\pi(x_1^2 + x_2^2)} \end{aligned} \quad (1.30)$$

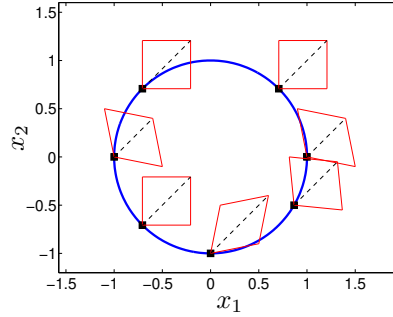


Figure 1.8: Ideal vortex. The fluid particle (i.e. its diagonal, see Fig. 1.4) does not rotate. The locations of the fluid particle is indicated by black, filled squares. The diagonals are shown as black dashed lines. The fluid particle is shown at $\theta = 0, \pi/4, 3\pi/4, \pi, 5\pi/4, 3\pi/2$ and $-\pi/6$.

Inserting Eq. 1.30 into Eq. 1.27 we get

$$v_1 = -\frac{\Gamma x_2}{2\pi(x_1^2 + x_2^2)}, \quad v_2 = \frac{\Gamma x_1}{2\pi(x_1^2 + x_2^2)}. \quad (1.31)$$

To verify that this flow is a potential flow, we need to show that the vorticity, $\omega_i = \varepsilon_{ijk} \partial v_k / \partial x_j$ is zero. Since it is a two-dimensional flow ($v_3 = \partial / \partial x_3 = 0$), $\omega_1 = \omega_2 = 0$, we only need to compute $\omega_3 = \partial v_2 / \partial x_1 - \partial v_1 / \partial x_2$. The velocity derivatives are obtained as

$$\frac{\partial v_1}{\partial x_2} = -\frac{\Gamma}{2\pi} \frac{x_1^2 - x_2^2}{(x_1^2 + x_2^2)^2}, \quad \frac{\partial v_2}{\partial x_1} = \frac{\Gamma}{2\pi} \frac{x_2^2 - x_1^2}{(x_1^2 + x_2^2)^2} \quad (1.32)$$

and we get

$$\omega_3 = \frac{\Gamma}{2\pi} \frac{1}{(x_1^2 + x_2^2)^2} (x_2^2 - x_1^2 + x_1^2 - x_2^2) = 0 \quad (1.33)$$

which shows that the flow is indeed a potential flow, i.e. *irrotational* ($\omega_i \equiv 0$). Note that the deformation is not zero, i.e.

$$S_{12} = \frac{1}{2} \left(\frac{\partial v_1}{\partial x_2} + \frac{\partial v_2}{\partial x_1} \right) = \frac{\Gamma}{2\pi} \frac{x_2^2}{(x_1^2 + x_2^2)^2} \quad (1.34)$$

Hence a fluid particle in an ideal vortex does deform but it does not rotate (i.e. its diagonal does not rotate, see Fig. 1.8).

It may be little confusing that the flow path forms a *vortex* but the flow itself has no *vorticity*. Thus one must be very careful when using the words “vortex” and “vorticity”. By vortex we usually mean a recirculation region of the mean flow. That the flow has no vorticity (i.e. no rotation) means that a fluid particle moves as illustrated in Fig. 1.8. As a fluid particle moves from position a to b – on its counter-clockwise-rotating path – the particle itself is not rotating. This is true for the whole flow field, except at the center where the fluid particle does rotate. This is a singular point as is seen from Eq. 1.27 for which $v_\theta \rightarrow \infty$.

Note that generally a vortex has vorticity, see Section 4.2. The ideal vortex is a very special flow case.

**vortex vs.
vorticity**

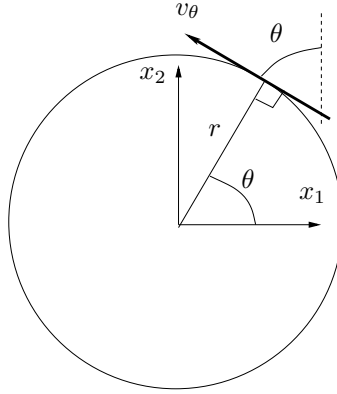


Figure 1.9: Transformation of v_θ into Cartesian components.

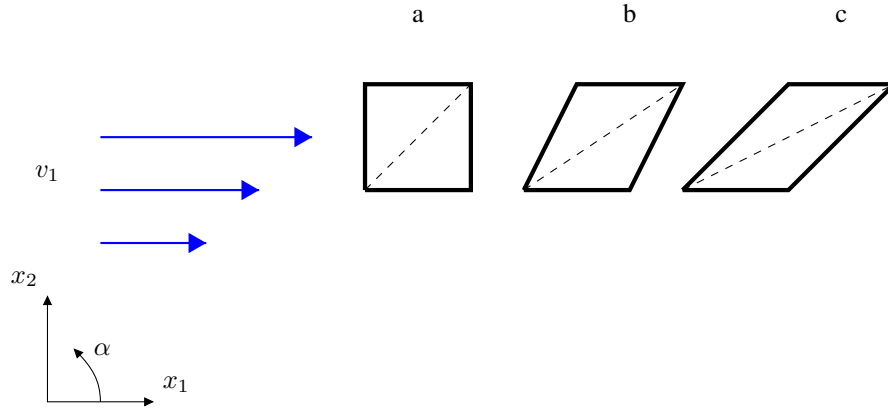


Figure 1.10: A shear flow. A fluid particle with vorticity. $v_1 = cx_2^2$.

1.7.2 Shear flow

Another example – which is rotational – is the lower half of fully-developed channel flow for which the velocity reads (see Eq. 3.28)

$$\frac{v_1}{v_{1,max}} = \frac{4x_2}{h} \left(1 - \frac{x_2}{h}\right), \quad v_2 = 0 \quad (1.35)$$

where $x_2 < h/2$, see Fig. 1.10. The vorticity vector for this flow reads

$$\omega_1 = \omega_2 = 0, \quad \omega_3 = \frac{\partial v_2}{\partial x_1} - \frac{\partial v_1}{\partial x_2} = -\frac{4}{h} \left(1 - \frac{2x_2}{h}\right) \quad (1.36)$$

When the fluid particle is moving from position a , via b to position c its has vorticity. Its vertical too edge move faster than its bottom edge. The horizontal edges stay horizontal because $v_2 = 0$. Its vertical edges are rotating in clockwise direction. The diagonal is rotating which really is the definition of rotation. Note that the positive rotating direction is defined as the counter-clockwise direction, indicated by a in Fig. 1.10. This is why the vorticity, ω_3 , in the lower half of the channel ($x_2 < h/2$) is negative. In the upper half of the channel the vorticity is positive because $\partial v_1 / \partial x_2 < 0$.

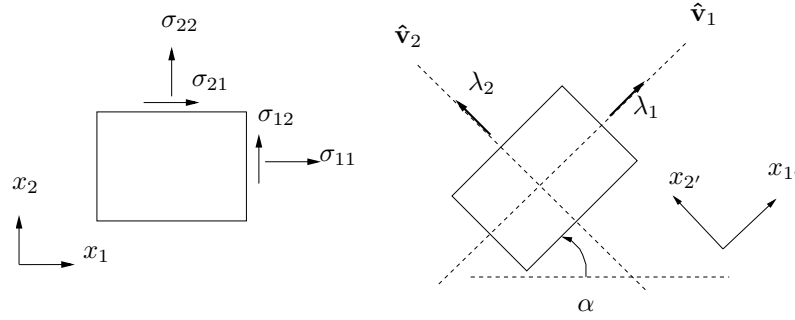


Figure 1.11: A two-dimensional fluid element. Left: in original state; right: rotated to principal coordinate directions. λ_1 and λ_2 denote eigenvalues; $\hat{\mathbf{v}}_1$ and $\hat{\mathbf{v}}_2$ denote unit eigenvectors.

It may be noted that for the flow in Fig. 1.10 the magnitude of the shear, S_{12} , and the vorticity, Ω_{12} , are equal but of opposite sign, i.e. $S_{12} = -\Omega_{12}$.

1.8 Eigenvalues and eigenvectors: physical interpretation

See also [3], Chapt. 2.5.5.

Consider a two-dimensional fluid (or solid) element, see Fig. 1.11. In the left figure it is oriented along the $x_1 - x_2$ coordinate system. On the surfaces act normal stresses (σ_{11} , σ_{22}) and shear stresses (σ_{12} , σ_{21}). The stresses form a tensor, σ_{ij} . Any tensor has eigenvectors and eigenvalues (also called principal vectors and principal values). Since σ_{ij} is symmetric, the eigenvalues are real (i.e. not imaginary). The eigenvalues are obtained from the characteristic equation, see [3], Chapt. 2.5.5 or Eq. 13.5 at p. 173. When the eigenvalues have been obtained, the eigenvectors can be computed. Given the eigenvectors, the fluid element is rotated α degrees so that its edges are aligned with the eigenvectors, $\hat{\mathbf{v}}_1 = \hat{\mathbf{x}}_{1'}$ and $\hat{\mathbf{v}}_2 = \hat{\mathbf{x}}_{2'}$, see right part of Fig. 1.11. Note that the sign of the eigenvectors is not defined, which means that the eigenvectors can equally well be chosen as $-\hat{\mathbf{v}}_1$ and/or $-\hat{\mathbf{v}}_2$. In the principal coordinates $x_{1'} - x_{2'}$ (right part of Fig. 1.11), there are no shear stresses on the surfaces of the fluid element. There are only normal stresses. This is the very definition of eigenvectors. Furthermore, the eigenvalues are the normal stresses in the principal coordinates, i.e. $\lambda_1 = \sigma_{1'1'}$ and $\lambda_2 = \sigma_{2'2'}$.

2 Governing flow equations

SEE also [3], Chaps. 5 and 8.1.

2.1 The Navier-Stokes equation

2.1.1 The continuity equation

The first equation is the continuity equation (the balance equation for mass) which reads [4]

$$\boxed{\dot{\rho} + \rho v_{i,i} = 0} \quad (2.1)$$

Change of notation gives

$$\frac{d\rho}{dt} + \rho \frac{\partial v_i}{\partial x_i} = 0 \quad (2.2)$$

For incompressible flow ($\rho = \text{const}$) we get

$$\frac{\partial v_i}{\partial x_i} = 0 \quad (2.3)$$

2.1.2 The momentum equation

The next equation is the momentum equation. We have formulated the constitutive law for Newtonian viscous fluids [4]

$$\begin{aligned} \sigma_{ij} &= -P\delta_{ij} + 2\mu S_{ij} - \frac{2}{3}\mu S_{kk}\delta_{ij} \\ \tau_{ij} &= 2\mu S_{ij} - \frac{2}{3}\mu S_{kk}\delta_{ij} \end{aligned} \quad (2.4)$$

Inserting Eq. 2.4 into the balance equations, Eq. 1.7, we get

$$\rho \frac{dv_i}{dt} = -\frac{\partial P}{\partial x_i} + \frac{\partial \tau_{ji}}{\partial x_j} + \rho f_i = -\frac{\partial P}{\partial x_i} + \frac{\partial}{\partial x_j} \left(2\mu S_{ij} - \frac{2}{3}\mu \frac{\partial v_k}{\partial x_k} \delta_{ij} \right) + \rho f_i \quad (2.5)$$

where μ denotes the dynamic viscosity. This is the *Navier-Stokes* equations (sometimes the continuity equation is also included in the name “Navier-Stokes”). It is also called the *transport equation for momentum*. Note that the stress tensor, σ_{ij} , depends only on the *symmetric* part (i.e. S_{ij} , see Eq. 1.11) of the velocity gradient. It is only the part of the velocity gradient that *deforms* the fluid (see Figs. 1.5 and 1.6) that appears in σ_{ij} . The part of the velocity gradient that *rotates* the fluid (i.e. Ω_{ij} , see Eq. 1.11 and Fig. 1.4) does not appear in σ_{ij} .

For incompressible flow, the last term in the diffusion term is zero because of the continuity equation (see Eq. 2.3) so that

$$\rho \frac{dv_i}{dt} = -\frac{\partial P}{\partial x_i} + \frac{\partial}{\partial x_j} \left[\mu \left(\frac{\partial v_i}{\partial x_j} + \frac{\partial u_j}{\partial x_i} \right) \right] + \rho f_i \quad (2.6)$$

Furthermore, if the viscosity, μ , is constant it can be moved outside the derivative. We can then re-write the first term in the parenthesis in Eq. 2.6 as

$$\frac{\partial}{\partial x_j} \left[\mu \left(\frac{\partial v_i}{\partial x_j} + \frac{\partial u_j}{\partial x_i} \right) \right] = \mu \frac{\partial}{\partial x_j} \left(\frac{\partial v_i}{\partial x_j} + \frac{\partial u_j}{\partial x_i} \right) = \mu \frac{\partial^2 v_i}{\partial x_j \partial x_j} \quad (2.7)$$

because of the continuity equation, i.e.

$$\mu \frac{\partial}{\partial x_j} \left(\frac{\partial v_j}{\partial x_i} \right) = \mu \frac{\partial}{\partial x_i} \left(\frac{\partial v_j}{\partial x_j} \right) = 0. \quad (2.8)$$

Equation 2.5 can now – for constant μ and incompressible flow – be written

$$\rho \frac{dv_i}{dt} = -\frac{\partial P}{\partial x_i} + \mu \frac{\partial^2 v_i}{\partial x_j \partial x_j} + \rho f_i \quad (2.9)$$

The viscous stress tensor then reads

$$\tau_{ij} = 2\mu S_{ij} = \mu \left(\frac{\partial v_i}{\partial x_j} + \frac{\partial v_j}{\partial x_i} \right) \quad (2.10)$$

In inviscid (potential) flow, there are no viscous (friction) forces. In this case, the Navier-Stokes equation reduces to the *Euler equations*

$$\rho \frac{dv_i}{dt} = -\frac{\partial P}{\partial x_i} + \rho f_i \quad (2.11)$$

**Euler
equations**

Exercise 13 Equation 1.7 states that mass times acceleration is equal to the sum of forces (per unit volume). Write out the momentum equation (without using the summation rule) for the x_1 direction and show the surface forces and the volume force on a small, square fluid element (see lecture notes of Toll & Ekh [4]). Now repeat it for the x_2 direction.

Exercise 14 Formulate the Navier-Stokes equation for incompressible flow but non-constant viscosity.

2.2 The energy equation

See also [3], Chaps. 6.4 and 8.1.

We have in Part I [4] derived the energy equation which reads

$$\boxed{\rho \dot{u} - v_{i,j} \sigma_{ji} + q_{i,i} = \rho z} \quad (2.12)$$

where u denotes internal energy (N.B.: in [4] it is denoted by e). q_i denotes the conductive heat flux and z the net radiative heat source. For simplicity, we neglect the radiation from here on. Change of notation gives

$$\rho \frac{du}{dt} = \sigma_{ji} \frac{\partial v_i}{\partial x_j} - \frac{\partial q_i}{\partial x_i} \quad (2.13)$$

In Part I [4] we formulated the constitutive law for the heat flux vector (Fourier's law)

$$q_i = -k \frac{\partial T}{\partial x_i} \quad (2.14)$$

Inserting the constitutive laws, Eqs. 2.4 and 2.14, into Eq. 2.13 gives

$$\rho \frac{du}{dt} = -P \frac{\partial v_i}{\partial x_i} + \underbrace{2\mu S_{ij} S_{ij} - \frac{2}{3} \mu S_{kk} S_{ii}}_{\Phi} + \frac{\partial}{\partial x_i} \left(k \frac{\partial T}{\partial x_i} \right) \quad (2.15)$$

where we have used $S_{ij}\partial v_i/\partial x_j = S_{ij}(S_{ij} + \Omega_{ij}) = S_{ij}S_{ij}$ because the product of a symmetric tensor, S_{ij} , and an anti-symmetric tensor, Ω_{ij} , is zero. The dissipation term, Φ , can be re-written as

$$\Phi = 2\mu \left(S_{ij}S_{ij} - \frac{1}{3}S_{kk}S_{ii} \right) = \left[2\mu \left(S_{ij} - \frac{1}{3}S_{kk}\delta_{ij} \right)^2 \right] > 0$$

which shows that Φ is positive. The dissipation represents irreversible viscous heating (i.e. transformation of kinetic energy into thermal energy); it is important at high-speed flow² (for example re-entry from outer space) and for highly viscous flows (lubricants). The first term on the right side represents reversible heating and cooling due to compression and expansion of the fluid. Equation 2.15 is the *transport equation for (internal) energy*, u .

Now we assume that the flow is incompressible (i.e. the velocity should be smaller than approximately 1/3 of the speed of sound) for which

$$du = c_p dT \quad (2.16)$$

where c_p is the heat capacity (see Part I) [4] so that Eq. 2.15 gives (c_p is assumed to be constant)

$$\rho c_p \frac{dT}{dt} = \Phi + \frac{\partial}{\partial x_i} \left(k \frac{\partial T}{\partial x_i} \right) \quad (2.17)$$

The dissipation term is simplified to $\Phi = 2\mu S_{ij}S_{ij}$ because $S_{ii} = \partial v_i/\partial x_i = 0$. If we furthermore assume that the heat conductivity coefficient is constant and that the fluid is a gas or a common liquid (i.e. not an lubricant oil) so that the viscous dissipation is negligible (i.e. $\Phi = 0$), we get

$$\frac{dT}{dt} = \alpha \frac{\partial^2 T}{\partial x_i \partial x_i} \quad (2.18)$$

where $\alpha = k/(\rho c_p)$ is the *thermal diffusivity*. The Prandtl number is defined as

$$Pr = \frac{\nu}{\alpha} \quad (2.19)$$

**thermal
diffusivity**

where $\nu = \mu/\rho$ is the kinematic viscosity. The physical meaning of the Prandtl number is the ratio of how well the fluid diffuses momentum to how well it diffuses internal energy (i.e. temperature).

The dissipation term, Φ , is neglected in Eq. 2.18 when one of two assumptions are valid:

1. The fluid is a gas with low velocity (lower than 1/3 of the speed of sound); this assumption was made when we assumed that the fluid is incompressible
2. The fluid is a common liquid (i.e. not an lubricant oil). In lubricant oils the viscous heating (i.e. the dissipation, Φ) is large. One example is the oil flow in a gearbox in a car where the temperature usually is more than 100°C higher when the car is running compared to when it is idle.

Exercise 15 Write out and simplify the dissipation term, Φ , in Eq. 2.15. The first term is positive and the second term is negative; are you sure that $\Phi > 0$?

²High-speed flows relevant for aeronautics will be treated in detail in the course “TME085 Compressible flow” in the MSc programme.

2.3 Transformation of energy

Now we will derive the equation for the kinetic energy, $k = v_i v_i / 2$. Multiply Eq. 1.7 with v_i

$$\rho v_i \frac{dv_i}{dt} - v_i \frac{\partial \sigma_{ji}}{\partial x_j} - v_i \rho f_i = 0 \quad (2.20)$$

Using the product rule backwards (Trick 2, see Eq. 8.4), the first term on the left side can be re-written

$$\rho v_i \frac{dv_i}{dt} = \frac{1}{2} \rho \frac{d(v_i v_i)}{dt} = \rho \frac{dk}{dt} \quad (2.21)$$

($v_i v_i / 2 = k$) so that

$$\rho \frac{dk}{dt} = v_i \frac{\partial \sigma_{ji}}{\partial x_j} + \rho v_i f_i \quad (2.22)$$

Re-write the stress-velocity term so that (Trick 1, see Eq. 8.2)

$$\rho \frac{dk}{dt} = \frac{\partial v_i \sigma_{ji}}{\partial x_j} - \sigma_{ji} \frac{\partial v_i}{\partial x_j} + \rho v_i f_i \quad (2.23)$$

This is the *transport equation for kinetic energy*, k . Adding Eq. 2.23 to Eq. 2.13 gives

$$\rho \frac{d(u + k)}{dt} = \frac{\partial \sigma_{ji} v_i}{\partial x_j} - \frac{\partial q_i}{\partial x_i} + \rho v_i f_i \quad (2.24)$$

This is an equation for the sum of internal and kinetic energy, $u + k$. This is the *transport equation for total energy*, $u + k$.

Let us take a closer look at Eqs. 2.13, 2.23 and 2.24. First we separate the term $\sigma_{ji} \partial v_i / \partial x_j$ in Eqs. 2.13 and 2.23 into work related to the pressure and viscous stresses respectively (see Eq. 1.9), i.e.

$$\sigma_{ji} \frac{\partial v_i}{\partial x_j} = \underbrace{-P \frac{\partial v_i}{\partial x_i}}_{\mathbf{a}} + \underbrace{\tau_{ji} \frac{\partial v_i}{\partial x_j}}_{\mathbf{b}=\Phi} \quad (2.25)$$

The following things should be noted.

- The physical meaning of the **a**-term in Eq. 2.25 – which includes the pressure, P – is heating/cooling by compression/expansion. This is a reversible process, i.e. no loss of energy but only transformation of energy.
- The physical meaning of the **b**-term in Eq. 2.25 – which includes the viscous stress tensor, τ_{ij} – is a dissipation, which means that kinetic energy is transformed to thermal energy. It is denoted Φ , see Eq. 2.15, and is called viscous dissipation. It is always positive and represents irreversible heating.
- The dissipation, Φ , appears as a sink term in the equation for the kinetic energy, k (Eq. 2.23) and it appears as a source term in the equation for the internal energy, u (Eq. 2.13). The transformation of kinetic energy into internal energy takes place through this source term. In incompressible flow for which the viscous term in Navier-Stokes can be simplified (see Eq. 2.9), the viscous term reads

$$\tau_{ji} \frac{\partial v_i}{\partial x_j} = \mu \frac{\partial v_i}{\partial x_j} \frac{\partial v_i}{\partial x_j} \quad (2.26)$$

which is the viscous dissipation. When arriving at this expression we use the fact that the second term in τ_{ij} in the Navier-Stokes (Eq. 2.9) is zero, i.e. we use $\tau_{ij} = \mu \frac{\partial v_i}{\partial x_j}$ (see 2.10). The viscous dissipation is very important in turbulent flow, cf. Eqs. 8.14 and 8.38.

- Φ does not appear in the equation for the total energy $u + k$ (Eq. 2.24); this makes sense since Φ represents a energy transfer between u and k and does not affect their sum, $u + k$.

Dissipation is very important in turbulence where transfer of energy takes place at several levels. First energy is transferred from the mean flow to the turbulent fluctuations. The physical process is called production of turbulent kinetic energy. Then we have transformation of kinetic energy from turbulence kinetic energy to thermal energy; this is turbulence dissipation (or heating). At the same time we have the usual viscous dissipation from the mean flow to thermal energy, but this is much smaller than that from the turbulence kinetic energy. For more detail, see Section 5.

2.4 Left side of the transport equations

So far, the left sides in transport equations have been formulated using the material derivative, d/dt . Let ψ denote a transported quantity (i.e. $\psi = v_i, u, T \dots$); the left side of the equation for momentum, thermal energy, total energy, temperature etc reads

$$\rho \frac{d\psi}{dt} = \rho \frac{\partial \psi}{\partial t} + \rho v_j \frac{\partial \psi}{\partial x_j} \quad \text{non-conservative} \quad (2.27)$$

This is often called the *non-conservative* Using the continuity equation, Eq. 2.2, it can be re-written as

$$\begin{aligned} \rho \frac{d\psi}{dt} &= \rho \frac{\partial \psi}{\partial t} + \rho v_j \frac{\partial \psi}{\partial x_j} + \underbrace{\psi \left(\frac{d\rho}{dt} + \rho \frac{\partial v_j}{\partial x_j} \right)}_{=0} = \\ &\underbrace{\rho \frac{\partial \psi}{\partial t}} + \rho v_j \frac{\partial \psi}{\partial x_j} + \underbrace{\psi \left(\frac{\partial \rho}{\partial t} + v_j \frac{\partial \rho}{\partial x_j} + \rho \frac{\partial v_j}{\partial x_j} \right)} \end{aligned} \quad (2.28)$$

The two underlined terms will form a time derivative term, and the other three terms can be collected into a convective term, i.e.

$$\rho \frac{d\psi}{dt} = \frac{\partial \rho \psi}{\partial t} + \frac{\partial \rho v_j \psi}{\partial x_j} \quad \text{conservative} \quad (2.29)$$

Thus, the left side of the temperature equation and the Navier-Stokes, for example, can be written in three different ways (by use of the chain-rule and the continuity equation)

$$\begin{aligned} \rho \frac{dv_i}{dt} &= \rho \frac{\partial v_i}{\partial t} + \rho v_j \frac{\partial v_i}{\partial x_j} = \frac{\partial \rho v_i}{\partial t} + \frac{\partial \rho v_j v_i}{\partial x_j} \\ \rho \frac{dT}{dt} &= \rho \frac{\partial T}{\partial t} + \rho v_j \frac{\partial T}{\partial x_j} = \frac{\partial \rho T}{\partial t} + \frac{\partial \rho v_j T}{\partial x_j} \end{aligned} \quad (2.30)$$

The continuity equation can also be written in three ways (by use of the chain-rule)

$$\frac{d\rho}{dt} + \rho \frac{\partial v_i}{\partial x_i} = \frac{\partial \rho}{\partial t} + v_i \frac{\partial \rho}{\partial x_i} + \rho \frac{\partial v_i}{\partial x_i} = \frac{\partial \rho}{\partial t} + \frac{\partial \rho v_i}{\partial x_i} \quad (2.31)$$

The forms on the right sides of Eqs. 2.30 and 2.31 are called the *conservative* form. When solving transport equations (such as the Navier-Stokes) numerically using finite volume methods, the left sides in the transport equation are always written as the expressions on the right side of Eqs. 2.30 and 2.31; in this way Gauss law can be used to transform the equations from a volume integral to a surface integral and thus ensuring that the transported quantities are *conserved*. The results may be inaccurate due to too coarse a numerical grid, but no mass, momentum, energy etc is lost (provided a transport equation for the quantity is solved): “what comes in goes out”.

2.5 Material particle vs. control volume (Reynolds Transport Theorem)

See also lecture notes of Toll & Ekh [4] and [3], Chapt. 5.2.

In Part I [4] we initially derived all balance equations (mass, momentum and energy) for a collection of *material particles*. The conservation of mass, $d/dt \int \rho dV = 0$, Newton’s second law, $d/dt \int \rho v_i = F_i$ etc were derived for a collection of particles in the volume V_{part} , where V_{part} is a volume that includes the same fluid particles all the time. This means that the volume, V_{part} , must be moving and it may expand or contract (if the density is non-constant), otherwise particles would move across its boundaries. The equations we have looked at so far (the continuity equation 2.3, the Navier-Stokes equation 2.9, the energy equations 2.15 and 2.23) are all given for a fixed control volume. How come? The answer is the Reynolds transport theorem, which converts the equations from being valid for a moving, deformable volume with a collection of particles, V_{part} , to being valid for a fixed volume, V . The Reynolds transport theorem reads (first line)

$$\begin{aligned} \frac{d}{dt} \int_{V_{part}} \Phi dV &= \int_V \left(\frac{d\Phi}{dt} + \Phi \frac{\partial v_i}{\partial x_i} \right) dV \\ &= \int_V \left(\frac{\partial \Phi}{\partial t} + v_i \frac{\partial \Phi}{\partial x_i} + \Phi \frac{\partial v_i}{\partial x_i} \right) dV = \int_V \left(\frac{\partial \Phi}{\partial t} + \frac{\partial v_i \Phi}{\partial x_i} \right) dV \\ &= \int_V \frac{\partial \Phi}{\partial t} dV + \int_S v_i n_i \Phi dS \end{aligned} \quad (2.32)$$

where V denotes a fixed non-deformable volume in space. The divergence of the velocity vector, $\partial v_i / \partial x_i$, on the first line represents the increase or decrease of V_{part} during dt . The divergence theorem was used to obtain the last line and S denotes the bounding surface of volume V . The last term on the last line represents the net flow of Φ across the fixed non-deformable volume, V . Φ in the equation above can be, e.g., ρ (mass), ρv_i (momentum) or ρu (energy). This equation applies to *any* volume at *every* instant and the restriction to a collection of a material particles is no longer necessary. Hence, in fluid mechanics the transport equations (Eqs. 2.2, 2.5, 2.13, ...) are valid both for a material collection of particles as well as for a *volume*; the latter is usually fixed (this is not necessary).

The left hand of the momentum equation, i.e. $\phi = \rho v_i$, is given on the first line in Eq. 2.30. However, if we want to write it as dv_i/dt (as in [4]) we start from the right

side of line 1 in Eq. 2.32, i.e.

$$\begin{aligned}
 \frac{d}{dt}(\rho v_i) + \rho v_i \frac{\partial v_k}{\partial x_k} &= v_i \frac{d\rho}{dt} + \rho \frac{dv_i}{dt} + \rho v_i \frac{\partial v_k}{\partial x_k} \\
 &= v_i \frac{\partial \rho}{\partial t} + \underbrace{v_i v_k \frac{\partial \rho}{\partial x_k}} + \rho \frac{dv_i}{dt} + \underbrace{\rho v_i \frac{\partial v_k}{\partial x_k}} \\
 &= \rho \frac{dv_i}{dt}
 \end{aligned}$$

because the underlined terms on line 2 are the continuity equation multiplied with v_i .

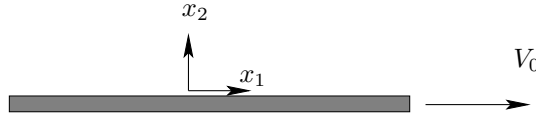


Figure 3.1: The plate moves to the right with speed V_0 for $t > 0$.

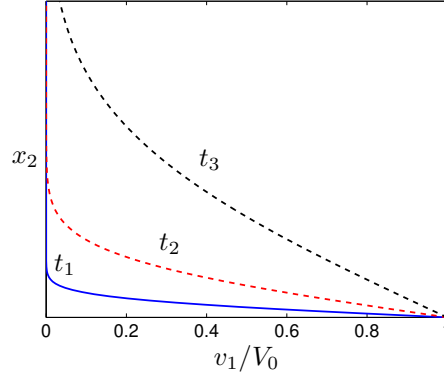


Figure 3.2: The v_1 velocity at three different times. $t_3 > t_2 > t_1$.

3 Solutions to the Navier-Stokes equation: three examples

3.1 The Rayleigh problem

IMAGINE the sudden incompressible motion of an infinitely long flat plate. For time greater than zero the plate is moving with the speed V_0 , see Fig. 3.1. Because the plate is infinitely long, there is no x_1 dependency. Hence the flow depends only on x_2 and t , i.e. $v_1 = v_1(x_2, t)$ and $p = p(x_2, t)$. Furthermore, $\partial v_1 / \partial x_1 = \partial v_3 / \partial x_3 = 0$ so that the continuity equation gives $\partial v_2 / \partial x_2 = 0$. At the lower boundary ($x_2 = 0$) and at the upper boundary ($x_2 \rightarrow \infty$) the velocity component $v_2 = 0$, which means that $v_2 = 0$ in the entire domain. So, Eq. 2.9 gives (no body forces, i.e. $f_1 = 0$) for the v_1 velocity component

$$\frac{\partial v_1}{\partial t} = \nu \frac{\partial^2 v_1}{\partial x_2^2} \quad (3.1)$$

where we have divided the equation by density so that $\nu = \mu / \rho$. The boundary conditions for Eq. 3.1 are

$$v_1(x_2, t = 0) = 0, \quad v_1(x_2 = 0, t) = V_0, \quad v_1(x_2 \rightarrow \infty, t) = 0 \quad (3.2)$$

The solution to Eq. 3.1 is shown in Fig. 3.2. For increasing time ($t_3 > t_2 > t_1$), the moving plate affects the fluid further and further away from the plate.

It turns out that the solution to Eq. 3.1 is a *similarity solution*; this means that the number of independent variables is reduced by one, in this case from two (x_2 and t) to one (η). The similarity variable, η , is related to x_2 and t as

**similarity
solution**

$$\eta = \frac{x_2}{2\sqrt{\nu t}} \quad (3.3)$$

If the solution of Eq. 3.1 depends only on η , it means that the solution for a given fluid will be the same (“similar”) for many (infinite) values of x_2 and t as long as the ratio $x_2/\sqrt{\nu t}$ is constant. Now we need to transform the derivatives in Eq. 3.1 from $\partial/\partial t$ and $\partial/\partial x_2$ to $d/d\eta$ so that it becomes a function of η only. We get

$$\begin{aligned}\frac{\partial v_1}{\partial t} &= \frac{dv_1}{d\eta} \frac{\partial \eta}{\partial t} = -\frac{x_2 t^{-3/2}}{4\sqrt{\nu}} \frac{dv_1}{d\eta} = -\frac{1}{2} \frac{\eta}{t} \frac{dv_1}{d\eta} \\ \frac{\partial v_1}{\partial x_2} &= \frac{dv_1}{d\eta} \frac{\partial \eta}{\partial x_2} = \frac{1}{2\sqrt{\nu t}} \frac{dv_1}{d\eta} \\ \frac{\partial^2 v_1}{\partial x_2^2} &= \frac{\partial}{\partial x_2} \left(\frac{\partial v_1}{\partial x_2} \right) = \frac{\partial}{\partial x_2} \left(\frac{1}{2\sqrt{\nu t}} \frac{dv_1}{d\eta} \right) = \frac{1}{2\sqrt{\nu t}} \frac{\partial}{\partial x_2} \left(\frac{dv_1}{d\eta} \right) = \frac{1}{4\nu t} \frac{d^2 v_1}{d\eta^2}\end{aligned}\quad (3.4)$$

We introduce a non-dimensional velocity

$$f = \frac{v_1}{V_0} \quad (3.5)$$

Inserting Eqs. 3.4 and 3.5 in Eq. 3.1 gives

$$\frac{d^2 f}{d\eta^2} + 2\eta \frac{df}{d\eta} = 0 \quad (3.6)$$

We have now successfully transformed Eq. 3.1 and reduced the number of independent variables from two to one. Now let us find out if the boundary conditions, Eq. 3.2, also can be transformed in a physically meaningful way; we get

$$\begin{aligned}v_1(x_2, t = 0) = 0 &\Rightarrow f(\eta \rightarrow \infty) = 0 \\ v_1(x_2 = 0, t) = V_0 &\Rightarrow f(\eta = 0) = 1 \\ v_1(x_2 \rightarrow \infty, t) = 0 &\Rightarrow f(\eta \rightarrow \infty) = 0\end{aligned}\quad (3.7)$$

Since we managed to transform both the equation (Eq. 3.1) and the boundary conditions (Eq. 3.7) we conclude that the transformation is suitable.

Now let us solve Eq. 3.6. Integration once gives

$$\frac{df}{d\eta} = C_1 \exp(-\eta^2) \quad (3.8)$$

Integration a second time gives

$$f = C_1 \int_0^\eta \exp(-\eta'^2) d\eta' + C_2 \quad (3.9)$$

The integral above is the error function

$$\text{erf}(\eta) \equiv \frac{2}{\sqrt{\pi}} \int_0^\eta \exp(-\eta'^2) d\eta' \quad (3.10)$$

At the limits, the error function takes the values 0 and 1, i.e. $\text{erf}(0) = 0$ and $\text{erf}(\eta \rightarrow \infty) = 1$. Taking into account the boundary conditions, Eq. 3.7, the final solution to Eq. 3.9 is (with $C_2 = 1$ and $C_1 = -2/\sqrt{\pi}$)

$$f(\eta) = 1 - \text{erf}(\eta) \quad (3.11)$$

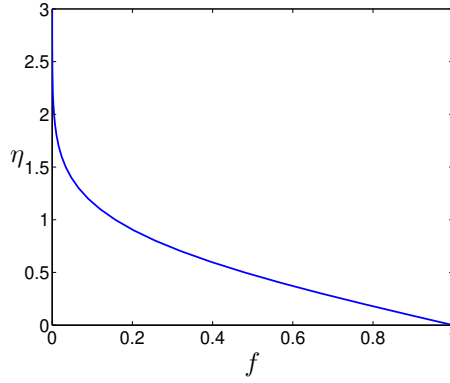


Figure 3.3: The velocity, $f = v_1/V_0$, given by Eq. 3.11.

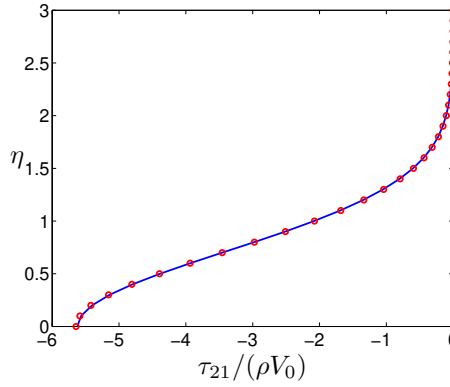


Figure 3.4: The shear stress for water ($\nu = 10^{-6}$) obtained from Eq. 3.12 at time $t = 100\,000$.

The solution is presented in Fig. 3.3. Compare this figure with Fig. 3.2 at p. 38; all graphs in that figure collapse into one graph in Fig. 3.3. To compute the velocity, v_1 , we pick a time t and insert x_2 and t in Eq. 3.3. Then f is obtained from Eq. 3.11 and the velocity, v_1 , is computed from Eq. 3.5. This is how the graphs in Fig. 3.2 were obtained.

From the velocity profile we can get the shear stress as

$$\tau_{21} = \mu \frac{\partial v_1}{\partial x_2} = \frac{\mu V_0}{2\sqrt{\nu t}} \frac{df}{d\eta} = -\frac{\mu V_0}{\sqrt{\pi \nu t}} \exp(-\eta^2) \quad (3.12)$$

where we used $\nu = \mu/\rho$. Figure 3.4 presents the shear stress, τ_{21} . The solid line is obtained from Eq. 3.12 and circles are obtained by evaluating the derivative, $df/d\eta$, numerically using central differences $(f_{j+1} - f_{j-1})/(\eta_{j+1} - \eta_{j-1})$. As can be seen from Fig. 3.4, the magnitude of the shear stress increases for decreasing η and it is largest at the wall, $\tau_w = -\rho V_0/\sqrt{\pi t}$

The vorticity, ω_3 , across the boundary layer is computed from its definition (Eq. 1.36)

$$\omega_3 = -\frac{\partial v_1}{\partial x_2} = -\frac{V_0}{2\sqrt{\nu t}} \frac{df}{d\eta} = \frac{V_0}{\sqrt{\pi \nu t}} \exp(-\eta^2) \quad (3.13)$$

From Fig. 3.2 at p. 38 it is seen that for large times, the moving plate is felt further and further out in the flow, i.e. the thickness of the boundary layer, δ , increases. Often

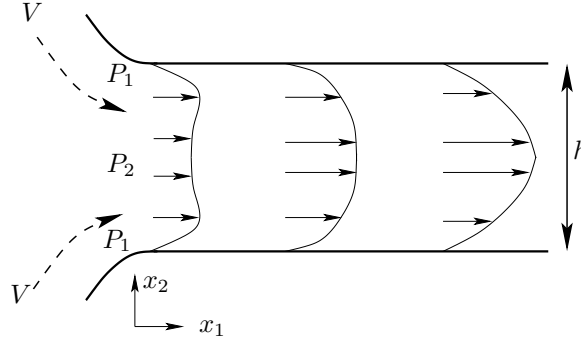


Figure 3.5: Flow in a horizontal channel. The inlet part of the channel is shown.

the boundary layer thickness is defined by the position where the local velocity, $v_1(x_2)$, reaches 99% of the freestream velocity. In our case, this corresponds to the point where $v_1 = 0.01V_0$. Find the point $f = v_1/V_0 = 0.01$ in Fig. 3.3; at this point $\eta \simeq 1.8$ (we can also use Eq. 3.11). Inserting $x_2 = \delta$ in Eq. 3.3 gives

$$\eta = 1.8 = \frac{\delta}{2\sqrt{\nu t}} \Rightarrow \delta = 3.6\sqrt{\nu t} \quad (3.14)$$

It can be seen that the boundary layer thickness increases with $t^{1/2}$. Equation 3.14 can also be used to estimate the *diffusion length*. After, say, 10 minutes the diffusion length for air and water, respectively, are

**diffusion
length**

$$\begin{aligned} \delta_{air} &= 10.8cm \\ \delta_{water} &= 2.8cm \end{aligned} \quad (3.15)$$

The diffusion length can also be used to estimate the thickness of a developing boundary layer, see Section 4.3.1.

Exercise 16 Consider the graphs in Fig. 3.3. Create this graph with Python/Matlab/Octave.

Exercise 17 Consider the graphs in Fig. 3.2. Note that no scale is used on the x_2 axis and that no numbers are given for t_1 , t_2 and t_3 . Create this graph with Python/Matlab/Octave for both air and engine oil. Choose suitable values on t_1 , t_2 and t_3 .

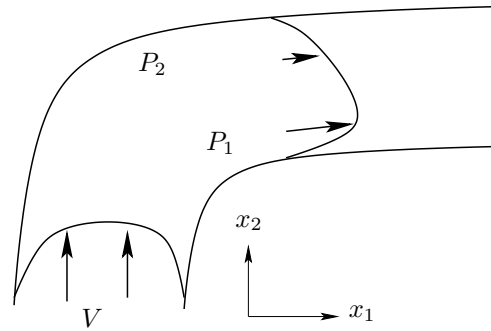
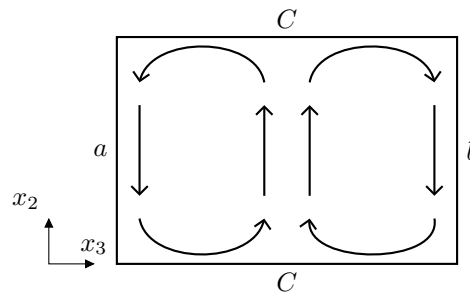
Exercise 18 Repeat the exercise above for the shear stress, τ_{21} , see Fig. 3.4.

3.2 Flow between two plates

Consider steady, incompressible flow in a two-dimensional channel, see Fig. 3.5, with constant physical properties (i.e. $\mu = \text{const}$).

3.2.1 Curved plates

Provided that the walls at the inlet are well curved, the velocity near the walls is larger than in the center, see Fig. 3.5. The reason is that the flow (with velocity V) following the curved wall must change its direction. The physical agent which accomplish this is the pressure gradient which forces the flow to follow the wall as closely as possible (if the wall is not sufficiently curved a separation will take place). Hence the pressure

**Figure 3.6:** Flow in a channel bend.**Figure 3.7:** Secondary flow in a duct bend.

in the center of the channel, P_2 , is higher than the pressure near the wall, P_1 . It is thus easier (i.e. less opposing pressure) for the fluid to enter the channel near the walls than in the center. This explains the high velocity near the walls.

The same phenomenon occurs in a channel bend, see Fig. 3.6. The flow V approaches the bend and the flow feels that it is approaching a bend through an increased pressure. The pressure near the outer wall, P_2 , must be higher than that near the inner wall, P_1 , in order to force the flow to turn. Hence, it is easier for the flow to sneak along the inner wall where the opposing pressure is smaller than near the outer wall: the result is a higher velocity near the inner wall than near the outer wall. In a three-dimensional duct or in a pipe, the pressure difference $P_2 - P_1$ creates secondary flow downstream the bend (i.e. a swirling motion in the $x_2 - x_3$ plane). If you sit on a fluid particle through the bend you're exposed to two forces:

- a centrifugal forces which tries to push you towards the outer wall
- and an opposing pressure force $P_2 - P_1$ per unit area

The pressure force is constant along the x_3 direction but the centrifugal is small along the walls a and b (because of the boundary layers along these walls) and it is large in the center $C - C$. Hence, the secondary flow is in the center ($C - C$) moving towards the outer wall..

3.2.2 Flat plates

The flow in the inlet section (Fig. 3.5) is two dimensional. Near the inlet the velocity is largest near the wall and further downstream the velocity is retarded near the walls due

to the large viscous shear stresses there. The flow is accelerated in the center because the integrated mass flow (from $x_2 = 0$ to h) at each x_1 must be constant because of continuity. The acceleration and retardation of the flow in the inlet region is “paid for” by a pressure loss which is rather high in the inlet region; if a separation occurs because of sharp corners at the inlet, the pressure loss will be even higher. For large x_1 the flow will be fully developed; the region until this occurs is called the *entrance region*, and the entrance length can, for moderately disturbed inflow, be estimated as [6]

$$\frac{x_{1,e}}{D_h} = 0.016 Re_{D_h} \equiv 0.016 \frac{VD_h}{\nu} \quad (3.16)$$

where V denotes the bulk (i.e. the mean) velocity, and $D_h = 4A/S_p$ where D_h , A and S_p denote the hydraulic diameter, the cross-sectional area and the perimeter, respectively. For flow between two plates we get $D_h = 2h$.

Let us find the governing equations for the fully developed flow region; in this region the flow does not change with respect to the streamwise coordinate, x_1 (i.e. $\partial v_1/\partial x_1 = \partial v_2/\partial x_1 = 0$). Since the flow is two-dimensional, it does not depend on the third coordinate direction, x_3 (i.e. $\partial/\partial x_3$), and the velocity in this direction is zero, i.e. $v_3 = 0$. Taking these restrictions into account the continuity equation can be simplified as (see Eq. 2.3)

$$\frac{\partial v_2}{\partial x_2} = 0 \quad (3.17)$$

Integration gives $v_2 = C_1$ and since $v_2 = 0$ at the walls, it means that

$$v_2 = 0 \quad (3.18)$$

across the entire channel (recall that we are dealing with the part of the channel where the flow is fully developed; in the inlet section $v_2 \neq 0$, see Fig. 3.5).

Now let us turn our attention to the momentum equation for v_2 . This is the vertical direction (x_2 is positive upwards, see Fig. 3.5). The gravity acts in the negative x_2 direction, i.e. $f_i = (0, -g, 0)$. The momentum equation can be written (see Eq. 2.9 at p. 32)

$$\rho \frac{dv_2}{dt} \equiv \rho v_1 \frac{\partial v_2}{\partial x_1} + \rho v_2 \frac{\partial v_2}{\partial x_2} = -\frac{\partial P}{\partial x_2} + \mu \frac{\partial^2 v_2}{\partial x_2^2} - \rho g \quad (3.19)$$

Since $v_2 = 0$ we get

$$\frac{\partial P}{\partial x_2} = -\rho g \quad (3.20)$$

Integration gives

$$P = -\rho g x_2 + C_1(x_1) \quad (3.21)$$

where the integration “constant” C_1 may be a function of x_1 but not of x_2 . If we denote the pressure at the lower wall (i.e. at $x_2 = 0$) as p we get

$$P = -\rho g x_2 + p(x_1) \quad (3.22)$$

Hence the pressure, P , decreases with vertical height. This agrees with our experience that the pressure decreases at high altitudes in the atmosphere and increases the deeper we dive into the sea. Usually the *hydrodynamic pressure*, p , is used in incompressible flow. This pressure is zero when the flow is *static*, i.e. when the velocity field is zero. However, when you want the *physical* pressure, the $\rho g x_2$ as well as the surrounding atmospheric pressure must be added.

**hydrodynamic
pressure**

We can now formulate the momentum equation in the streamwise direction

$$\rho \frac{dv_1}{dt} \equiv \rho v_1 \frac{\partial v_1}{\partial x_1} + \rho v_2 \frac{\partial v_1}{\partial x_2} = -\frac{dp}{dx_1} + \mu \frac{\partial^2 v_1}{\partial x_2^2} \quad (3.23)$$

where P was replaced by p using Eq. 3.22. Since $v_2 = \partial v_1 / \partial x_1 = 0$ the left side is zero so

$$\mu \frac{\partial^2 v_1}{\partial x_2^2} = \frac{dp}{dx_1} \quad (3.24)$$

Since the left side is a function of x_2 and the right side is a function of x_1 , we conclude that they both are equal to a constant (i.e. Eq. 3.24 is independent of x_1 and x_2). The velocity, v_1 , is zero at the walls, i.e

$$v_1(0) = v_1(h) = 0 \quad (3.25)$$

where h denotes the height of the channel, see Fig. 3.5. Integrating Eq. 3.24 twice and using Eq. 3.25 gives

$$v_1 = -\frac{h}{2\mu} \frac{dp}{dx_1} x_2 \left(1 - \frac{x_2}{h}\right) \quad (3.26)$$

The minus sign on the right side appears because the pressure is decreasing for increasing x_1 ; the pressure is *driving* the flow. The negative pressure gradient is constant (see Eq. 3.24) and can be written as $-dp/dx_1 = \Delta p/L$.

The velocity takes its maximum in the center, i.e. for $x_2 = h/2$, and reads

$$v_{1,max} = \frac{h}{2\mu} \frac{\Delta p}{L} \frac{h}{2} \left(1 - \frac{1}{2}\right) = \frac{h^2}{8\mu} \frac{\Delta p}{L} \quad (3.27)$$

We often write Eq. 3.26 on the form

$$\frac{v_1}{v_{1,max}} = \frac{4x_2}{h} \left(1 - \frac{x_2}{h}\right) \quad (3.28)$$

The mean velocity (often called the bulk velocity) is obtained by integrating Eq. 3.28 across the channel, i.e.

$$v_{1,mean} = \frac{v_{1,max}}{h} \int_0^h \frac{4x_2}{h} \left(1 - \frac{x_2}{h}\right) dx_2 = \frac{2}{3} v_{1,max} \quad (3.29)$$

The velocity profile is shown in Fig. 3.8

Since we know the velocity profile, we can compute the wall shear stress. Equation 3.26 gives

$$\tau_w = \mu \frac{\partial v_1}{\partial x_2} = -\frac{h}{2} \frac{dp}{dx_1} = \frac{h}{2} \frac{\Delta p}{L} \quad (3.30)$$

Actually, this result could have been obtained by simply taking a force balance of a slice of the flow far downstream.

This flow is analyzed in Appendix C.

3.2.3 Force balance, channel flow

We continue to consider fully developed flow between two parallel plates. To formulate a force balance in the x_1 direction, we start with Eq. 1.7 which reads for $i = 1$

$$\rho \frac{dv_1}{dt} = \frac{\partial \sigma_{j1}}{\partial x_j} \quad (3.31)$$

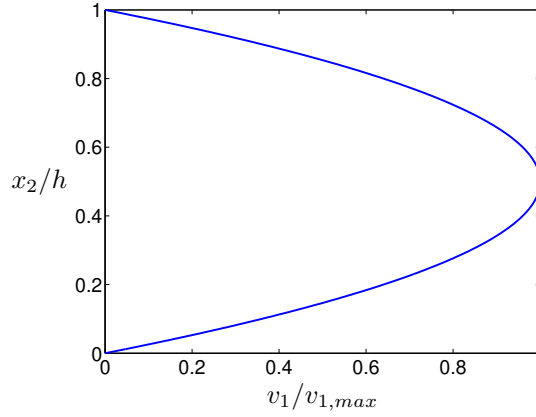


Figure 3.8: The velocity profile in fully developed channel flow, Eq. 3.28.

The left hand side is zero since the flow is fully developed. Forces act on a volume and its bounding surface. Hence we integrate Eq. 3.31 over the volume of a slice (length L), see Fig. 3.9

$$0 = \int_V \frac{\partial \sigma_{j1}}{\partial x_j} dV \quad (3.32)$$

Recall that this is the form on which we originally derived the momentum balance (Newton's second law) in Part I. [4] Now use Gauss divergence theorem

$$0 = \int_V \frac{\partial \sigma_{j1}}{\partial x_j} dV = \int_S \sigma_{j1} n_j dS \quad (3.33)$$

The bounding surface consists in our case of four surfaces (lower, upper, left and right) so that

$$0 = \int_{S_{left}} \sigma_{j1} n_j dS + \int_{S_{right}} \sigma_{j1} n_j dS + \int_{S_{lower}} \sigma_{j1} n_j dS + \int_{S_{upper}} \sigma_{j1} n_j dS \quad (3.34)$$

The normal vector on the lower, upper, left and right are $n_{i,lower} = (0, -1, 0)$, $n_{i,upper} = (0, 1, 0)$, $n_{i,left} = (-1, 0, 0)$, $n_{i,right} = (1, 0, 0)$. Inserting the normal vectors and using Eq. 1.9 give

$$0 = - \int_{S_{left}} (-p + \tau_{11}) dS + \int_{S_{right}} (-p + \tau_{11}) dS - \int_{S_{lower}} \tau_{21} dS + \int_{S_{upper}} \tau_{21} dS \quad (3.35)$$

$\tau_{11} = 0$ because $\partial v_1 / \partial x_1 = 0$ (fully developed flow). The shear stress at the upper and lower surfaces, τ_{21} , have opposite sign because $\mu(\partial v_1 / \partial x_2)_{lower} = -\mu(\partial v_1 / \partial x_2)_{upper}$. Using this and Eq. 3.22 give ($p = p(x_1)$ and τ_w is constant and can thus be taken out in front of the integration)

$$0 = p_1 W h - p_2 W h - 2\tau_w L W \quad (3.36)$$

where $\tau_w = \mu(\partial v_1 / \partial x_2)_{lower}$ and W is the width (in x_3 direction) of the two plates (for convenience we set $W = 1$). With $\Delta p = p_1 - p_2$ we get Eq. 3.30.

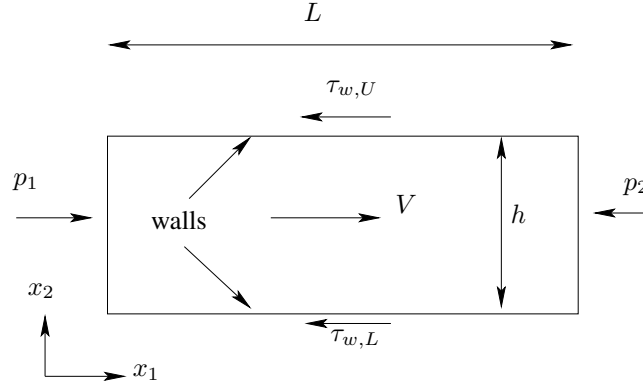


Figure 3.9: Force balance of the flow between two plates.

3.2.4 Balance equation for the kinetic energy

In this subsection we will use the equation for kinetic energy, Eq. 2.23. Let us integrate this equation in the same way as we did for the force balance. The left side of Eq. 2.23 is zero because we assume that the flow is fully developed; using Eq. 1.9 gives

$$\begin{aligned}
 0 &= \frac{\partial v_i \sigma_{ji}}{\partial x_j} - \sigma_{ji} \frac{\partial v_i}{\partial x_j} + \underbrace{\rho v_i f_i}_{=0} \\
 &= -\frac{\partial v_j p}{\partial x_j} + \frac{\partial v_i \tau_{ji}}{\partial x_j} + p \delta_{ij} \frac{\partial v_i}{\partial x_j} - \underbrace{\tau_{ji} \frac{\partial v_i}{\partial x_j}}_{\Phi}
 \end{aligned} \tag{3.37}$$

On the first line $v_i f_i = v_1 f_1 + v_2 f_2 = 0$ because $v_2 = f_1 = 0$. The third term on the second line $p \delta_{ij} \partial v_i / \partial x_j = p \partial v_i / \partial x_i = 0$ because of continuity. The last term corresponds to the viscous dissipation term, Φ (i.e. loss due to friction), see Eq. 2.25 (term **b**). Now we integrate the equation over a volume

$$0 = \int_V \left(-\frac{\partial p v_j}{\partial x_j} + \frac{\partial \tau_{ji} v_i}{\partial x_j} - \Phi \right) dV \tag{3.38}$$

Gauss divergence theorem on the two first terms gives

$$0 = \int_S (-p v_j + \tau_{ji} v_i) n_j dS - \int_V \Phi dV \tag{3.39}$$

where S is the surface bounding the volume. The unit normal vector is denoted by n_j which points *out* from the volume. For example, on the right surface in Fig. 3.9 it is $n_j = (1, 0, 0)$ and on the lower surface it is $n_j = (0, -1, 0)$. Now we apply Eq. 3.39 to the fluid enclosed by the flat plates in Fig. 3.9. The second term is zero on all four surfaces and the first term is zero on the lower and upper surfaces (see Exercises below). We replace the pressure P with p using Eq. 3.22 so that

$$\begin{aligned}
 \int_{S_{left} \& S_{right}} (-p v_1 + \rho g x_2 v_1) n_1 dS &= -(p_2 - p_1) \int_{S_{left} \& S_{right}} v_1 n_1 dS \\
 &= \Delta p v_{1,mean} W h
 \end{aligned} \tag{3.40}$$

because $\rho g x_2 n_1 v_1$ on the left and right surfaces cancels; p can be taken out of the integral as it does not depend on x_2 . Finally we get

$$\Delta p = \frac{1}{Whv_{1,mean}} \int_V \Phi dV \quad (3.41)$$

3.3 Two-dimensional boundary layer flow over flat plate

The equations for steady, two-dimensional, incompressible boundary layer flow reads (x_1 and x_2 denote streamwise and wall-normal coordinates, respectively)

$$\begin{aligned} v_1 \frac{\partial v_1}{\partial x_1} + v_2 \frac{\partial v_1}{\partial x_2} &= \nu \frac{\partial^2 v_1}{\partial x_2^2} \\ \frac{\partial p}{\partial x_2} &= 0 \\ \frac{\partial v_1}{\partial x_1} + \frac{\partial v_2}{\partial x_2} &= 0 \end{aligned} \quad (3.42)$$

where the pressure gradient is omitted in the v_1 momentum equation because $\partial p / \partial x_1 = 0$ along a flat plate in infinite surroundings. The boundary conditions are

$$\begin{aligned} x_2 = 0 : v_1 = v_2 = 0 & \quad (\text{at the wall}) \\ x_2 \rightarrow \infty : v_1 \rightarrow V_{1,\infty}, v_2 = 0 & \quad (\text{far from the wall}) \end{aligned} \quad (3.43)$$

Let's introduce the *stream function* Ψ , which is useful when re-writing the two-dimensional Navier-Stokes equations. It is defined as

stream-function

$$v_1 = \frac{\partial \Psi}{\partial x_2}, \quad v_2 = -\frac{\partial \Psi}{\partial x_1} \quad (3.44)$$

With the velocity field expressed in Ψ , the continuity equations is automatically satisfied which is easily shown by inserting Eq. 3.44 into the continuity equation

$$\frac{\partial v_1}{\partial x_1} + \frac{\partial v_2}{\partial x_2} = \frac{\partial^2 \Psi}{\partial x_1 \partial x_2} - \frac{\partial^2 \Psi}{\partial x_2 \partial x_1} = 0 \quad (3.45)$$

Inserting Eq. 3.44 into the streamwise momentum equation gives

$$\frac{\partial \Psi}{\partial x_2} \frac{\partial^2 \Psi}{\partial x_1 \partial x_2} - \frac{\partial \Psi}{\partial x_1} \frac{\partial^2 \Psi}{\partial x_2^2} = \nu \frac{\partial^3 \Psi}{\partial x_2^3} \quad (3.46)$$

The boundary conditions for the stream function read

$$\begin{aligned} x_2 = 0 : \Psi = \frac{\partial \Psi}{\partial x_2} &= 0 \quad (\text{at the wall}) \\ x_2 \rightarrow \infty : \frac{\partial \Psi}{\partial x_2} &\rightarrow V_{1,\infty} \quad (\text{far from the wall}) \end{aligned} \quad (3.47)$$

As in Section 3.1 we want to transform the partial differential equation, Eq. 3.46, into an ordinary differential equation. In Section 3.1 we replaced x_1 and t with the new non-dimensional variable η . Now we want to replace x_1 and x_2 with a new dimensionless variable, say ξ . At the same time we define a new dimensionless stream function, $g(\xi)$, as

$$\xi = \left(\frac{V_{1,\infty}}{\nu x_1} \right)^{1/2} x_2, \quad \Psi = (\nu V_{1,\infty} x_1)^{1/2} g \quad (3.48)$$

First we need the derivatives $\partial\xi/\partial x_1$ and $\partial\xi/\partial x_2$

$$\begin{aligned}\frac{\partial\xi}{\partial x_1} &= -\frac{1}{2} \left(\frac{V_{1,\infty}}{\nu x_1} \right)^{1/2} \frac{x_2}{x_1} = -\frac{\xi}{2x_1} \\ \frac{\partial\xi}{\partial x_2} &= \left(\frac{V_{1,\infty}}{\nu x_1} \right)^{1/2} = \frac{\xi}{x_2}\end{aligned}\quad (3.49)$$

Now we express the first derivatives of Ψ in Eq. 3.46 as derivatives of g , i.e. (g' denotes $dg/d\xi$)

$$\begin{aligned}\frac{\partial\Psi}{\partial x_1} &= \frac{\partial}{\partial x_1} \left((\nu V_{1,\infty} x_1)^{1/2} \right) g + (\nu V_{1,\infty} x_1)^{1/2} g' \frac{\partial\xi}{\partial x_1} \\ &= \frac{1}{2} \left(\frac{\nu V_{1,\infty}}{x_1} \right)^{1/2} g - (\nu V_{1,\infty} x_1)^{1/2} g' \frac{\xi}{2x_1} \\ &= \frac{1}{2} \left(\frac{\nu V_{1,\infty}}{x_1} \right)^{1/2} (g - \xi g') \\ \frac{\partial\Psi}{\partial x_2} &= \frac{\partial}{\partial x_2} \left((\nu V_{1,\infty} x_1)^{1/2} \right) g + (\nu V_{1,\infty} x_1)^{1/2} \frac{\partial\xi}{\partial x_2} g' = V_{1,\infty} g'\end{aligned}\quad (3.50)$$

The second and third derivatives of Ψ read

$$\begin{aligned}\frac{\partial^2\Psi}{\partial x_2^2} &= V_{1,\infty} g'' \frac{\partial\xi}{\partial x_2} = V_{1,\infty} \left(\frac{V_{1,\infty}}{\nu x_1} \right)^{1/2} g'' = V_{1,\infty} \frac{\xi}{x_2} g'' \\ \frac{\partial^3\Psi}{\partial x_2^3} &= V_{1,\infty} \left(\frac{V_{1,\infty}}{\nu x_1} \right)^{1/2} g''' \frac{\partial\xi}{\partial x_2} = V_{1,\infty} \frac{V_{1,\infty}}{\nu x_1} g''' = V_{1,\infty} \left(\frac{\xi}{x_2} \right)^2 g''' \\ \frac{\partial^2\Psi}{\partial x_1 \partial x_2} &= V_{1,\infty} g'' \frac{\partial\xi}{\partial x_1} = -\frac{\xi}{2x_1} V_{1,\infty} g''\end{aligned}\quad (3.51)$$

Inserting Eqs. 3.50 and 3.51 into Eq. 3.46 gives

$$\begin{aligned}-V_{1,\infty} g' \frac{\xi}{2x_1} V_{1,\infty} g'' - \left(\frac{1}{2} \left(\frac{\nu V_{1,\infty}}{x_1} \right)^{1/2} (g - \xi g') \right) V_{1,\infty} \left(\frac{V_{1,\infty}}{\nu x_1} \right)^{1/2} g'' \\ = \nu \frac{V_{1,\infty}^2}{\nu x_1} g'''\end{aligned}\quad (3.52)$$

Divide by $V_{1,\infty}^2$ and multiply by x_1 gives

$$-g' \frac{\xi}{2} g'' - \frac{1}{2} (g - \xi g') g'' = g'''\quad (3.53)$$

so that

$$\frac{1}{2} g g'' + g''' = 0\quad (3.54)$$

This equation was derived (and solved numerically!) by Blasius in his PhD thesis 1907 [7, 8]. The numerical solution is given in Table 3.1. The flow is analyzed in Appendix 33.

Exercise 19 For the fully developed flow, compute the vorticity, ω_i , using the exact solution (Eq. 3.28).

ξ	g	g'	g''
0	0.000000000E+00	0.000000000E+00	3.320573362E-01
0.2	6.640999715E-03	6.640779210E-02	3.319838371E-01
0.4	2.655988402E-02	1.327641608E-01	3.314698442E-01
0.6	5.973463750E-02	1.989372524E-01	3.300791276E-01
0.8	1.061082208E-01	2.647091387E-01	3.273892701E-01
1.0	1.655717258E-01	3.297800312E-01	3.230071167E-01
1.2	2.379487173E-01	3.937761044E-01	3.165891911E-01
1.4	3.229815738E-01	4.562617647E-01	3.078653918E-01
1.6	4.203207655E-01	5.167567844E-01	2.966634615E-01
1.8	5.295180377E-01	5.747581439E-01	2.829310173E-01
2.0	6.500243699E-01	6.297657365E-01	2.667515457E-01
2.2	7.811933370E-01	6.813103772E-01	2.483509132E-01
2.4	9.222901256E-01	7.289819351E-01	2.280917607E-01
2.6	1.072505977E+00	7.724550211E-01	2.064546268E-01
2.8	1.230977302E+00	8.115096232E-01	1.840065939E-01
3.0	1.396808231E+00	8.460444437E-01	1.613603195E-01
3.2	1.569094960E+00	8.760814552E-01	1.391280556E-01
3.4	1.746950094E+00	9.017612214E-01	1.178762461E-01
3.6	1.929525170E+00	9.233296659E-01	9.808627878E-02
3.8	2.116029817E+00	9.411179967E-01	8.012591814E-02
4.0	2.305746418E+00	9.555182298E-01	6.423412109E-02
4.2	2.498039663E+00	9.669570738E-01	5.051974749E-02
4.4	2.692360938E+00	9.758708321E-01	3.897261085E-02
4.6	2.888247990E+00	9.826835008E-01	2.948377201E-02
4.8	3.085320655E+00	9.877895262E-01	2.187118635E-02
5.0	3.283273665E+00	9.915419002E-01	1.590679869E-02
5.2	3.481867612E+00	9.942455354E-01	1.134178897E-02
5.4	3.680919063E+00	9.961553040E-01	7.927659815E-03
5.6	3.880290678E+00	9.974777682E-01	5.431957680E-03
5.8	4.079881939E+00	9.983754937E-01	3.648413667E-03
6.0	4.279620923E+00	9.989728724E-01	2.402039844E-03
6.2	4.479457297E+00	9.993625417E-01	1.550170691E-03
6.4	4.679356615E+00	9.996117017E-01	9.806151170E-04
6.6	4.879295811E+00	9.997678702E-01	6.080442648E-04
6.8	5.079259772E+00	9.998638190E-01	3.695625701E-04
7.0	5.279238811E+00	9.999216041E-01	2.201689553E-04
7.2	5.479226847E+00	9.999557173E-01	1.285698072E-04
7.4	5.679220147E+00	9.999754577E-01	7.359298339E-05
7.6	5.879216466E+00	9.999866551E-01	4.129031111E-05
7.8	6.079214481E+00	9.999928812E-01	2.270775140E-05
8.0	6.279213431E+00	9.999962745E-01	1.224092624E-05
8.2	6.479212887E+00	9.999980875E-01	6.467978611E-06
8.4	6.679212609E+00	9.999990369E-01	3.349939753E-06
8.6	6.879212471E+00	9.999995242E-01	1.700667989E-06
8.8	7.079212403E+00	9.999997695E-01	8.462841214E-07

Table 3.1: Blasius numerical solution of laminar flow along a flat plate.

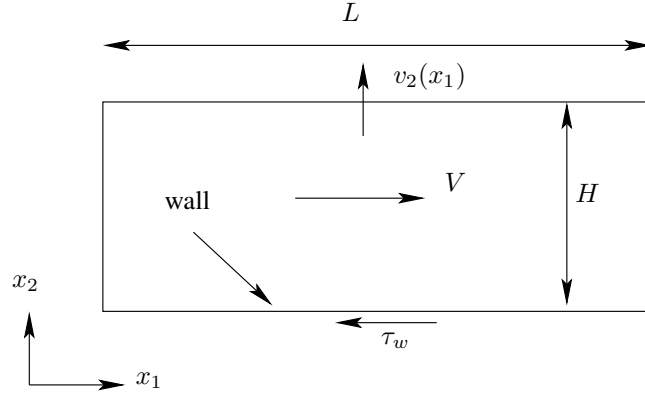


Figure 3.10: Force balance of boundary layer flow along a flat plate.

Exercise 20 Show that the first and second terms in Eq. 3.39 are zero on the upper and the lower surfaces in Fig. 3.9.

Exercise 21 Show that the second term in Eq. 3.39 is zero also on the left and right surfaces in Fig. 3.9 (assume fully developed flow).

Exercise 22 Using the exact solution, compute the dissipation, Φ , for the fully developed flow.

Exercise 23 From the dissipation, compute the pressure drop. Is it the same as that obtained from the force balance (if not, find the error; it should be!).

3.3.1 Momentum balance, boundary layer

Let's make a momentum balance for the boundary layer in the same way as we did for fully-developed channel flow in Section 3.2.3. The left boundary (see Fig. 3.10) is located upstream of the plate, i.e. at $x < 0$, see Fig. 3.3.1. Note that here – contrary to the channel flow – we do not have any pressure gradient. At the upper boundary we also have an outflow because the right boundary includes a boundary layer meaning that the outflow here is smaller than the inflow at the left boundary. Hence, the right side of the momentum equation reads (cf. Eq. 3.34)

$$0 = \int_{S_{lower}} \sigma_{j1} n_j dS = - \int_{S_{lower}} \sigma_{21} = - \int_{S_{lower}} \tau_w dS \quad (3.55)$$

using Eq. 1.9 and $n_j = (0, -1, 0)$. Only the contribution from the lower boundary appears. The reason is that there are no pressure forces on the left and right (or, rather, they cancel each other) and there is no shear stress on the top boundary since $\partial v_1 / \partial x_2 = 0$. The other difference compared to the channel flow in Section 3.2.3 is that the left side of Eq. 3.31 is not zero. It reads

$$\rho \frac{dv_1}{dt} \equiv \frac{\partial v_j v_1}{\partial x_j}. \quad (3.56)$$

Gauss divergence theorem gives

$$\int_V \frac{\partial v_j v_1}{\partial x_j} dV = \int_{S_{left}} v_j v_1 n_j dS + \int_{S_{right}} v_j v_1 n_j dS + \int_{S_{top}} v_j v_1 n_j dS \quad (3.57)$$

where the contribution at the lower boundary is zero since the velocity is zero at the walls. The unit normal vector at the left, right and top boundaries are $(1, 0, 0)$, $(-1, 0, 0)$ and $(0, 1, 0)$, respectively, which gives

$$\int_V \frac{\partial v_j v_1}{\partial x_j} dV = \int_{S_{right}} v_1^2 dS - \int_{S_{left}} v_1^2 dS + \int_{S_{top}} v_1 v_2 dS \quad (3.58)$$

At the left boundary $v_1 = V_\infty$ which gives

$$\int_V \frac{\partial v_j v_1}{\partial x_j} dV = \int_S (v_1^2 - V_{1,\infty}^2) dS + \int_{S_{top}} v_1 v_2 dS \quad (3.59)$$

Combining Eqs. 3.55 and 3.59 we can write (assuming that the extent of the integration domain in the third direction is one)

$$\tau_w = \frac{1}{L} \left[\int_S (V_{1,\infty}^2 - v_1^2) dx_2 + \int_{S_{top}} v_1 v_2 dx_1 \right] \quad (3.60)$$

We find one important difference between fully-developed channel flow and boundary layer flow: the flow in channel flow is driven by a pressure gradient (the pressure decreases) whereas in the boundary layer the “force” to overcome the opposing wall shear stress is achieved by decreasing momentum in the convective term. Making a balance of the mass flow and combining it with Eq. 3.60 the expression for the momentum thickness, 33.2, is derived.

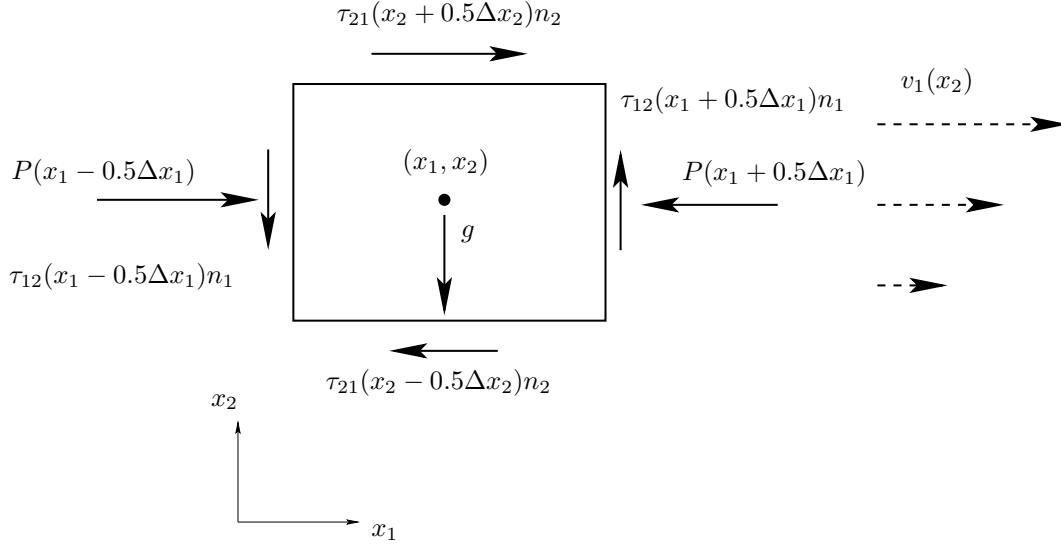


Figure 4.1: Surface forces acting on a fluid particle. The fluid particle is located in the lower half of fully developed channel flow. The v_1 velocity is given by Eq. 3.28 and $v_2 = 0$. Hence $\tau_{11} = \tau_{22} = \partial\tau_{12}/\partial x_1 = 0$ and $-\partial\tau_{21}/\partial x_2 > 0$. The v_1 velocity field is indicated by dashed vectors.

4 Vorticity equation and potential flow

4.1 Vorticity and rotation

VORTICITY, ω_i , was introduced in Eq. 1.12 at p. 22. As shown in Fig. 1.4 at p. 25, vorticity is connected to rotation of a fluid particle. Figure 4.1 shows the surface forces acting on a fluid particle in a shear flow. Looking at Fig. 4.1 it is obvious that only the shear stresses are able to rotate the fluid particle; the pressure and the normal viscous stresses act through the center of the fluid particle and are thus not able to affect rotation of the fluid particle. Note that the v_2 momentum equation (see Eqs. 2.4 and 3.32) requires that the vertical viscous stresses in Fig. 4.1 are in balance. The v_1 momentum equation requires that the horizontal viscous stresses balance the pressure difference. Furthermore, you may notice that $\tau_{12} \neq \tau_{21}$ in Fig. 4.1. The reason is that τ_{21} is drawn at a larger x_2 where the velocity derivative $\partial v_1/\partial x_2$ is larger than at the position where τ_{12} is drawn.

Let us have a look at the momentum equations in order to show that the viscous terms indeed can be formulated with the vorticity vector, ω_i . In incompressible flow the viscous terms read (see Eqs. 2.4, 2.5 and 2.7)

$$\frac{\partial \tau_{ji}}{\partial x_j} = \mu \frac{\partial^2 v_i}{\partial x_j \partial x_j} \quad (4.1)$$

The right side can be re-written using the tensor identity

$$\begin{aligned} \frac{\partial^2 v_i}{\partial x_j \partial x_j} &= \frac{\partial^2 v_j}{\partial x_j \partial x_i} - \left(\frac{\partial^2 v_j}{\partial x_j \partial x_i} - \frac{\partial^2 v_i}{\partial x_j \partial x_j} \right) \\ &= \underbrace{\frac{\partial}{\partial x_i} \left(\frac{\partial v_j}{\partial x_j} \right)}_{=0} - \varepsilon_{inm} \varepsilon_{mjk} \frac{\partial^2 v_k}{\partial x_j \partial x_n} = -\varepsilon_{inm} \varepsilon_{mjk} \frac{\partial^2 v_k}{\partial x_j \partial x_n} \end{aligned} \quad (4.2)$$

where the first on the second line is zero because of continuity. Let's verify that

$$\left(\frac{\partial^2 v_j}{\partial x_j \partial x_i} - \frac{\partial^2 v_i}{\partial x_j \partial x_j} \right) = \varepsilon_{inm} \varepsilon_{mjk} \frac{\partial^2 v_k}{\partial x_j \partial x_n} \quad (4.3)$$

Use the $\varepsilon - \delta$ -identity (see Table B.1 at p. 287)

$$\varepsilon_{inm} \varepsilon_{mjk} \frac{\partial^2 v_k}{\partial x_j \partial x_n} = (\delta_{ij} \delta_{nk} - \delta_{ik} \delta_{nj}) \frac{\partial^2 v_k}{\partial x_j \partial x_n} = \frac{\partial^2 v_k}{\partial x_i \partial x_k} - \frac{\partial^2 v_i}{\partial x_j \partial x_j} \quad (4.4)$$

which shows that Eq. 4.3 is correct. At the right side of Eq. 4.3 we recognize the vorticity, $\omega_m = \varepsilon_{mjk} \partial v_k / \partial x_j$, so that

$$\frac{\partial^2 v_i}{\partial x_j \partial x_j} = -\varepsilon_{inm} \frac{\partial \omega_m}{\partial x_n} \quad (4.5)$$

In vector notation the identity Eq. 4.5 reads

$$\nabla^2 \mathbf{v} = \nabla(\nabla \cdot \mathbf{v}) - \nabla \times \nabla \times \mathbf{v} = -\nabla \times \boldsymbol{\omega} \quad (4.6)$$

Using Eq. 4.5, Eq. 4.1 reads

$$\frac{\partial \tau_{ji}}{\partial x_j} = -\mu \varepsilon_{inm} \frac{\partial \omega_m}{\partial x_n} \quad (4.7)$$

Let's look at Eq. 4.7 for the v_1 equation in two dimensions. Setting $i = 1$ gives

$$\frac{\partial \tau_{j1}}{\partial x_j} = -\mu \varepsilon_{1nm} \frac{\partial \omega_m}{\partial x_n} = -\mu \varepsilon_{123} \frac{\partial \omega_3}{\partial x_2} - \mu \varepsilon_{132} \frac{\partial \omega_2}{\partial x_3} = -\frac{\partial \omega_3}{\partial x_2} + \frac{\partial \omega_2}{\partial x_3} = -\frac{\partial \omega_3}{\partial x_2} \quad (4.8)$$

since $\omega_2 = 0$. Inserting Eq. 1.12 gives

$$\frac{\partial \tau_{j1}}{\partial x_j} = -\frac{\partial}{\partial x_2} \left(\varepsilon_{3jk} \frac{\partial v_k}{\partial x_j} \right) = -\frac{\partial}{\partial x_2} \left(\varepsilon_{321} \frac{\partial v_1}{\partial x_2} + \varepsilon_{312} \frac{\partial v_2}{\partial x_1} \right) = -\frac{\partial}{\partial x_2} \left(-\frac{\partial v_1}{\partial x_2} + \frac{\partial v_2}{\partial x_1} \right)$$

Changing the order of derivatation for the second term gives

$$\frac{\partial \tau_{j1}}{\partial x_j} = \frac{\partial}{\partial x_2} \left(\frac{\partial v_1}{\partial x_2} \right) - \frac{\partial}{\partial x_1} \left(\frac{\partial v_2}{\partial x_2} \right)$$

Using the continuity equation for the last term gives

$$\frac{\partial \tau_{j1}}{\partial x_j} = \frac{\partial}{\partial x_2} \left(\frac{\partial v_1}{\partial x_2} \right) + \frac{\partial}{\partial x_1} \left(\frac{\partial v_1}{\partial x_1} \right)$$

and now we have shown – again – that Eqs. 4.7 and 4.8 are indeed correct.

Thus, there is a one-to-one relation between the viscous term and vorticity: no viscous terms means no vorticity and vice versa. An imbalance in shear stresses (left side of Eq. 4.7) causes a change in vorticity, i.e. generates vorticity (right side of Eq. 4.7). Hence, inviscid flow (i.e. friction-less flow) has no rotation. (The exception is when vorticity is transported *into* an inviscid region, but also in that case no vorticity is generated or destroyed: it stays constant, unaffected.) Inviscid flow is often called *irrotational* flow (i.e. no rotation) or *potential* flow. The vorticity is always created at **potential** boundaries, see Section 4.3.1.

The main points that we have learnt in this section are:

1. The viscous terms are responsible for creating vorticity; this means that the vorticity can not be created or destroyed in inviscid (friction-less) flow
2. The viscous terms in the momentum equations can be expressed in ω_i ; considering Item 1 this was to be expected.

Exercise 24 Prove the first equality of Eq. 4.5 using the ε - δ -identity.

Exercise 25 Write out Eq. 4.7 for $i = 1$ and verify that it is satisfied.

4.2 The vorticity transport equation in three dimensions

Up to now we have talked quite a lot about vorticity. We have learnt that physically it means rotation of a fluid particle and that it is only the viscous terms that can cause rotation of a fluid particle. The terms inviscid (no friction), irrotational and potential flow all denote *frictionless* flow which is equivalent to zero (change in) vorticity. There is a small difference between the three terms because there may be vorticity in inviscid flow that is convected into the flow at the inlet(s); but also in this case the vorticity is not affected once it has entered the inviscid flow region. However, usually no distinction is made between the three terms. **frictionless**

In this section we will derive the transport equation for vorticity in incompressible flow. As usual we start with the Navier-Stokes equation, Eq. 2.9 at p. 32. First, we re-write the convective term of the incompressible momentum equation (Eq. 2.9) as

$$v_j \frac{\partial v_i}{\partial x_j} = v_j (S_{ij} + \Omega_{ij}) = v_j \left(S_{ij} - \frac{1}{2} \varepsilon_{ijk} \omega_k \right) \quad (4.9)$$

where Eq. 1.19 on p. 23 was used. Inserting $S_{ij} = (\partial v_i / \partial x_j + \partial v_j / \partial x_i) / 2$ and multiplying by two gives

$$2v_j \frac{\partial v_i}{\partial x_j} = v_j \left(\frac{\partial v_i}{\partial x_j} + \frac{\partial v_j}{\partial x_i} \right) - \varepsilon_{ijk} v_j \omega_k \quad (4.10)$$

The second term on the right side can be written as (Trick 2, see Eq. 8.4)

$$v_j \frac{\partial v_j}{\partial x_i} = \frac{1}{2} \frac{\partial (v_j v_j)}{\partial x_i} = \frac{\partial k}{\partial x_i} \quad (4.11)$$

where $k = v_j v_j / 2$. Equation 4.10 can now be written as

$$v_j \frac{\partial v_i}{\partial x_j} = \underbrace{\frac{\partial k}{\partial x_i}}_{\text{no rotation}} - \underbrace{\varepsilon_{ijk} v_j \omega_k}_{\text{rotation}} \quad (4.12)$$

The last term on the right side is the vector product of \mathbf{v} and $\boldsymbol{\omega}$, i.e. $\mathbf{v} \times \boldsymbol{\omega}$.

The trick we have achieved is to split the convective term into one term without rotation (first term on the right side of Eq. 4.12) and one term including rotation (second term on the right side). Inserting Eq. 4.12 into the incompressible momentum equation (Eq. 2.9) yields

$$\frac{\partial v_i}{\partial t} + \underbrace{\frac{\partial k}{\partial x_i}}_{\text{no rotation}} - \underbrace{\varepsilon_{ijk} v_j \omega_k}_{\text{rotation}} = -\frac{1}{\rho} \frac{\partial P}{\partial x_i} + \nu \frac{\partial^2 v_i}{\partial x_j \partial x_j} + f_i \quad (4.13)$$

The volume source is in most engineering flows represented by the gravity, i.e. $f_i = g_i$.

From Eq. 4.13 we get Crocco's theorem for steady inviscid flow

$$\varepsilon_{ijk} v_j \omega_k = \frac{\partial}{\partial x_i} \left(\frac{P}{\rho} + k \right) - f_i = \frac{\partial}{\partial x_i} \underbrace{\left(\frac{P}{\rho} + k + \phi \right)}_{P_0/\rho} \quad (4.14)$$

where $\partial \phi / \partial x_i = -f_i$ is the potential of the body force. In vector notation, Eq. 4.14 reads

$$\mathbf{v} \times \boldsymbol{\omega} = \frac{1}{\rho} \nabla(P_0) \quad (4.15)$$

These equations states that the gradient of stagnation pressure, P_0 , is orthogonal to both the velocity and vorticity vector.

Since the vorticity vector in Eq. 1.12 is defined by the cross product $\varepsilon_{pqi} \partial v_i / \partial x_q$ ($\nabla \times \mathbf{v}$ in vector notation, see Exercise 8), we start by applying the operator $\varepsilon_{pqi} \partial / \partial x_q$ to the Navier-Stokes equation (Eq. 4.13) so that

$$\begin{aligned} & \varepsilon_{pqi} \frac{\partial^2 v_i}{\partial t \partial x_q} + \varepsilon_{pqi} \frac{\partial^2 k}{\partial x_i \partial x_q} - \varepsilon_{pqi} \varepsilon_{ijk} \frac{\partial v_j \omega_k}{\partial x_q} \\ &= -\varepsilon_{pqi} \frac{1}{\rho} \frac{\partial^2 P}{\partial x_i \partial x_q} + \nu \varepsilon_{pqi} \frac{\partial^3 v_i}{\partial x_j \partial x_j \partial x_q} + \varepsilon_{pqi} \frac{\partial g_i}{\partial x_q} \end{aligned} \quad (4.16)$$

where the body force f_i was replaced by g_i . We know that ε_{ijk} is anti-symmetric in all indices, and hence the second term on line 1 and the first term on line 2 are zero (product of a symmetric and an anti-symmetric tensor). The last term on line 2 is zero because the gravitation vector, g_i , is constant (it is zero even if it is non-constant, because it can be expressed as a potential, see Eq. 4.32). The last term on line 1 is re-written using the ε - δ identity (see Table B.1 at p. 287)

$$\begin{aligned} \varepsilon_{pqi} \varepsilon_{ijk} \frac{\partial v_j \omega_k}{\partial x_q} &= (\delta_{pj} \delta_{qk} - \delta_{pk} \delta_{qj}) \frac{\partial v_j \omega_k}{\partial x_q} = \frac{\partial v_p \omega_k}{\partial x_k} - \frac{\partial v_q \omega_p}{\partial x_q} \\ &= v_p \frac{\partial \omega_k}{\partial x_k} + \omega_k \frac{\partial v_p}{\partial x_k} - v_q \frac{\partial \omega_p}{\partial x_q} - \omega_p \frac{\partial v_q}{\partial x_q} \end{aligned} \quad (4.17)$$

Using the definition of ω_i we find that its divergence

$$\frac{\partial \omega_i}{\partial x_i} = \frac{\partial}{\partial x_i} \left(\varepsilon_{ijk} \frac{\partial v_k}{\partial x_j} \right) = \varepsilon_{ijk} \frac{\partial^2 v_k}{\partial x_j \partial x_i} = 0 \quad (4.18)$$

is zero (product of a symmetric and an anti-symmetric tensor). Using the continuity equation ($\partial v_q / \partial x_q = 0$) and Eq. 4.18, Eq. 4.17 can be written

$$\varepsilon_{pqi} \varepsilon_{ijk} \frac{\partial v_j \omega_k}{\partial x_q} = \omega_k \frac{\partial v_p}{\partial x_k} - v_k \frac{\partial \omega_p}{\partial x_k} \quad (4.19)$$

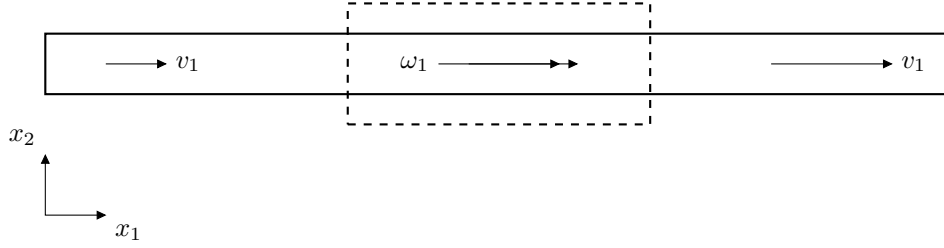


Figure 4.2: Vortex stretching. Dashed lines denote fluid element before stretching. $\frac{\partial v_1}{\partial x_1} > 0$.

The second term on line 2 in Eq. 4.16 can be written as

$$\nu \varepsilon_{pqi} \frac{\partial^3 v_i}{\partial x_j \partial x_j \partial x_q} = \nu \frac{\partial^2}{\partial x_j \partial x_j} \left(\varepsilon_{pqi} \frac{\partial v_i}{\partial x_q} \right) = \nu \frac{\partial^2 \omega_p}{\partial x_j \partial x_j} \quad (4.20)$$

Inserting Eqs. 4.19 and 4.20 into Eq. 4.16 gives finally

$$\frac{d\omega_p}{dt} \equiv \frac{\partial \omega_p}{\partial t} + v_k \frac{\partial \omega_p}{\partial x_k} = \omega_k \frac{\partial v_p}{\partial x_k} + \nu \frac{\partial^2 \omega_p}{\partial x_j \partial x_j} \quad (4.21)$$

We recognize the usual unsteady term, the convective term and the diffusive term. Furthermore, we have got rid of the pressure gradient term. That makes sense, because as mentioned in connection to Fig. 4.1, the pressure cannot affect the rotation (i.e. the vorticity) of a fluid particle since the pressure acts through its center. Equation 4.21 has a new term on the right-hand side which represents amplification and bending or tilting of the vorticity lines. If we write it term-by-term it reads

$$\omega_k \frac{\partial v_p}{\partial x_k} = \begin{cases} \omega_1 \frac{\partial v_1}{\partial x_1} + \omega_2 \frac{\partial v_1}{\partial x_2} + \omega_3 \frac{\partial v_1}{\partial x_3}, & p = 1 \\ \omega_1 \frac{\partial v_2}{\partial x_1} + \omega_2 \frac{\partial v_2}{\partial x_2} + \omega_3 \frac{\partial v_2}{\partial x_3}, & p = 2 \\ \omega_1 \frac{\partial v_3}{\partial x_1} + \omega_2 \frac{\partial v_3}{\partial x_2} + \omega_3 \frac{\partial v_3}{\partial x_3}, & p = 3 \end{cases} \quad (4.22)$$

The diagonal terms in this matrix represent *vortex stretching*. Imagine a slender, cylindrical fluid particle with vorticity ω_i and introduce a cylindrical coordinate system with the x_1 -axis as the cylinder axis and r_2 as the radial coordinate (see Fig. 4.2) so that $\omega_i = (\omega_1, 0, 0)$. We assume that a positive $\partial v_1 / \partial x_1$ is acting on the fluid cylinder; it will act as a source in Eq. 4.21 increasing ω_1 and it will stretch the cylinder. The volume of the fluid element must stay constant during the stretching (the incompressible continuity equation), which means that the radius, r , of the cylinder will decrease. For high *Reynolds numbers*, the viscous term is negligible. Hence, the viscous forces on the surface is small. This means that the angular momentum, $r^2 \omega_1$, is constant during the elongation (stretching) of the cylinder which gives an increased ω_1 . We see that vortex stretching will either make a fluid element longer and thinner with larger ω_1 (as in the example above) or shorter and thicker (when $\partial v_1 / \partial x_1 < 0$). The illustration given here is mainly relevant when a fluid particle actually rotates (as it does in turbulent flow, see Section 5).

The off-diagonal terms in Eq. 4.22 represent *vortex tilting*. Again, take a slender

Vortex stretching

Re number= ratio of convective to viscous term

Vortex tilting

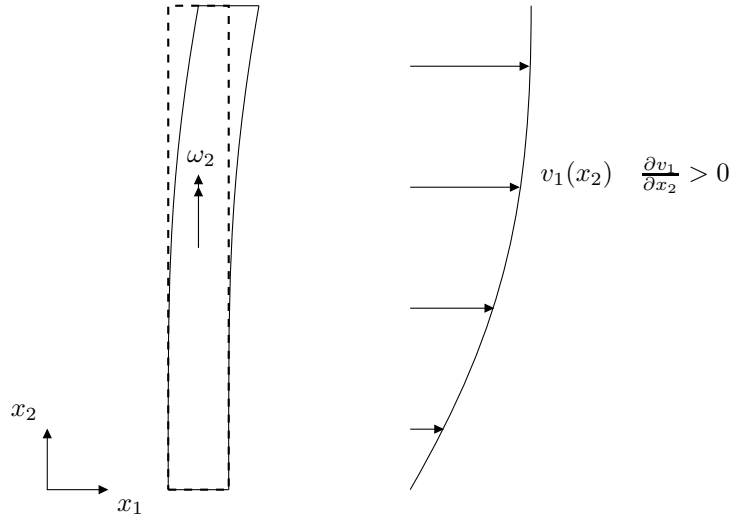


Figure 4.3: Vortex tilting. Dashed lines denote fluid element before bending or tilting.

fluid particle, but this time with its axis aligned with the x_2 axis, see Fig. 4.3. Assume it has a vorticity, ω_2 , and that the velocity surrounding velocity field is $v_1 = v_1(x_2)$. The velocity gradient $\partial v_1 / \partial x_2$ will tilt the fluid particle so that it rotates in clock-wise direction. The second term $\omega_2 \partial v_1 / \partial x_2$ in line one in Eq. 4.22 gives a contribution to ω_1 . This means that vorticity in the x_2 direction, through the source term $\omega_2 \partial v_1 / \partial x_2$, creates vorticity in the x_1 direction..

Vortex stretching and tilting are physical phenomena which act in three dimensions: fluid which initially is two dimensional becomes quickly three dimensional through these phenomena. Vorticity is useful when explaining why turbulence must be three-dimensional, see Section 5.4.

4.3 The vorticity transport equation in two dimensions

It is obvious that the vortex stretching/tilting has no influence in two dimensions; in this case the vortex stretching/tilting term vanishes because the vorticity vector is orthogonal to the velocity vector (for a 2D flow the velocity vector reads $v_i = (v_1, v_2, 0)$ and the vorticity vector reads $\omega_i = (0, 0, \omega_3)$ so that the scalar product is zero, i.e. $\omega_k \partial v_p / \partial x_k = 0$). Thus in two dimensions the vorticity equation reads

$$\frac{d\omega_3}{dt} = \nu \frac{\partial^2 \omega_3}{\partial x_\alpha \partial x_\alpha} \quad (4.23)$$

(Greek indices are used to indicate that they take values 1 or 2). If the Prandtl number is one ($Pr = 1$), this equation is exactly the same as the transport equation for temperature in incompressible flow, see Eq. 2.18. This means that vorticity is convected and diffused in the same way as temperature. In fully developed channel flow, for example,

the vorticity and the temperature equations reduce to (cf. Eq. 3.24)

$$0 = \nu \frac{\partial^2 \omega_3}{\partial x_2^2} \quad (4.24a)$$

$$0 = k \frac{\partial^2 T}{\partial x_2^2} \quad (4.24b)$$

For the temperature equation the heat flux is given by $q_2 = -k\partial T/\partial x_2$; with a hot lower wall and a cold upper wall (constant wall temperatures) the heat flux is constant for all x_2 and goes from the lower wall to the upper wall. We have the same situation for the vorticity. Its gradient, i.e. the vorticity flux, $\gamma_2 = -\nu\partial\omega_3/\partial x_2$, is constant across the channel, see Eq. 3.27 (you have plotted this quantity in TME226 Assignment 1). Equation 4.24 is turned into relations for q_2 and γ_2 by integration

$$\gamma_{wall} = \gamma_2 \quad (4.25a)$$

$$q_{wall} = q_2 \quad (4.25b)$$

If the wall-normal temperature derivative $\partial T/\partial x_2 = 0$ at both walls (*adiabatic* walls), the heat flux at the walls, q_{wall} , will be zero and the temperature will be equal to an arbitrary constant in the entire domain. It is only when the wall-normal temperature derivative at the walls are non-zero that a temperature field is created in the domain. The same is true for ω_3 : if $\nu\partial\omega_3/\partial x_2 = -\gamma_2 = 0$ at the walls, the flow will not include any vorticity. Hence, vorticity is – in the same way as temperature – generated at the walls.

4.3.1 Boundary layer thickness from the Rayleigh problem

In Section 3.1 we studied the Rayleigh problem (unsteady diffusion). As shown above, the two-dimensional unsteady temperature equation is identical to the two-dimensional unsteady equation for vorticity. The diffusion time, t , or the diffusion length, δ , in Eq. 3.14 can now be used to estimate the thickness of a developing boundary layer (recall that the limit between the boundary layer and the outer free-stream region can be defined by vorticity: inside the vorticity is non-zero and outside it is zero).

In a boundary layer, the streamwise pressure gradient is zero, see Eq. 3.42. This means that

$$\mu \frac{\partial^2 v_1}{\partial x_2^2} \Big|_{wall} = 0$$

because, at the wall, the only non-zero terms in the Navier-Stokes equation are the streamwise pressure gradient and the wall-normal diffusion term (see, for example, Eqs. 2.9 and 3.23). Hence, the flux of vorticity

$$\gamma_2 = -\nu \frac{\partial \omega_3}{\partial x_2} \Big|_{wall} = \nu \frac{\partial^2 v_1}{\partial x_2^2} \Big|_{wall} = 0 \quad (4.26)$$

(recall that $(\partial v_2/\partial x_1)_{wall} = 0$) along the wall which means that no vorticity is created along the boundary. The vorticity in a developing boundary layer is created at the leading edge of the plate (note that in channel flow, vorticity is indeed created along the walls because in this case the streamwise pressure gradient is not zero). The vorticity generated at the leading edge is transported along the wall by convection and at the same time it is transported by diffusion away from the wall.

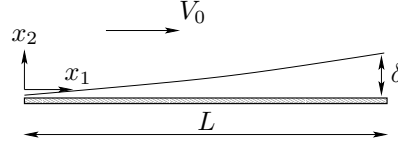


Figure 4.4: Boundary layer. The boundary layer thickness, δ , increases for increasing stream-wise distance from leading edge ($x_1 = 0$).

Below we will estimate the boundary layer thickness using the expression derived for the Rayleigh problem. In a boundary layer there is vorticity and outside the boundary layer it is zero (in the Rayleigh flow problem, the vorticity is created at time $t = 0^+$ when the plate instantaneously accelerates from rest to velocity V_0). Hence, if we can estimate how far from the wall the vorticity diffuses, this gives us an estimation of the boundary layer thickness.

Consider the boundary layer in Fig. 4.4. The boundary layer thickness at the end of the plate is $\delta(L)$. The time it takes for a fluid particle to travel from the leading edge of the plate to $x = L$ is L/V_0 (in the Rayleigh problem this corresponds to the flow field after time $t = L/V_0$). During this time vorticity will be transported by diffusion in the x_2 direction the length δ according to Eq. 3.14. If we assume that the fluid is air with the speed $V_0 = 3\text{m/s}$ and that the length of the plate $L = 2\text{m}$ we get from Eq. 3.14 that $\delta(L) = 1.2\text{cm}$.

Exercise 26 Note that the estimate above is not quite accurate because in the Rayleigh problem we assumed that the convective terms are zero, but in a developing boundary layer, as in Fig. 4.4, they are not ($v_2 \neq 0$ and $\partial v_1 / \partial x_1 \neq 0$). The proper way to solve the problem is to use Blasius solution, see Section 3.3. Blasius solution gives (see Eq. 33.1)

$$\frac{\delta}{L} = \frac{5}{Re_L^{1/2}}, \quad Re_L = \frac{V_0 L}{\nu} \quad (4.27)$$

Compute what $\delta(L)$ you get from Eq. 4.27.

Exercise 27 Assume that we have a developing flow in a pipe (radius R) or between two flat plates (separation distance h). We want to find out how long distance it takes for the the boundary layers to merge. Equation 3.14 can be used with $\delta = R$ or h . Make a comparison with this and Eq. 3.16.

4.4 Potential flow

IN potential flow, the velocity vector can be expressed as the gradient of its potential Φ , see Eq. 1.22. The vorticity is then zero by definition since the curl of the divergence is zero. This is easily seen by inserting Eq. 1.22 ($v_i = \partial\Phi/\partial x_i$) into the definition of the vorticity, Eq. 1.12, i.e.

$$\omega_i = \epsilon_{ijk} \frac{\partial v_k}{\partial x_j} = \epsilon_{ijk} \frac{\partial^2 \Phi}{\partial x_j \partial x_k} = 0 \quad (4.28)$$

since ϵ_{ijk} is anti-symmetric in indices j and k and $\partial^2 \Phi / \partial x_j \partial x_k$ is symmetric in j and k . Inserting Eq. 1.22 into the continuity equation, Eq. 2.3, gives

$$0 = \frac{\partial v_i}{\partial x_i} = \frac{\partial}{\partial x_i} \left(\frac{\partial \Phi}{\partial x_i} \right) = \frac{\partial^2 \Phi}{\partial x_i \partial x_i} \quad (4.29)$$

i.e. the potential satisfies the Laplace equation. This is of great important since many analytical methods exist for the Laplace equation.

4.4.1 The Bernoulli equation

The velocity field in potential flow is thus given by the continuity equation, Eq. 4.29 (together with Eq. 1.22). Do we have any use of the Navier-Stokes equation? The answer is yes: this equation provides the pressure field. We use the Navier-Stokes equation (Eq. 4.13) with the viscous term expressed as in Eq. 4.5

$$\frac{\partial v_i}{\partial t} + \frac{\partial k}{\partial x_i} - \epsilon_{ijk} v_j \omega_k = -\frac{1}{\rho} \frac{\partial P}{\partial x_i} - \nu \epsilon_{imn} \frac{\partial \omega_m}{\partial x_n} + f_i \quad (4.30)$$

Since $\omega_i = 0$ in potential (irrotational) flow, we get (with $f_i = g_i$) and using $k = v_i v_i / 2 = v^2 / 2$

$$\frac{\partial}{\partial t} \left(\frac{\partial \Phi}{\partial x_i} \right) + \frac{1}{2} \frac{\partial v^2}{\partial x_i} = -\frac{1}{\rho} \frac{\partial P}{\partial x_i} + g_i \quad (4.31)$$

where v_i in the unsteady term was replaced by its potential (Eq. 1.22). The gravity force can be expressed as a force potential, $g_i = -\partial \mathcal{X} / \partial x_i$ (see Eq. 4.14), because it is *conservative*. The gravity force is conservative because when integrating this force, the work (i.e. the integral) depends only on the starting and ending points of the integral: in mathematics this is called an *exact* differential. **conservative force**

Inserting $g_i = -\partial \mathcal{X} / \partial x_i$ in Eq. 4.31 gives

$$\frac{\partial}{\partial x_i} \left(\frac{\partial \Phi}{\partial t} + \frac{v^2}{2} + \frac{P}{\rho} + \mathcal{X} \right) = 0 \quad (4.32)$$

Integration gives the famous Bernoulli equation

$$\frac{\partial \Phi}{\partial t} + \frac{v^2}{2} + \frac{P}{\rho} + \mathcal{X} = C(t) \quad (4.33)$$

where $\mathcal{X} = -g_i x_i$. In steady flow, we get

$$\frac{v^2}{2} + \frac{P}{\rho} - g_3 x_3 = C \quad (4.34)$$

where $g_i = (0, 0, g_3)$. Using the height, $gh = -g_3 x_3$, we get the more familiar form

$$\frac{v^2}{2} + \frac{P}{\rho} + gh = C \quad (4.35)$$

4.4.2 Complex variables for potential solutions of plane flows

Complex analysis is a suitable tool for studying potential flow. We start this section by repeating some basics of complex analysis. For real functions, the value of a partial derivative, $\partial f / \partial x$, at $x = x_0$ is defined by making x approach x_0 and then evaluating $(f(x + x_0) - f(x)) / x_0$. The total derivative, df / dt , is defined by approaching the point $x_{10}, x_{20}, x_{30}, t$ as a linear combination of all independent variables (cf. Eq. 1.1).

A complex derivative of a complex variable is defined as $(f(z + z_0) - f(z)) / z_0$ where $z = x + iy$ and $f = u + iv$. We can approach the point z_0 both in the real coordinate direction, x , and in the imaginary coordinate direction, y . The complex derivative is defined only if the value of the derivative is independent of how we approach the point z_0 . Hence

$$\begin{aligned} \frac{df}{dz} &= \lim_{\Delta z \rightarrow 0} \frac{f(z_0 + \Delta z) - f(z_0)}{\Delta z} \\ &= \lim_{\Delta x \rightarrow 0} \frac{f(x_0 + \Delta x, iy_0) - f(x_0, iy_0)}{\Delta x} = \lim_{\Delta y \rightarrow 0} \frac{f(x_0, iy_0 + i\Delta y) - f(x_0, iy_0)}{i\Delta y}. \end{aligned} \quad (4.36)$$

The second line can be written as

$$\frac{\partial f}{\partial x} = \frac{1}{i} \frac{\partial f}{\partial y} = \frac{i}{i^2} \frac{\partial f}{\partial y} = -i \frac{\partial f}{\partial y} \quad (4.37)$$

since $i^2 = -1$. Inserting $f = u + iv$ and taking the partial derivative of f we get

$$\begin{aligned} \frac{\partial f}{\partial x} &= \frac{\partial u}{\partial x} + i \frac{\partial v}{\partial x} \\ -i \frac{\partial f}{\partial y} &= -i \frac{\partial u}{\partial y} - i^2 \frac{\partial v}{\partial y} = -i \frac{\partial u}{\partial y} + \frac{\partial v}{\partial y} \end{aligned} \quad (4.38)$$

Using Eq. 4.37 gives

$$\frac{\partial u}{\partial x} = \frac{\partial v}{\partial y}, \quad \frac{\partial u}{\partial y} = -\frac{\partial v}{\partial x} \quad (4.39)$$

Equations 4.39 are called the *Cauchy-Riemann* equations. Another way to derive Eq. 4.39 is found [here](#).

So far the complex plane has been expressed as $z = x + iy$. It can also be expressed in polar coordinates (see Fig. 4.5)

$$z = re^{i\theta} = r(\cos \theta + i \sin \theta) \quad (4.40)$$

Now we return to fluid mechanics and potential flow. Let us introduce a complex potential, f , based on the stream function, Ψ (Eq. 3.44), and the velocity potential, Φ (Eq. 1.22)

$$f = \Phi + i\Psi \quad (4.41)$$

Recall that for potential (i.e. inviscid, $\nu = 0$) two-dimensional, incompressible flow, the velocity potential satisfies the Laplace equation, see for example Eq. 4.29. The stream function also satisfies the Laplace equation in potential flow where the vorticity, ω_i , is zero. This is easily seen by taking the divergence of the stream function, Eq. 3.44

$$\frac{\partial^2 \Psi}{\partial x_1^2} + \frac{\partial^2 \Psi}{\partial x_2^2} = -\frac{\partial v_2}{\partial x_1} + \frac{\partial v_1}{\partial x_2} = -\omega_3 = 0 \quad (4.42)$$

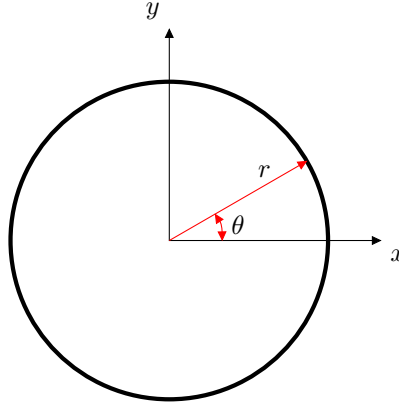


Figure 4.5: The complex plane in polar coordinates. Real and imaginary axes correspond to the horizontal and vertical axes, respectively.

see Eq. 1.13. Hence the complex potential, f , also satisfies the Laplace equation. Furthermore, f also satisfies the Cauchy-Riemann equations, Eq. 4.39, since

$$\frac{\partial \Phi}{\partial x} = \frac{\partial \Psi}{\partial y} = v_1 \quad \text{and} \quad \frac{\partial \Phi}{\partial y} = -\frac{\partial \Psi}{\partial x} = v_2 \quad (4.43)$$

see Eqs. 3.44 and 1.22. Thus we can conclude that f defined as in Eq. 4.41 is differentiable, i.e. df/dz exists. We have now defined a complex function, $f = \Phi + i\Psi$ which satisfies Laplace equation and which has a physical meaning in fluid dynamics.

4.4.3 $f \propto z^n$

Now we will give some examples of $f(z)$ which correspond to useful engineering flows. The procedure is as follows:

- assume that $f \propto z^n$ is complex potential
- verify that this is true (see, e.g, Eqs. 4.44 and 4.46)
- choose an n and find out what physical flow the complex potential describes

We can choose any exponent n in $f \propto z^n$ and multiply with any constant in order to get a physical, meaningful flow. The solution

$$f = C_1 z^n \quad (4.44)$$

is one example. Let's first verify that this is a solution of the Laplace equation (i.e. the continuity equation, 4.29 and that the flow is inviscid, $\omega_3 = 0$, Eq. 4.42). Taking the first and the second derivatives of Eq. 4.44 gives

$$\begin{aligned} \frac{\partial f}{\partial x} &= C_1 n (x + iy)^{n-1} \\ \frac{\partial^2 f}{\partial x^2} &= C_1 n(n-1)(x + iy)^{n-2} \\ \frac{\partial f}{\partial y} &= C_1 n i (x + iy)^{n-1} \\ \frac{\partial^2 f}{\partial^2 y} &= C_1 n(n-1)i^2 (x + iy)^{n-2} = -C_1 n(n-1)(x + iy)^{n-2} \end{aligned} \quad (4.45)$$

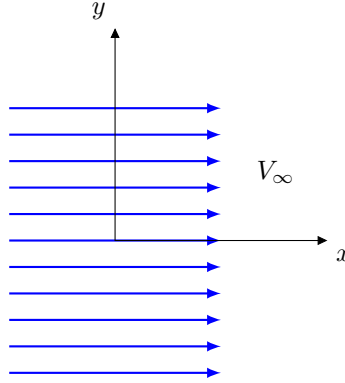


Figure 4.6: Parallel flow.

We find that the Laplace equation is indeed zero, i.e.

$$\frac{\partial^2 f}{\partial x^2} + \frac{\partial^2 f}{\partial y^2} = 0 \quad (4.46)$$

4.4.3.1 Parallel flow

When we set $n = 1$ in Eq. 4.44 we get ($C_1 = V_\infty$)

$$f = V_\infty z = V_\infty(x + iy) \quad (4.47)$$

The stream function, Ψ , is equal to the imaginary part, see Eq. 4.41. Equation 4.43 gives the velocity components

$$v_1 = \frac{\partial \Psi}{\partial y} = V_\infty \quad \text{and} \quad v_2 = -\frac{\partial \Psi}{\partial x} = 0 \quad (4.48)$$

The flow is shown in Fig. 4.6.

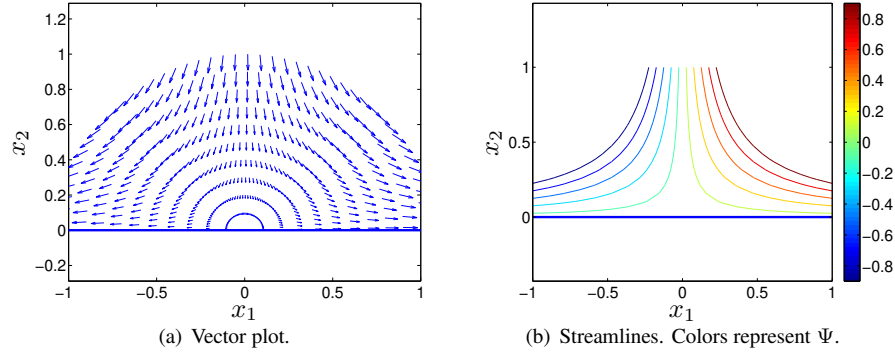
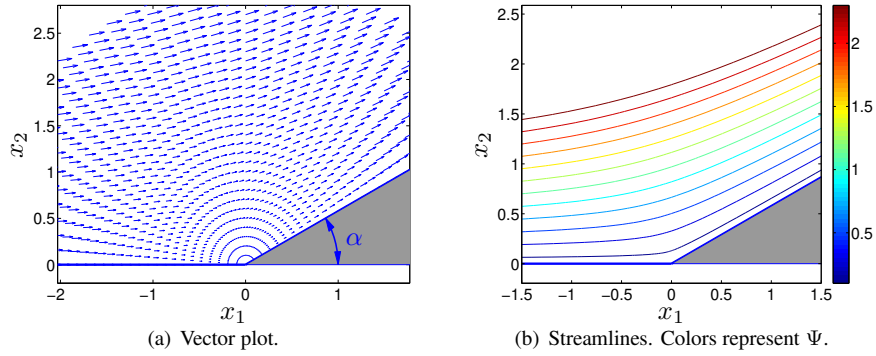
4.4.3.2 Stagnation flow

When we set $n = 2$ in Eqs. 4.44 we get (inviscid) stagnation flow onto a wall. The stream function, Ψ , corresponds to the imaginary part of f , see Eq. 4.41 so that ($C_1 = 1$)

$$\Psi = z^2 \quad (4.49)$$

The solution in form of a vector plot and contour plot of the stream function is given in Fig. 4.7. The flow impinges at the wall at $x_2 = 0$. The stream function is zero along the symmetry line, $x_1 = 0$, and it is negative to the left and positive to the right. The velocity components are obtained as

$$\begin{aligned} v_1 &= \frac{\partial \Psi}{\partial y} = 2x = 2x_1 \\ v_2 &= -\frac{\partial \Psi}{\partial x} = -2y = -2x_2 \end{aligned} \quad (4.50)$$

**Figure 4.7:** Potential flow. Stagnation flow.**Figure 4.8:** c

actionPotential flow. The lower boundary for $x_1 < 0$ can either be a wall (concave corner) or symmetry line (wedge).

Recall that since the flow is inviscid (no friction), the boundary condition on the wall is slip, i.e. a frictionless wall (same as a symmetric boundary). Note that this flow is the same as we looked at in Section 1.2 except that the velocities are here twice as large because we chose $C_1 = 1$ (see Eq. 1.4).

4.4.3.3 Flow over a wedge and flow in a concave corner.

Next we set $n = 6/5$. When n is not an integer, it is convenient to express f in polar coordinates

$$f = C_1 (re^{i\theta})^n = C_1 r^n e^{in\theta} = C_1 r^n (\cos(n\theta) + i \sin(n\theta)) \quad (4.51)$$

With $n = 6/5$ we get (inviscid) flow over a wedge and flow over a concave corner (n should be in the interval $1 < n < 2$). The stream function, the imaginary part of f , is given by (Eqs. 4.41 and 4.51)

$$\Psi = r^{6/5} \sin(6\theta/5) \quad (4.52)$$

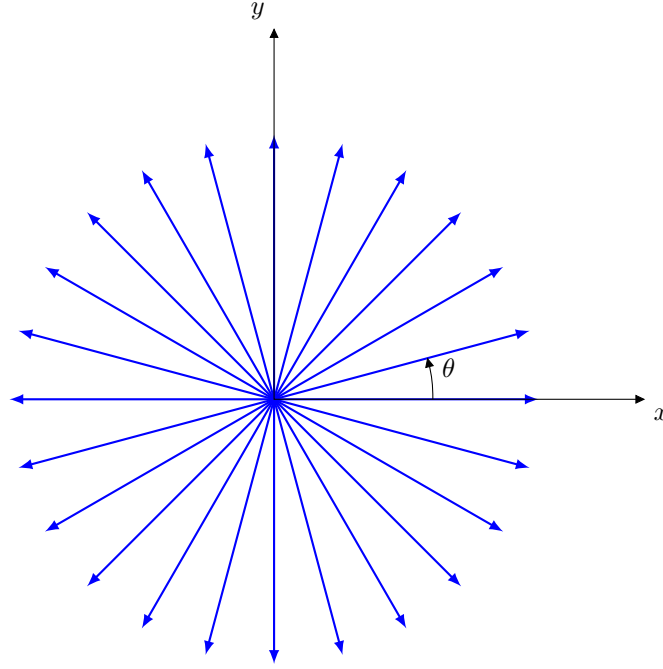


Figure 4.9: Line source. $\dot{m} > 0$

($C_1 = 1$) and the velocity components read

$$\begin{aligned} v_r &= \frac{1}{r} \frac{\partial \Psi}{\partial \theta} = \frac{6}{5} r^{1/6} \cos(6\theta/5) \\ v_\theta &= -\frac{\partial \Psi}{\partial r} = -\frac{6}{5} r^{1/6} \sin(6\theta/5) \end{aligned} \quad (4.53)$$

The velocity vector field and the stream function are presented in Fig. 4.8. The stream function is zero along the lower boundary. Note that $\theta = 0$ at the wedge, i.e. $0 \leq \theta \leq 5/6\pi$. The angle, α , in Fig. 4.8a is given by

$$\alpha = \frac{(n-1)\pi}{n} = \frac{\pi}{6} \quad (4.54)$$

4.4.4 Analytical solutions for a line source

The complex potential for a line source reads

$$f = \frac{\dot{m}}{2\pi} \ln z \quad (4.55)$$

where \dot{m} is the strength of the source; the physical meaning of \dot{m} is volume flow assuming that the extent of the domain in the third coordinate direction, x_3 , is one. First, we need to make sure that this solution satisfies the Laplace equation. The first

and second derivatives read

$$\begin{aligned}\frac{\partial f}{\partial x} &= \frac{\dot{m}}{2\pi z} \\ \frac{\partial^2 f}{\partial x^2} &= -\frac{\dot{m}}{2\pi z^2} \\ \frac{\partial f}{\partial y} &= \frac{i\dot{m}}{2\pi z} \\ \frac{\partial^2 f}{\partial x^2} &= -i^2 \frac{\dot{m}}{2\pi z^2} = \frac{\dot{m}}{2\pi z^2}\end{aligned}\tag{4.56}$$

which shows that the Laplace equation is satisfied.

Writing Eq. 4.55 on polar form gives

$$f = \frac{\dot{m}}{2\pi} \ln(re^{i\theta}) = \frac{\dot{m}}{2\pi} (\ln r + \ln(e^{i\theta})) = \frac{\dot{m}}{2\pi} (\ln r + i\theta)\tag{4.57}$$

The stream function corresponds to the imaginary part of f and we get

$$\begin{aligned}v_r &= \frac{1}{r} \frac{\partial \Psi}{\partial \theta} = \frac{\dot{m}}{2\pi r} \\ v_\theta &= -\frac{\partial \Psi}{\partial r} = 0\end{aligned}\tag{4.58}$$

We find that the physical flow is in the radial direction, see Fig. 4.9. If $\dot{m} > 0$, the flow is outwards directed and for $\dot{m} < 0$ it is going inwards toward origo. When origo is approached, the velocity, v_r , tends to infinity. Hence, Eq. 4.58 gives nonphysical flow near origo. The reason is that the inviscid assumption (zero viscosity) is not valid in this region.

It was mentioned above that the physical meaning of \dot{m} is volume flow. This is easily seen by integrating v_r (Eq. 4.58) over a cylindrical surface as

$$\int_0^1 dx_3 \int_0^{2\pi} v_r r d\theta = \int_0^1 dx_3 \int_0^{2\pi} \frac{\dot{m}}{2\pi r} r d\theta = \frac{\dot{m}}{2\pi} \int_0^1 \int_0^{2\pi} dx_3 d\theta = \dot{m}.\tag{4.59}$$

4.4.5 Analytical solutions for a vortex line

A line vortex is another example of a complex potential; it is very similar to Eq. 4.55 and reads

$$f = -i \frac{\Gamma}{2\pi} \ln z\tag{4.60}$$

which on polar form reads (cf. Eq. 4.57)

$$f = -\frac{\Gamma}{2\pi} (i \ln r - \theta)\tag{4.61}$$

From the stream function (the imaginary part of f) we get (cf. Eq. 4.58)

$$\begin{aligned}v_r &= \frac{1}{r} \frac{\partial \Psi}{\partial \theta} = 0 \\ v_\theta &= -\frac{\partial \Psi}{\partial r} = \frac{\Gamma}{2\pi r}\end{aligned}\tag{4.62}$$

This flow was introduced in Section 1.7.1 (where we called it an ideal vortex line) as an example of a flow with no vorticity. The flow is in the positive θ direction along lines

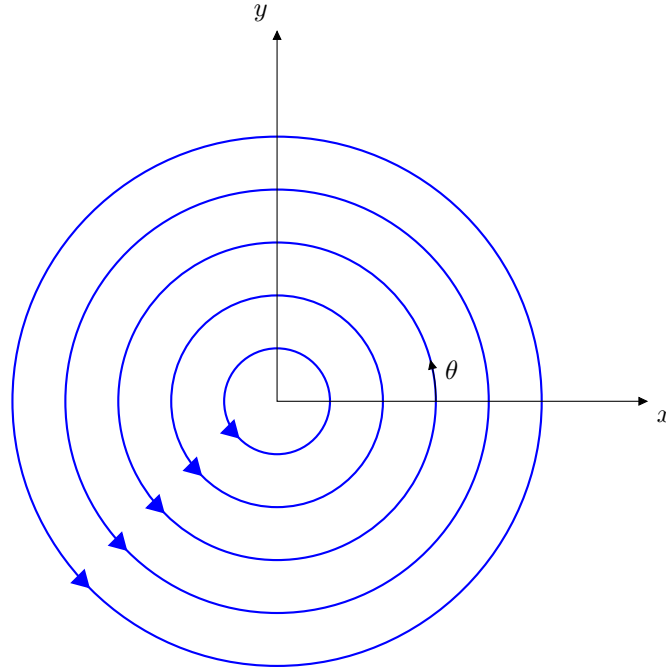
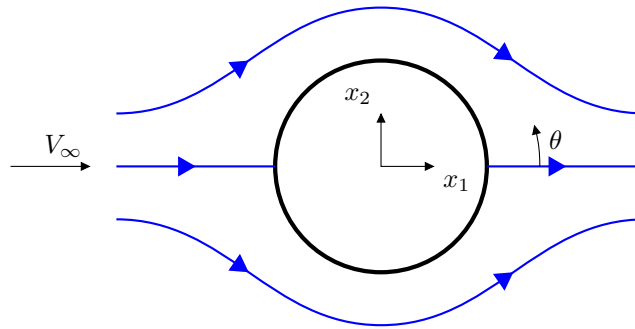


Figure 4.10: Vortex line.

Figure 4.11: Flow around a cylinder of radius r_0 .

of constant radius, see Fig. 4.10. The circulation, Γ , appears in the expression of v_θ . It was introduced in Section 1.7. It is defined as a closed line integral along line C , see Eq. 1.23 and can be expressed as an integral of the vorticity over surface S bounded by line C , see Eq. 1.25 and Fig. 1.7.

4.4.6 Analytical solutions for flow around a cylinder

The complex potential for the flow around a cylinder can be found by combining a doublet and a parallel flow. A doublet consists of a line source (strength \dot{m}) and sink (strength $-\dot{m}$) separated by a distance ε in the x_1 direction (line sources were introduced in Section 4.4.4). Imagine that we move the source and the sink closer to each other and at the same time we increase their strength $|\dot{m}|$ so that the product $\mu = \dot{m}\varepsilon$

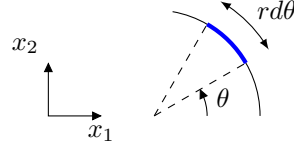


Figure 4.12: Flow around a cylinder of radius r_0 . Integration of surface pressure.

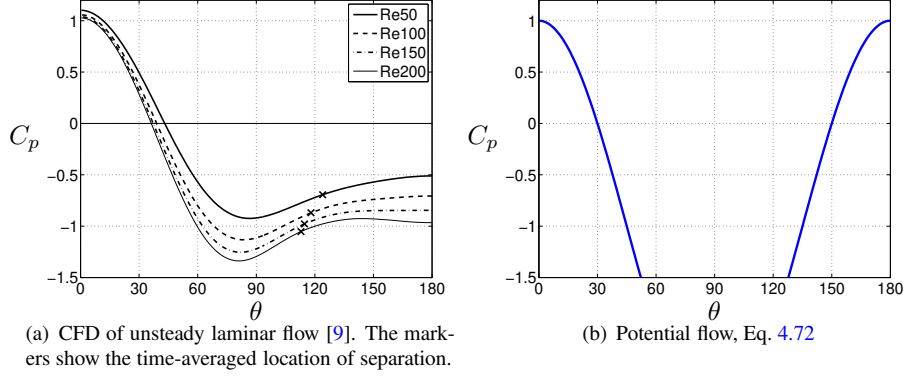


Figure 4.13: Pressure coefficients.

stays constant. The resulting complex potential is

$$f = \frac{\mu}{\pi z} \quad (4.63)$$

When adding the complex potential of parallel flow, see Eq. 4.47, we get

$$f = \frac{\mu}{\pi z} + V_\infty z \quad (4.64)$$

Now we define the radius of a cylinder, r_0 , as

$$r_0^2 = \mu/(\pi V_\infty) \quad (4.65)$$

so that

$$f = \frac{V_\infty r_0^2}{z} + V_\infty z \quad (4.66)$$

On polar form it reads

$$\begin{aligned} f &= \frac{V_\infty r_0^2}{r e^{i\theta}} + V_\infty r e^{i\theta} = V_\infty \left(\frac{r_0^2}{r} e^{-i\theta} + r e^{i\theta} \right) \\ &= V_\infty \left(\frac{r_0^2}{r} (\cos \theta - i \sin \theta) + r (\cos \theta + i \sin \theta) \right) \end{aligned} \quad (4.67)$$

The stream function reads (imaginary part)

$$\Psi = V_\infty \left(r - \frac{r_0^2}{r} \right) \sin \theta \quad (4.68)$$

Now we can compute the velocity components

$$\begin{aligned} v_r &= \frac{1}{r} \frac{\partial \Psi}{\partial \theta} = V_\infty \left(1 - \frac{r_0^2}{r^2} \right) \cos \theta \\ v_\theta &= -\frac{\partial \Psi}{\partial r} = -V_\infty \left(1 + \frac{r_0^2}{r^2} \right) \sin \theta \end{aligned} \quad (4.69)$$

We find that $v_r = 0$ for $r = r_0$ as intended (thanks to the definition in Eq. 4.65). We are not interested in the solution inside the cylinder ($r < r_0$). Furthermore, we see that the tangential velocity is zero at $\theta = 0$ and π ; hence these points correspond to the stagnation points, see Fig. 4.11. The velocity field at the cylinder surface, $r = r_0$, reads

$$\begin{aligned} v_{r,s} &= 0 \\ v_{\theta,s} &= -2V_\infty \sin \theta \end{aligned} \quad (4.70)$$

where index s denotes surface. Note that the local velocity gets twice as large as the freestream velocity at the top ($\theta = \pi/2$) and the bottom ($\theta = -\pi/2$) of the cylinder. The surface pressure is obtained from Bernoulli equation (see Eq. 4.35)

$$\frac{V_\infty^2}{2} + \frac{P_\infty}{\rho} = \frac{v_{\theta,s}^2}{2} + \frac{p_s}{\rho} \Rightarrow p_s = P_\infty + \rho \frac{V_\infty^2 - v_{\theta,s}^2}{2} \quad (4.71)$$

where we neglected the gravitation term. The surface pressure is usually expressed as a pressure coefficient

$$C_p \equiv \frac{p_s - P_\infty}{\rho V_\infty^2 / 2} = 1 - \frac{v_{\theta,s}^2}{V_\infty^2} = 1 - 4 \sin^2 \theta \quad (4.72)$$

using Eq. 4.70.

It should be stressed that although Eqs. 4.70 and 4.72 are exact they are not realistic because of the strict requirement that the flow should be inviscid. This requirement is valid neither in the boundary layers nor in the wake; the boundary layers may be thin but the wake is a large part of the domain. Figure 4.13 presents the pressure coefficient for potential flow and accurate unsteady CFD of two-dimensional viscous flow [9] (the Reynolds number is sufficiently low for the flow to be laminar); Eqs. 2.3 and 2.9 are solved numerically [9]. The potential solution agrees rather well with viscous flow up to $\theta \simeq 20^\circ$.

How do we find the lift and drag force? The only force (per unit area) that acts on the cylinder surface is the pressure (in viscous flow there would also be a viscous stress, but it is usually much smaller). To find the lift force, F_L , we simply integrate the pressure over the surface. Usually the lift force is expressed as a lift coefficient, C_L , which is scaled with the dynamic pressure $\rho V_\infty^2 / 2$. The lift coefficient is obtained as

$$\begin{aligned} C_L &= \frac{F_L}{\rho V_\infty^2 / 2} = - \int_0^1 dx_3 \int_0^{2\pi} \frac{p_s}{\rho V_\infty^2 / 2} \sin \theta r_0 d\theta \\ &= -r_0 \int_0^1 dx_3 \int_0^{2\pi} (1 - 4 \sin^2 \theta) \sin \theta d\theta \\ &= -r_0 \left[-\cos \theta - 4 \left(\frac{1}{12} \cos(3\theta) - \frac{3}{4} \cos \theta \right) \right]_0^{2\pi} = 0 \end{aligned} \quad (4.73)$$

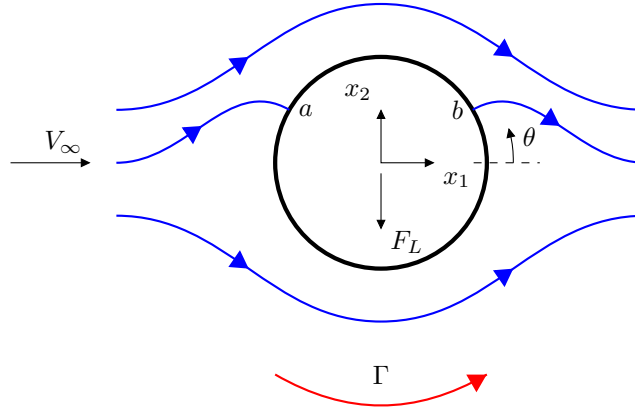


Figure 4.14: Flow around a cylinder of radius r_0 with additional circulation which give a (negative) lift force, see Eq. 4.84.

The $\sin \theta$ on the first line appears because we project the pressure force in the vertical direction (see Fig. 4.12) and minus sign is because pressure acts inwards, see Eq. 1.9 and Fig. 4.1. We assume in Eq. 4.73 that the length of the cylinder in the x_3 direction is one. The drag coefficient is computed as

$$\begin{aligned} C_D &= \frac{F_D}{\rho V_\infty^2/2} = - \int_0^1 dx_3 \int_0^{2\pi} (1 - 4 \sin^2 \theta) \cos \theta r_0 d\theta \\ &= -r_0 \int_0^1 dx_3 \int_0^{2\pi} \left[\sin \theta - \frac{4}{3} \sin^3 \theta \right]_0^{2\pi} = 0 \end{aligned} \quad (4.74)$$

The $\cos \theta$ on the first line appears because we project the pressure force in the horizontal direction (see Fig. 4.12). Equations 4.73 and 4.74 give $C_L = C_D = 0$; hence we find that inviscid flow around a cylinder creates neither lift nor drag. The reason is that the pressure is symmetric both with respect to $x_1 = 0$ and $x_2 = 0$. The lift force on the lower surface side cancels the force on the upper side. Same argument for the drag force: the pressure force on the upstream surface cancels that on the downstream surface.

4.4.7 Analytical solutions for flow around a cylinder with circulation

We will now introduce a second example of potential flow around cylinders, which is by far the most important one from engineering point of view. Here we will introduce the use of additional circulation which alters the locations of the stagnation points and creates lift. This approach is used in potential methods for predicting flow around airfoils in aeronautics (mainly helicopters) and windpower engineering.

We add the complex potential of a vortex line (see Eq. 4.60) to Eq. 4.66 so that

$$f = \frac{V_\infty r_0^2}{z} + V_\infty z - i \frac{\Gamma}{2\pi} \ln z \quad (4.75)$$

On polar form it reads (see Eqs. 4.61 and 4.67)

$$f = V_\infty \left(\frac{r_0^2}{r} (\cos \theta - i \sin \theta) + r (\cos \theta + i \sin \theta) \right) - \frac{\Gamma}{2\pi} (i \ln r - \theta) \quad (4.76)$$

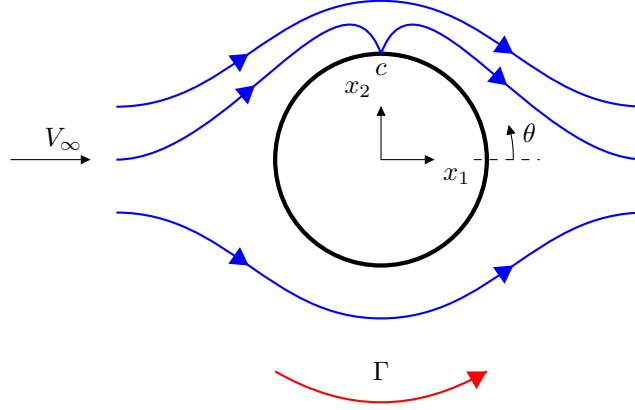


Figure 4.15: Flow around a cylinder of radius r_0 with maximal additional circulation.

The imaginary part gives the stream function

$$\Psi = V_{\infty} \left(r - \frac{r_0^2}{r} \right) \sin \theta - \frac{\Gamma}{2\pi} \ln r \quad (4.77)$$

We get the velocity components as (see Eqs. 4.62 and 4.69)

$$\begin{aligned} v_r &= \frac{1}{r} \frac{\partial \Psi}{\partial \theta} = V_{\infty} \left(1 - \frac{r_0^2}{r^2} \right) \cos \theta \\ v_{\theta} &= -\frac{\partial \Psi}{\partial r} = -V_{\infty} \left(1 + \frac{r_0^2}{r^2} \right) \sin \theta + \frac{\Gamma}{2\pi r} \end{aligned} \quad (4.78)$$

The effect of the added vortex line is, as expected, to increase v_{θ} while leaving v_r unaffected. The larger the circulation, the larger v_{θ} .

The velocity at the surface, $r = r_0$, reads

$$\begin{aligned} v_{r,s} &= 0 \\ v_{\theta,s} &= -2V_{\infty} \sin \theta + \frac{\Gamma}{2\pi r_0} \end{aligned} \quad (4.79)$$

Now let's find the location of the stagnation points, i.e. where $v_{\theta,s} = 0$. Equation 4.79 gives

$$2V_{\infty} \sin \theta_{stag} = \frac{\Gamma}{2\pi r_0} \Rightarrow \theta_{stag} = \arcsin \left(\frac{\Gamma}{4\pi r_0 V_{\infty}} \right) \quad (4.80)$$

The two angles that satisfy this equation are located in the first and second quadrants. The two positions are indicated with a and b in Fig. 4.14. For a limiting value of the circulation, Γ_{max} , the two locations s and b will merge at $\theta = \pi/2$, denoted with c in Fig. 4.15,

$$\Gamma_{max} = 4\pi V_{\infty} r_0. \quad (4.81)$$

This corresponds to the maximum value of the circulation for which there is a stagnation point on the cylinder surface. For circulation larger than Γ_{max} , the stagnation point will be located above the cylinder.

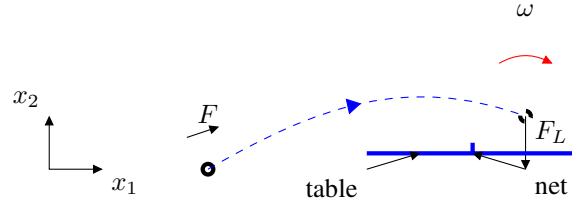


Figure 4.16: Table tennis. The loop uses the Magnus effect. Side view.

The pressure is obtained from Bernoulli equation as (see Eq. 4.72)

$$\begin{aligned} C_p &= 1 - \frac{v_{\theta,s}^2}{V_\infty^2} = 1 - \left(-2 \sin \theta + \frac{\Gamma}{2\pi r_0 V_\infty} \right)^2 \\ &= 1 - 4 \sin^2 \theta + \frac{4\Gamma \sin \theta}{2\pi r_0 V_\infty} - \left(\frac{\Gamma}{2\pi r_0 V_\infty} \right)^2 \end{aligned} \quad (4.82)$$

We found in Section 4.4.6 that a cylinder without circulation gives neither drag nor lift, see Eqs. 4.73 and 4.74. What about the present case? Let's compute the lift. We found in Eq. 4.73 that the two first terms in Eq. 4.82 give no contribution to the lift. The last term cannot give any contribution to the lift because it is constant on the entire surface. Hence we only need to include the third term in Eq. 4.82 so that

$$\begin{aligned} C_L &= \frac{F_L}{\rho V_\infty^2/2} = - \int_0^1 dx_3 \int_0^{2\pi} \frac{p_s}{\rho V_\infty^2/2} \sin \theta r_0 d\theta \\ &= -r_0 \int_0^1 dx_3 \int_0^{2\pi} \frac{2\Gamma \sin \theta}{\pi r_0 V_\infty} \sin \theta d\theta \\ &= - \left[\frac{\Gamma \theta}{\pi V_\infty} - \frac{\Gamma}{2\pi V_\infty} \sin(2\theta) \right]_0^{2\pi} = -\frac{2\Gamma}{V_\infty} \end{aligned} \quad (4.83)$$

We find that the lift force on a unit length of the cylinder can be computed from the circulation as

$$F_L = -\rho V_\infty \Gamma \quad (4.84)$$

This relation is valid for any body and it is called the *Kutta-Joukowski* law who – independent of each other – formulated it. The reason to the sign of the lift force can easily be seen from Fig. 4.14. The stagnation points, where the pressure is largest, are located at the top of the cylinder and hence the pressure is higher on the top than on the bottom. The "lift" force is acting downwards, i.e. in the negative x_2 direction.

The drag is, however, still zero. In Eq. 4.74 we found that the first and the second terms in Eq. 4.82 gives no contribution to drag. Hence, we only need to consider the third terms. In the drag integral (see Eq. 4.74), this term in Eq. 4.82 gives rise to a term proportional to $\sin \theta \cos \theta$ whose contribution is zero. Hence, the additional circulation does not give rise to any drag.

4.4.7.1 The Magnus effect

Circulation around a cylinder is very similar to a rotating cylinder. Instead of adding a circulation, we let the cylinder rotate with speed ω . A rotating cylinder produces lift. This has interesting application in sports, for example football, table tennis and golf.

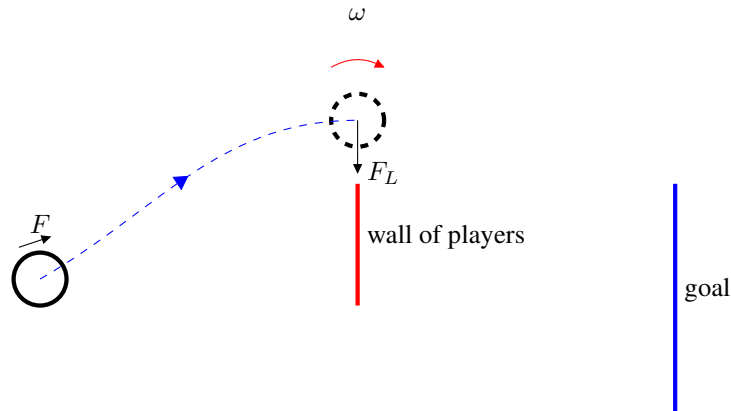


Figure 4.17: Football. A free-kick uses the Magnus effect. Top view

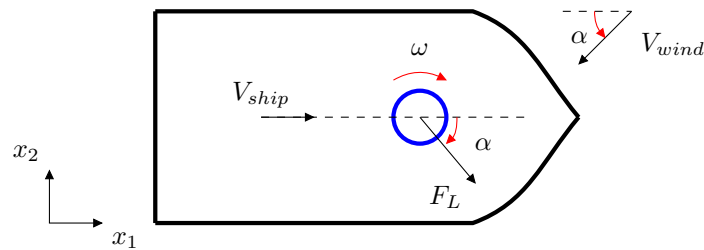


Figure 4.18: Flettner rotor (in blue) on a ship. The relative velocity between the ship and the wind is $V_{wind} + V_{ship}$. The ship moves with speed V_{ship} . Top view.

In table tennis, the ball must hit the table on the side of the opponent. One way to improve the chance that this will happen is to make a loop. This means that you hit the ball slightly on the top. The ball experiences a force, F , when you hit it (see Fig. 4.16) and this force makes it rotate with rotation speed ω (clockwise direction). The rotation causes a lift, F_L , which acts downwards so that the ball drops down quickly and (hopefully) hits the table on the other side of the net. The lift force is downwards because the stagnation points are located on the upper surface. Recall that the relative velocity of the air is in the negative x_1 direction.

Another example where the Magnus effect is important is golf. Here the object is often vice versa. You want the ball to go as far as possible. Hence you hit it with a slice so that it spins with a positive ω (counter-clockwise). The result is a lift force in the positive x_2 direction which makes the ball go further.

A final sports example is football. Here the lift is used sideways. Imagine there is a free-kick rather close to the opponents' goal, see Fig. 4.17. The opponents erect a wall of players between the goal and the location of the free-kick. The player who makes the free-kick wants to make the ball go on the left side of the wall; after the wall of players, the ball should turn right towards the goal. The Magnus effect helps to achieve this. The player hits the ball with her/his left foot on the left side of the ball which creates a force F on the ball. This makes the ball rotate clockwise, see Fig. 4.17, and creates a lift force so that the ball after it has passed the wall turns to the right towards the goal. The reason that the ball turns to the right first after the wall (and not before) is that the forward momentum created by F (the player) is much larger than F_L .

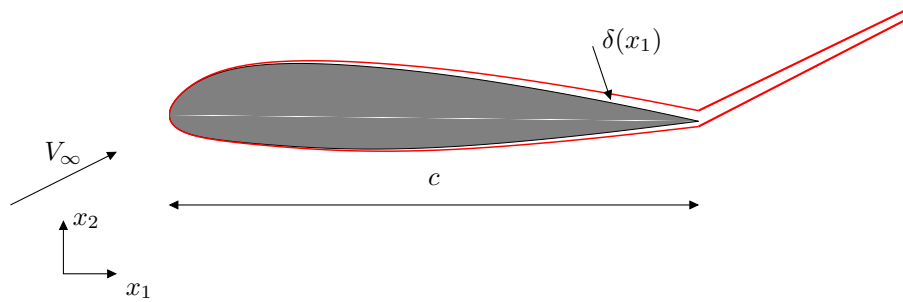


Figure 4.19: Airfoil. The boundary layers, $\delta(x_1)$, and the wake illustrated in red. $x_1 = 0$ and $x_1 = c$ at leading and trailing edge, respectively.

When looking at Figs. 4.16 and 4.17 I know it may be confusing to understand the direction of the force. The trick is to imagine that the ball is still/non-moving and the wind is coming towards it with speed $-V_{ball}$. Then we see that the rotation and on-coming speed $-V_{ball}$ "co-operates" at the lower side and thereby increasing the total speed on the lower side compared to the upper side. Bernoulli (Eq.4.35) then gives a lower pressure on the lower side of the ball compared to the upper side which gives a downward force.

If you are interested in football you may be pleased to learn that by use of fluid dynamics it is now scientifically proven that it was much harder to make a good freekick in 2010 worldcup than in 2014 [10]. Figure 7b in that paper is particularly interesting.

As an experiment, two identical freekicks are made with the football used at the 2013 FIFA Confederations. The freekicks are made 25m from the goal. The initial velocity of the football is 30 m/s. The result of the two freekicks is that the two footballs reach the goal three meters from each other in the vertical direction. Why? Because the ball was rotated 45 degrees before the second freekick (see Figs. 2c,d) in [10].

Finally we give an engineering example of the use of the Magnus effect. The first Flettner rotors on ships were produced in 1924. It has recently gained new interest as the cost of fuel is rising. A Flettner rotor is a rotating cylinder (or many) on a ship, see Fig. 4.18. The diameter of this rotor can be a couple of meter and have a length (i.e. height) of 10 – 20 meter. The ship is moving to the right with speed V_{ship} . The wind comes towards the ship from the left-front (relative wind at an angle of $\pi/4$). The Flettner rotor rotates in the clockwise direction. The Magnus effect creates a force in the orthogonal direction to the relative windspeed, i.e. at an angle of $-\pi/4$. Note that if the wind comes from the right instead of from the left, the rotor should rotate in the counter-clockwise direction. The additional propulsion force is $F_L \cos(\alpha)$. The Division of Fluid Dynamics recently took part in an EU project where we studied the flow around rotating cylinders in relation to Flettner rotors [11].

4.4.8 The flow around an airfoil

Flow around airfoils is a good example where potential methods are useful. These methods are still in use in wind engineering and for helicopters. At the Division of

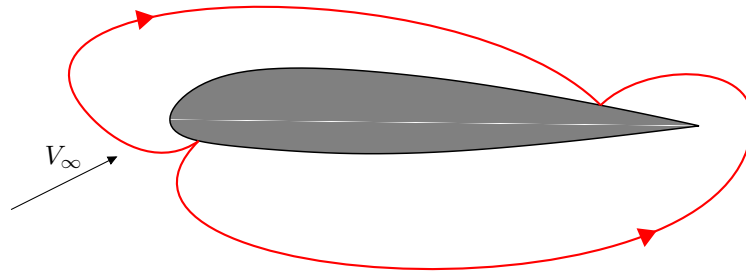


Figure 4.20: Airfoil. Streamlines from potential flow. Rear stagnation point at the upper surface (suction side).

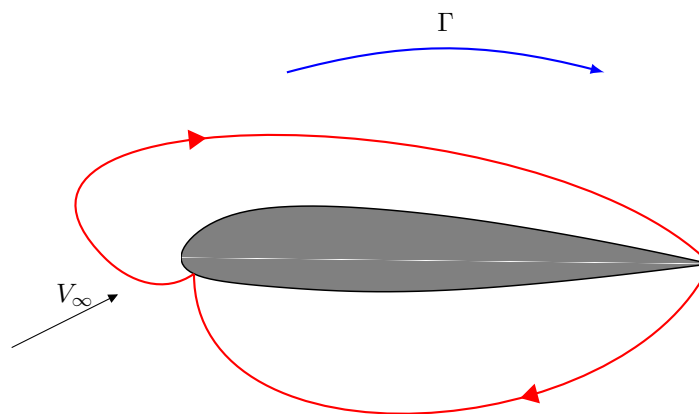


Figure 4.21: Airfoil. Streamlines from potential flow with added circulation. Rear stagnation point at the trailing edge.

Fluid Dynamics we had a PhD project where we used potential methods for computing the aerodynamic loads for wind turbine rotor blades [5, 12].

The flow around airfoils is a good example where the flow can be treated as inviscid in large part of the flow. For low angles of attack (which is the case for, for example, an aircraft in cruise conditions) the boundary layers and the wake are thin. Outside these regions the flow is essentially inviscid.

Figure 4.19 (see also Fig. 16.1) shows a two-dimensional airfoil. The boundary layers and the wake are illustrated in red. The boundary layer is thinner on the pressure (lower) side than on the suction (upper) side. It grows slightly thicker towards the trailing edge (denoted by $\delta(x_1)$ in Fig. 4.19). When this flow is computed using potential methods, the location of the front stagnation point is reasonably well captured, see Fig. 4.20. However, the stagnation point near the trailing edge is located on the suction side which is clearly nonphysical. The flow on the pressure (lower) side cannot be expected to make a 180° turn at the trailing edge and then go in the negative x_1 direction towards the stagnation point located on the suction side.

The solution is to move the stagnation points in the same way as we did for the cylinder flow in Section 4.4.7. We want to move the rear stagnation point towards the trailing edge. This is achieved by adding a circulation in the clockwise direction, see Fig. 4.21. The magnitude of the circulation is determined by the requirement that the stagnation point should be located at the trailing edge. This is called the *Kutta condition*. The added circulation is negative (clockwise). In aeronautics, the sign of circulation is usually changed so that $\Gamma_{aeronautic} = -\Gamma$. The lift of a two-dimensional airfoil (or a two-dimensional section of a three-dimensional airfoil) is then computed as (see Eq. 4.84)

$$F_L = \rho V_\infty \Gamma_{aeronautic} \quad (4.85)$$

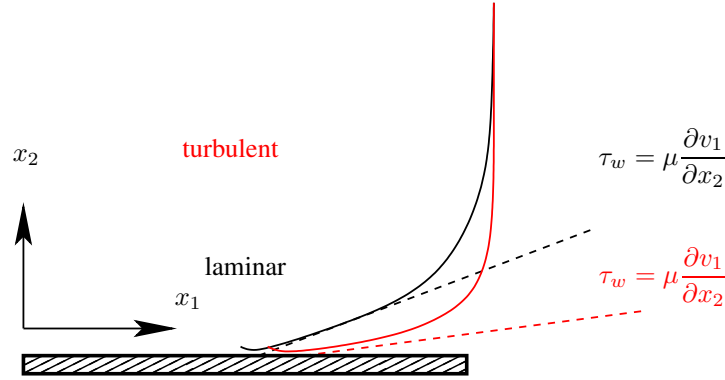


Figure 5.1: Laminar and turbulent boundary layer.

5 Turbulence

5.1 Introduction

ALMOST all fluid flow which we encounter in daily life is turbulent. Typical examples are flow around (as well as *in*) cars, aeroplanes and buildings. The boundary layers and the wakes around and after bluff bodies such as cars, aeroplanes and buildings are turbulent. Also the flow and combustion in engines, both in piston engines and gas turbines and combustors, are highly turbulent. Air movements in rooms are turbulent, at least along the walls where wall-jets are formed. Hence, when we compute fluid flow it will most likely be turbulent. In turbulent flow we usually divide the velocities in one time-averaged part \bar{v}_i , which is independent of time (when the mean flow is steady), and one fluctuating part v'_i so that $v_i = \bar{v}_i + v'_i$.

There is no definition on turbulent flow, but it has a number of characteristic features (see Pope [13] and Tennekes & Lumley [14]) such as:

I. Irregularity. Turbulent flow is irregular and chaotic (they may seem random, but they are governed by Navier-Stokes equation, Eq. 2.9). The flow consists of a spectrum of different scales (eddy sizes). We do not have any exact definition of an *turbulent eddy*, but we suppose that it exists in a certain region in space for a certain time and that it is subsequently destroyed (by the cascade process or by dissipation, see below). It has a characteristic velocity and length (called a velocity and length scale). The region covered by a large eddy may well enclose also smaller eddies. The largest eddies are of the order of the flow geometry (i.e. boundary layer thickness, jet width, etc). At the other end of the spectrum we have the smallest eddies which are dissipated by viscous forces (stresses) into thermal energy resulting in a temperature increase. Even though turbulence is chaotic it is deterministic and is described by the Navier-Stokes equations.

II. Diffusivity. In turbulent flow the diffusivity increases compared to laminar flow, see Fig. 5.1. The turbulence increases the exchange of momentum in e.g. boundary layers, and reduces or delays thereby separation at bluff bodies such as cylinders, airfoils and cars. The increased diffusivity also increases the resistance (wall friction) and heat transfer in internal flows such as in channels and pipes.

III. Large Reynolds Numbers. Turbulent flow occurs at high Reynolds number. For example, the transition to turbulent flow in pipes occurs that $Re_D \simeq 2300$, and in

turbulent
eddy

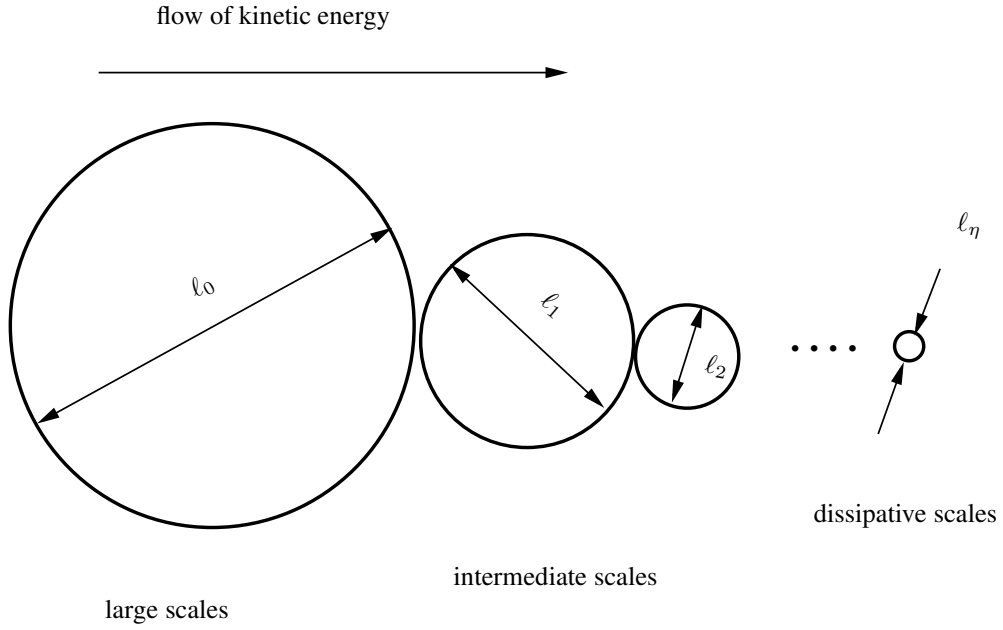


Figure 5.2: Cascade process with a spectrum of eddies. The energy-containing eddies are denoted by v_0 ; ℓ_1 and ℓ_2 denotes the size of the eddies in the inertial subrange such that $\ell_2 < \ell_1 < \ell_0$; ℓ_η is the size of the dissipative eddies.

boundary layers at $Re_x \simeq 500\,000$.

IV. Three-Dimensional. Turbulent flow is always three-dimensional and unsteady. However, when the equations are time averaged, we can treat the flow as two-dimensional (if the geometry is two-dimensional).

V. Dissipation. Turbulent flow is dissipative, which means that kinetic energy in the small (dissipative) eddies are transformed into thermal energy. The small eddies receive the kinetic energy from slightly larger eddies. The slightly larger eddies receive their energy from even larger eddies and so on. The largest eddies extract their energy from the mean flow. This process of transferring energy from the largest turbulent scales (eddies) to the smallest is called the *cascade process*, see Fig. 45.5.

VI. Continuum. Even though we have small turbulent scales in the flow they are much larger than the molecular scale and we can treat the flow as a continuum.

**cascade
process**

5.2 Turbulent scales

The largest scales are of the order of the flow geometry (the boundary layer thickness, for example), with length scale ℓ_0 and velocity scale v_0 . These scales extract kinetic energy from the mean flow which has a time scale comparable to the large scales, i.e.

$$\frac{\partial \bar{v}_1}{\partial x_2} \sim t_0^{-1} \sim v_0 / \ell_0 \quad (5.1)$$

Part of the kinetic energy of the large scales is lost to slightly smaller scales with which the large scales interact. Through the *cascade process*, kinetic energy is in this way transferred from the largest scale to the smallest scales. At the smallest scales the frictional forces (viscous stresses) become large and the kinetic energy is transformed

(dissipated) into thermal energy. The kinetic energy transferred per unit time from eddy-to-eddy (from an eddy to a slightly smaller eddy) is the same for each eddy size. Although the kinetic energy is mostly transferred from large to small scales, it may instantaneously go the other way, i.e. from small scales to large scales. It may even happen that kinetic energy goes from fluctuations to the mean flow; this happens when the production term, P^k , is negative, see Item II on p. 105.

The dissipation is denoted by ε which is energy per unit time and unit mass ($\varepsilon = [m^2/s^3]$). The dissipation is proportional to the kinematic viscosity, ν , times the fluctuating velocity gradient up to the power of two (see Section 8.2). The friction forces exist of course at all scales, but they are largest at the smallest eddies. In reality a small fraction is dissipated at all scales. However it is assumed that most of the energy that goes into the large scales per unit time (say 90%) is finally dissipated at the smallest (dissipative) scales.

The smallest scales where dissipation occurs are called the Kolmogorov scales whose velocity scale is denoted by v_η , length scale by ℓ_η and time scale by τ_η . We assume that these scales are determined by viscosity, ν , and dissipation, ε . The argument is as follows.

viscosity: Since the kinetic energy is destroyed by viscous forces it is natural to assume that viscosity plays a part in determining these scales; the larger viscosity, the larger scales.

dissipation: The amount of energy per unit time that is to be dissipated is ε . The more energy that is to be transformed from kinetic energy to thermal energy, the larger the velocity gradients must be.

Having assumed that the dissipative scales are determined by viscosity and dissipation, we can express v_η , ℓ_η and τ_η in ν and ε using dimensional analysis. We write

$$\begin{array}{rcl} v_\eta & = & \nu^a \varepsilon^b \\ [m/s] & = & [m^2/s] [m^2/s^3] \end{array} \quad (5.2)$$

where below each variable its dimensions are given. The dimensions of the left and the right side must be the same. We get two equations, one for meters $[m]$

$$1 = 2a + 2b, \quad (5.3)$$

and one for seconds $[s]$

$$-1 = -a - 3b, \quad (5.4)$$

which give $a = b = 1/4$. In the same way we obtain the expressions for ℓ_η and τ_η so that

$$v_\eta = (\nu\varepsilon)^{1/4}, \quad \ell_\eta = \left(\frac{\nu^3}{\varepsilon}\right)^{1/4}, \quad \tau_\eta = \left(\frac{\nu}{\varepsilon}\right)^{1/2} \quad (5.5)$$

5.3 Energy spectrum

As mentioned above, the turbulence fluctuations are composed of a wide range of scales. We can think of them as eddies, see Fig. 5.2. It turns out that it is often convenient to use Fourier series to analyze turbulence. In general, any periodic function, g ,

with a period of $2L$ (i.e. $g(x) = g(x + 2L)$), can be expressed as a Fourier series, i.e.

$$g(x) = \frac{1}{2}a_0 + \sum_{n=1}^{\infty} (a_n \cos(\kappa_n x) + b_n \sin(\kappa_n x)) \quad (5.6)$$

where x is a spatial coordinate and

$$\kappa_n = \frac{n\pi}{L} \quad \text{or} \quad \kappa = \frac{2\pi}{L}. \quad (5.7)$$

κ_n is called the wavenumber. The Fourier coefficients are given by

$$a_n = \frac{1}{L} \int_{-L}^L g(x) \cos(\kappa_n x) dx$$

$$b_n = \frac{1}{L} \int_{-L}^L g(x) \sin(\kappa_n x) dx$$

Parseval's formula states that

$$\int_{-L}^L g^2(x) dx = \frac{L}{2} a_0^2 + L \sum_{n=1}^{\infty} (a_n^2 + b_n^2) \quad (5.8)$$

For readers not familiar to Fourier series, a brief introduction is given in Appendix A1. An example of a Fourier series and spectra are given in Appendix 36. Let g be a fluctuating velocity component, say v'_1 . The left side of Eq. 5.8 expresses v'^2_1 in physical space (vs. x) and the right side v'^2_1 in wavenumber space (vs. κ_n). The reader who is not familiar to the term “wavenumber”, is probably more familiar to “frequency”. In that case, express g in Eq. 5.6 as a series in *time* rather than in *space*. Then the left side of Eq. 5.8 expresses v'^2_1 as a function of time and the right side expresses v'^2_1 as a function of frequency.

The turbulent scales are distributed over a range of scales which extends from the largest scales which interact with the mean flow to the smallest scales where dissipation occurs, see Fig. 5.2. Let us think about how the kinetic energy of the eddies varies with eddy size. Intuitively we assume that large eddies have large fluctuating velocities which implies large kinetic energy, $v'_i v'_i / 2$. It is convenient to study the kinetic energy of each eddy size in wavenumber space. In wavenumber space the energy of eddies can be expressed as

$$E(\kappa) d\kappa \quad (5.9)$$

where Eq. 5.9 expresses the contribution from the scales with wavenumber between κ and $\kappa + d\kappa$ to the turbulent kinetic energy k . The energy spectrum, $E(\kappa)$, corresponds to $g^2(\kappa)$ in Eq. 5.8. The dimension of wavenumber is one over length; thus we can think of wavenumber as proportional to the inverse of an eddy's diameter, i.e. $\kappa \propto 1/d$. The total turbulent kinetic energy is obtained by integrating over the whole wavenumber space, i.e.

$$k = \int_0^{\infty} E(\kappa) d\kappa = L \sum g^2(\kappa_n) \quad (5.10)$$

Think of this equation as a way to compute the kinetic energy by first sorting all eddies by size (i.e. wavenumber), then computing the kinetic energy of each eddy size (i.e. $E(\kappa) d\kappa$), and finally summing the kinetic energy of all eddy sizes (i.e. carrying out the

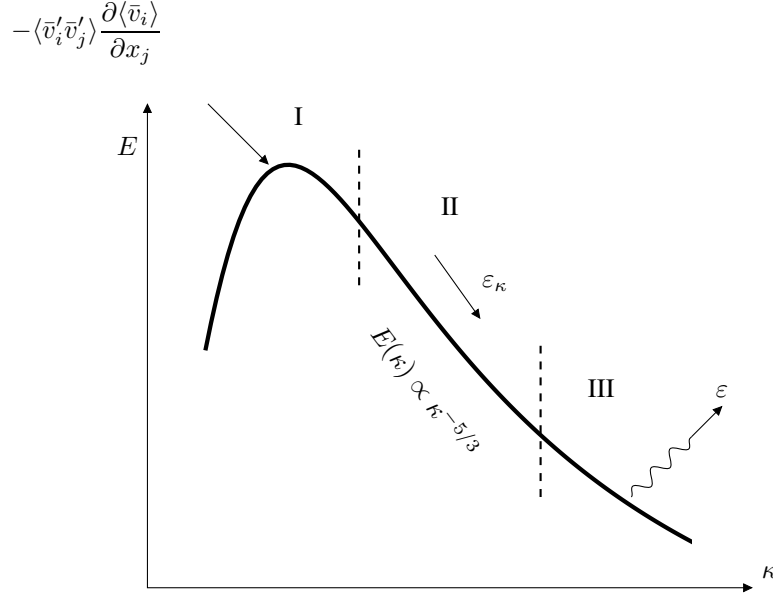


Figure 5.3: Spectrum for turbulent kinetic energy, k . I: Range for the large, energy containing eddies. II: the inertial subrange. III: Range for small, isotropic scales. The wavenumber, κ , is proportional to the inverse of the length scale of a turbulent eddy, ℓ_κ , i.e. $\kappa \propto \ell_\kappa^{-1}$. For a discussion of ε_κ vs. ε , see Section 8.2.2.

integration). Note that the physical meaning of E is kinetic energy *per unit wavenumber* of eddies of size $\ell_\kappa \propto \kappa^{-1}$. Hence the dimension of E is v^2/κ , see Eq. 5.10; for a discussion on the dimension of E , see Appendix 36.

The kinetic energy is the sum of the kinetic energy of the three fluctuating velocity components, i.e.

$$k = \frac{1}{2} (\overline{v_1'^2} + \overline{v_2'^2} + \overline{v_3'^2}) = \frac{1}{2} \overline{v_i' v_i'} \quad (5.11)$$

The spectrum of E is shown in Fig. 5.3. We find region I, II and III which are discussed below.

- I. In this region we have the large eddies which carry most of the energy. These eddies interact with the mean flow and extract energy from the mean flow. This energy transfer takes place via the production term, P^k , in the transport equation for turbulent kinetic energy, see Eq. 8.14. Part of the energy extracted per unit time by the largest eddies is transferred (per unit time) to slightly smaller scales. The eddies' velocity and length scales are v_0 and ℓ_0 , respectively.
- III. Dissipation range. The eddies are small and isotropic and it is here that the dissipation occurs. The energy transfer from turbulent kinetic energy to thermal energy (increased temperature) is governed by ε in the transport equation for turbulent kinetic energy, see Eq. 8.14. The scales of the eddies are described by the Kolmogorov scales (see Eq. 5.5)
- II. Inertial subrange. The existence of this region requires that the Reynolds number is high (fully turbulent flow). The eddies in this region represent the mid-region.

The turbulence is also in this region isotropic. This region is a “transport region” (i.e. in wavenumber space) in the cascade process. The “transport” in wavenumber space is called *spectral transfer*. Energy per time unit, $P^k = \varepsilon$, is coming from the large eddies at the lower part of this range and is transferred per unit time to the dissipation range at the higher part. Note that the relation $P^k = \{\text{dissipation at small scales}\}$, see Fig. 5.3, is given by the assumption of the cascade process, i.e. that the energy transfer per unit time from eddy-size-to-eddy-size is the same for all eddy sizes.

**spectral
transfer**

The kinetic energy, $k_\kappa = v'_{\kappa,i} v'_{\kappa,i} / 2$, of an eddy of size (lengthscale), $1/\kappa$, represents the kinetic energy of all eddies of this size. The kinetic energy of all eddies (of all size) is computed by Eq. 5.11. The eddies in this region are independent of both the large, energy-containing eddies and the eddies in the dissipation range. One can argue that the eddies in this region should be characterized by the spectral transfer of energy per unit time (ε) and the size of the eddies, $1/\kappa$. Dimensional analysis gives

$$\begin{aligned} E &= \kappa^a \varepsilon^b \\ [m^3/s^2] &= [1/m] [m^2/s^3] \end{aligned} \quad (5.12)$$

We get two equations, one for meters $[m]$

$$3 = -a + 2b,$$

and one for seconds $[s]$

$$-2 = -3b,$$

so that $b = 2/3$ and $a = -5/3$. Inserted in Eq. 5.12 we get

$$E(\kappa) = C_K \varepsilon^{2/3} \kappa^{-5/3} \quad (5.13)$$

where the Kolmogorov constant $C_K \simeq 1.5$. This is a very important law (Kolmogorov spectrum law or the $-5/3$ law) which states that, if the flow is fully turbulent (high Reynolds number), the energy spectra should exhibit a $-5/3$ -decay in the inertial region (region II, Fig. 5.3).

Above we state that the eddies in Region II and III are *isotropic*. This means that – in average – the eddies have no preferred direction, i.e. the fluctuations in all directions are the same so that $\overline{v_1'^2} = \overline{v_2'^2} = \overline{v_3'^2}$. Note that is not true instantaneously, i.e. in general $v_1' \neq v_2' \neq v_3'$. Furthermore, isotropic turbulence implies that if a coordinate direction is switched (i.e. rotated 180°), nothing should change. For example if the x_1 coordinate direction is rotated 180° the $\overline{v_1' v_2'}$ should remain the same, i.e. $\overline{v_1' v_2'} = -\overline{v_1' v_2'}$. This is possible only if $\overline{v_1' v_2'} = 0$. Hence, all shear stresses are zero in isotropic turbulence. Using our knowledge in tensor notation, we know that an isotropic tensor can be written as $\text{const.} \cdot \delta_{ij}$. Hence, the Reynolds stress tensor for small scales can be written as $\overline{v_i' v_j'} = \text{const.} \delta_{ij}$ which, again, shows us that the shear stresses are zero in isotropic turbulence.

**isotropic
turbulence**

As discussed on p. 79, the concept of the cascade process assumes that the energy extracted per unit time by the large turbulent eddies is transferred (per unit time) by non-linear interactions through the inertial range to the dissipative range where the kinetic energy is transformed (per unit time) to thermal energy (increased temperature). The spectral transfer rate of kinetic energy from eddies of size $1/\kappa$ to slightly smaller eddies can be estimated as follows. An eddy loses (part of) its kinetic energy during

one revolution. The kinetic energy of the eddy is proportional to v_κ^2 and the time for one revolution is proportional to ℓ_κ/v_κ . Hence, the energy spectral transfer rate, ε_κ , for an eddy of length scale $1/\kappa$ can be estimated as (see Fig. 5.3)

$$\varepsilon_\kappa \sim \frac{v_\kappa^2}{t_\kappa} \sim \frac{v_\kappa^2}{\ell_\kappa/v_\kappa} \sim \frac{v_\kappa^3}{\ell_\kappa} \quad (5.14)$$

Kinetic energy is transferred per unit time to smaller and smaller eddies until the transfer takes place by dissipation (i.e. increased temperature) at the Kolmogorov scales. In the inertial subrange, the cascade process assumes that $\varepsilon_\kappa = \varepsilon$. Applying Eq. 5.14 for the large energy-containing eddies gives

$$\varepsilon_0 \sim \frac{v_0^2}{\ell_0/v_0} \sim \frac{v_0^3}{\ell_0} \sim \varepsilon_\kappa = \varepsilon \quad (5.15)$$

The dissipation at small scales (large wavenumbers) is determined by how much energy per unit time enters the cascade process at the large scales (small wavenumbers). We can now estimate the ratio between the large eddies (with v_0 and ℓ_0) to the Kolmogorov eddies (v_η and ℓ_η). Equations 5.5 and 5.15 give

$$\begin{aligned} \frac{v_0}{v_\eta} &= (\nu\varepsilon)^{-1/4} v_0 = (\nu v_0^3/\ell_0)^{-1/4} v_0 = (v_0 \ell_0/\nu)^{1/4} = Re^{1/4} \\ \frac{\ell_0}{\ell_\eta} &= \left(\frac{\nu^3}{\varepsilon}\right)^{-1/4} \ell_0 = \left(\frac{\nu^3 \ell_0}{v_0^3}\right)^{-1/4} \ell_0 = \left(\frac{\nu^3}{v_0^3 \ell_0^3}\right)^{-1/4} = Re^{3/4} \\ \frac{\tau_0}{\tau_\eta} &= \left(\frac{\nu \ell_0}{v_0^3}\right)^{-1/2} \tau_0 = \left(\frac{v_0^3}{\nu \ell_0}\right)^{1/2} \frac{\ell_0}{v_0} = \left(\frac{v_0 \ell_0}{\nu}\right)^{1/2} = Re^{1/2} \end{aligned} \quad (5.16)$$

where $Re = v_0 \ell_0/\nu$. We find that the ratio of the velocity, length and time scales of the energy-containing eddies to the Kolmogorov eddies increases with increasing Reynolds number. This means that the eddy range (wavenumber range) of the intermediate region (region II, the inertial region) increases with increasing Reynolds number. Hence, the larger the Reynolds number, the larger the wavenumber range of the intermediate range where the eddies are independent of both the large scales and the viscosity. or in other words: the larger the Reynolds number, the larger the difference between the largest and the smallest scales. This is the very reason why it is so expensive (in terms of computer power) to solve the Navier-Stokes equations. With a computational grid we must resolve all eddies. Hence, as the Reynolds number increases, the number of grid cells increases rapidly, see Eq. 28.1.

5.4 The cascade process created by vorticity

The interaction between vorticity and velocity gradients is an essential ingredient to create and maintain turbulence. Disturbances are amplified by interaction between the vorticity vector and the velocity gradients; the disturbances are turned into chaotic, three-dimensional fluctuations, i.e. into turbulence. Two idealized phenomena in this interaction process can be identified: vortex stretching and vortex tilting.

The equation for the instantaneous vorticity ($\omega_i = \bar{\omega}_i + \omega'_i$) reads (see Eq. 4.21)

$$\begin{aligned} \frac{\partial \omega_i}{\partial t} + v_j \frac{\partial \omega_i}{\partial x_j} &= \omega_j \frac{\partial v_i}{\partial x_j} + \nu \frac{\partial^2 \omega_i}{\partial x_j \partial x_j} \\ \omega_i &= \epsilon_{ijk} \frac{\partial v_k}{\partial x_j} \end{aligned} \quad (5.17)$$

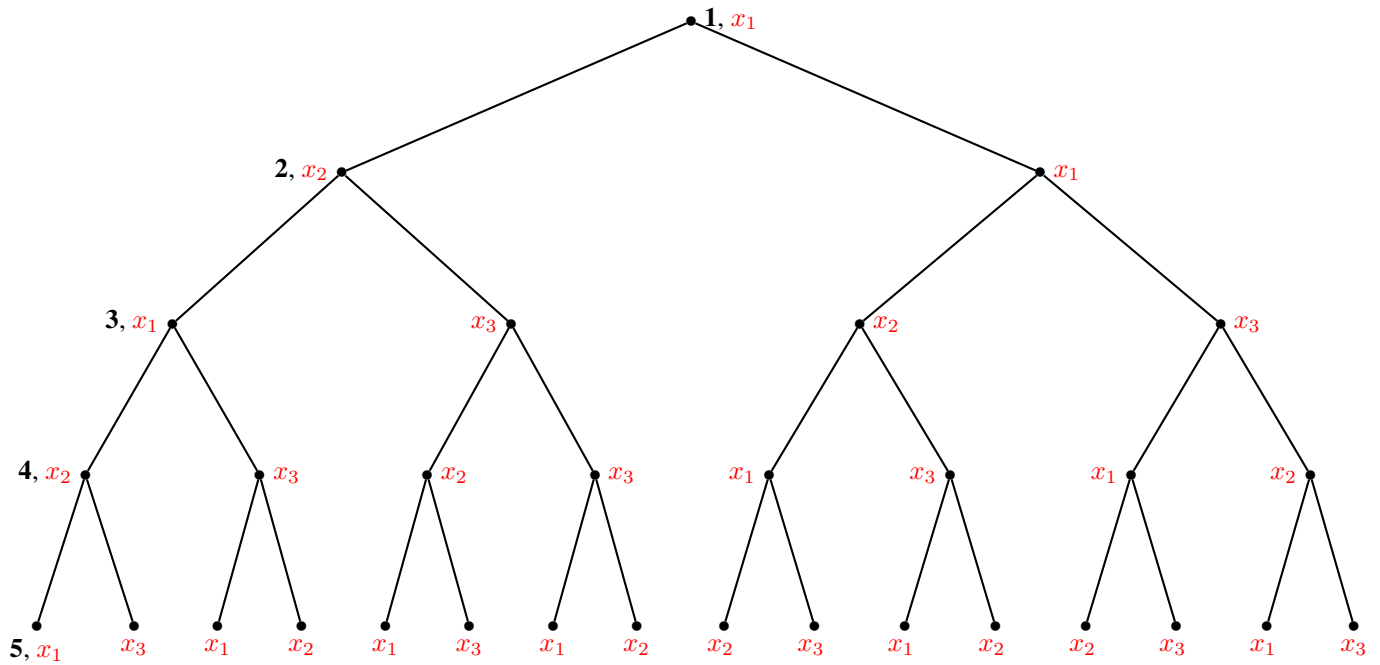


Figure 5.4: Family tree of turbulent eddies (see also Table 5.1). Five generations (indicated in bold). Orientation of eddy is indicated in red. The large original eddy, with axis aligned in the x_1 direction, is 1st generation. Adapted from [15].

generation	x₁	x₂	x₃
1 st	1	0	0
2 nd	0	1	1
3 rd	2	1	1
4 th	2	3	3
5 th	6	5	5
6 th	10	11	11
7 th	22	21	21

Table 5.1: Number of eddies at each generation with their axis aligned in the x_1 , x_2 or x_3 direction, see Fig. 5.4.

As we learnt in Section 4.2 this equation is not an ordinary convection-diffusion equation: it has an additional term on the right side which represents amplification and rotation/tilting of the vorticity lines (the first term on the right side). The $i = j$ components of this term represent (see Eq. 4.22) *vortex stretching*. A positive $\partial v'_1 / \partial x_1$ will stretch the cylinder, see Fig. 4.2 and from the requirement that the volume must not change (incompressible continuity equation) we find that the radius of the cylinder will decrease. We may neglect the viscosity since viscous diffusion at high Reynolds number is much smaller than the turbulent one and since viscous dissipation occurs at small scales (see p. 78). Thus we can assume that there are no viscous stresses acting on the cylindrical fluid element surface which means that the angular momentum

$$r^2 \omega'_1 = \text{const.} \quad (5.18)$$

remains constant as the radius of the fluid element decreases. Note that also the circulation, Γ – which is the integral of the tangential velocity round the perimeter, see Eq. 1.23 – is constant. Equation 5.18 shows that the vorticity increases if the radius decreases (and vice versa). As was mentioned above, the continuity equation shows that stretching results in a decrease of the radius of a slender fluid element and an increase of the vorticity component (i.e. the tangential velocity component) aligned with the element. For example, an extension of a fluid element in one direction (x_1 direction) decreases the length scales in the x_2 direction and increases ω'_1 , see Fig. 5.5. At the same time, vortex tilting creates small-scale vorticity in the x_2 and x_3 direction, ω'_2 and ω'_3 . The increased ω'_1 means that the velocity fluctuation in the x_2 direction is increased, see Fig. 5.6. The increased v'_2 velocity component will stretch smaller fluid elements aligned in the x_2 direction, see Fig. 5.6. This will increase their vorticity ω'_2 and decrease their radius. In the same way will the increased ω'_1 also stretch a fluid element aligned in the x_3 direction and increase ω'_3 and decrease its radius. At each stage, the length scale of the eddies – whose velocity scale are increased – decreases. Figure 5.4 illustrates how a large eddy whose axis is oriented in the x_1 axis in a few generations creates – through vortex stretching – smaller and smaller eddies with larger and larger velocity gradients. Here a generation is related to a wavenumber in the energy spectrum (Fig. 5.3); young generations correspond to high wavenumbers. The smaller the eddies, the less the original orientation of the large eddy is recalled. In other words, the small eddies “don’t remember” the characteristics of their original ancestor. The small eddies have no preferred direction. They are *isotropic*. The creation of multiple eddies by vortex stretching from one original eddies is illustrated in Fig. 5.4 and Table 5.1. The large original eddy (1^{st} generation) is aligned in the x_1 direction. It creates eddies in the x_2 and x_3 direction (2^{nd} generation); the eddies in the x_2 direction create new eddies in the x_1 and x_3 (3^{rd} generation) and so on. For each generation the eddies become more and more isotropic as they get smaller.

The $i \neq j$ components in the first term on the right side in Eq. 4.22 represent *vortex tilting*. Again, take a slender fluid element, now with its axis aligned with the x_2 axis, Fig. 4.3. The velocity gradient $\partial v_1 / \partial x_2$ (or $\partial v'_1 / \partial x_2$, which is equivalent) will tilt the fluid element so that it rotates in the clock-wise direction. As a result, the second term $\omega_2 \partial v_1 / \partial x_2$ in line one in Eq. 4.22 gives a contribution to ω_1 (and ω'_1). This shows how vorticity in one direction is transferred to the other two directions through vortex tilting.

Vortex stretching and vortex tilting qualitatively explain how interaction between vorticity and velocity gradient create vorticity in all three coordinate directions from a disturbance which initially was well defined in one coordinate direction. Once this

**Vortex
stretching**

**Vortex
tilting**

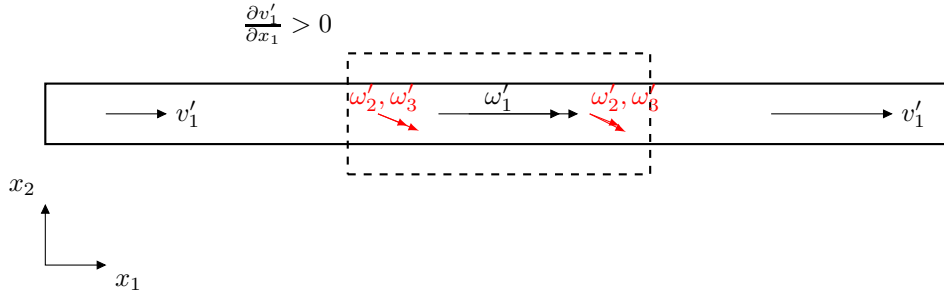


Figure 5.5: A fluid element is stretched by $\frac{\partial v'_1}{\partial x_1} > 0$. Its radius decreases (from dashed line to solid line).

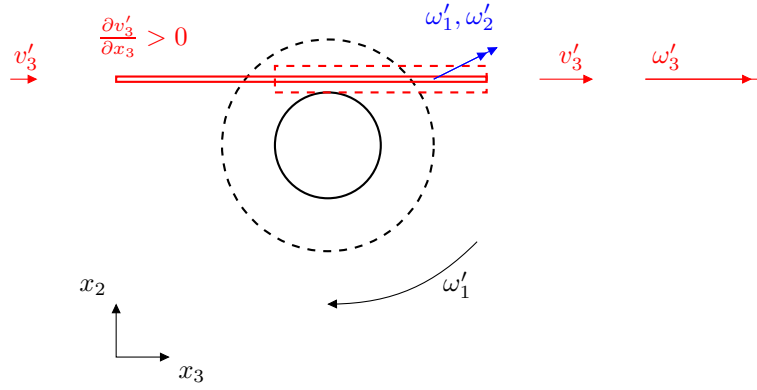


Figure 5.6: The rotation rate of the fluid element (black circles) in Fig. 5.5 increases and its radius decreases. This creates a positive $\frac{\partial v'_3}{\partial x_3} > 0$ which stretches the small red fluid element aligned in the x_3 direction and increases ω'_3 . The radius of the red fluid element decreases.

process has started it continues, because vorticity generated by vortex stretching and vortex tilting interacts with the velocity field and creates further vorticity and so on. The vorticity and velocity field becomes chaotic and three-dimensional: turbulence has been created. The turbulence is also maintained by these processes.

From the discussion above we can now understand why turbulence always must be three-dimensional (Item IV on p. 78). If the instantaneous flow is two-dimensional ($x_1 - x_2$ plane) we find that the vortex-stretching/tilting term on the right side of Eq. 5.17 vanishes because the vorticity vector and the velocity vector are orthogonal. The only non-zero component of vorticity vector is ω_3 because

$$\begin{aligned}\omega_1 &= \frac{\partial v_3}{\partial x_2} - \frac{\partial v_2}{\partial x_3} \equiv 0 \\ \omega_2 &= \frac{\partial v_1}{\partial x_3} - \frac{\partial v_3}{\partial x_1} \equiv 0.\end{aligned}$$

Since $v_3 = 0$, we get $\omega_j \partial v_i / \partial x_j = 0$.

We have seen that the diffusion term in Navier-Stokes include only the strain-rate tensor, S_{ij} , not the vorticity tensor, Ω_{ij} . Here we will show that it is only the strain-rate tensor that creates vorticity, the vorticity tensor does not. The vortex stretching term (Eq. 5.17) read

$$\omega_j \frac{\partial v_i}{\partial x_j}$$

Replace the velocity gradient by

$$s_{ij} + \Omega_{ij}$$

and then replace

$$\Omega_{ij}$$

using Eq. 1.19 which gives

because the product of a symmetric tensor, $\omega_k \omega_i$, and an anti-symmetric tensor, ε_{ijk} , is zero. Hence, vorticity is also created only by s_{ij} .

6 Turbulent mean flow

6.1 Time averaged Navier-Stokes

WHEN the flow is turbulent it is preferable to decompose the instantaneous variables (for example the velocity components and the pressure) into a mean value and a fluctuating value, i.e.

$$\begin{aligned} v_i &= \bar{v}_i + v'_i \\ p &= \bar{p} + p' \end{aligned} \quad (6.1)$$

where the bar, $\bar{\cdot}$, denotes the time averaged value defined as

$$\bar{v} = \frac{1}{2T} \int_{-T}^T v dt. \quad (6.2)$$

where T is sufficiently large. When we time average Eq. 6.1 we get

$$\bar{v}_i = \overline{\bar{v}_i + v'_i} = \bar{v}_i + \overline{v'_i} \quad (6.3)$$

where we used the fact that $\overline{\bar{v}_i} = \bar{v}_i$, see Section 8.1.4. Hence, Eq. 6.3 gives

$$\overline{v'_i} = 0, \quad \overline{p'} = 0 \quad (6.4)$$

One reason why we decompose the variables is that when we measure flow quantities we are usually interested in their mean values rather than their time histories. Another reason is that when we want to solve the Navier-Stokes equation numerically it would require a very fine grid to resolve all turbulent scales and it would also require a fine resolution in time (turbulence is always unsteady).

The continuity equation and the Navier-Stokes equation for incompressible flow with constant viscosity read

$$\frac{\partial v_i}{\partial x_i} = 0 \quad (6.5)$$

$$\rho \frac{\partial v_i}{\partial t} + \rho \frac{\partial v_i v_j}{\partial x_j} = -\frac{\partial p}{\partial x_i} + \mu \frac{\partial^2 v_i}{\partial x_j \partial x_j} \quad (6.6)$$

The gravitation term, $-\rho g_i$, has been omitted which means that the p is the *hydrodynamic* pressure (i.e. when $v_i \equiv 0$, then $p \equiv 0$, see p. 43). Inserting Eq. 6.1 into the continuity equation (6.5)

$$\frac{\partial \overline{\bar{v}_i + v'_i}}{\partial x_i} = \frac{\partial \bar{v}_i}{\partial x_i} + \frac{\partial \overline{v'_i}}{\partial x_i} = \frac{\partial \bar{v}_i}{\partial x_i} = \frac{\partial \bar{v}_i}{\partial x_i} \quad (6.7)$$

where we used the fact that $\overline{v'_i} = 0$ (see Eq. 6.4 and $\overline{\bar{v}_i} = \bar{v}_i$, see section 8.1.4).

Next, we use the decomposition in Navier-Stokes equation (Eq. 6.6)

$$\underbrace{\rho \frac{\partial (\bar{v}_i + v'_i)}{\partial t}}_I + \underbrace{\rho \frac{\partial (\bar{v}_i + v'_i)(\bar{v}_j + v'_j)}{\partial x_j}}_{II} = -\underbrace{\frac{\partial (\bar{p} + p')}{\partial x_i}}_{III} + \underbrace{\mu \frac{\partial^2 (\bar{v}_i + v'_i)}{\partial x_j \partial x_j}}_{IV} \quad (6.8)$$

Let us consider the equation term-by-term.

Term I:

$$\frac{\partial(\bar{v}_i + v'_i)}{\partial t} = \frac{\partial \bar{v}_i}{\partial t} + \frac{\partial v'_i}{\partial t} = \frac{\partial \bar{v}_i}{\partial t} = \frac{\partial \bar{v}_i}{\partial t}$$

We assume that the mean flow, \bar{v}_i , is steady, and hence the term is zero.

Term II:

$$\begin{aligned} \frac{\partial(\bar{v}_i + v'_i)(\bar{v}_j + v'_j)}{\partial x_j} &= \frac{\partial \bar{v}_i \bar{v}_j + \bar{v}_i v'_j + v'_i \bar{v}_j + v'_i v'_j}{\partial x_j} \\ &= \frac{\partial \bar{v}_i \bar{v}_j}{\partial x_j} + \frac{\partial \bar{v}_i v'_j}{\partial x_j} + \frac{\partial v'_i \bar{v}_j}{\partial x_j} + \frac{\partial v'_i v'_j}{\partial x_j} \end{aligned}$$

- Section 8.1.4 shows that $\bar{v}_i \bar{v}_j = \bar{v}_i \bar{v}_j$.
- Section 8.1.3 shows that $\bar{v}_i v'_j = \bar{v}_i v'_j = 0$ and $\bar{v}_j v'_i = \bar{v}_j v'_i = 0$

Hence, Term II reads

$$\frac{\partial \bar{v}_i \bar{v}_j}{\partial x_j} + \frac{\partial v'_i v'_j}{\partial x_j}$$

Term III:

$$\frac{\partial(\bar{p} + p')}{\partial x_i} = \frac{\partial \bar{p}}{\partial x_i} + \frac{\partial p'}{\partial x_i} = \frac{\partial \bar{p}}{\partial x_i}$$

Term IV:

$$\frac{\partial^2(\bar{v}_i + v'_i)}{\partial x_j \partial x_j} = \frac{\partial^2 \bar{v}_i}{\partial x_j \partial x_j} + \frac{\partial^2 v'_i}{\partial x_j \partial x_j} = \frac{\partial^2 \bar{v}_i}{\partial x_j \partial x_j}$$

Now we can finally write the *time averaged* continuity equation and Navier-Stokes equation

$$\frac{\partial \bar{v}_i}{\partial x_i} = 0 \quad (6.9)$$

$$\rho \frac{\partial \bar{v}_i \bar{v}_j}{\partial x_j} = -\frac{\partial \bar{p}}{\partial x_i} + \frac{\partial}{\partial x_j} \left(\mu \frac{\partial \bar{v}_i}{\partial x_j} - \rho \overline{v'_i v'_j} \right) \quad (6.10)$$

It is assumed that the mean flow is steady. This equation is the time-averaged Navier-Stokes equation and it is often called the *Reynolds Averaged Navier-Stokes* (RANS) equation. A new term $\overline{\rho v'_i v'_j}$ appears on the right side of Eq. 6.10 which is called the *Reynolds stress tensor*. The tensor is symmetric (for example $\overline{v'_1 v'_2} = \overline{v'_2 v'_1}$). It represents correlations between fluctuating velocities. It is an additional stress term due to turbulence (fluctuating velocities) and it is unknown. We need a model for $\overline{v'_i v'_j}$ to close the equation system in Eq. 6.10. This is called the *closure problem*: the number of unknowns (ten: three velocity components, pressure, six stresses) is larger than the number of equations (four: the continuity equation and three components of the Navier-Stokes equations).

RANS

closure problem

The continuity equation applies both for the instantaneous velocity, v_i (Eq. 6.5), and for the time-averaged velocity, \bar{v}_i (Eq. 6.9); hence it applies also for the fluctuating velocity, v'_i , i.e.

$$\frac{\partial v'_i}{\partial x_i} = 0 \quad (6.11)$$

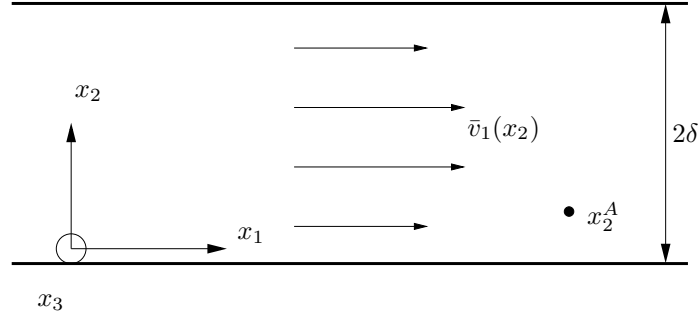


Figure 6.1: Flow between two infinite parallel plates. The width (i.e. length in the x_3 direction) of the plates, Z_{max} , is much larger than the separation between the plates, i.e. $Z_{max} \gg \delta$.

6.1.1 Boundary-layer approximation

For boundary-layer type of flow (i.e. boundary layers along a flat plate, channel flow, pipe flow, jet and wake flow, etc.) the following relations apply

$$\bar{v}_2 \ll \bar{v}_1, \quad \frac{\partial \bar{v}_1}{\partial x_1} \ll \frac{\partial \bar{v}_1}{\partial x_2}, \quad (6.12)$$

Assume steady ($\partial/\partial t = 0$), two-dimensional ($\bar{v}_3 = \partial/\partial x_3 = 0$) boundary-layer flow. First we re-write the left side of Eq. 6.10 using the continuity equation

$$\rho \frac{\partial \bar{v}_i \bar{v}_j}{\partial x_j} = \rho \bar{v}_j \frac{\partial \bar{v}_i}{\partial x_j} + \underbrace{\rho \bar{v}_i \frac{\partial \bar{v}_j}{\partial x_j}}_{=0} = \rho \bar{v}_j \frac{\partial \bar{v}_i}{\partial x_j} \quad (6.13)$$

Using Eq. 6.13, Eq. 6.10 can be written

$$\rho \bar{v}_1 \frac{\partial \bar{v}_1}{\partial x_1} + \rho \bar{v}_2 \frac{\partial \bar{v}_1}{\partial x_2} = -\frac{\partial \bar{p}}{\partial x_1} + \frac{\partial}{\partial x_2} \left[\underbrace{\mu \frac{\partial \bar{v}_1}{\partial x_2} - \overline{\rho v'_1 v'_2}}_{\tau_{12,tot}} \right] \quad (6.14)$$

x_1 and x_2 denote the streamwise and wall-normal coordinate, respectively, see Fig. 6.1. Note that the two terms on the left side are of the same order, because they both include the product of one large (\bar{v}_1 or $\partial/\partial x_2$) and one small (\bar{v}_2 or $\partial/\partial x_1$) part.

In addition to the viscous shear stress, $\mu \partial \bar{v}_1 / \partial x_2$, an additional *turbulent* one – a **shear stress** Reynolds shear stress – appears on the right side of Eq. 6.14. The total shear stress is thus

$$\tau_{12,tot} = \mu \frac{\partial \bar{v}_1}{\partial x_2} - \overline{\rho v'_1 v'_2} \quad (6.15)$$

6.2 Wall region in fully developed channel flow

The region near the wall is very important. Here the velocity gradient is largest as the velocity drops down to zero at the wall over a very short distance. One important quantity is the wall shear stress which is defined as

$$\tau_w = \mu \left. \frac{\partial \bar{v}_1}{\partial x_2} \right|_w \quad (6.16)$$

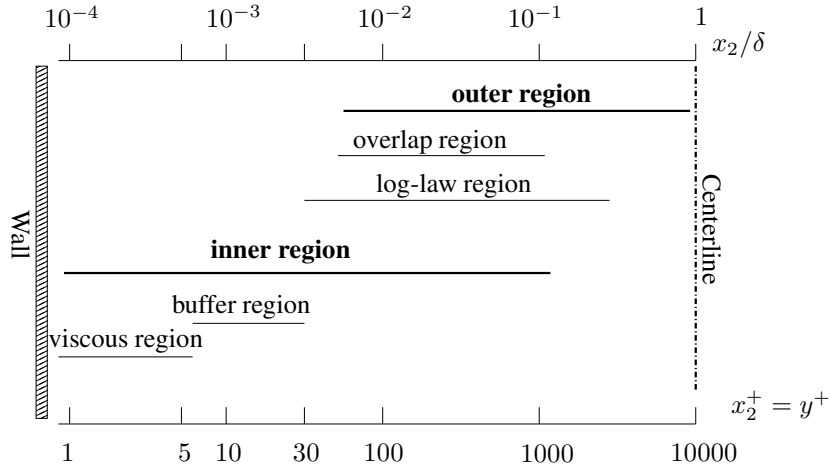


Figure 6.2: The wall region (adapted from Ch.7 in [13]) for $Re_\tau = 10\,000$. δ denotes half width of the channel, see Fig. 6.1 and $x_2^+ = x_2 u_\tau / \nu$ denotes the normalized wall distance.

From the wall shear stress, we can define a *wall friction velocity*, u_τ , as

$$\tau_w = \rho u_\tau^2 \Rightarrow u_\tau = \left(\frac{\tau_w}{\rho} \right)^{1/2} \quad (6.17)$$

**wall
friction
velocity**

In order to take a closer look at the near-wall region, let us, again, consider fully developed channel flow between two infinite plates, see Fig. 6.1. In fully developed channel flow, the streamwise derivative of the streamwise velocity component is zero (this *is* the definition of fully developed flow), i.e. $\partial \bar{v}_1 / \partial x_1 = 0$. The continuity equation gives now $\bar{v}_2 = 0$, see Eq. 3.18 at p. 43. The first term on the left side of Eq. 6.14 is zero because we have fully developed flow ($\partial \bar{v}_1 / \partial x_1 = 0$) and the last term is zero because $\bar{v}_2 \equiv 0$. The streamwise momentum equation, Eq. 6.14, can now be written

$$0 = -\frac{\partial \bar{p}}{\partial x_1} + \frac{\partial}{\partial x_2} \left(\mu \frac{\partial \bar{v}_1}{\partial x_2} - \overline{\rho v'_1 v'_2} \right) \quad (6.18)$$

We know that the first term is a function only of x_1 and the two terms in parenthesis are functions of x_2 only; hence they must be constant (see Eq. 3.24 and the text related to this equation), i.e.

$$\begin{aligned} -\frac{\partial \bar{p}}{\partial x_1} &= \text{constant} \\ \frac{\partial}{\partial x_2} \left(\mu \frac{\partial \bar{v}_1}{\partial x_2} - \overline{\rho v'_1 v'_2} \right) &= \frac{\partial \tau_{12,tot}}{\partial x_2} = \text{constant} \end{aligned} \quad (6.19)$$

where the total stress, $\tau_{12,tot}$, is given by Eq. 6.15. Integrating Eq. 6.18 from $x_2 = 0$ to x_2 gives

$$\tau_{12,tot}(x_2) - \tau_w = \frac{\partial \bar{p}}{\partial x_1} x_2 \Rightarrow \tau_{12,tot} = \tau_w + \frac{\partial \bar{p}}{\partial x_1} x_2 = \tau_w \left(1 - \frac{x_2}{\delta} \right) \quad (6.20)$$

At the last step we used the fact that the pressure gradient balances the wall shear stress, i.e. $-\partial \bar{p} / \partial x_1 = \tau_w / \delta$, see Eq. 3.30 (note that $h = 2\delta$) and Eq. 6.39.

The wall region can be divided into one outer and one inner region, see Fig. 6.2. The inner region includes the viscous region, $x_2^+ \lesssim 5$ (dominated by the viscous diffusion), and the logarithmic region, $x_2^+ \gtrsim 30$ (dominated by turbulent diffusion); the logarithmic region is sometimes called the *inertial region*, because the turbulent stresses stem from the inertial (i.e. the non-linear convection) term. The buffer region acts as a transition region between these two regions where viscous diffusion of streamwise momentum is gradually replaced by turbulent diffusion. In the inner region, the total shear stress is approximately constant and equal to the wall shear stress τ_w , see Fig. 6.3. Note that the total shear stress is constant only close to the wall (Fig. 6.3b); further away from the wall it decreases (in fully developed channel flow it decreases linearly with the distance from the wall, see Eq. 6.20 and Fig. 6.3a). The Reynolds shear stress vanishes at the wall because $v'_1 = v'_2 = 0$, and the viscous shear stress attains its wall-stress value $\tau_w = \rho u_\tau^2$. As we go away from the wall the viscous stress decreases and the turbulent one increases and at $x_2^+ \simeq 11$ they are approximately equal. In the logarithmic layer the viscous stress is negligible compared to the Reynolds stress.

At the wall, the velocity gradient is directly related to the wall shear stress, i.e. (see Eq. 6.16 and 6.17)

$$\left. \frac{\partial \bar{v}_1}{\partial x_2} \right|_w = \frac{\tau_w}{\mu} = \frac{\rho}{\mu} u_\tau^2 = \frac{1}{\nu} u_\tau^2 \quad (6.21)$$

Integration gives (recall that both ν and u_τ^2 are constant)

$$\bar{v}_1 = \frac{1}{\nu} u_\tau^2 x_2 + C_1$$

Since the velocity, \bar{v}_1 , is zero at the wall, the integration constant $C_1 = 0$ so that

$$\frac{\bar{v}_1}{u_\tau} = \frac{u_\tau x_2}{\nu} \quad (6.22)$$

Equation 6.22 is expressed in *inner scaling* (or wall scaling) which means that \bar{v}_1 and x_2 are normalized with quantities related to the wall, i.e. the friction velocity stemming from the wall shear stress and the viscosity (here we regard viscosity as a quantity related to the wall, since the flow is dominated by viscosity). The plus-sign ('+') is used to denote inner scaling, i.e.

$$\begin{aligned} \bar{v}_1^+ &\equiv \frac{\bar{v}_1}{u_\tau} \\ x_2^+ &\equiv \frac{u_\tau x_2}{\nu} \end{aligned} \quad (6.23)$$

Now equation Eq. 6.22 can then be written as

$$\bar{v}_1^+ = x_2^+ \quad (6.24)$$

From the friction velocity and the viscosity we can define the *viscous length scale*, ℓ_ν , for the near-wall region as

$$x_2^+ = x_2 / \ell_\nu \Rightarrow \ell_\nu = \frac{\nu}{u_\tau} \quad (6.25)$$

Further away from the wall at $30 \lesssim x_2^+ \lesssim 3000$ (or $0.003 \lesssim x_2 / \delta \lesssim 0.3$), we encounter the *log-law region*, see Fig. 6.2. In this region the flow is assumed to be

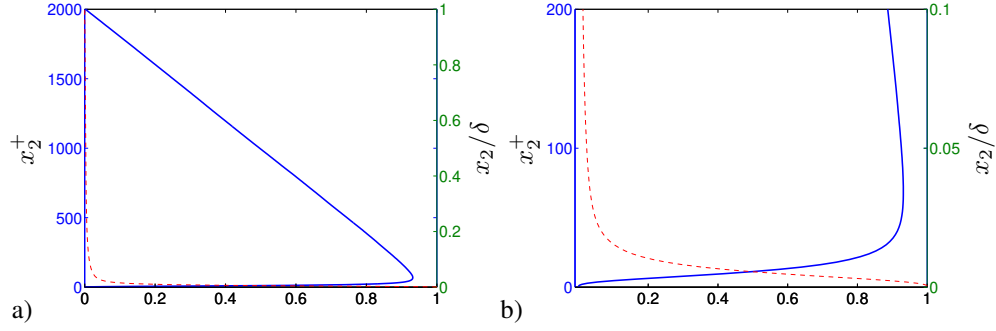


Figure 6.3: Reynolds shear stress. $Re_\tau = 2000$. a) lower half of the channel; b) zoom near the wall. DNS (Direct Numerical Simulation) data [16, 17]. — : $-\rho \overline{v_1' v_2'} / \tau_w$; - - : $\mu(\partial^2 \bar{v}_1 / \partial x_2^2) / \tau_w$.

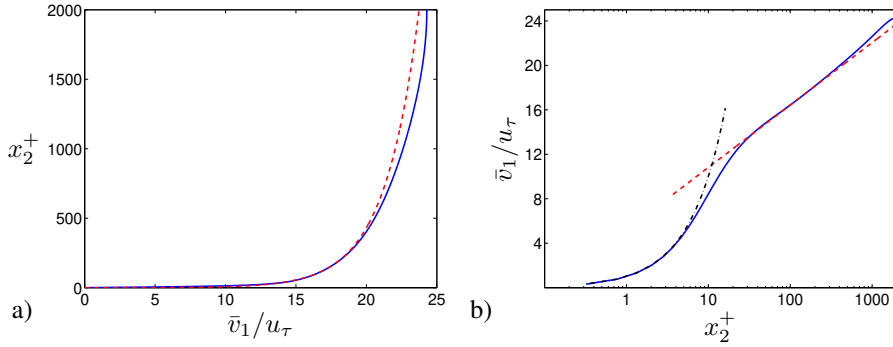


Figure 6.4: Velocity profiles in fully developed channel flow. $Re_\tau = 2000$. — : DNS (Direct Numerical Simulation) data [16, 17]; - - : $\bar{v}_1 / u_\tau = (\ln x_2^+) / 0.41 + 5.2$; - · - : $\bar{v}_1 / u_\tau = x_2^+$.

independent of viscosity. The Reynolds shear stress, $\overline{\rho v_1' v_2'}$, is in the region $x_2^+ \lesssim 200$ (i.e. $x_2 / \delta \lesssim 0.1$) fairly constant and approximately equal to the wall shear stress, i.e.

$$\tau_w = \rho \overline{|v_1' v_2'|} \quad (6.26)$$

see Fig. 6.3b. Hence the friction velocity, u_τ , is a suitable velocity scale in the inner logarithmic region; it is used in the entire region.

What about the length scale? Near the wall, an eddy cannot be larger than the distance to the wall and it is the distance to the wall that sets an upper limit on the eddy-size. Hence it seems reasonable to take the wall distance as the characteristic length scale; a constant, κ , is added so that

$$\ell = \kappa x_2. \quad (6.27)$$

where κ is the von Kármán constant, $\kappa = 0.41$. The velocity gradient can now be estimated as

$$\frac{\partial \bar{v}_1}{\partial x_2} = \frac{u_\tau}{\kappa x_2} \quad (6.28)$$

based on the velocity scale, u_τ , and the length scale κx_2 . Another way of deriving the expression in Eq. 6.28 is to use the Boussinesq assumption (see Eq. 11.33) in which a turbulent Reynolds stress is assumed to be equal to the product between the turbulent

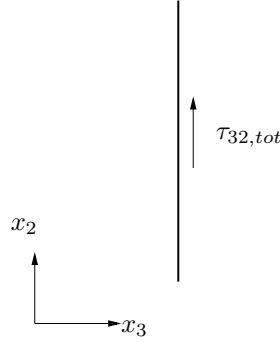


Figure 6.5: Symmetry plane of channel flow.

viscosity and the velocity gradient as

$$-\overline{v_1' v_2'} = \nu_t \frac{\partial \bar{v}_1}{\partial x_2} \quad (6.29)$$

The turbulent viscosity, ν_t , represents the turbulence and has the same dimension as ν , i.e. $[m^2/s]$. Hence ν_t can be expressed as a product of a turbulent velocity scale and a turbulent length scale, and in the log-law region that gives

$$\nu_t = u_\tau \kappa x_2 \quad (6.30)$$

so that Eq. 6.29 gives (inserting $-\overline{v_1' v_2'} = u_\tau^2$)

$$u_\tau^2 = \kappa u_\tau x_2 \frac{\partial \bar{v}_1}{\partial x_2} \Rightarrow \frac{\partial \bar{v}_1}{\partial x_2} = \frac{u_\tau}{\kappa x_2} \quad (6.31)$$

In non-dimensional form Eqs. 6.28 and 6.31 read

$$\frac{\partial \bar{v}_1^+}{\partial x_2^+} = \frac{1}{\kappa x_2^+} \quad (6.32)$$

Integration gives now

$$\begin{aligned} \bar{v}_1^+ &= \frac{1}{\kappa} \ln(x_2^+) + B \quad \text{or} \\ \frac{\bar{v}_1}{u_\tau} &= \frac{1}{\kappa} \ln\left(\frac{x_2 u_\tau}{\nu}\right) + B \end{aligned} \quad (6.33)$$

where B is an integration constant. Equation 6.33 is the logarithmic law due to von Kármán [18]. The constant, κ , is called the von Kármán constant. The constants in the log-law are usually set to $\kappa = 0.41$ and $B = 5.2$.

log-law

As can be seen in Fig. 6.2 the log-law applies for $x_2^+ \lesssim 3000$ ($x_2/\delta \lesssim 0.3$). Figure 6.4 – where the Reynolds number is lower than in Fig. 6.2 – shows that the log-law fit the DNS (Direct Numerical Simulation) up to $x_2^+ \lesssim 500$ ($x_2/\delta \lesssim 0.25$). Hence, the upper limit for the validity of the log-law is dependent on Reynolds number; the larger the Reynolds number, the larger the upper limit.

In the outer region of the boundary layer, the relevant length scale is the boundary layer thickness. The resulting velocity law is the *defect law*

$$\frac{\bar{v}_{1,c} - \bar{v}_1}{u_\tau} = F_D\left(\frac{x_2}{\delta}\right) \quad (6.34)$$

where c denotes centerline. The velocity in the log-region and the outer region (often called the wake region) can be written as

$$\frac{\bar{v}_1}{u_\tau} = \frac{1}{\kappa} \ln(y^+) + B + \frac{2\Pi}{\kappa} \sin^2\left(\frac{\pi x_2}{2\delta}\right) \quad (6.35)$$

where $\kappa = 0.38$, $B = 4.1$ and $\Pi = 0.5$ are taken from boundary layer flow [19–21].

6.3 Reynolds stresses in fully developed channel flow

The flow is two-dimensional ($\bar{v}_3 = 0$ and $\partial/\partial x_3 = 0$). Consider the $x_2 - x_3$ plane, see Fig. 6.5. Since nothing changes in the x_3 direction, the viscous shear stress

$$\tau_{32} = \mu \left(\frac{\partial \bar{v}_3}{\partial x_2} + \frac{\partial \bar{v}_2}{\partial x_3} \right) = 0 \quad (6.36)$$

because $\bar{v}_3 = \partial \bar{v}_2 / \partial x_3 = 0$. The turbulent part shear stress, $\overline{\rho v'_2 v'_3}$, can be expressed using the Boussinesq assumption (see Eq. 11.33)

$$-\overline{\rho v'_2 v'_3} = \mu_t \left(\frac{\partial \bar{v}_3}{\partial x_2} + \frac{\partial \bar{v}_2}{\partial x_3} \right) = 0 \quad (6.37)$$

and it is also zero since $\bar{v}_3 = \partial \bar{v}_2 / \partial x_3 = 0$. With the same argument, $\overline{v'_1 v'_3} = 0$. However note that $\overline{v'^2_3} = \overline{v'^2_3} \neq 0$. The reason is that although the *time-averaged* flow is two-dimensional (i.e. $\bar{v}_3 = 0$), the instantaneous turbulent flow is always three-dimensional and unsteady. Hence $v_3 \neq 0$ and $v'_3 \neq 0$ so that $v'^2_3 \neq 0$. Consider, for example, the time series $v_3 = v'_3 = (-0.25, 0.125, 0.125, -0.2, 0.2)$. This gives

$$\bar{v}_3 = (-0.25 + 0.125 + 0.125 - 0.2 + 0.2)/5 = 0$$

but

$$\overline{v'^2_3} = \overline{v'^2_3} = [(-0.25)^2 + 0.125^2 + 0.125^2 + (-0.2)^2 + 0.2^2] / 5 = 0.03475 \neq 0.$$

Figure 6.3 presents the Reynolds and the viscous shear stresses for fully developed flow. As can be seen, the viscous shear stress is negligible except very near the wall. It is equal to one near the wall and decreases rapidly for increasing wall distance. On the other hand, the Reynolds shear stress is zero at the wall (because the fluctuating velocities are zero at the wall) and increases for increasing wall distance. The intersection of the two shear stresses takes place at $x_2^+ \simeq 11$.

Looking at Eq. 6.18 we find that it is not really the shear stress that is interesting, but its gradient. The gradient of the shear stress, $-\partial(\overline{\rho v'_1 v'_2})/\partial x_2$ and $\mu \partial^2 \bar{v}_1 / \partial x_2^2$ represent, together with the pressure gradient, $-\partial \bar{p} / \partial x_1$, the *forces* acting on the fluid. Figure 6.6 presents the forces. Start by looking at Fig. 6.6b which shows the forces in the region away from the wall, see the red fluid particle in Fig. 6.7. The pressure gradient is constant and equal to one: this is the force *driving* the flow. This agrees – fortunately – with our intuition. We can imagine that the fluid (air, for example) is driven by a fan. Another way to describe the behaviour of the pressure is to say that there is a pressure drop. The pressure must decrease in the streamwise direction so that the pressure gradient term, $-\partial \bar{p} / \partial x_1$, in Eq. 6.18 takes a positive value which pushes the flow in the x_1 direction. The force that balances the pressure gradient is the gradient of the Reynolds shear stress. This is the force *opposing* the movement of the fluid. This

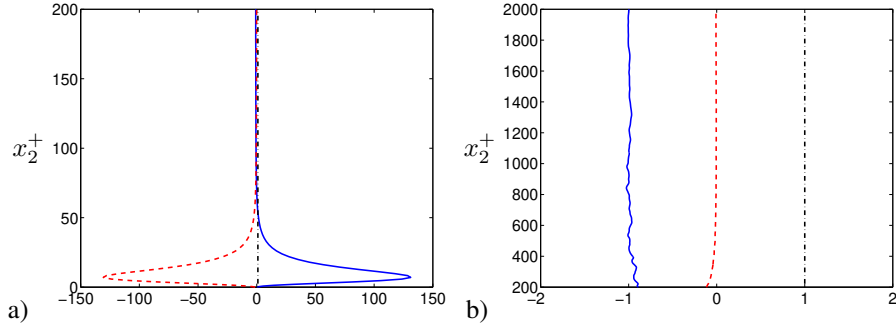


Figure 6.6: Fully developed channel flow. $Re_\tau = 2000$. Forces in the \bar{v}_1 equation, see Eq. 6.18. a) near the lower wall of the channel; b) lower half of the channel excluding the near-wall region. DNS (Direct Numerical Simulation) data [16, 17]. — : $-\rho(\partial \bar{v}_1' v_2' / \partial x_2) / \tau_w$; - - : $\mu(\partial^2 \bar{v}_1 / \partial x_2^2) / \tau_w$; - · - : $-(\partial \bar{p} / \partial x_1) / \tau_w$.

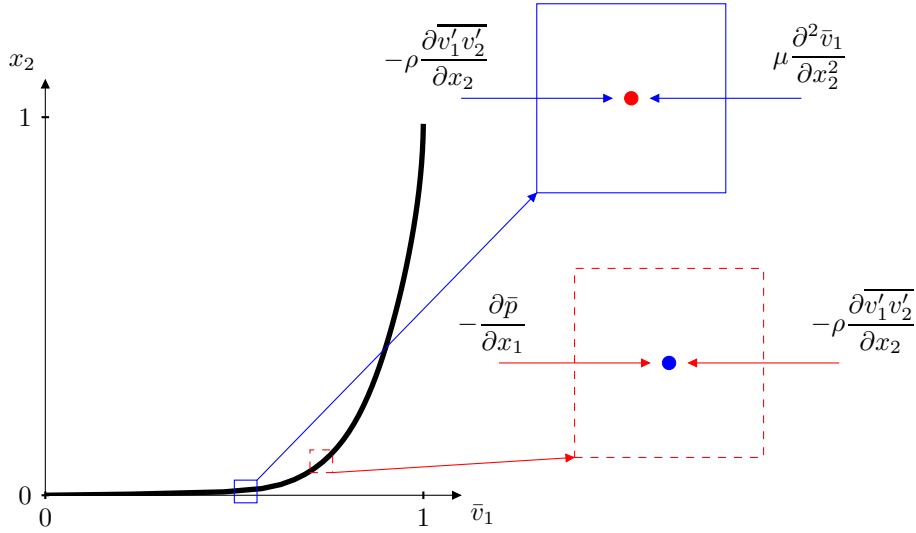


Figure 6.7: Forces in a boundary layer. The red (dashed line) and the blue (solid line) fluid particle are located at $x_2^+ \simeq 400$ and $x_2^+ \simeq 20$, respectively (see Fig. 6.6).

opposing force has its origin at the walls due to the viscous wall force (viscous shear stress multiplied by area).

Now let us have a look at the forces in the near-wall region, see Fig. 6.6a. Here the forces are two orders of magnitude larger than in Fig. 6.6b but they act over a very thin region ($x_2^+ \leq 40$ or $x_2/\delta < 0.02$). In this region the Reynolds shear stress gradient term is *driving* the flow and the opposing force is the viscous force, see the blue fluid particle in Fig. 6.7. We can of course make a force balance for a section of the channel, as we did for laminar flow, see Eq. 3.36 at p. 45 and Fig. 3.9 at p. 46 which reads

$$0 = \bar{p}_1 Z_{max} 2\delta - \bar{p}_2 Z_{max} 2\delta - 2\tau_w L Z_{max} \quad (6.38)$$

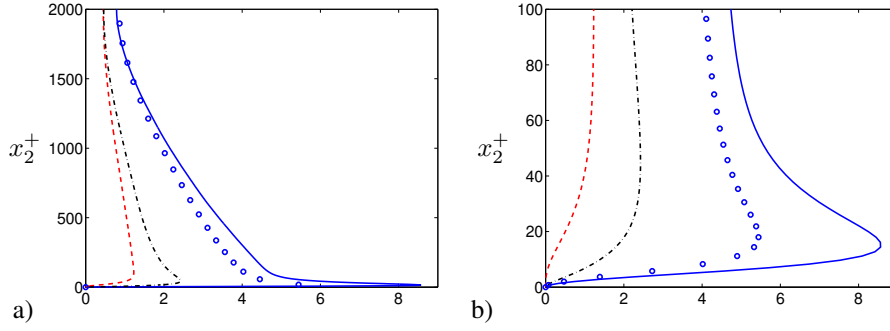


Figure 6.8: Normal Reynolds stresses and turbulent kinetic energy. $Re_\tau = 2000$. DNS (Direct Numerical Simulation) data [16, 17]. — : $\overline{\rho v_1'^2}/\tau_w$; - - : $\overline{\rho v_2'^2}/\tau_w$; - · - : $\overline{\rho v_3'^2}/\tau_w$; ○ : k/u_τ^2 .

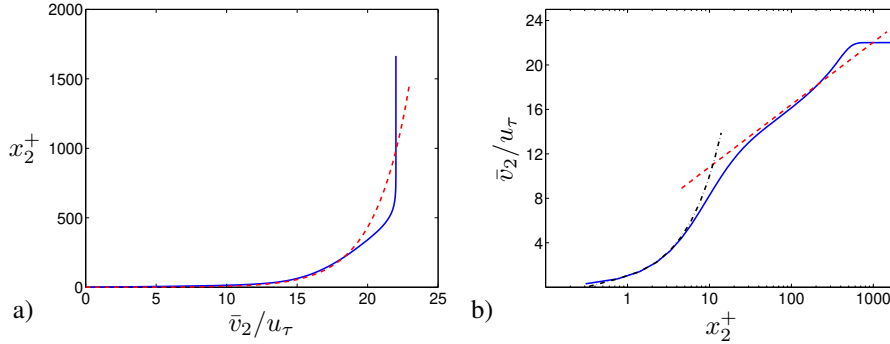


Figure 6.9: Velocity profiles in a boundary layer along a flat plate. — : DNS (Direct Numerical Simulation) data [22]; - - : $\bar{v}_2/u_\tau = (\ln x_2^+)/0.41 + 5.2$; - · - : $\bar{v}_2/u_\tau = x_2^+$.

where L is the length of the section. We get

$$\frac{\Delta \bar{p}}{L} = -\frac{\partial \bar{p}}{\partial x_1} = \frac{\tau_w}{\delta} \quad (6.39)$$

As can be seen the pressure drop is directly related to the wall shear stress. In turbulent flow the velocity profile in the center region is much flatter than in laminar flow (cf. Fig. 6.4 and Fig. 3.8 at p. 45). This makes the velocity gradient near the wall (and the wall shear stress, τ_w) much larger in turbulent flow than in laminar flow: Eq. 6.39 shows why the pressure drop is larger in the former case compared to the latter; or — in other words — why a larger fan is required to push the flow in turbulent flow than in laminar flow.

Figure 6.8 presents the normal Reynolds stresses, $\overline{\rho v_1'^2}$, $\overline{\rho v_2'^2}$ and $\overline{\rho v_3'^2}$. As can be seen, the streamwise stress is largest and the wall-normal stress is smallest. The former is largest because the mean flow is in this direction; the latter is smallest because the turbulent fluctuations are damped by the wall. The turbulent kinetic energy, $k = \overline{v_i' v_i'}/2$, is also included. Note that this is smaller than $\overline{v_1'^2}$.

6.4 Boundary layer

Up to now we have mainly discussed fully developed channel flow. What is the difference between that flow and a boundary layer flow? First, in a boundary layer flow

the convective terms are not zero (or negligible), i.e. the left side of Eq. 6.14 is not zero. The flow in a boundary layer is continuously developing, i.e. its thickness, δ , increases continuously for increasing x_1 . The flow in a boundary layer is described by Eq. 6.14. Second, in a boundary layer flow the wall shear stress is not determined by the pressure drop (indeed it is zero); the total shear stress is balanced by the convective terms. Third, the outer part of the boundary layer is highly intermittent, consisting of turbulent/non-turbulent motion.

However, the inner region of a boundary layer ($x_2/\delta < 0.1$) is principally the same as for the fully developed channel flow, see Fig. 6.9: the linear and the log-law regions are very similar for the two flows. However, in boundary layer flow the log-law is valid only up to approximately $x_2/\delta \simeq 0.1$ (compared to approximately $x_2/\delta \simeq 0.3$ in channel flow)

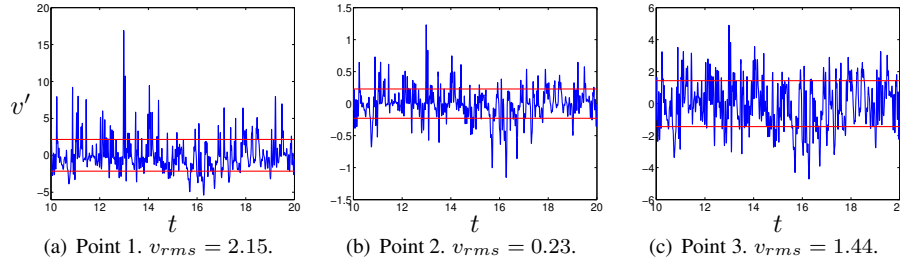


Figure 7.1: Time history of v' . Horizontal red lines show $\pm v_{rms}$.

7 Probability density functions

SOME statistical information is obtained by forming the mean and second moments, for example \bar{v} and $\overline{v'^2}$, as was done in Section 6. The *root-mean-square* (RMS) can be defined from the second moment as

$$v_{rms} = \left(\overline{v'^2} \right)^{1/2} \quad (7.1)$$

**root-mean-square
RMS**

The RMS is the same as the *standard deviation* which is equal to the square-root of the *variance*. In order to extract more information, probability density function is a useful statistical tool to analyze turbulence. From the velocity signals we can compute the probability densities (sometimes called *histograms*). With a probability density, f_v , of the v velocity, the mean velocity is computed as

**standard
deviation
variance**

$$\bar{v} = \int_{-\infty}^{\infty} v f_v(v) dv \quad (7.2)$$

Normalize the probability functions, so that

$$\int_{-\infty}^{\infty} f_v(v) dv = 1 \quad (7.3)$$

Here we integrate over v . The mean velocity can of course also be computed by integrating over time, as we do when we define a time average, (see Eq. 6.1 at p. 88), i.e.

$$\bar{v} = \frac{1}{2T} \int_{-T}^T v dt \quad (7.4)$$

where T is “sufficiently” large.

Consider the probability density functions of the fluctuations. The second moment corresponds to the variance of the fluctuations (or the square of the RMS, see Eq. 7.1), i.e.

$$\overline{v'^2} = \int_{-\infty}^{\infty} v'^2 f_{v'}(v') dv' \quad (7.5)$$

As in Eq. 7.4, $\overline{v'^2}$ is usually computed by integrating in time, i.e.

$$\overline{v'^2} = \frac{1}{2T} \int_{-T}^T v'^2(t) dt$$

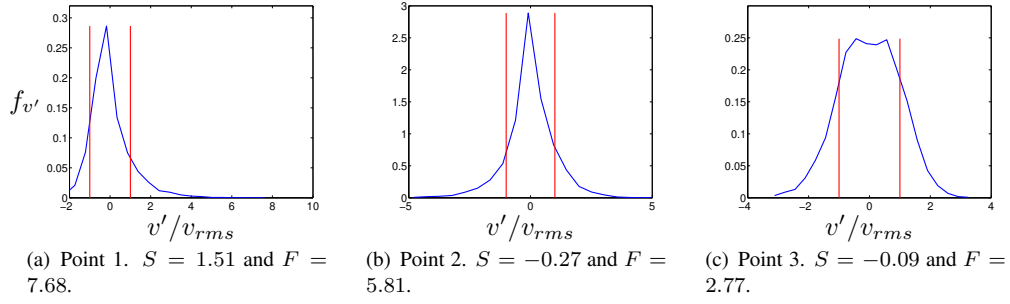


Figure 7.2: Probability density functions of time histories in Fig. 7.1. Vertical red lines show $\pm v_{rms}$. The skewness, S , and the flatness, F , are given for the three time histories.

A probability density function is symmetric if positive values are as frequent and large as the negative values. Figure 7.1 presents the time history of the v' history at three different points in a flow (note that $v' = 0$). The red horizontal lines indicate the RMS value of v' . The resulting probability densities functions are shown in Fig. 7.2. The red vertical lines show plus and minus RMS of v' . Let us analyze the data at the three points.

Point 1. The time history of the velocity fluctuation (Fig. 7.1a) shows that there exists large positive values but no large negative values. The positive values are often larger than $+v_{rms}$ (the peak is actually close to $8v_{rms}$) but the negative values are seldom smaller than $-v_{rms}$. This indicates that the distribution of v' is skewed towards the positive side. This is confirmed in the PDF distribution, see Fig. 7.2a.

Point 2. The fluctuations at this point are much smaller and the positive values are as large as the negative values; this means that the PDF should be symmetric which is confirmed in Fig. 7.2b. The extreme values of v' are approximately $\pm 1.5v_{rms}$, see Figs. 7.1b and 7.2b.

Point 3. At this point the time history (Fig. 7.1c) shows that the fluctuations are clustered around zero and much values are within $\pm v_{rms}$. The time history shows that the positive and the negative values have the same magnitude. The PDF function in Fig. 7.2c confirms that there are many value around zero, that the extreme value are small and that positive and negative values are equally frequent (i.e. the PDF is symmetric).

In Fig. 7.2 we can judge whether the PDF is symmetric, but instead of “looking” at the probability density functions, we should use a definition of the degree of symmetry, which is the *skewness*. It is defined as

skewness

$$\overline{v'^3} = \int_{-\infty}^{\infty} v'^3 f_{v'}(v') dv'$$

and is commonly normalized by v_{rms}^3 , so that the skewness, $S_{v'}$, of v' is defined as

$$S_{v'} = \frac{1}{v_{rms}^3} \int_{-\infty}^{\infty} v'^3 f_{v'}(v') dv' = \frac{1}{2v_{rms}^3 T} \int_{-T}^T v'^3(t) dt$$

Note that f must be normalized (see Eq. 7.3).

There is yet another statistical quantity which sometimes is used for describing turbulent fluctuations, namely the *flatness*. The variance (the square of RMS) tells us how large the fluctuations are in average, but it does not tell us if the time history includes few very large fluctuations or if all are rather close to v_{rms} . The flatness gives this information, and it is defined computed from v'^4 and normalized by v_{rms}^4 , i.e.

$$F = \frac{1}{v_{rms}^4} \int_{-\infty}^{\infty} v'^4 f_{v'}(v) dv$$

The fluctuations at Point 1 (see Fig. 7.1a) includes some samples which are very large and hence its flatness is large (see caption in Fig. 7.2a), whereas the fluctuation for Point 3 all mostly clustered within $\pm 2v_{rms}$ giving a small flatness, see Fig. 7.1c and the caption in Fig. 7.2c. For a Gaussian distribution

$$f(v') = \frac{1}{v_{rms}} \exp\left(-\frac{(v' - v_{rms})^2}{2v_{rms}^2}\right)$$

for which $F = 3$.

8 Transport equations for turbulent kinetic energy

IN this section and Section 9 we will derive various transport equations. There are two tricks which often will be used. Both tricks simply use the product rule for derivative backwards.

Trick 1: Using the product rule we get

$$\frac{\partial A_i B_j}{\partial x_k} = A_i \frac{\partial B_j}{\partial x_k} + B_j \frac{\partial A_i}{\partial x_k} \quad (8.1)$$

This expression can be re-written as

$$A_i \frac{\partial B_j}{\partial x_k} = \frac{\partial A_i B_j}{\partial x_k} - B_j \frac{\partial A_i}{\partial x_k} \quad (8.2)$$

and then we call it the “product rule backwards”.

Trick 2: Using the product rule we get

$$\frac{1}{2} \frac{\partial A_i A_i}{\partial x_j} = \frac{1}{2} \left(A_i \frac{\partial A_i}{\partial x_j} + A_i \frac{\partial A_i}{\partial x_j} \right) = A_i \frac{\partial A_i}{\partial x_j} \quad (8.3)$$

This trick is usually used backwards, i.e.

$$A_i \frac{\partial A_i}{\partial x_j} = \frac{1}{2} \frac{\partial A_i A_i}{\partial x_j} \quad (8.4)$$

8.1 Rules for time averaging

8.1.1 What is the difference between $\overline{v'_1 v'_2}$ and $\overline{v'_1} \overline{v'_2}$?

Using Eq. 6.2 we get

$$\overline{v'_1 v'_2} = \frac{1}{2T} \int_{-T}^T v'_1 v'_2 dt.$$

whereas

$$\overline{v'_1} \overline{v'_2} = \left(\frac{1}{2T} \int_{-T}^T v'_1 dt \right) \left(\frac{1}{2T} \int_{-T}^T v'_2 dt \right)$$

We take a numerical example. Assume that we have a time-series of four time instants with the values of v'_1 and v'_2 as

$$v'_1 = [0.2, -0.3, 0.18, -0.08]$$

$$v'_2 = [0.15, -0.25, 0.04, 0.06]$$

$$\overline{v'_1} = \frac{1}{N} \sum_{n=1}^N v'_{1,n} = (0.2 - 0.3 + 0.18 - 0.08)/4 = 0$$

$$\overline{v'_2} = \frac{1}{N} \sum_{n=1}^N v'_{2,n} = (0.15 - 0.25 + 0.04 + 0.06)/4 = 0$$

so that

$$\overline{v'_1} \overline{v'_2} = \left(\frac{1}{N} \sum_{n=1}^N v'_{1,n} \right) \left(\frac{1}{N} \sum_{n=1}^N v'_{2,n} \right) = 0 \cdot 0 = 0$$

However, the time average of their product is not zero, i.e.

$$\overline{v'_1 v'_2} = \frac{1}{N} \sum_{n=1}^N v'_{1,n} v'_{2,n} = (0.2 \cdot 0.15 + 0.3 \cdot 0.25 + 0.18 \cdot 0.04 - 0.08 \cdot 0.06) / 4 = 0.02685$$

8.1.2 What is the difference between $\overline{v'^2_1}$ and $\overline{v_1'}^2$?

Using Eq. 6.2 we get

$$\overline{v'^2_1} = \frac{1}{2T} \int_{-T}^T v'^2_1 dt.$$

whereas

$$\overline{v_1'}^2 = \left(\frac{1}{2T} \int_{-T}^T v'_1 dt \right)^2.$$

The numerical example gives

$$\overline{v'^2_1} = \frac{1}{N} \sum_{n=1}^N v'^2_{1,n} = (0.2^2 + 0.3^2 + 0.18^2 + 0.08^2) / 4 = 0.0422$$

$$\overline{v'^2_2} = \frac{1}{N} \sum_{n=1}^N v'^2_{2,n} = (0.15^2 + 0.25^2 + 0.04^2 + 0.06^2) / 4 = 0.02255$$

but

$$\overline{v_1'}^2 = \left(\frac{1}{N} \sum_{n=1}^N v'_{1,n} \right)^2 = [(0.2 - 0.3 + 0.18 - 0.08) / 4]^2 = 0$$

$$\overline{v_2'}^2 = \left(\frac{1}{N} \sum_{n=1}^N v'_{2,n} \right)^2 = [(0.15 - 0.25 + 0.04 + 0.06) / 4]^2 = 0$$

8.1.3 Show that $\overline{\bar{v}_1 v'^2_1} = \bar{v}_1 \overline{v'^2_1}$

Using Eq. 6.2 we get

$$\overline{\bar{v}_1 v'^2_1} = \frac{1}{2T} \int_{-T}^T \bar{v}_1 v'^2_1 dt$$

and since \bar{v} does not depend on t we can take it out of the integral as

$$\bar{v}_1 \frac{1}{2T} \int_{-T}^T v'^2_1 dt = \bar{v}_1 \overline{v'^2_1}$$

Now let us do it with numerical values. Assume that $\bar{v}_1 = 10$.

$$\begin{aligned} \overline{\bar{v}_1 v'^2_1} &= \frac{1}{N} \sum_{n=1}^N \left(\frac{1}{N} \sum_{m=1}^N v_{1,m} \right) v'^2_{1,n} = \\ &= (10 \cdot 0.2^2 + 10 \cdot 0.3^2 + 10 \cdot 0.18^2 + 10 \cdot 0.08^2) / 4 = 0.422 \end{aligned}$$

$$\begin{aligned} \bar{v}_1 \overline{v'^2_1} &= \left(\frac{1}{N} \sum_{n=1}^N v_{1,n} \right) \left(\frac{1}{N} \sum_{n=1}^N v'^2_{1,n} \right) = \\ &= [10 \cdot (0.2^2 + 0.3^2 + 0.18^2 + 0.08^2) / 4] = 0.422 \end{aligned}$$

8.1.4 Show that $\bar{\bar{v}}_1 = \bar{v}_1$

Using Eq. 6.2 we get

$$\bar{\bar{v}}_1 = \frac{1}{2T} \int_{-T}^T \bar{v}_1 dt$$

and since \bar{v} does not depend on t we can take it out of the integral as

$$\bar{v}_1 \frac{1}{2T} \int_{-T}^T dt = \bar{v}_1 \frac{1}{2T} 2T = \bar{v}_1$$

With numerical values we get

$$\bar{\bar{v}}_1 = \frac{1}{N} \sum_{n=1}^N = (10 + 10 + 10 + 10)/4 = 10 = \bar{v}_1$$

8.2 The Exact k Equation

The equation for turbulent kinetic energy, $k = \frac{1}{2} \overline{v'_i v'_i}$, is derived from the Navier-Stokes equation. Again, we assume incompressible flow (constant density) and constant viscosity (cf. Eq. 6.6). We subtract Eq. 6.10 from Eq. 6.6 and divide by density, multiply by v'_i and time average which gives

$$\begin{aligned} & \overline{v'_i \frac{\partial}{\partial x_j} [v_i v_j - \bar{v}_i \bar{v}_j]} = \\ & -\frac{1}{\rho} \overline{v'_i \frac{\partial}{\partial x_i} [p - \bar{p}]} + \overline{\nu v'_i \frac{\partial^2}{\partial x_j \partial x_j} [v_i - \bar{v}_i]} + \overline{\frac{\partial v'_i v'_j}{\partial x_j} v'_i} \end{aligned} \quad (8.5)$$

Using $v_j = \bar{v}_j + v'_j$, the left side can be rewritten as

$$\overline{v'_i \frac{\partial}{\partial x_j} [(\bar{v}_i + v'_i)(\bar{v}_j + v'_j) - \bar{v}_i \bar{v}_j]} = \overline{v'_i \frac{\partial}{\partial x_j} [\bar{v}_i v'_j + v'_i \bar{v}_j + v'_i v'_j]}. \quad (8.6)$$

Using the continuity equation $\partial v'_j / \partial x_j = 0$ (see Eq. 6.11), the first term is rewritten as

$$\overline{v'_i \frac{\partial}{\partial x_j} (\bar{v}_i v'_j)} = \overline{v'_i v'_j \frac{\partial \bar{v}_i}{\partial x_j}}. \quad (8.7)$$

For the second term in Eq. 8.6 we start using $\partial \bar{v}_j / \partial x_j = 0$

$$\overline{v'_i \frac{\partial}{\partial x_j} (v'_i \bar{v}_j)} = \overline{\bar{v}_j v'_i \frac{\partial v'_i}{\partial x_j}} \quad (8.8)$$

Next, we use **Trick 2**

$$\bar{v}_j \left(\overline{v'_i \frac{\partial v'_i}{\partial x_j}} \right) = \bar{v}_j \frac{\partial}{\partial x_j} \left(\overline{\frac{1}{2} v'_i v'_i} \right) = \bar{v}_j \frac{\partial}{\partial x_j} (k) = \frac{\partial}{\partial x_j} (\bar{v}_j k) \quad (8.9)$$

The third term in Eq. 8.6 can be written as (replace \bar{v}_j by v'_j and use the same technique as in Eq. 8.9)

$$\frac{1}{2} \frac{\partial}{\partial x_j} \overline{(v'_j v'_i v'_i)}. \quad (8.10)$$

The first term on the right side of Eq. 8.5 is re-written using **Trick 1**

$$-\frac{1}{\rho} \overline{v'_i \frac{\partial p'}{\partial x_i}} = -\frac{1}{\rho} \overline{\frac{\partial p' v'_i}{\partial x_i}} + \frac{1}{\rho} \overline{p' \frac{\partial v'_i}{\partial x_i}} = -\frac{1}{\rho} \overline{\frac{\partial p' v'_i}{\partial x_i}} \quad (8.11)$$

where the continuity equation was used at the last step. The second term on the right side of Eq. 8.5 can be written

$$\overline{\nu v'_i \frac{\partial^2 v'_i}{\partial x_j \partial x_j}} = \overline{\nu v'_i \frac{\partial}{\partial x_j} \left(\frac{\partial v'_i}{\partial x_j} \right)} = \overline{\nu \frac{\partial}{\partial x_j} \left(v'_i \frac{\partial v'_i}{\partial x_j} \right)} - \overline{\nu \frac{\partial v'_i}{\partial x_j} \frac{\partial v'_i}{\partial x_j}} \quad (8.12)$$

applying **Trick 1** ($A = v'_i$ and $B = \partial v'_i / \partial x_j$). For the first term in Eq. 8.12 we use the same trick as in Eq. 8.9 so that

$$\begin{aligned} \overline{\nu \frac{\partial}{\partial x_j} \left(v'_i \frac{\partial v'_i}{\partial x_j} \right)} &= \overline{\nu \frac{\partial}{\partial x_j} \left(\frac{1}{2} \left(v'_i \frac{\partial v'_i}{\partial x_j} + v'_i \frac{\partial v'_i}{\partial x_j} \right) \right)} = \\ &= \overline{\nu \frac{\partial}{\partial x_j} \left(\frac{1}{2} \left(\frac{\partial v'_i v'_i}{\partial x_j} \right) \right)} = \overline{\nu \frac{1}{2} \frac{\partial^2 v'_i v'_i}{\partial x_j \partial x_j}} = \overline{\nu \frac{\partial^2 k}{\partial x_j \partial x_j}} \end{aligned} \quad (8.13)$$

The last term on the right side of Eq. 8.5 is zero because it is time averaging of a fluctuation, i.e. $\overline{\bar{a} \bar{b}'} = \bar{a} \bar{b}' = 0$. Now we can assemble the transport equation for the turbulent kinetic energy. Equations 8.7, 8.9, 8.11, 8.12 and 8.13 give

$$\underbrace{\frac{\partial \bar{v}_j k}{\partial x_j}}_I = \underbrace{-\overline{v'_j v'_j} \frac{\partial \bar{v}_i}{\partial x_j}}_{II} - \underbrace{\frac{\partial}{\partial x_j} \left[\frac{1}{\rho} \overline{v'_j p'} + \frac{1}{2} \overline{v'_j v'_i v'_i} - \nu \frac{\partial k}{\partial x_j} \right]}_{III} - \underbrace{\overline{\nu \frac{\partial v'_i}{\partial x_j} \frac{\partial v'_i}{\partial x_j}}}_{IV} \quad (8.14)$$

The terms in Eq. 8.14 have the following meaning.

I Convection.

II Production, P^k . The large turbulent scales extract energy from the mean flow. This term (including the minus sign) is almost always positive. It may happen that the production is negative which means that turbulent kinetic energy is transferred from the fluctuations to the mean flow. In turbulent flow which includes recirculation, this often occurs locally in small regions.

The production is largest for the energy-containing eddies, i.e. for small wavenumbers, see Fig. 5.3. This term originates from the convection term (the first term on the right side of Eq. 8.6). It can be noted that the production term is an acceleration term, $v'_j \partial \bar{v}_i / \partial x_j$, multiplied by a fluctuating velocity, v'_i , i.e. the product of an inertial force per unit mass (acceleration) and a fluctuating velocity. A force multiplied with a velocity corresponds to work per unit time. When the acceleration term and the fluctuating velocity are in opposite directions (i.e. when $P^k > 0$), the mean flow performs work on the fluctuating velocity field. When the production term is **negative**, it means that the fluctuations are doing work on the mean flow field. In this case, v'_j and the acceleration term, $v'_j \partial \bar{v}_i / \partial x_j$, have the same sign.

Using Eq. 1.11, the production terms reads

$$P^k = -\overline{v'_i v'_j} \frac{\partial \bar{v}_i}{\partial x_j} = -\overline{v'_i v'_j} (\bar{S}_{ij} + \bar{\Omega}_{ij}) = -\overline{v'_i v'_j} \bar{S}_{ij} \quad (8.15)$$

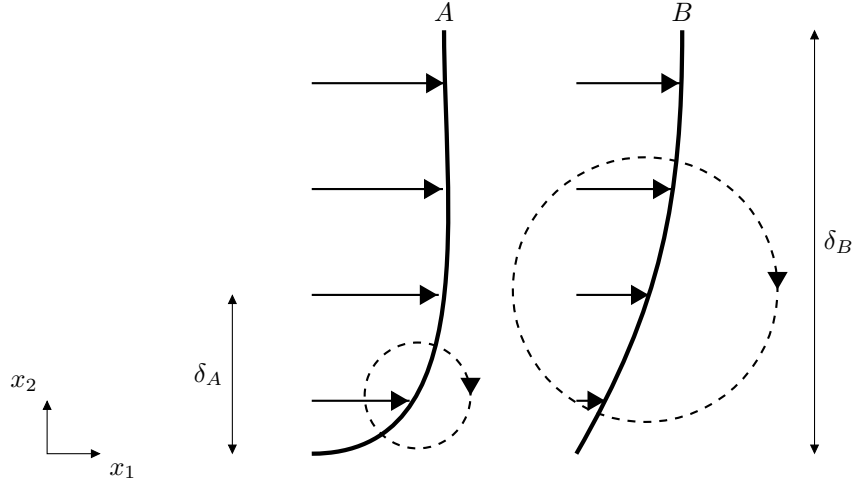


Figure 8.1: The size of the largest eddies (dashed lines) for different velocity profiles.

(the product of the symmetric tensor, $\overline{v'_i v'_j}$, and the anti-symmetric tensor, $\bar{\Omega}_{ij}$, is zero). Thus it is only the symmetric part of the velocity gradient (\bar{S}_{ij} , the part that *deforms* a fluid element) that creates turbulence. The production does not depend on $\bar{\Omega}_{ij}$, the part of the velocity gradient that rotates a fluid element. This is consistent with the fact that the stress tensor, σ_{ij} , depends only on S_{ij} , not on Ω_{ij} , see discussion below Eq. 2.5.

- III The two first terms represent **turbulent diffusion** by pressure-velocity fluctuations, and velocity fluctuations, respectively. The last term is viscous diffusion. The velocity-fluctuation term originates from the convection term (the last term on the right side of Eq. 8.6).
- IV **Dissipation**, ε . This term is responsible for transformation of kinetic energy at small scales to thermal energy. The term (excluding the minus sign) is always positive (it consists of velocity gradients squared). It is largest for large wavenumbers, see Fig. 5.3. The dissipation term stems from the viscous term (see Eq. 8.12) in the Navier-Stokes equation. It can be written as $\overline{v'_i \partial \tau'_{ij} / \partial x_j}$, see Eq. 4.1. The divergence of τ'_{ij} is a force vector (per unit mass), i.e. $T'_i = \partial \tau'_{ij} / \partial x_j$. The dissipation term can now be written $\overline{v'_i T'_i}$, which is a scalar product between two vectors. When the viscous stress vector is in the opposite direction to the fluctuating velocity, the term is negative (i.e. it is dissipative); this means that the viscous stress vector performs work and transforms kinetic energy into internal energy.

The transport equation for k can also be written in a simplified easy-to-read symbolic form as

$$C^k = P^k + D^k - \varepsilon \quad (8.16)$$

where C^k , P^k , D^k and ε correspond to terms I-IV in Eq. 8.14.

Above, it is stated that the production takes place at the large energy-containing eddies, i.e. we assume that the large eddies contribute much more to the production term more than the small eddies. There are two arguments for this:

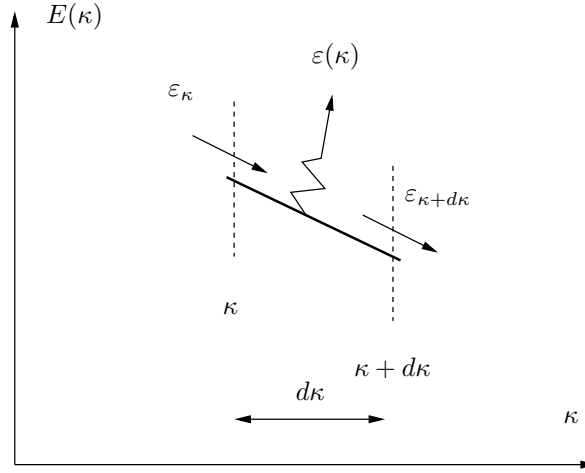


Figure 8.2: Zoom of the energy spectrum for a wavenumber located in Region II or III, see Fig. 5.3.

1. The Reynolds stresses (which appear in P^k) are larger for large eddies than for small eddies.
2. The mean flow generates large eddies which will have same time scale as the mean velocity gradient, $\partial \bar{v}_i / \partial x_j$. In the fully turbulent region of a boundary layer, for example, both time scales are proportional to $\kappa x_2 / u_\tau$. The time scale of the velocity gradient is given by $\kappa x_2 / u_\tau$, see Eq. 6.28, and the time scale of a large eddy is also given by $\ell_0 / v_0 = \kappa x_2 / u_\tau$. Figure 8.1 shows how different velocity profiles create different largest eddies. The largest eddies created by the velocity profile *A* are much smaller than those created by the velocity profile *B*, because the gradient of profile *A* acts over a much shorter length than the gradient of profile *B*.

In the cascade process (see Section 5.3) we assume that the viscous dissipation, ε , takes place at the smallest scales. How do we know that the majority of the dissipation takes place at the smallest scales? First, let us investigate how the time scale varies with eddy size. Consider the inertial subrange. let us denote the energy that is transferred in spectral space (i.e. from eddy-to-eddy) per unit time by ε_κ . How large is ε – that is generating heat – at wavenumber κ , which we here denote $\varepsilon(\kappa)$ (see Section 8.2.2 and Fig. 8.2)? Recall that the viscous dissipation, ε , is expressed as viscosity times the square of the velocity gradient, see Eq. 8.14. The velocity gradient for an eddy characterized by velocity v_κ and lengthscale ℓ_κ can be estimated as

$$\left(\frac{\partial v}{\partial x} \right)_\kappa \propto \frac{v_\kappa}{\ell_\kappa} \propto (v_\kappa^2)^{1/2} \kappa \quad (8.17)$$

since $\ell_\kappa \propto \kappa^{-1}$. We know that the energy spectrum (see Eqs. 5.10 and 5.13),

$$E(\kappa) \propto k_\kappa / \kappa \propto v_\kappa^2 / \kappa \propto \kappa^{-5/3} \Rightarrow v_\kappa^2 \propto \kappa^{-2/3} \quad (8.18)$$

in the inertial region. Inserting Eq. 8.18 into Eq. 8.17 gives

$$\left(\frac{\partial v}{\partial x} \right)_\kappa \propto (\kappa^{-2/3})^{1/2} \kappa \propto \kappa^{-1/3} \kappa \propto \kappa^{2/3} \quad (8.19)$$

Thus the viscous dissipation at wavenumber κ can be estimated as (see the last term in Eq. 8.14)

$$\varepsilon = \nu \overline{\frac{\partial v'_i}{\partial x_j} \frac{\partial v'_i}{\partial x_j}} \Rightarrow \varepsilon(\kappa) \propto \left(\frac{\partial v}{\partial x} \right)_\kappa^2 \propto \kappa^{4/3}, \quad (8.20)$$

i.e. $\varepsilon(\kappa)$ does indeed increase for increasing wavenumber.

The energy transferred from eddy-to-eddy per unit time in spectral space can also be used for estimating the velocity gradient of an eddy. The cascade process assumes that this energy transfer per unit time is the same for each eddy size, i.e. $\varepsilon_\kappa = \varepsilon = v_\kappa^3 / \ell_\kappa = \ell_\kappa^2 / \tau_\kappa^3 = \ell_0^2 / \tau_0^3$, see Eq. 5.14. We find from $\ell_\kappa^2 / \tau_\kappa^3 = \ell_0^2 / \tau_0^3$ that for decreasing eddy size (decreasing ℓ_κ), the time scale, τ_κ , also decreases, i.e.

$$\tau_\kappa = \left(\frac{\ell_\kappa}{\ell_0} \right)^{2/3} \tau_0 \quad (8.21)$$

where τ_0 and ℓ_0 are constants (they are given by the flow we're looking at, for example a boundary layer which has the large scales, τ_0 and ℓ_0). Hence

$$\left(\frac{\partial v}{\partial x} \right)_\kappa \propto \frac{v_\kappa}{\ell_\kappa} \propto \tau_\kappa^{-1} \propto \ell_\kappa^{-2/3} \propto \kappa^{2/3}, \quad (8.22)$$

which is the same as Eq. 8.19.

8.2.1 Expressing dissipation with s_{ij} ; non-isotropic dissipation

The Navier-Stokes for incompressible flow (Eq. 2.6) expressed in s_{ij} reads

$$\frac{dv_i}{dt} = -\frac{1}{\rho} \frac{\partial p}{\partial x_i} + 2\nu \frac{\partial s_{ij}}{\partial x_j} \quad (8.23)$$

The corresponding RANS equation (Eq. 6.10) reads

$$\frac{d\bar{v}_i}{dt} = -\frac{1}{\rho} \frac{\partial \bar{p}}{\partial x_i} + 2\nu \frac{\partial \bar{s}_{ij}}{\partial x_j} - \frac{\partial \overline{v'_i v'_j}}{\partial x_j} \quad (8.24)$$

The v'_i equation is obtained by subtracting Eq. 8.24 from Eq. 8.23

$$\frac{dv'_i}{dt} = -\frac{1}{\rho} \frac{\partial p'}{\partial x_i} + 2\nu \frac{\partial s'_{ij}}{\partial x_j} + \frac{\partial \overline{v'_i v'_j}}{\partial x_j}$$

Multiplying by v'_i and time-averaging gives

$$\overline{v'_i \frac{dv'_i}{dt}} = -\frac{1}{\rho} \overline{v'_i \frac{\partial p'}{\partial x_i}} + 2\nu \overline{v'_i \frac{\partial s'_{ij}}{\partial x_j}} + \overline{v'_i \frac{\partial \overline{v'_i v'_j}}{\partial x_j}}$$

Re-write the viscous term as

$$\begin{aligned} 2\nu \overline{v'_i \frac{\partial s'_{ij}}{\partial x_j}} &= 2\nu \overline{\frac{\partial v'_i s'_{ij}}{\partial x_j}} - 2\nu \overline{\frac{\partial v'_i}{\partial x_j} s'_{ij}} = 2\nu \overline{\frac{\partial v'_i s'_{ij}}{\partial x_j}} - 2\nu \overline{(s'_{ij} + \Omega'_{ij}) s'_{ij}} \\ &= 2\nu \overline{\frac{\partial v'_i s'_{ij}}{\partial x_j}} - 2\nu \overline{s'_{ij} s'_{ij}} \end{aligned}$$

The last term (we use fact that the product of a symmetric and anti-symmetric tensor is zero, i.e. $s'_{ij}\Omega'_{ij} = 0$, and Eq. 1.11) can be written

$$2\nu\overline{s'_{ij}s'_{ij}} = 2\nu\overline{s'_{ij}(s'_{ij} + \Omega'_{ij})} = \nu\overline{\left(\frac{\partial v'_i}{\partial x_j} + \frac{\partial v'_j}{\partial x_i}\right)\frac{\partial v'_i}{\partial x_j}}$$

This dissipation is sometimes called the non-isotropic dissipation [2]; the usual dissipation, ε (term IV in Eq. 8.14), is then the isotropic dissipation.

8.2.2 Spectral transfer dissipation ε_κ vs. “true” viscous dissipation, ε

As a final note to the discussion in the previous section, it may be useful to look at the difference between the spectral transfer dissipation ε_κ , and the “true” viscous dissipation, ε ; the former is the energy transferred from eddy-to-eddy per unit time, and the latter is the energy transformed per unit time to internal energy (i.e. increased temperature) for the entire spectrum (occurring mainly at the small, dissipative scales), see Fig. 5.3. Now consider Fig. 8.2 which shows a zoom of the energy spectrum. We assume that no mean flow energy production occurs between κ and $\kappa + d\kappa$, i.e. the region may be in the $-5/3$ region or in the dissipation region. Turbulent kinetic per unit time energy enters at wavenumber κ at a rate of ε_κ and leaves at wavenumber $\kappa + d\kappa$ a rate of $\varepsilon_{\kappa+d\kappa}$. If κ and $\kappa + d\kappa$ are located in the inertial region (i.e. the $-5/3$ region), then the usual assumption is that $\varepsilon_\kappa \simeq \varepsilon_{\kappa+d\kappa}$ and that there is no viscous dissipation to internal energy, i.e. $\varepsilon(\kappa) \simeq 0$. If there is viscous dissipation at wavenumber κ (which indeed is the case if the zoomed region is located in the dissipative region), then $\varepsilon(\kappa)$ is simply obtained through an energy balance per unit time, i.e.

$$\varepsilon(\kappa) = \varepsilon_{\kappa+d\kappa} - \varepsilon_\kappa \quad (8.25)$$

8.3 The Exact k Equation: 2D Boundary Layers

In 2D boundary-layer flow, for which $\partial/\partial x_2 \gg \partial/\partial x_1$ and $\bar{v}_2 \ll \bar{v}_1$, the exact k equation reads

$$\begin{aligned} \frac{\partial \bar{v}_1 k}{\partial x_1} + \frac{\partial \bar{v}_2 k}{\partial x_2} &= -\overline{v'_1 v'_2} \frac{\partial \bar{v}_1}{\partial x_2} \\ &\quad - \frac{\partial}{\partial x_2} \left[\frac{1}{\rho} \overline{p' v'_2} + \frac{1}{2} \overline{v'_2 v'_i v'_i} - \nu \frac{\partial k}{\partial x_2} \right] - \nu \overline{\frac{\partial v'_i}{\partial x_j} \frac{\partial v'_i}{\partial x_j}} \end{aligned} \quad (8.26)$$

Note that the dissipation includes all derivatives. This is because the dissipation term is at its largest for small, isotropic scales for which all derivatives are of the same order and hence the usual boundary-layer approximation $\partial/\partial x_1 \ll \partial/\partial x_2$ does not apply for these scales.

Figure 8.3 presents the terms in Eq. 8.26 for fully developed channel flow. The left side is – since the flow is fully developed – zero. In the outer region (Fig. 8.3b) all terms are negligible except the production term and the dissipation term which balance each other. This is called *local equilibrium*, see p. 111. Closer to the wall (Fig. 8.3a) the other terms do also play a role. Note that the production and the dissipation terms close to the wall are two orders of magnitude larger than in the logarithmic region (Fig. 8.3b). At the wall the turbulent fluctuations are zero which means that the production term is zero. Since the region near the wall is dominated by viscosity the turbulent diffusion terms due to pressure and velocity are also small. The dissipation term and the viscous

local equilibrium

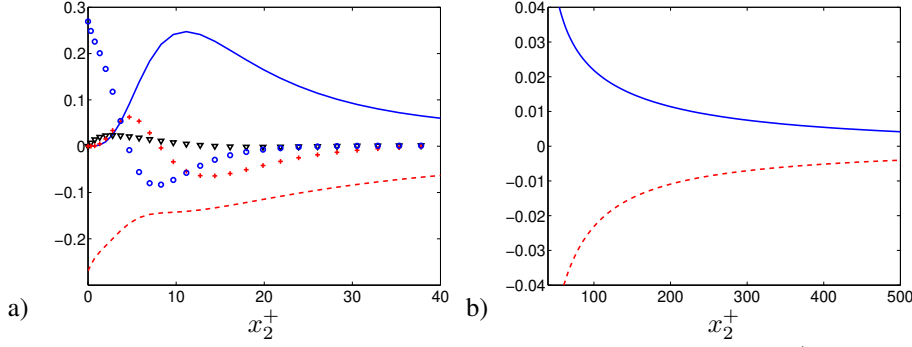


Figure 8.3: Channel flow at $Re_\tau = 2000$. Terms in the k equation scaled by u_τ^4/ν . $Re_\tau = 2000$. a) Zoom near the wall; b) Outer region. DNS (Direct Numerical Simulation) data [16, 17].
—: P^k ; - - - : $-\varepsilon$; ∇ : $-\partial \overline{v'p'}/\partial x_2$; +: $-\partial \overline{v'_2 v'_i v'_i}/2/\partial x_2$; \circ : $\nu \partial^2 k/\partial x_2^2$.

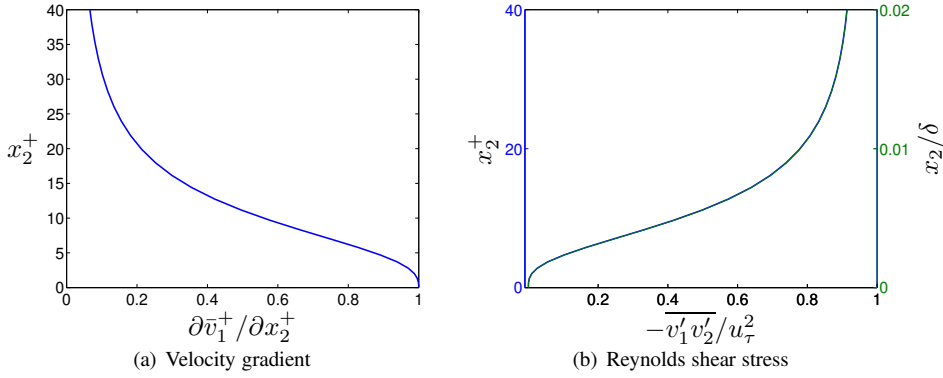


Figure 8.4: Channel flow at $Re_\tau = 2000$. DNS (Direct Numerical Simulation) data [16, 17].

diffusion term attain their largest value at the wall and they must be equal to each other since all other terms are zero or negligible.

The turbulence kinetic energy is produced by its main source term, the production term, $P^k = -\overline{v'_1 v'_2} \partial \overline{v_1}/\partial x_2$. The velocity gradient is largest at the wall (see Fig. 8.4a) where the shear stress is zero (see Fig. 8.4b)); the former decreases and the magnitude of the latter increases with wall distance and their product takes its maximum at $x_2^+ \simeq 11$. Since P^k is largest here so is also k , see Fig. 6.8. k is transported in the x_2 direction by viscous and turbulent diffusion and it is destroyed (i.e. dissipated) by ε .

8.4 Spatial vs. spectral energy transfer

In Section 5.3 we discussed *spectral* transfer of turbulent kinetic energy from large to small eddies (which also applies to the transport of the Reynolds stresses). In Section 8.2 we derived the equation for *spatial* transport of turbulent kinetic energy. How are the spectral transfer and the spatial transport related? The reason that we in Section 5.3 only talked about spectral transfer was that we assumed homogeneous turbulence in which the spatial derivatives of the time-averaged turbulent quantities are zero, for example $\partial \overline{v_1'^2}/\partial x_i = 0$, $\partial k/\partial x_i = 0$ etc. (Note that the derivatives of the *instantaneous* turbulent fluctuations are non-zero even in homogeneous turbulence, i.e.

**homogeneous
turbulence**

$\partial v'_1/\partial x_i \neq 0$; the instantaneous flow field in turbulent flow is – as we mentioned at the beginning of this section, p. 78 – *always* three-dimensional and unsteady). In homogeneous turbulence the spatial transport terms (i.e. the convective term, term **I**, and the diffusion terms, term **III** in Eq. 8.14) are zero. Hence, in homogeneous turbulence there is no time-averaged spatial transport. However, there is *spectral transfer* of turbulent kinetic energy which takes place in wavenumber space, from large to small eddies. The production term (term **II** in Eq. 8.14) corresponds to the process in which large energy-containing eddies extract energy from the mean flow. The dissipation term (term **IV** in Eq. 8.14) corresponds to transformation of the turbulent kinetic energy at the small eddies to thermal energy. However, real flows are hardly ever homogeneous. Some flows may have one or two homogeneous directions. Consider, for example, fully developed channel turbulent flow. If the channel walls are very long and wide compared to the distance between the walls, 2δ , then the turbulence (and the flow) is homogeneous in the streamwise direction and the spanwise direction, i.e. $\partial \bar{v}_1/\partial x_1 = 0$, $\partial \bar{v}_i'^2/\partial x_1 = 0$, $\partial \bar{v}_i'^2/\partial x_3 = 0$ etc.

In non-homogeneous turbulence, the cascade process is not valid. Consider a large, turbulent eddy at a position x_2^A (see Fig. 6.1) in fully developed channel flow. The instantaneous turbulent kinetic energy, $k_\kappa = v'_{\kappa,i} v'_{\kappa,i}/2$, of this eddy may either be transferred in wavenumber space or transported in physical (spatial) space, or both. It may first be transported in physical space towards the center, and there lose its kinetic energy to smaller eddies. This should be kept in mind when thinking in terms of the cascade process. Large eddies which extract their energy from the mean flow may not give their energy to the slightly smaller eddies as assumed in Figs. 5.3 and 5.2, but k_κ may first be transported in physical space and then transferred in spectral space (i.e. to a smaller eddy).

In the inertial range (Region II), however, the cascade process is still a good approximation even in non-homogeneous turbulence. The reason is that the transfer of turbulent kinetic energy, k_κ , from eddy-to-eddy, occurs at a much faster rate than the spatial transport by convection and diffusion. In other words, the time scale of the cascade process is much smaller than that of convection and diffusion which have no time to transport k_κ in space before it is passed on to a smaller eddy by the cascade process. We say that the turbulence at these scales is in *local equilibrium*. The turbulence in the buffer layer and the logarithmic layer of a boundary layer (see Fig. 6.2) is in local equilibrium. In Townsend [23], this is (approximately) stated as:

**local
equilibrium**

the local rates of turbulent kinetic energy (i.e. production and dissipation) are so large that aspects of the turbulent motion concerned with these processes are independent of conditions elsewhere in the flow.

This statement simply means that production is equal to dissipation, i.e. $P^k = \varepsilon$, see Fig. 8.3.

In summary, care should be taken in non-homogeneous turbulence, regarding the validity of the cascade process for the large scales (Region I).

8.5 The overall effect of the transport terms

The overall effect (i.e. the net effect) of the production term is to increase k , i.e. if we integrate the production term over the entire domain, V , we get

$$\int_V P^k dV > 0 \quad (8.27)$$

Similarly, the net effect of the dissipation term is a negative contribution, i.e.

$$\int_V -\varepsilon dV < 0 \quad (8.28)$$

What about the overall effect of the *transport* terms, i.e. convection and diffusion? Integration of the convection term over the entire volume, V , gives, using Gauss divergence law,

$$\int_V \frac{\partial \bar{v}_j k}{\partial x_j} dV = \int_S \bar{v}_j k n_j dS \quad (8.29)$$

where S is the bounding surface of V . This shows that the net effect of the convection term occurs only at the boundaries. Inside the domain, the convection merely transports k without adding or subtracting anything to the integral of k , $\int_V k dV$; the convection acts as a source term in part of the domain, but in the remaining part of the domain it acts as an equally large sink term. Similarly for the diffusion term, we get

$$\begin{aligned} & - \int_V \frac{\partial}{\partial x_j} \left(\frac{1}{2} \overline{v'_j v'_k v'_k} + \frac{1}{\rho} \overline{p' v'_j} - \nu \frac{\partial k}{\partial x_j} \right) V \\ &= - \int_S \left(\frac{1}{2} \overline{v'_j v'_k v'_k} + \frac{1}{\rho} \overline{p' v'_j} - \nu \frac{\partial k}{\partial x_j} \right) n_j dS \end{aligned} \quad (8.30)$$

The only net contribution occurs at the boundaries. Hence, Eqs. 8.29 and 8.30 show that the transport terms only – as the word implies – *transports* k without giving any net effect except at the boundaries. Mathematically these terms are called *divergence terms*, i.e. they can both be written as the divergence of a vector A_j ,

$$\frac{\partial A_j}{\partial x_j} \quad (8.31)$$

**divergence
terms**

where A_j for the convection and the diffusion term reads

$$A_j = \begin{cases} \bar{v}_j k & \text{convection term} \\ - \left(\frac{1}{2} \overline{v'_j v'_k v'_k} + \frac{1}{\rho} \overline{p' v'_j} - \nu \frac{\partial k}{\partial x_j} \right) & \text{diffusion term} \end{cases} \quad (8.32)$$

8.6 The transport equation for $\bar{v}_i \bar{v}_i / 2$

The equation for $K = \bar{v}_i \bar{v}_i / 2$ is derived in the same way as that for $\overline{v'_i v'_i} / 2$. Multiply the time-averaged Navier-Stokes equations, Eq. 6.10, by \bar{v}_i so that

$$\bar{v}_i \frac{\partial \bar{v}_i \bar{v}_j}{\partial x_j} = -\frac{1}{\rho} \bar{v}_i \frac{\partial \bar{p}}{\partial x_i} + \nu \bar{v}_i \frac{\partial^2 \bar{v}_i}{\partial x_j \partial x_j} - \bar{v}_i \frac{\partial \overline{v'_i v'_j}}{\partial x_j}. \quad (8.33)$$

Using the continuity equation and **Trick 2** the term on the left side can be rewritten as

$$\bar{v}_i \frac{\partial \bar{v}_i \bar{v}_j}{\partial x_j} = \bar{v}_j \bar{v}_i \frac{\partial \bar{v}_i}{\partial x_j} = \bar{v}_j \frac{\frac{1}{2} \partial \bar{v}_i \bar{v}_i}{\partial x_j} = \frac{\partial \bar{v}_j K}{\partial x_j} \quad (8.34)$$

The viscous term in Eq. 8.33 is rewritten in the same way as the viscous term in Section 8.2, see Eqs. 8.12 and 8.13, i.e.

$$\nu \bar{v}_i \frac{\partial^2 \bar{v}_i}{\partial x_j \partial x_j} = \nu \frac{\partial^2 K}{\partial x_j \partial x_j} - \nu \frac{\partial \bar{v}_i}{\partial x_j} \frac{\partial \bar{v}_i}{\partial x_j}. \quad (8.35)$$

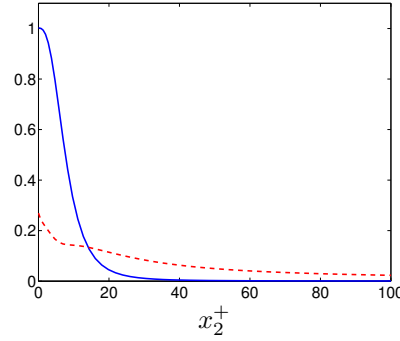


Figure 8.5: Channel flow at $Re_\tau = 2000$. Comparison of mean and fluctuating dissipation terms, see Eqs. 8.39 and 8.40. Both terms are normalized by u_τ^4/ν . DNS (Direct Numerical Simulation) data [16, 17]. — : $\nu(\partial \bar{v}_1 / \partial x_2)^2$; - - : ε .

Equations 8.34 and 8.35 inserted in Eq. 8.33 gives

$$\frac{\partial \bar{v}_j K}{\partial x_j} = \nu \frac{\partial^2 K}{\partial x_j \partial x_j} - \frac{\bar{v}_i}{\rho} \frac{\partial \bar{p}}{\partial x_i} - \nu \frac{\partial \bar{v}_i}{\partial x_j} \frac{\partial \bar{v}_i}{\partial x_j} - \bar{v}_i \frac{\partial \overline{v'_i v'_j}}{\partial x_j}. \quad (8.36)$$

The last term is rewritten using **Trick 1** as

$$-\bar{v}_i \frac{\partial \overline{v'_i v'_j}}{\partial x_j} = -\frac{\partial \overline{v_i v'_i v'_j}}{\partial x_j} + \overline{v'_i v'_j} \frac{\partial \bar{v}_i}{\partial x_j}. \quad (8.37)$$

Note that the first term on the right side differs to the corresponding term in Eq. 8.14 by a factor of two since **Trick 2** cannot be used because $\bar{v}_i \neq v'_i$. Inserted in Eq. 8.36 gives (cf. Eq. 8.14)

$$\frac{\partial \bar{v}_j K}{\partial x_j} = \underbrace{\overline{v'_i v'_j} \frac{\partial \bar{v}_i}{\partial x_j}}_{-P^k, \text{ sink}} - \frac{\bar{v}_i}{\rho} \frac{\partial \bar{p}}{\partial x_i} - \frac{\partial}{\partial x_j} \left(\overline{v_i v'_i v'_j} - \nu \frac{\partial K}{\partial x_j} \right) - \underbrace{\nu \frac{\partial \bar{v}_i}{\partial x_j} \frac{\partial \bar{v}_i}{\partial x_j}}_{\varepsilon_{mean}, \text{ sink}} \quad (8.38)$$

On the left side we have the usual convective term. On the right side we find:

- loss of energy to k due to the production term
- work performed by the pressure gradient; in channel flow, for example, this term gives a positive contribution to K (as expected) since $-\bar{v}_1 \partial \bar{p} / \partial x_1 > 0$
- diffusion by velocity-stress interaction
- viscous diffusion.
- viscous dissipation, ε_{mean} . This corresponds to the dissipation term in Eq. 2.23; if you replace v_i with \bar{v}_i and use the continuity equation to get rid of the second velocity gradient in \bar{S}_{ij} you find that the dissipation term in Eq. 2.23 (see Eq. 2.26), is identical to ε_{mean} .

Note that the first term in Eq. 8.38 is the same as the first term in Eq. 8.14 but with opposite sign: here we clearly can see that the main source term in the k equation (the production term) appears as a sink term in the K equation.

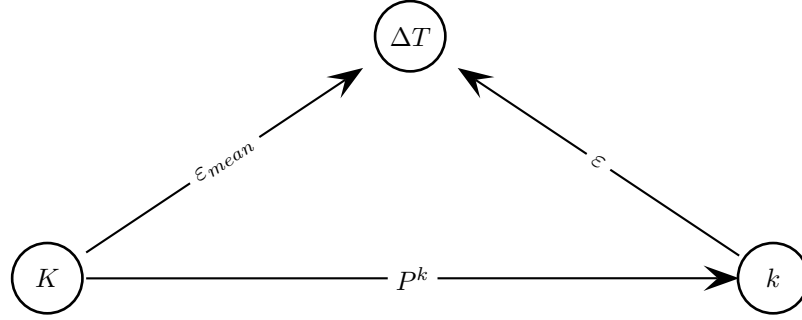


Figure 8.6: Transfer of energy between mean kinetic energy (K), turbulent kinetic energy (k) and internal energy (denoted as an increase in temperature, ΔT). $K = \frac{1}{2} \bar{v}_i \bar{v}_i$ and $k = \frac{1}{2} \overline{v'_i v'_i}$.

In the K equation the dissipation term and the negative production term (representing loss of kinetic energy to the k field) read

$$-\nu \frac{\partial \bar{v}_i}{\partial x_j} \frac{\partial \bar{v}_i}{\partial x_j} + \overline{v'_i v'_j} \frac{\partial \bar{v}_i}{\partial x_j}, \quad (8.39)$$

and in the k equation the production and the dissipation terms read

$$-\overline{v'_i v'_j} \frac{\partial \bar{v}_i}{\partial x_j} - \nu \frac{\partial v'_i}{\partial x_j} \frac{\partial v'_i}{\partial x_j} \quad (8.40)$$

The gradient of the time-averaged velocity field, \bar{v}_i , is much smoother than the gradient of the fluctuating velocity field, v'_i . Hence, the dissipation by the turbulent fluctuations, ε , in the turbulent region (logarithmic region and further out from walls), is much larger than the dissipation by the mean flow (left side of Eq. 8.39). This is seen in Fig. 8.5 ($x_2^+ \gtrsim 15$). The energy flow from the mean flow to internal energy is illustrated in Fig. 8.6. The major part of the energy flow goes from K to k and then to dissipation.

In the viscous-dominated wall region ($x_2^+ \lesssim 5$), the mean dissipation, $\nu(\partial \bar{v}_1 / \partial x_2)^2$, is much larger than ε , see Fig. 8.5. At the wall, the mean dissipation takes the value $\nu = 1/2000$ (normalized by u_τ^4/ν).

11 Reynolds stress models and two-equation models

11.1 Mean flow equations

11.1.1 Flow equations

For incompressible turbulent flow, all variables are divided into a mean part (time averaged) and fluctuating part. For the velocity vector this means that v_i is divided into a mean part \bar{v}_i and a fluctuating part v'_i so that $v_i = \bar{v}_i + v'_i$. Time average and we get (see Eq. 6.9 at p. 89):

$$\frac{\partial \bar{v}_i}{\partial x_i} = 0 \quad (11.1)$$

$$\frac{\partial \rho_0 \bar{v}_i}{\partial t} + \frac{\partial}{\partial x_j} (\rho_0 \bar{v}_i \bar{v}_j) = -\frac{\partial \bar{p}}{\partial x_i} + \mu \frac{\partial^2 \bar{v}_i}{\partial x_j \partial x_j} - \frac{\partial \tau_{ij}}{\partial x_j} - \beta \rho_0 (\bar{\theta} - \theta_0) g_i \quad (11.2)$$

(note that θ denotes temperature) where ρ_0 is a constant reference density, the volume force $f_i = -\beta(\bar{\theta} - \theta_0)g_i$ and the turbulent stress tensor (also called *Reynolds stress tensor*) is written as:

$$\tau_{ij} = \overline{\rho_0 v'_i v'_j} \quad (11.3)$$

**Reynolds
stress
tensor**

The pressure, \bar{p} , denotes the hydrodynamic pressure, see Eq. 3.22, which means that when the flow is still (i.e. $\bar{v}_i \equiv 0$), then the pressure is zero (i.e. $\bar{p} \equiv 0$). We have assumed that the temperature variations are small (typically smaller than 10 °C) so that the density variations can be neglected (using ρ_0) in all terms except the gravity term. This is called the *Boussinesq approximation*.

**Boussinesq
approximation**

The body force f_i – which was omitted for convenience in Eq. 6.9 – has here been re-introduced. The body force in Eq. 11.2 is due to buoyancy, i.e. density differences. The basic form of the buoyancy force is $f_i = g_i$ where g_i denotes gravitational acceleration. Since the pressure, \bar{p} , is defined as the hydrodynamic pressure we have re-written the buoyancy source as

$$\rho_0 f_i \rightarrow (\rho - \rho_0) g_i \quad (11.4)$$

so that $\bar{p} \equiv 0$ when $\bar{v}_i \equiv 0$ (note that the true pressure decreases upwards as $\rho g \Delta h$ where Δh denotes change in height). To understand that $\bar{v}_i = 0$ is solution when $\bar{p} = 0$, set $\partial \bar{p} / \partial x_i = 0$ in Eq. 11.2. We see that $\bar{v}_i = 0$ is a solution. $\partial \bar{p} / \partial x_i = 0$ means that the $\bar{p} = \text{const}$ in the entire domain. Then we set $\bar{p} = 0$ in one point which so that $\bar{p} = 0$ in the entire domain. Now we let density in Eq. 11.4 depend on pressure and temperature, and differentiation gives

$$d\rho = \left(\frac{\partial \rho}{\partial \theta} \right)_p d\theta + \left(\frac{\partial \rho}{\partial p} \right)_\theta dp \quad (11.5)$$

Our flow is incompressible, which means that the density does not depend on pressure, i.e. $\partial \rho / \partial p = 0$; it may, however, depend on temperature and mixture composition. Hence the last term in Eq. 11.5 is zero and we introduce the volumetric thermal expansion, β , so that

$$\begin{aligned} \beta &= -\frac{1}{\rho_0} \left(\frac{\partial \rho}{\partial \theta} \right)_p \Rightarrow \\ d\rho &= -\rho_0 \beta d\theta \Rightarrow \rho - \rho_0 = -\beta \rho_0 (\theta - \theta_0) \end{aligned} \quad (11.6)$$

where β is a physical property which is tabulated in physical handbooks. For a perfect gas it is simply $\beta = \theta^{-1}$ (with θ in degrees Kelvin). Now we can re-write the buoyancy term as

$$(\rho - \rho_0)g_i = -\rho_0\beta(\bar{\theta} - \theta_0)g_i \quad (11.7)$$

which is the last term in Eq. 11.2. Consider the case where x_3 is vertically upwards. Then $g_i = (0, 0, -g)$ and a large temperature in Eq. 11.7 results in a force vertically upwards, which agrees well with our intuition.

11.1.2 Temperature equation

The instantaneous temperature, θ , is also decomposed into a mean and a fluctuating component as $\theta = \bar{\theta} + \theta'$. The transport equation for θ reads (see Eq. 2.18 where temperature was denoted by T)

$$\frac{\partial \theta}{\partial t} + \frac{\partial v_i \theta}{\partial x_i} = \alpha \frac{\partial^2 \theta}{\partial x_i \partial x_i} \quad (11.8)$$

where $\alpha = k/(\rho c_p)$, see Eq. 2.18 on p. 33. Introducing $\theta = \bar{\theta} + \theta'$ we get

$$\frac{\partial \bar{\theta}}{\partial t} + \frac{\partial \bar{v}_i \bar{\theta}}{\partial x_i} = \alpha \frac{\partial^2 \bar{\theta}}{\partial x_i \partial x_i} - \frac{\partial \overline{v'_i \theta'}}{\partial x_i} \quad (11.9)$$

The last term on the right side is an additional term whose physical meaning is turbulent heat flux vector. This is similar to the Reynolds stress tensor on the right side of the time-averaged momentum equation, Eq. 11.2. The total heat flux vector – viscous plus turbulent – in Eq. 11.9 reads (cf. Eq. 2.14)

$$-\frac{q_{i,tot}}{\rho c_p} = -\frac{q_i}{\rho c_p} - \frac{q_{i,turb}}{\rho c_p} = \alpha \frac{\partial \bar{\theta}}{\partial x_i} - \overline{v'_i \theta'} \quad (11.10)$$

11.2 The exact $\overline{v'_i v'_j}$ equation

Now we want to solve the time-averaged continuity equation (Eq. 11.1) and the three momentum equations (Eq. 11.2). Unfortunately there are ten unknowns; the four usual ones (\bar{v}_i, \bar{p}) plus six turbulent stresses, $\overline{v'_i v'_j}$. We must *close* this equation system; it is called the *closure problem*. We must find some new equations for the turbulent stresses. We need a turbulence model.

**closure
problem**

The most comprehensive turbulence model is to derive exact transport equations for the turbulent stresses. An exact equation for the Reynolds stresses can be derived from the Navies-Stokes equation. It is emphasized that this equation is exact; or, rather, as exact as the Navier-Stokes equations. The derivation follows the steps below.

- Set up the momentum equation for the instantaneous velocity $v_i = \bar{v}_i + v'_i \rightarrow$ Eq. (A)
- Time average \rightarrow equation for \bar{v}_i , Eq. (B)
- Subtract Eq. (B) from Eq. (A) \rightarrow equation for v'_i , Eq. (C)
- Do the same procedure for $v_j \rightarrow$ equation for v'_j , Eq. (D)
- Multiply Eq. (C) with v'_j and Eq. (D) with v'_i , time average and add them together \rightarrow equation for $\overline{v'_i v'_j}$

In Section 9 at p. 115 these steps are given in some detail. More details can also be found in [24] (set the SGS tensor to zero, i.e. $\tau_{ij}^a = 0$).

The final $\overline{v'_i v'_j}$ -equation (Reynolds Stress equation) reads (see Eq. 9.12)

$$\begin{aligned}
 \frac{\partial \overline{v'_i v'_j}}{\partial t} + \underbrace{\overline{v_k \frac{\partial v'_i v'_j}{\partial x_k}}}_{C_{ij}} = & \underbrace{-\overline{v'_i v'_k} \frac{\partial \bar{v}_j}{\partial x_k} - \overline{v'_j v'_k} \frac{\partial \bar{v}_i}{\partial x_k}}_{P_{ij}} + \underbrace{\frac{p'}{\rho} \left(\frac{\partial v'_i}{\partial x_j} + \frac{\partial v'_j}{\partial x_i} \right)}_{\Pi_{ij}} \\
 & - \underbrace{\frac{\partial}{\partial x_k} \left[\overline{v'_i v'_j v'_k} + \frac{p' v'_j}{\rho} \delta_{ik} + \frac{p' v'_i}{\rho} \delta_{jk} \right]}_{D_{ij,t}} + \underbrace{\nu \frac{\partial^2 \overline{v'_i v'_j}}{\partial x_k \partial x_k}}_{D_{ij,\nu}} \\
 & \underbrace{-g_i \beta \overline{v'_j \theta'} - g_j \beta \overline{v'_i \theta'}}_{G_{ij}} - \underbrace{2\nu \frac{\partial v'_i}{\partial x_k} \frac{\partial v'_j}{\partial x_k}}_{\varepsilon_{ij}}
 \end{aligned} \tag{11.11}$$

where $D_{ij,t}$ and $D_{ij,\nu}$ denote turbulent and viscous diffusion, respectively. The total diffusion reads $D_{ij} = D_{ij,t} + D_{ij,\nu}$. This is analogous to the momentum equation where we have gradients of viscous and turbulent stresses which correspond to viscous and turbulent diffusion. Equation 11.11 can symbolically be written

$$C_{ij} = P_{ij} + \Pi_{ij} + D_{ij} + G_{ij} - \varepsilon_{ij}$$

where

C_{ij} Convection

P_{ij} Production

Π_{ij} Pressure-strain

D_{ij} Diffusion

G_{ij} Buoyancy production

ε_{ij} Dissipation

Which terms in Eq. 11.11 are known and which are unknown? First, let's think about which physical quantities we solve for.

\bar{v}_i is obtained from the momentum equation, Eq. 11.2

$\overline{v'_i v'_j}$ is obtained from the modeled $\overline{v'_i v'_j}$ equation, Eq. 11.101

Hence the following terms in Eq. 11.11 are known (i.e. they do not need to be modeled)

- The left side
- The production term, P_{ij}
- The viscous part of the diffusion term, D_{ij} , i.e. D_{ij}^ν
- The buoyancy term, G_{ij} (provided that a transport equation is solved for $\overline{v'_i \theta'}$, Eq. 11.22; if not, $\overline{v'_i \theta'}$ is obtained from the Boussinesq assumption, Eq. 11.35)

11.3 The exact $\overline{v'_i \theta'}$ equation

If temperature variations occur we must solve for the mean temperature field, see Eq. 11.9. Then we need the unknown turbulent heat fluxes, $\overline{v'_i \theta'}$. To derive its transport equation, start with the equation for the fluctuating temperature. Subtract Eq. 11.9 from Eq. 11.8

$$\frac{\partial \theta'}{\partial t} + \frac{\partial}{\partial x_k} (v'_k \bar{\theta} + \bar{v}_k \theta' + v'_k \theta') = \alpha \frac{\partial^2 \theta'}{\partial x_k \partial x_k} - \frac{\partial \overline{v'_k \theta'}}{\partial x_k} \quad (11.12)$$

To get the equation for the fluctuating velocity, v'_i , subtract the equation for the mean velocity \bar{v}_i (Eq. 11.2) from the equation for the instantaneous velocity, v_i (Eq. 6.6) so that

$$\frac{\partial v'_i}{\partial t} + \frac{\partial}{\partial x_k} (v'_k \bar{v}_i + \bar{v}_k v'_i + v'_k v'_i) = -\frac{1}{\rho} \frac{\partial p'}{\partial x_i} + \nu \frac{\partial^2 v'_i}{\partial x_k \partial x_k} + \frac{\partial \overline{v'_i v'_k}}{\partial x_k} - g_i \beta \theta' \quad (11.13)$$

Multiply Eq. 11.12 with v'_i and multiply Eq. 11.13 with θ' , add them together and time average

$$\begin{aligned} \frac{\partial \overline{v'_i \theta'}}{\partial t} + \overline{v'_i \frac{\partial}{\partial x_k} (v'_k \bar{\theta} + \bar{v}_k \theta' + v'_k \theta')} + \overline{\theta' \frac{\partial}{\partial x_k} (\bar{v}_i v'_k + \bar{v}_k v'_i + v'_i v'_k)} \\ = -\overline{\frac{\theta'}{\rho} \frac{\partial p'}{\partial x_i}} + \alpha \overline{v'_i \frac{\partial^2 \theta'}{\partial x_k \partial x_k}} + \nu \overline{\theta' \frac{\partial^2 v'_i}{\partial x_k \partial x_k}} - g_i \beta \overline{\theta' \theta'} \end{aligned} \quad (11.14)$$

The Reynolds stress term in Eq. 11.13 multiplied by θ' and time averaged is zero, i.e.

$$\frac{\partial \overline{v'_i v'_j \theta'}}{\partial x_k} = \frac{\partial \overline{v'_i v'_j}}{\partial x_k} \overline{\theta'} = 0$$

If you have forgotten the rules for time-averaging, see Section 8.1.

The first term in the two parentheses on line 1 in Eq. 11.14 are combined into two production terms (using the continuity equation, $\partial v'_k / \partial x_k = 0$)

$$\overline{v'_i v'_k \frac{\partial \bar{\theta}}{\partial x_k}} + \overline{v'_k \theta' \frac{\partial \bar{v}}{\partial x_k}} \quad (11.15)$$

The second term in the two parenthesis on the first line of Eq. 11.14 are re-written using the continuity equation

$$\overline{v'_i \frac{\partial \bar{v}_k \theta'}{\partial x_k}} + \overline{\theta' \frac{\partial \bar{v}_k v'_i}{\partial x_k}} = \bar{v}_k \left(\overline{v'_i \frac{\partial \theta'}{\partial x_k}} + \overline{\theta' \frac{\partial v'_i}{\partial x_k}} \right) \quad (11.16)$$

Now the two terms can be merged (product rule backwards, Trick 1)

$$\bar{v}_k \left(\overline{v'_i \frac{\partial \theta'}{\partial x_k}} + \overline{\theta' \frac{\partial v'_i}{\partial x_k}} \right) = \bar{v}_k \frac{\partial \overline{v'_i \theta'}}{\partial x_k} = \frac{\partial \bar{v}_k \overline{v'_i \theta'}}{\partial x_k} \quad (11.17)$$

where we used the continuity equation to obtain the right side. The last two terms on the first line in Eq. 11.14 are re-cast into turbulent diffusion terms using the same procedure as in Eqs. 11.16 and 11.17

$$\overline{v'_i \frac{\partial}{\partial x_k} (v'_k \theta')} + \overline{\theta' \frac{\partial}{\partial x_k} (v'_i v'_k)} = \frac{\partial \overline{v'_i v'_k \theta'}}{\partial x_k} \quad (11.18)$$

The viscous diffusion terms on the right side are re-written using the product rule backwards (Trick 1, see p. 102)

$$\begin{aligned}\overline{\alpha v'_i \frac{\partial^2 \theta'}{\partial x_k \partial x_k}} &= \overline{\alpha v'_i \frac{\partial}{\partial x_k} \left(\frac{\partial \theta'}{\partial x_k} \right)} = \alpha \frac{\partial}{\partial x_k} \left(\overline{v'_i \frac{\partial \theta'}{\partial x_k}} \right) - \alpha \overline{\frac{\partial \theta'}{\partial x_k} \frac{\partial v'_i}{\partial x_k}} \\ \overline{\nu \theta' \frac{\partial^2 v'_i}{\partial x_k \partial x_k}} &= \overline{\nu \theta' \frac{\partial}{\partial x_k} \left(\frac{\partial v'_i}{\partial x_k} \right)} = \nu \frac{\partial}{\partial x_k} \left(\overline{\theta' \frac{\partial v'_i}{\partial x_k}} \right) - \nu \overline{\frac{\partial \theta'}{\partial x_k} \frac{\partial v'_i}{\partial x_k}}\end{aligned}\quad (11.19)$$

Inserting Eqs. 11.15, 11.17, 11.18 and 11.19 into Eq. 11.14 gives the transport equation for the heat flux vector $\overline{v'_i \theta'}$

$$\begin{aligned}\frac{\partial \overline{v'_i \theta'}}{\partial t} + \frac{\partial}{\partial x_k} \overline{v_k v'_i \theta'} &= \underbrace{-\overline{v'_i v'_k} \frac{\partial \bar{\theta}}{\partial x_k}}_{P_{i\theta}} - \underbrace{\overline{v'_k \theta'} \frac{\partial \bar{v}_i}{\partial x_k}}_{\Pi_{i\theta}} - \underbrace{\frac{\overline{\theta'} \partial p'}{\rho \partial x_i}}_{\Pi_{i\theta}} - \underbrace{\frac{\partial}{\partial x_k} \overline{v'_k v'_i \theta'}}_{D_{i\theta,t}} \\ &+ \underbrace{\alpha \frac{\partial}{\partial x_k} \left(\overline{v'_i \frac{\partial \theta'}{\partial x_k}} \right)}_{D_{i\theta,\nu}} + \underbrace{\nu \frac{\partial}{\partial x_k} \left(\overline{\theta' \frac{\partial v'_i}{\partial x_k}} \right)}_{\varepsilon_{i\theta}} - \underbrace{(\nu + \alpha) \frac{\partial v'_i}{\partial x_k} \frac{\partial \theta'}{\partial x_k}}_{\varepsilon_{i\theta}} - \underbrace{g_i \beta \overline{\theta'^2}}_{G_{i\theta}}\end{aligned}\quad (11.20)$$

where $P_{i\theta}$, $\Pi_{i\theta}$ and $D_{i\theta,t}$ denote the production, scramble and turbulent diffusion term, respectively. The production term includes one term with the mean velocity gradient and one with the mean temperature gradient. On the last line, $D_{i\theta,\nu}$, $\varepsilon_{i\theta}$ and $G_{i\theta}$ denote viscous diffusion, dissipation and buoyancy term, respectively. The unknown terms – $\Pi_{i\theta}$, $D_{i\theta}$, $\varepsilon_{i\theta}$, $G_{i\theta}$ – have to be modeled as usual; this is out of the scope of the present course but the interested reader is referred to [25].

It can be noted that there is no usual viscous diffusion term in Eq. 11.20. The reason is that the viscous diffusion coefficients are different in the v_i equation and the θ equation (ν in the former case and α in the latter). However, if $\nu \simeq \alpha$ (which corresponds to a Prandtl number of unity, i.e. $Pr = \nu/\alpha \simeq 1$, see Eq. 2.19), the diffusion term in Eq. 11.20 assumes the familiar form

$$\begin{aligned}&\alpha \frac{\partial}{\partial x_k} \left(\overline{v'_i \frac{\partial \theta'}{\partial x_k}} \right) + \nu \frac{\partial}{\partial x_k} \left(\overline{\theta' \frac{\partial v'_i}{\partial x_k}} \right) \\ &= \alpha \frac{\partial^2 \overline{v'_i \theta'}}{\partial x_k \partial x_k} - \alpha \frac{\partial}{\partial x_k} \left(\overline{\theta' \frac{\partial v'_i}{\partial x_k}} \right) + \nu \frac{\partial^2 \overline{v'_i \theta'}}{\partial x_k \partial x_k} - \nu \frac{\partial}{\partial x_k} \left(\overline{v'_i \frac{\partial \theta'}{\partial x_k}} \right) \\ &\simeq \left(\nu + \frac{\nu}{Pr} \right) \frac{\partial^2 \overline{v'_i \theta'}}{\partial x_k \partial x_k} - \nu \frac{\partial}{\partial x_k} \left(\overline{\theta' \frac{\partial v'_i}{\partial x_k}} \right) - \nu \frac{\partial}{\partial x_k} \left(\overline{v'_i \frac{\partial \theta'}{\partial x_k}} \right) \\ &= \left(\nu + \frac{\nu}{Pr} \right) \frac{\partial^2 \overline{v'_i \theta'}}{\partial x_k \partial x_k} - D_{i\theta,\nu}\end{aligned}\quad (11.21)$$

where $D_{i\theta,\nu}$ cancels the corresponding term in Eq. 11.20 if $\alpha = \nu$. Often the viscous diffusion is simplified in this way. Hence, if $\alpha \simeq \nu$ the transport equation for $\overline{v'_i \theta'}$ can be simplified as

$$\begin{aligned}\frac{\partial \overline{v'_i \theta'}}{\partial t} + \frac{\partial}{\partial x_k} \overline{v_k v'_i \theta'} &= \underbrace{-\overline{v'_i v'_k} \frac{\partial \bar{\theta}}{\partial x_k}}_{P_{i\theta}} - \underbrace{\overline{v'_k \theta'} \frac{\partial \bar{v}_i}{\partial x_k}}_{\Pi_{i\theta}} - \underbrace{\frac{\overline{\theta'} \partial p'}{\rho \partial x_i}}_{\Pi_{i\theta}} - \underbrace{\frac{\partial}{\partial x_k} \overline{v'_k v'_i \theta'}}_{D_{i\theta,t}} \\ &+ \underbrace{\left(\nu + \frac{\nu}{Pr} \right) \frac{\partial^2 \overline{v'_i \theta'}}{\partial x_k \partial x_k}}_{D_{i\theta,\nu}} - \underbrace{(\nu + \alpha) \frac{\partial v'_i}{\partial x_k} \frac{\partial \theta'}{\partial x_k}}_{\varepsilon_{i\theta}} - \underbrace{g_i \beta \overline{\theta'^2}}_{G_{i\theta}}\end{aligned}\quad (11.22)$$

The same question arises as for the $\overline{v'_i v'_j}$ equation: which terms need to be modeled in Eq. 11.22? The following quantities are known:

\bar{v}_i is obtained from the momentum equation, Eq. 11.2

$\bar{\theta}$ is obtained from the temperature equation, Eq. 11.9

$\overline{v'_i v'_j}$ is obtained from the modeled $\overline{v'_i v'_j}$ equation, Eq. 11.101

$\overline{v'_i \theta'}$ is obtained from the modeled $\overline{v'_i \theta'}$ equation

Hence the following terms in Eq. 11.22 are known (i.e. they do not need to be modeled)

- The left side
- The production term, $P_{i\theta}$
- The viscous diffusion term, $D_{i\theta, \nu}$
- The buoyancy term, $G_{i\theta}$ (provided that a transport equation is solved for $\overline{\theta'^2}$; if not, $\overline{\theta'^2}$ is usually modeled via a relation to k)

11.4 The k equation

The turbulent kinetic energy is the sum of all normal Reynolds stresses, i.e.

$$k = \frac{1}{2} (\overline{v_1'^2} + \overline{v_2'^2} + \overline{v_3'^2}) \equiv \frac{1}{2} \overline{v'_i v'_i}$$

By taking the trace (setting indices $i = j$) of the equation for $\overline{v'_i v'_j}$ and dividing by two we get the equation for the turbulent kinetic energy:

$$\begin{aligned} \frac{\partial k}{\partial t} + \underbrace{\bar{v}_j \frac{\partial k}{\partial x_j}}_{C^k} = & - \underbrace{\overline{v'_i v'_j} \frac{\partial \bar{v}_i}{\partial x_j}}_{P^k} - \underbrace{\nu \frac{\partial \overline{v'_i v'_j}}{\partial x_j} \frac{\partial \bar{v}_i}{\partial x_j}}_{\varepsilon} \\ & - \underbrace{\frac{\partial}{\partial x_j} \left\{ \overline{v'_j \left(\frac{p'}{\rho} + \frac{1}{2} v'_i v'_i \right)} \right\}}_{D_t^k} + \underbrace{\nu \frac{\partial^2 k}{\partial x_j \partial x_j}}_{D_\nu^k} - \underbrace{g_i \beta \overline{v'_i \theta'}}_{G^k} \end{aligned} \quad (11.23)$$

where – as in the $\overline{v'_i v'_j}$ equation – D_t^k and D_ν^k denotes turbulent and viscous diffusion, respectively. The total diffusion reads $D^k = D_t^k + D_\nu^k$. Equation 11.23 can symbolically be written:

$$C^k = P^k + D^k + G^k - \varepsilon \quad (11.24)$$

The known quantities in Eq. 11.23 are:

\bar{v}_i is obtained from the momentum equation, Eq. 11.2

k is obtained from the modeled k equation, Eq. 11.97

Hence the following terms in Eq. 11.23 are known (i.e. they do not need to be modeled)

- The left side
- The viscous diffusion term, $D_{i, \nu}^k$
- The buoyancy term, G_{ij} (provided that a transport equation is solved for $\overline{v'_i \theta'}$, Eq. 11.22; if not, $\overline{v'_i \theta'}$ is obtained from the Boussinesq assumption, Eq. 11.35)

11.5 The ε equation

Two quantities are usually used in eddy-viscosity model to express the turbulent viscosity. In the $k - \varepsilon$ model, k and ε are used. The turbulent viscosity is estimated – using dimensional analysis – as the product of a turbulent velocity, \mathcal{U} , and length scale, \mathcal{L} ,

$$\nu_t \propto \mathcal{U}\mathcal{L} \quad (11.25)$$

The velocity scale is taken as $k^{1/2}$ and the length scale as $k^{3/2}/\varepsilon$ which gives

$$\nu_t = C_\mu \frac{k^2}{\varepsilon}$$

where $C_\mu = 0.09$. An exact equation for the transport equation for the dissipation

$$\varepsilon = \nu \frac{\partial v'_i}{\partial x_j} \frac{\partial v'_i}{\partial x_j}$$

can be derived (see, e.g., [26]), but it is very complicated and in the end many terms are found negligible. It is much easier to look at the k equation, Eq. 11.24, and to setup a similar equation for ε . The transport equation should include a convective term, C^ε , a diffusion term, D^ε , a production term, P^ε , a production term due to buoyancy, G^ε , and a destruction term, Ψ^ε , i.e.

$$C^\varepsilon = P^\varepsilon + D^\varepsilon + G^\varepsilon - \Psi^\varepsilon \quad (11.26)$$

The production and destruction terms, P^k and ε , in the k equation are used to formulate the corresponding terms in the ε equation. The terms in the k equation have the dimension $[m^2/s^3]$ (look at the unsteady term, $\partial k/\partial t$) whereas the terms in the ε equation have the dimension $[m^2/s^4]$ (cf. $\partial \varepsilon/\partial t$). Hence, we must multiply P^k and ε by a quantity which has the dimension $[1/s]$. One quantity with this dimension is the mean velocity gradient which might be relevant for the production term, but not for the destruction. A better choice should be $\varepsilon/k = [1/s]$. Hence, we get

$$P^\varepsilon + G^\varepsilon - \Psi^\varepsilon = \frac{\varepsilon}{k} (c_{\varepsilon 1} P^k + c_{\varepsilon 1} G^k - c_{\varepsilon 2} \varepsilon) \quad (11.27)$$

where we have added new unknown coefficients in front of each term. The turbulent diffusion term is expressed in the same way as that in the k equation (see Eq. 11.40) but with its own turbulent Prandtl number, σ_ε (see Eq. 11.37), i.e.

$$D^\varepsilon = \frac{\partial}{\partial x_j} \left[\left(\nu + \frac{\nu_t}{\sigma_\varepsilon} \right) \frac{\partial \varepsilon}{\partial x_j} \right] \quad (11.28)$$

The final form of the ε transport equation reads

$$\frac{\partial \varepsilon}{\partial t} + \bar{v}_j \frac{\partial \varepsilon}{\partial x_j} = \frac{\varepsilon}{k} (c_{\varepsilon 1} P^k + c_{\varepsilon 1} G^k - c_{\varepsilon 2} \varepsilon) + \frac{\partial}{\partial x_j} \left[\left(\nu + \frac{\nu_t}{\sigma_\varepsilon} \right) \frac{\partial \varepsilon}{\partial x_j} \right] \quad (11.29)$$

Note that this is a *modeled* equation since we have modeled the production, destruction and turbulent diffusion terms.

For details on how to derive the constants, see [27].

11.6 The Boussinesq assumption

In the Boussinesq assumption an eddy (i.e. a *turbulent*) viscosity is introduced to model the unknown Reynolds stresses in Eq. 11.2. Consider the diffusion terms in the incompressible momentum equation in the case of non-constant viscosity (see Eq. 2.6)

$$\frac{\partial}{\partial x_j} \left\{ \nu \left(\frac{\partial \bar{v}_i}{\partial x_j} + \frac{\partial \bar{v}_j}{\partial x_i} \right) - \overline{v'_i v'_j} \right\} \quad (11.30)$$

Now we want to replace the Reynolds stress tensor, $\overline{v'_i v'_j}$, by a turbulent viscosity, ν_t , so that the diffusion terms can be written

$$\frac{\partial}{\partial x_j} \left\{ (\nu + \nu_t) \left(\frac{\partial \bar{v}_i}{\partial x_j} + \frac{\partial \bar{v}_j}{\partial x_i} \right) \right\} \quad (11.31)$$

Note that ν_t is not constant. Identification of Eqs. 11.30 and 11.31 gives

$$-\overline{v'_i v'_j} = \nu_t \left(\frac{\partial \bar{v}_i}{\partial x_j} + \frac{\partial \bar{v}_j}{\partial x_i} \right) \quad (11.32)$$

This is identical to the assumption for the Newtonian, viscous stress for incompressible flow, see Eq. 2.4. Equation 11.32 is not valid upon contraction³ (the right side will be zero due to continuity, but not the left side). Hence we add the trace of the left side to the right side so that

$$\overline{v'_i v'_j} = -\nu_t \left(\frac{\partial \bar{v}_i}{\partial x_j} + \frac{\partial \bar{v}_j}{\partial x_i} \right) + \frac{1}{3} \delta_{ij} \overline{v'_k v'_k} = -2\nu_t \bar{s}_{ij} + \frac{2}{3} \delta_{ij} k \quad (11.33)$$

Now the equation is valid also when it is contracted (i.e taking the trace); after contraction both left and right side are equal (as they must be) to $\overline{v'_i v'_i} = 2k$. When Eq. 11.33 is included in Eq. 11.2 we replace six turbulent stresses with one new unknown (the turbulent viscosity, ν_t). This is of course a drastic simplification. With the Boussinesq assumption the momentum equation reads (see Eq. 11.2 and 11.33)

$$\begin{aligned} & \frac{\partial \rho_0 \bar{v}_i}{\partial t} + \frac{\partial}{\partial x_j} (\rho_0 \bar{v}_i \bar{v}_j) \\ &= -\frac{\partial \bar{p}_B}{\partial x_i} + \frac{\partial}{\partial x_j} \left[(\mu + \mu_t) \left(\frac{\partial \bar{v}_i}{\partial x_j} + \frac{\partial \bar{v}_j}{\partial x_i} \right) \right] - \beta \rho_0 (\bar{\theta} - \theta_0) g_i \end{aligned} \quad (11.34)$$

where the turbulent kinetic energy (last term in Eq. 11.33) has been incorporated in the pressure, i.e. $\bar{p}_B = \bar{p} + 2k/3$. There is a fundamental difference between μ and μ_t : μ is different for each fluid (water, air, methane, ...) and depends mainly on temperature; μ_t depends on the flow, i.e. it is function of the location ($\mu_t = \mu_t(x_i)$).

If the mean temperature equation, Eq. 11.9, is solved for, we need an equation for the heat flux vector, $\overline{v'_i \theta'}$. One option is to solve its transport equation, Eq. 11.22. However, it is more common to use an eddy-viscosity model for the heat flux vector. The Boussinesq assumption reads

$$\overline{v'_i \theta'} = -\alpha_t \frac{\partial \bar{\theta}}{\partial x_i} \quad (11.35)$$

³contraction means that i is set to j

where α_t denotes the turbulent thermal diffusivity. Note that this is the same assumption as Fourier's law for a Newtonian flux, see Eq. 2.14. The turbulent thermal diffusivity, α_t , is usually obtained from the turbulent viscosity as

$$\alpha_t = \frac{\nu_t}{\sigma_\theta} \quad (11.36)$$

where σ_θ is the turbulent Prandtl number; it is an empirical constant which is usually set to $0.7 \leq \sigma_\theta \leq 0.9$. The physical meaning of the turbulent Prandtl number, σ_θ , is analogous to the physical meaning of the usual Prandtl number, see Eq. 2.19; it defines how efficient the turbulence transports (by diffusion) momentum compared to how efficient it transports thermal energy, i.e.

$$\sigma_\theta = \frac{\nu_t}{\alpha_t} \quad (11.37)$$

It is important to recognize that the viscosity (ν), the Prandtl number (Pr), the thermal diffusivity (α) are *physical* parameters which depend on the fluid (e.g. water or air) and its conditions (e.g. temperature). However, the turbulent viscosity (ν_t), the turbulent thermal diffusivity (α_t) and the turbulent Prandtl number (σ_θ) depend on the *flow* (e.g. mean flow gradients and turbulence).

11.7 Modeling assumptions

Now we will compare the modeling assumptions for the unknown terms in the $\overline{v'_i v'_j}$, $\overline{v'_i \theta'}$, k and ε equations and formulate modeling assumptions for the remaining terms in the Reynolds stress equation. This will give us the Reynolds Stress Model [RSM] (also called the Reynolds Stress Transport Model [RSTM]) where a (modeled) transport equation is solved for each stress. Later on, we will introduce a simplified algebraic model, which is called the Algebraic Stress Model [ASM] (this model is also called Algebraic Reynolds Stress Model, ARSM)

Summary of physical meaning:

P_{ij} , $P_{i\theta}$ and P^k are production terms of $\overline{v'_i v'_j}$, $\overline{v'_i \theta'}$ and k

G_{ij} , $G_{i\theta}$ and G^k are production terms of $\overline{v'_i v'_j}$, $\overline{v'_i \theta'}$ and k due to buoyancy

$D_{ij,t}$, $D_{i\theta,t}$, D_t^k are the turbulent diffusion terms of $\overline{v'_i v'_j}$, $\overline{v'_i \theta'}$ and k

$\Pi_{i\theta}$ is the pressure-scramble terms of $\overline{v'_i \theta'}$

Π_{ij} is the pressure-strain correlation term, which promotes isotropy of the turbulence

ε_{ij} , $\varepsilon_{i\theta}$ and ε are dissipation of $\overline{v'_i v'_j}$, $\overline{v'_i \theta'}$ and k , respectively. The dissipation takes place at the small-scale turbulence.

11.7.1 Production terms

In RSM and ASM the production terms are computed exactly

$$\begin{aligned} P_{ij} &= -\overline{v'_i v'_k} \frac{\partial \bar{v}_j}{\partial x_k} - \overline{v'_j v'_k} \frac{\partial \bar{v}_i}{\partial x_k}, & P^k &= \frac{1}{2} P_{ii} = -\overline{v'_i v'_j} \frac{\partial \bar{v}_i}{\partial x_j} \\ P_{i\theta} &= -\overline{v'_i v'_k} \frac{\partial \bar{\theta}}{\partial x_k} - \overline{v'_k \theta'} \frac{\partial \bar{v}_i}{\partial x_k} \end{aligned} \quad (11.38)$$

k is usually not solved for in RSM but a length-scale equation (i.e. ε or ω) is always part of an RSM and that equation includes P^k .

In the $k - \varepsilon$ model, the Reynolds stresses in the production term are computed using the Boussinesq assumption, which gives

$$\begin{aligned}
 -\overline{v'_i v'_j} &= \nu_t \left(\frac{\partial \bar{v}_i}{\partial x_j} + \frac{\partial \bar{v}_j}{\partial x_i} \right) - \frac{2}{3} \delta_{ij} k \\
 P^k &= \left\{ \nu_t \left(\frac{\partial \bar{v}_i}{\partial x_j} + \frac{\partial \bar{v}_j}{\partial x_i} \right) - \frac{2}{3} \delta_{ij} k \right\} \frac{\partial \bar{v}_i}{\partial x_j} \\
 &= \nu_t \left(\frac{\partial \bar{v}_i}{\partial x_j} + \frac{\partial \bar{v}_j}{\partial x_i} \right) \frac{\partial \bar{v}_i}{\partial x_j} = \nu_t 2 \bar{s}_{ij} (\bar{s}_{ij} + \Omega_{ij}) = 2 \nu_t \bar{s}_{ij} \bar{s}_{ij} \\
 \bar{s}_{ij} &= \frac{1}{2} \left(\frac{\partial \bar{v}_i}{\partial x_j} + \frac{\partial \bar{v}_j}{\partial x_i} \right), \quad \Omega_{ij} = \frac{1}{2} \left(\frac{\partial \bar{v}_i}{\partial x_j} - \frac{\partial \bar{v}_j}{\partial x_i} \right), \quad \frac{\partial \bar{v}_i}{\partial x_j} = \bar{s}_{ij} + \Omega_{ij}
 \end{aligned} \tag{11.39}$$

where on the third line we used the fact that $\bar{s}_{ij} \Omega_{ij} = 0$ because the product between a symmetric tensor (\bar{s}_{ij}) and an asymmetric tensor (Ω_{ij}) is zero. The incompressibility condition, $\partial \bar{v}_i / \partial x_i = 0$, was used to obtain the third line.

11.7.2 Diffusion terms

The diffusion terms in the k and ε -equations in the $k - \varepsilon$ model are modeled using the standard gradient hypothesis which reads

$$\begin{aligned}
 D^k &= \frac{\partial}{\partial x_j} \left[\left(\nu + \frac{\nu_t}{\sigma_k} \right) \frac{\partial k}{\partial x_j} \right] \\
 D^\varepsilon &= \frac{\partial}{\partial x_j} \left[\left(\nu + \frac{\nu_t}{\sigma_\varepsilon} \right) \frac{\partial \varepsilon}{\partial x_j} \right]
 \end{aligned} \tag{11.40}$$

The gradient hypothesis simply assumes that turbulent diffusion acts as to even out all inhomogeneities. In other words, it assumes that the turbulent diffusion term, D^k , transports k from regions where k is large to regions where k is small. The turbulent diffusion flux of k is expressed as

$$d_{j,t}^k = \frac{1}{2} \overline{v'_j v'_i v'_i} = - \frac{\nu_t}{\sigma_k} \frac{\partial k}{\partial x_j} \tag{11.41}$$

Note that this is the same assumption as Fourier's law for a Newtonian flux, see Eq. 2.14. Only the triple correlations are included since the pressure diffusion usually is negligible (see Fig. 8.3 at p. 110). Taking the divergence of Eq. 11.41 (including the minus sign in Eq. 11.23) gives the turbulent diffusion term in Eq. 11.40.

Solving the equations for the Reynolds stresses, $\overline{v'_i v'_j}$, opens possibilities for a more advanced model of the turbulent diffusion terms. Equation 11.41 assumes that if the gradient is zero in x_j direction, then there is no diffusion flux in that direction. A more general gradient hypothesis can be formulated without this limitation, e.g.

$$d_{j,t,G}^k \propto \overline{v'_j v'_k} \frac{\partial k}{\partial x_k} \tag{11.42}$$

which is called the general gradient diffusion hypothesis (GGDH). It was derived in [28] from the transport equation of the triple correlation $\overline{v'_j v'_i v'_i}$. In GGDH the turbulent

flux $d_{1,t,G}^k$, for example, is computed as

$$d_{1,t,G}^k \propto \overline{v'_1 v'_1} \frac{\partial k}{\partial x_1} + \overline{v'_1 v'_2} \frac{\partial k}{\partial x_2} + \overline{v'_1 v'_3} \frac{\partial k}{\partial x_3} \quad (11.43)$$

Hence, even if $\partial k / \partial x_1 = 0$ the diffusion flux $d_{1,t,G}^k$ may be non-zero. A quantity of dimension $[s]$ must be added to get the correct dimension, and as in Eq. 11.27 we take k/ε so that

$$d_{j,t,G}^k = c_k \frac{k}{\varepsilon} \overline{v'_j v'_k} \frac{\partial k}{\partial x_k} \quad (11.44)$$

The diffusion term, D_t^k , in the k equation is obtained by taking the divergence of this equation

$$D_t^k = \frac{\partial d_{j,t,G}^k}{\partial x_j} = \frac{\partial}{\partial x_j} \left(c_k \frac{k}{\varepsilon} \overline{v'_j v'_k} \frac{\partial k}{\partial x_k} \right) \quad (11.45)$$

This diffusion model may be used when the k equation is solved in an RSM or an ASM. The corresponding diffusion terms for the ε and $\overline{v'_i v'_j}$ equations read

$$\begin{aligned} D_t^\varepsilon &= \frac{\partial}{\partial x_j} \left(c_\varepsilon \frac{k}{\varepsilon} \overline{v'_j v'_k} \frac{\partial \varepsilon}{\partial x_k} \right) \\ D_{ij,t} &= \frac{\partial}{\partial x_k} \left(c_k \frac{k}{\varepsilon} \overline{v'_i v'_j v'_k} \frac{\partial \varepsilon}{\partial x_m} \right) \end{aligned} \quad (11.46)$$

Equation 11.46 often causes numerical problems. A more stable alternative is to model the diffusion terms as in 11.40 which for $\overline{v'_i v'_j}$ reads

$$D_{ij,t} = \frac{\partial}{\partial x_m} \left(\frac{\nu_t}{\sigma_k} \frac{\partial \overline{v'_i v'_j}}{\partial x_m} \right) \quad (11.47)$$

11.7.3 Dissipation term, ε_{ij}

The dissipation term ε_{ij} (see Eq. 11.11) is active for the small-scale turbulence. Because of the cascade process and vortex stretching (see Figs. 5.3 and 5.4) the small-scale turbulence is isotropic. This means that the velocity fluctuations of the small-scale turbulence have no preferred direction, see p. 82. This gives:

1. $\overline{v_1'^2} = \overline{v_2'^2} = \overline{v_3'^2}$.
2. All shear stresses are zero, i.e.

$$\overline{v'_i v'_j} = 0 \quad \text{if } i \neq j$$

because the fluctuations in two different coordinate directions are not correlated.

What applies for the small-scale fluctuations (Items 1 and 2, above) must also apply for the gradients of the fluctuations, i.e.

$$\begin{aligned} \frac{\partial \overline{v'_1 v'_1}}{\partial x_k \partial x_k} &= \frac{\partial \overline{v'_2 v'_2}}{\partial x_k \partial x_k} = \frac{\partial \overline{v'_3 v'_3}}{\partial x_k \partial x_k} \\ \frac{\partial \overline{v'_i v'_j}}{\partial x_k \partial x_k} &= 0 \quad \text{if } i \neq j \end{aligned} \quad (11.48)$$

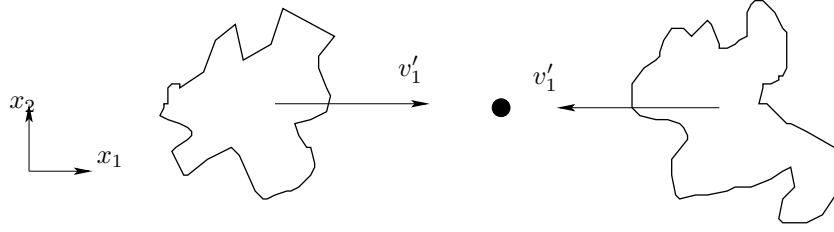


Figure 11.1: Physical illustration of the pressure-strain term.

The relations in Eq. 11.48 are conveniently expressed in tensor notation as

$$\varepsilon_{ij} = \frac{2}{3}\varepsilon\delta_{ij} \quad (11.49)$$

where the factor $2/3$ is included so that $\varepsilon = \frac{1}{2}\varepsilon_{ii}$ is satisfied, see Eqs. 11.11 and 11.23.

11.7.4 Slow pressure-strain term

The pressure-strain term, Π_{ij} , makes a large contribution to the $\overline{v'_i v'_j}$ equation. In Section 9 it was shown that for channel flow it is negative for the streamwise equation, $\overline{v'^2_1}$, and positive for the wall-normal, $\overline{v'^2_2}$, and spanwise, $\overline{v'^2_3}$, equations. Furthermore, it acts as a sink term for the shear stress equation. In summary, it was shown that the term acts as to make the turbulence more *isotropic*, i.e. decreasing the large normal stresses and the magnitude of the shear stress and increasing the small normal stresses. The pressure-strain term is often called the *Robin Hood* terms, because it “takes from the rich and gives to the poor”.

The role of the pressure strain can be described in physical terms as follows. Assume that two fluid particles with fluctuating velocities v'_1 bounce into each other at O so that $\partial v'_1 / \partial x_1 < 0$, see Fig. 11.1. As a result the fluctuating pressure p' increases at O so that

$$p' \frac{\partial v'_1}{\partial x_1} < 0$$

The fluid in the x_1 direction is performing work, moving fluid particles against the pressure gradient. The kinetic energy lost in the x_1 direction is transferred to the x_2 and x_3 directions and we assume that the collision makes fluid particles move in the other two directions, i.e.

$$\frac{\partial v'_2}{\partial x_2} > 0, \quad \frac{\partial v'_3}{\partial x_3} > 0 \quad (11.50)$$

Indeed, if $\partial v'_1 / \partial x_1 < 0$, the continuity equation gives $\partial v'_2 / \partial x_2 + \partial v'_3 / \partial x_3 > 0$. However, in Eq. 11.50 we assume that not only their sum is positive but also that they both are positive. If this is to happen the kinetic energy in the x_1 direction must be larger than that in the x_2 and x_3 direction, i.e. $\overline{v'^2_1} > \overline{v'^2_2}$ and $\overline{v'^2_1} > \overline{v'^2_3}$. If $\overline{v'^2_3} \simeq \overline{v'^2_1}$, the pressure strain re-distributes kinetic energy from both $\overline{v'^2_1}$ and $\overline{v'^2_3}$ to $\overline{v'^2_2}$.

Now let's assume that $\overline{v'^2_1} > \overline{v'^2_2}$ and $\overline{v'^2_1} > \overline{v'^2_3}$. The amount of kinetic energy transferred from the x_1 direction to the x_2 and x_3 directions, should be proportional to

the difference of their energies, i.e.

$$\begin{aligned} \overline{p' \frac{\partial v'_1}{\partial x_1}} &\propto -\frac{\rho}{2t} \left[\left(\overline{v_1'^2} - \overline{v_2'^2} \right) + \left(\overline{v_1'^2} - \overline{v_3'^2} \right) \right] \\ &= -\frac{\rho}{t} \left[\overline{v_1'^2} - \frac{1}{2} \left(\overline{v_2'^2} + \overline{v_3'^2} \right) \right] = -\frac{\rho}{t} \left[\frac{3}{2} \overline{v_1'^2} - \frac{1}{2} \left(\overline{v_1'^2} + \overline{v_2'^2} + \overline{v_3'^2} \right) \right] = -\frac{\rho}{t} \left(\frac{3}{2} \overline{v_1'^2} - k \right) \end{aligned} \quad (11.51)$$

where t denotes a turbulent timescale. The expression in Eq. 11.51 applies only to the normal stresses, i.e. the principal axis of $v'_i v'_j$. Let us show that by transforming the fluctuations to a coordinate system which is rotated an angle $\alpha = \pi/4$ then $\overline{p'(\partial v'_1/\partial x_2 + \partial v'_2/\partial x_1)} \propto -\overline{v'_1 v'_2}$ ($\alpha = \pi/4$ corresponds to the special case when the normal stresses are equal). We express Eq. 11.51 in principal coordinates, (x_{1*}, x_{2*}) , and then transform the equation to (x_1, x_2) by rotating it angle $\alpha = \pi/4$, see Appendix 53.1. Replacing u_{12} in Eq. 53.6b by $v'_1 v'_2$ we get

$$\overline{v'_1 v'_2} = 0.5 \left(\overline{v_{1*}'^2} - \overline{v_{2*}'^2} \right) \quad (11.52)$$

since $\overline{v'_{1*} v'_{2*}} = \overline{v'_{2*} v'_{1*}}$. Now we have transformed the right side of Eq. 11.51 (the right side on the first line). Next step is to transform the left side, i.e. the velocity gradients. We use Eqs. 53.6b and 53.6c: replacing u_{12} and u_{21} by $\partial v'_1/\partial x_2$ and $\partial v'_2/\partial x_1$, respectively, and adding them gives

$$\frac{\partial v'_2}{\partial x_1} + \frac{\partial v'_1}{\partial x_2} = \frac{\partial v'_{1*}}{\partial x_{1*}} - \frac{\partial v'_{2*}}{\partial x_{2*}} \quad (11.53)$$

the pressure-strain term in Eqs. 11.11 and 11.51 can be written

$$\overline{p' \left(\frac{\partial v'_2}{\partial x_1} + \frac{\partial v'_1}{\partial x_2} \right)} = \overline{p' \left(\frac{\partial v'_{1*}}{\partial x_{1*}} - \frac{\partial v'_{2*}}{\partial x_{2*}} \right)} \quad (11.54)$$

Now we apply Eq. 11.51 in the x_{1*} and $-x_{2*}$ directions (looking at the right side of Eq. 11.54) so that

$$\overline{p' \left(\frac{\partial v'_{1*}}{\partial x_{1*}} - \frac{\partial v'_{2*}}{\partial x_{2*}} \right)} \propto -\frac{3\rho}{2t} \left(\overline{v_{1*}'^2} - \overline{v_{2*}'^2} \right) \quad (11.55)$$

Inserting Eqs. 11.52 and 11.54 into Eq. 11.55 gives finally

$$\overline{p' \left(\frac{\partial v'_2}{\partial x_1} + \frac{\partial v'_1}{\partial x_2} \right)} \propto -\frac{3}{t} \rho \overline{v'_1 v'_2} \quad (11.56)$$

This shows that the pressure-strain term acts as a sink term in the shear stress equation. Thus, Eqs. 11.51 and 11.56 lead as to write

$$\Phi_{ij,1} \equiv \overline{p' \left(\frac{\partial v'_i}{\partial x_j} + \frac{\partial v'_j}{\partial x_i} \right)} = -c_1 \rho \frac{\varepsilon}{k} \left(\overline{v'_i v'_j} - \frac{2}{3} \delta_{ij} k \right) \quad (11.57)$$

where Φ denotes the *modeled* pressure-strain term and subscript 1 means the slow part; the concept “slow” and “rapid” is discussed at p. 142. We have introduced the turbulent time scale $t = k/\varepsilon$ and a constant c_1 . This pressure-strain model for the slow part was proposed by Rotta in 1951 [29].

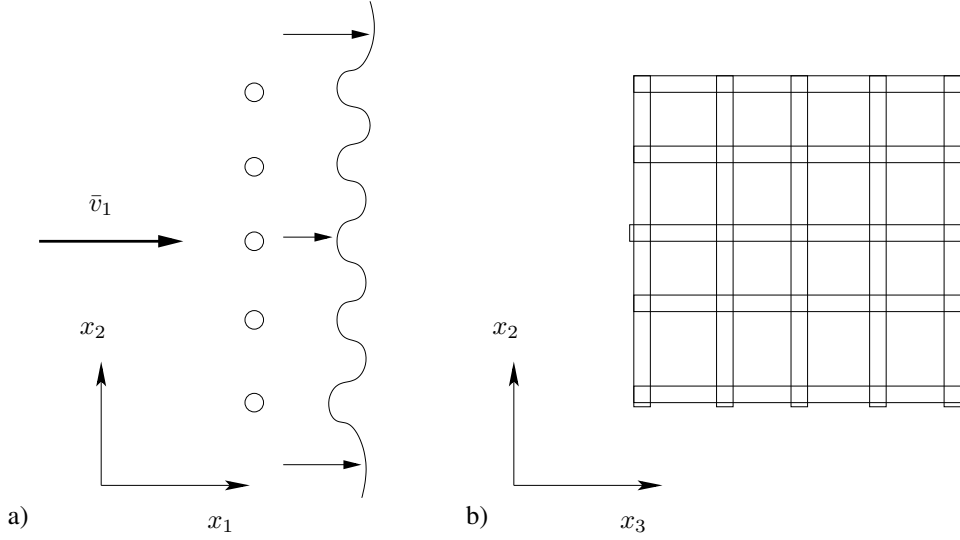


Figure 11.2: Decaying grid turbulence. The circles (a) and the thin rectangles (b) illustrates part of the grid which consists of a mesh of circular cylinders.

Let us investigate how Eq. 11.57 behaves for decaying grid turbulence, see Fig. 11.2. Flow from left with velocity \bar{v}_1 passes through a grid. The grid creates velocity gradients behind the grid which generates turbulence. Further downstream the velocity gradients are smoothed out and the mean flow becomes constant. From this point and further downstream the flow represents anisotropic turbulence (homogeneous in the x_2 and x_3 directions) which is slowly approaching isotropic turbulence; furthermore the turbulence is slowly dying (i.e. decaying) due to dissipation. The exact $\overline{v'_i v'_j}$ equation for this flow reads (no production or diffusion because of homogeneity)

$$\bar{v}_1 \frac{d\overline{v'_i v'_j}}{dx_1} = \frac{p'}{\rho} \left(\frac{\partial v'_i}{\partial x_j} + \frac{\partial v'_j}{\partial x_i} \right) - \varepsilon_{ij} \quad (11.58)$$

Rotta's pressure-strain model is supposed to reduce anisotropy. Thus it should be interesting to re-write Eq. 11.58 expressed in the normalized anisotropy Reynolds stress tensor which is defined as

$$a_{ij} = \frac{\overline{v'_i v'_j}}{k} - \frac{2}{3} \delta_{ij} \quad (11.59)$$

Note that when the turbulence is isotropic, then $a_{ij} = 0$. We introduce a_{ij} (Eq. 11.59), Rotta's model (Eq. 11.57) and the model for the dissipation tensor (11.49) into Eq. 11.58 so that

$$\bar{v}_1 \left(\frac{d(k a_{ij})}{dx_1} + \delta_{ij} \frac{2}{3} \frac{dk}{dx_1} \right) = -c_1 \varepsilon a_{ij} - \frac{2}{3} \delta_{ij} \varepsilon \quad (11.60)$$

Analogously to Eq. 11.58, the k equation in decaying grid turbulence reads

$$\bar{v}_1 \frac{dk}{dx_1} = -\varepsilon \quad (11.61)$$

Inserting Eq. 11.61 in Eq. 11.60, the left side reads

$$\begin{aligned}\bar{v}_1 a_{ij} \frac{dk}{dx_1} + \bar{v}_1 k \frac{da_{ij}}{dx_1} + \frac{2}{3} \delta_{ij} \bar{v}_1 \frac{dk}{dx_1} &= \left(a_{ij} + \frac{2}{3} \delta_{ij} \right) \bar{v}_1 \frac{dk}{dx_1} + k \bar{v}_1 \frac{da_{ij}}{dx_1} \\ &= - \left(a_{ij} + \frac{2}{3} \delta_{ij} \right) \varepsilon + k \bar{v}_1 \frac{da_{ij}}{dx_1}\end{aligned}$$

Dividing by k and inserting into Eq. 11.60 we get

$$\bar{v}_1 \frac{da_{ij}}{dx_1} = -c_1 \frac{\varepsilon}{k} a_{ij} - \frac{2}{3} \delta_{ij} \frac{\varepsilon}{k} + \frac{\varepsilon}{k} a_{ij} + \frac{2}{3} \delta_{ij} \frac{\varepsilon}{k} = \frac{\varepsilon}{k} a_{ij} (1 - c_1) \quad (11.62)$$

Provided that $c_1 > 1$ Rotta's model does indeed reduce non-isotropy as it should.

The model of the slow pressure-strain term in Eq. 11.57 can be extended by including terms which are non-linear in $\overline{v'_i v'_j}$. To make it general it is enough to include terms which are quadratic in $\overline{v'_i v'_j}$, since according to the Cayley-Hamilton theorem, a second-order tensor satisfies its own characteristic equation (see Section 1.20 in [30]); this means that terms that are cubic in $\overline{v'_i v'_j}$ (i.e. $\overline{v'_i v'_j}^3 = \overline{v'_i v'_k} \overline{v'_k v'_m} \overline{v'_m v'_j}$) can be expressed in terms that are linear and quadratic in $\overline{v'_i v'_j}$. The most general form of $\Phi_{ij,1}$ can be formulated as [31]

$$\begin{aligned}\Phi_{ij,1} &= -c_1 \rho \left[\varepsilon a_{ij} + c'_1 \left(a_{ik} a_{kj} - \frac{1}{3} \delta_{ij} a_{k\ell} a_{\ell k} \right) \right] \\ a_{ij} &= \frac{\overline{v'_i v'_j}}{k} - \frac{2}{3} \delta_{ij}\end{aligned} \quad (11.63)$$

a_{ij} is an anisotropy tensor whose trace is zero. In isotropic flow all its components are zero. Note that the right side is trace-less (i.e. the trace is zero). This should be so since the exact form of Φ_{ij} is trace-less, i.e. $\Phi_{ii} = 2p' \partial v'_i / \partial x_i = 0$.

11.7.5 Rapid pressure-strain term

Above a model for the slow part of the pressure-strain term was developed using physical arguments. Here we will carry out a mathematical derivation of a model for the rapid part of the pressure-strain term.

The notation “rapid” comes from a classical problem in turbulence called the rapid distortion problem, where a very strong velocity gradient $\partial \bar{v}_i / \partial x_j$ is imposed so that initially the second term (the slow term) can be neglected, see Eq. 11.65. It is assumed that the effect of the mean gradients is much larger than the effect of the turbulence, i.e.

$$\left| \frac{\partial \bar{v}_i}{\partial x_j} \right| / (\varepsilon/k) \rightarrow \infty \quad (11.64)$$

Thus in this case it is the first term in Eq. 11.65 which gives the most “rapid” response in p' . The second “slow” term becomes important first at a later stage when turbulence has been generated.

Now we want to derive an exact equation for the pressure-strain term, Π_{ij} . Since it includes the fluctuating pressure, p' , we start by deriving an exact equation for p' starting from Navier-Stokes equations.

1. Take the divergence of the incompressible Navier-Stokes equation assuming constant viscosity (see Eq. 6.6) i.e. $\frac{\partial}{\partial x_i} \left(v_j \frac{\partial v_i}{\partial x_j} \right) = \dots \Rightarrow \text{Equation A.}$

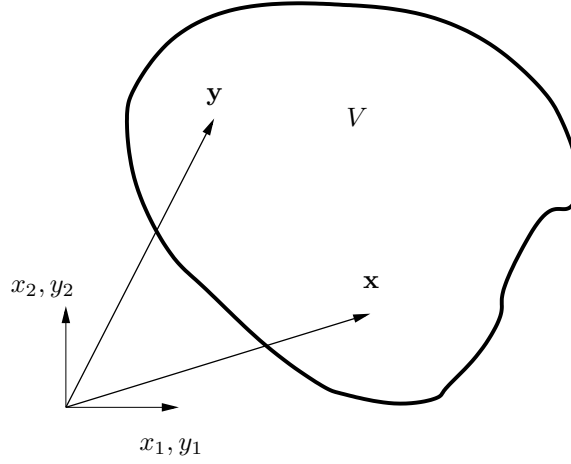


Figure 11.3: The exact solution to Eq. 11.66. The integral is carried out for all points, \mathbf{y} , in volume V .

2. Take the divergence of the incompressible time-averaged Navier-Stokes equation assuming constant viscosity (see Eq. 6.10) i.e. $\frac{\partial}{\partial x_i} \left(\bar{v}_j \frac{\partial \bar{v}_i}{\partial x_j} \right) = \dots \Rightarrow$ Equation **B**.

Subtraction of Equation **B** from Equation **A** gives a Poisson equation for the fluctuating pressure p'

$$\frac{1}{\rho} \frac{\partial^2 p'}{\partial x_j \partial x_j} = - \underbrace{2 \frac{\partial \bar{v}_i}{\partial x_j} \frac{\partial v'_j}{\partial x_i}}_{\text{rapid term}} - \underbrace{\frac{\partial^2}{\partial x_i \partial x_j} \left(v'_i v'_j - \overline{v'_i v'_j} \right)}_{\text{slow term}} \quad (11.65)$$

The factor two in the rapid term appears because when taking the divergence of the convective term there are two identical terms, see right-side of Eq. 8.6. For a Poisson equation

$$\frac{\partial^2 \varphi}{\partial x_j \partial x_j} = f \quad (11.66)$$

there exists an exact analytical solution given by Green's formula, see Appendix 54 (it is derived from Gauss divergence law)

$$\varphi(\mathbf{x}) = -\frac{1}{4\pi} \int_V \frac{f(\mathbf{y}) dy_1 dy_2 dy_3}{|\mathbf{y} - \mathbf{x}|} \quad (11.67)$$

where the integrals at the boundaries vanish because it is assumed that $f \rightarrow 0$ at the boundaries, see Fig. 11.3. Applying Eq. 11.67 on Eq. 11.65 gives

$$p'(\mathbf{x}) = \frac{\rho}{4\pi} \int_V \left[\underbrace{2 \frac{\partial \bar{v}_i(\mathbf{y})}{\partial y_j} \frac{\partial v'_j(\mathbf{y})}{\partial y_i}}_{\text{rapid term}} + \underbrace{\frac{\partial^2}{\partial y_i \partial y_j} \left(v'_i(\mathbf{y}) v'_j(\mathbf{y}) - \overline{v'_i(\mathbf{y}) v'_j(\mathbf{y})} \right)}_{\text{slow term}} \right] \frac{d\mathbf{y}^3}{|\mathbf{y} - \mathbf{x}|} \quad (11.68)$$

where $d\mathbf{y}^3 = dy_1 dy_2 dy_3$. Now make two assumptions in Eq. 11.68:

- i) the turbulence is homogeneous (i.e. the spatial derivative of all time-averaged fluctuating quantities is zero). This means that the last term in square brackets is zero. This requirement is not as drastic as it may sound (although very few turbulent flows are homogeneous). This term is indeed very small compared to the second derivative of the instantaneous fluctuations, $v'_i(\mathbf{y})v'_j(\mathbf{y})$.
- ii) the variation of $\partial\bar{v}_i/\partial x_j$ in space is small. The same argument can be used as above: the mean gradient $\partial\bar{v}_i/\partial x_j$ varies indeed much more slowly than the instantaneous velocity gradient, $\partial v'_j(\mathbf{y})/\partial y_i$

Assumption i) means that the last term in the integral in Eq. 11.68 is zero, i.e.

$$\frac{\partial^2 \overline{v'_i v'_j}}{\partial y_i \partial y_j} = 0$$

Assumption ii) means that the mean velocity gradient can be taken outside the integral. Now multiply Eq. 11.68 with $\partial v'_i/\partial x_j + \partial v'_j/\partial x_i$. Since this term is not a function of \mathbf{y} it can be moved in under the integral. We obtain after time averaging

$$\begin{aligned} & \overline{\frac{1}{\rho} p'(\mathbf{x}) \left(\frac{\partial v'_i(\mathbf{x})}{\partial x_j} + \frac{\partial v'_j(\mathbf{x})}{\partial x_i} \right)} \\ &= \frac{\partial \bar{v}_k(\mathbf{x})}{\partial x_\ell} \underbrace{\frac{1}{2\pi} \int_V \left(\frac{\partial v'_i(\mathbf{x})}{\partial x_j} + \frac{\partial v'_j(\mathbf{x})}{\partial x_i} \right) \frac{\partial v'_\ell(\mathbf{y})}{\partial y_k} \frac{d\mathbf{y}^3}{|\mathbf{y} - \mathbf{x}|}}_{M_{ijk\ell}} \\ &+ \underbrace{\frac{1}{4\pi} \int_V \left(\frac{\partial v'_i(\mathbf{x})}{\partial x_j} + \frac{\partial v'_j(\mathbf{x})}{\partial x_i} \right) \frac{\partial^2}{\partial y_k \partial y_\ell} (v'_k(\mathbf{y})v'_\ell(\mathbf{y})) \frac{d\mathbf{y}^3}{|\mathbf{y} - \mathbf{x}|}}_{A_{ij}} \end{aligned} \quad (11.69)$$

Note that the mean velocity gradient, $\partial\bar{v}/\partial x_\ell$, is taken at point \mathbf{x} because it has been moved out of the integral. In order to understand this better, consider the integral

$$f(x) = \int_0^L \frac{g(\xi)d\xi}{|x - \xi|} \quad (11.70)$$

Note that x and ξ are coordinates along the same axis (think of them as two different points along the x axis). If the two points, x and ξ , are far from each other, then the denominator is large and the contribution to the integral is small. Hence, we only need to consider ξ points which are close to x . If we assume that $g(\xi)$ varies slowly with ξ , $g(\xi)$ can be moved out of the integral and since x is close to ξ , Eq. 11.70 can be written as

$$f(x) = g(x) \int_0^L \frac{d\xi}{|x - \xi|} \quad (11.71)$$

Going from Eq. 11.70 to Eq. 11.71 corresponds to moving the mean velocity gradient out of the integral. Equation 11.69 can be written on shorter form as

$$\frac{p'}{\rho} \left(\frac{\partial v'_i}{\partial x_j} + \frac{\partial v'_j}{\partial x_i} \right) = A_{ij} + M_{ijk\ell} \frac{\partial \bar{v}_k}{\partial x_\ell} = \Phi_{ij,1} + \Phi_{ij,2} \quad (11.72)$$

where the first term represents the slow term, $\Phi_{ij,1}$ (see Eq. 11.57), and second term is the rapid term, $\Phi_{ij,2}$ (index 2 denotes the rapid part).

Now we will take a closer look at the rapid part (i.e. the second term) of $M_{ijk\ell}$. The second term of $M_{ijk\ell}$ in the integral in Eq. 11.69 can be rewritten as

$$\begin{aligned} \frac{\partial v'_j(\mathbf{x})}{\partial x_i} \frac{\partial v'_\ell(\mathbf{y})}{\partial y_k} &= \frac{\partial}{\partial y_k} \left(\overline{v'_\ell(\mathbf{y}) \frac{\partial v'_j(\mathbf{x})}{\partial x_i}} \right) - \overline{v'_\ell(\mathbf{y}) \frac{\partial^2 v'_j(\mathbf{x})}{\partial y_k \partial x_i}} \\ &= \frac{\partial^2}{\partial y_k \partial x_i} \left(\overline{v'_\ell(\mathbf{y}) v'_j(\mathbf{x})} \right) - \frac{\partial}{\partial y_k} \left(\overline{v'_j(\mathbf{x}) \frac{\partial v'_\ell(\mathbf{y})}{\partial x_i}} \right) \\ &= \frac{\partial^2}{\partial y_k \partial x_i} \left(\overline{v'_\ell(\mathbf{y}) v'_j(\mathbf{x})} \right) \end{aligned} \quad (11.73)$$

$\partial^2 v'_j(\mathbf{x}) / \partial y_k \partial x_i$ on line 1 is zero because $v'_j(\mathbf{x})$ is not a function of \mathbf{y} . For the same reason the last term on line 2 is zero.

Note that the terms above as well as in Eq. 11.69 are two-point correlations, the two points being \mathbf{x} and \mathbf{y} . Introduce the distance vector between the two points

$$r_i = y_i - x_i \quad (11.74)$$

Differentiating Eq. 11.74 gives

$$\frac{\partial}{\partial r_i} = \frac{\partial}{\partial y_i} - \frac{\partial}{\partial x_i} \quad (11.75)$$

Equation 11.74 is a coordinate transformation where we replace x_i and y_i with

- I. x_i and r_i , or
- II. y_i and r_i .

Assumption *i*) at p. 143 gives that $\partial / \partial x_i = 0$ (Item I) or $\partial / \partial y_i = 0$ (Item II). In other words, the two-point correlations are independent of where in space the two points are located; they are only dependent on the distance between the two points (i.e. r_i). Hence we can replace the spatial derivative by the distance derivative, i.e.

$$\begin{aligned} \frac{\partial}{\partial x_i} &= -\frac{\partial}{\partial r_i} \\ \frac{\partial}{\partial y_i} &= \frac{\partial}{\partial r_i} \end{aligned} \quad (11.76)$$

We can now write $M_{ijk\ell}$ in Eq. 11.69, using Eqs. 11.73 and 11.76, as

$$\begin{aligned} M_{ijk\ell} &= -\frac{1}{2\pi} \int_V \left[\frac{\partial^2}{\partial r_k \partial r_i} \left(\overline{v'_\ell v'_j} \right) + \frac{\partial^2}{\partial r_k \partial r_j} \left(\overline{v'_\ell v'_i} \right) \right] \frac{d\mathbf{r}^3}{|\mathbf{r}|} \\ &= a_{ijk\ell} + a_{jik\ell} \end{aligned} \quad (11.77)$$

It can be shown that $a_{ijk\ell}$ is symmetric with respect to index j and ℓ (recall that v'_ℓ and v'_j are not at the same point but separated by r_i), i.e.

$$a_{ijk\ell} = a_{ilkj} \quad (11.78)$$

see Appendix 39 on p. 361. Furthermore, Eq. 11.77 is independent of in which order the two derivatives are taken, so that $a_{ijk\ell}$ is symmetric with respect to i and k , i.e.

$$a_{ijk\ell} = a_{kjil} \quad (11.79)$$

Now let us formulate a general expression of $a_{ijk\ell}$ which is linear in $\overline{v'_i v'_j}$ and symmetric in (j, ℓ) and (i, k) . We get

$$\begin{aligned} a_{ijk\ell} = & c_1 \overline{\delta_{ik} v'_j v'_\ell} \\ & + c_2 \overline{\delta_{j\ell} v'_i v'_k} \\ & + c_3 (\overline{\delta_{ij} v'_k v'_\ell} + \overline{\delta_{kj} v'_i v'_\ell} + \overline{\delta_{i\ell} v'_k v'_j} + \overline{\delta_{k\ell} v'_i v'_j}) \\ & + c_4 \delta_{j\ell} \delta_{ik} k \\ & + c_5 (\delta_{ij} \delta_{k\ell} + \delta_{jk} \delta_{i\ell}) k \end{aligned} \quad (11.80)$$

Each line is symmetric in (j, ℓ) and (i, k) . For example, on line 3, term 1 & term 3 and term 2 & term 4 are symmetric with respect to j and ℓ and term 1 & term 2 and term 3 & term 4 are symmetric with respect to i and k .

Consider Eq. 11.69. Here it is seen that if $i = j$ then $M_{ijk\ell} = 0$ due to the continuity equation; looking at Eq. 11.77 we get

$$a_{iik\ell} = 0 \quad (11.81)$$

Applying this condition to Eq. 11.80 gives

$$\begin{aligned} 0 = & c_1 \overline{\delta_{ik} v'_i v'_\ell} + c_2 \overline{\delta_{i\ell} v'_i v'_k} + c_3 (3 \overline{v'_k v'_\ell} + \overline{\delta_{ki} v'_i v'_\ell} + \overline{\delta_{i\ell} v'_k v'_i} + \overline{\delta_{k\ell} v'_i v'_i}) \\ & + c_4 \delta_{i\ell} \delta_{ik} k + c_5 (3 \delta_{k\ell} + \delta_{ik} \delta_{i\ell}) k \\ = & c_1 \overline{v'_k v'_\ell} + c_2 \overline{v'_\ell v'_k} + c_3 (3 \overline{v'_k v'_\ell} + \overline{v'_k v'_\ell} + \overline{v'_k v'_\ell} + 2 \delta_{k\ell} k) \\ & + c_4 \delta_{k\ell} k + c_5 (3 \delta_{k\ell} + \delta_{k\ell}) k \\ = & \overline{v'_k v'_\ell} (c_1 + c_2 + 5c_3) + k \delta_{k\ell} (c_4 + 2c_3 + 4c_5) \end{aligned} \quad (11.82)$$

Green's third formula reads (see Appendix 39 on p. 361)

$$a_{ijil} = 2 \overline{v'_i v'_\ell} \quad (11.83)$$

Using Eq. 11.83 in Eq. 11.80 gives

$$\begin{aligned} 2 \overline{v'_j v'_\ell} = & 3c_1 \overline{v'_j v'_\ell} + c_2 \overline{\delta_{j\ell} v'_i v'_i} + c_3 (\overline{\delta_{ij} v'_i v'_\ell} + \overline{\delta_{ij} v'_i v'_\ell} + \overline{\delta_{i\ell} v'_i v'_j} + \overline{\delta_{i\ell} v'_i v'_j}) \\ & + (3c_4 \delta_{j\ell} + c_5 (\delta_{ij} \delta_{i\ell} + \delta_{ji} \delta_{i\ell})) k \\ = & 3c_1 \overline{v'_j v'_\ell} + 2c_2 \delta_{j\ell} k + 4c_3 \overline{v'_j v'_\ell} + (3c_4 + 2c_5) \delta_{j\ell} k \\ = & \overline{v'_j v'_\ell} (3c_1 + 4c_3) + \delta_{j\ell} k (2c_2 + 3c_4 + 2c_5) \end{aligned} \quad (11.84)$$

Equations 11.82 and 11.84 give four equations

$$\begin{aligned} c_1 + c_2 + 5c_3 = 0, \quad c_4 + 2c_3 + 4c_5 = 0 \\ 3c_1 + 4c_3 - 2 = 0, \quad 2c_2 + 3c_4 + 2c_5 = 0 \end{aligned} \quad (11.85)$$

for the five unknown constants. Let us express all constants in c_2 which gives

$$c_1 = \frac{4c_2 + 10}{11}, \quad c_3 = -\frac{3c_2 + 2}{11}, \quad c_4 = -\frac{50c_2 + 4}{55}, \quad c_5 = \frac{20c_2 + 6}{55} \quad (11.86)$$

Inserting Eq. 11.86 into Eq. 11.80 and 11.72 gives

$$\begin{aligned}
 \phi_{ij,2} &= M_{ijk\ell} \frac{\partial \bar{v}_k}{\partial x_\ell} = (a_{ijk\ell} + a_{jik\ell}) \frac{\partial \bar{v}_k}{\partial x_\ell} \\
 &= c_1 \left(\overline{v'_j v'_\ell} \frac{\partial \bar{v}_i}{\partial x_\ell} + \overline{v'_i v'_\ell} \frac{\partial \bar{v}_j}{\partial x_\ell} \right) + c_2 \left(\overline{v'_i v'_k} \frac{\partial \bar{v}_k}{\partial x_j} + \overline{v'_j v'_k} \frac{\partial \bar{v}_k}{\partial x_i} \right) \\
 &+ c_3 \left(2\delta_{ij} \overline{v'_k v'_\ell} \frac{\partial \bar{v}_k}{\partial x_\ell} + \overline{v'_i v'_\ell} \frac{\partial \bar{v}_j}{\partial x_\ell} + \overline{v'_j v'_\ell} \frac{\partial \bar{v}_i}{\partial x_\ell} + \overline{v'_k v'_j} \frac{\partial \bar{v}_k}{\partial x_i} + \overline{v'_k v'_i} \frac{\partial \bar{v}_k}{\partial x_j} \right) \\
 &+ c_4 k \left(\frac{\partial \bar{v}_i}{\partial x_j} + \frac{\partial \bar{v}_j}{\partial x_i} \right) + c_5 k \left(\frac{\partial \bar{v}_j}{\partial x_i} + \frac{\partial \bar{v}_i}{\partial x_j} \right)
 \end{aligned} \tag{11.87}$$

We find that the c_1 term and the second and third part of the c_3 term can be merged. Furthermore, the c_2 term and the third and fourth part of the c_3 term can be merged as well as the c_4 and c_5 terms; using Eq. 11.85 we get

$$\begin{aligned}
 \phi_{ij,2} &= -\frac{c_2 + 8}{11} P_{ij} - \frac{8c_2 - 2}{11} \mathcal{D}_{ij} + \frac{6c_2 + 4}{11} P^k + \frac{4 - 60c_2}{55} k \bar{s}_{ij} \\
 \mathcal{D}_{ij} &= -\overline{v'_i v'_k} \frac{\partial \bar{v}_k}{\partial x_j} - \overline{v'_j v'_k} \frac{\partial \bar{v}_k}{\partial x_i}
 \end{aligned} \tag{11.88}$$

Finally we re-write this equation so that it is expressed in trace-less tensors

$$\begin{aligned}
 \Phi_{ij,2} &= -\rho \frac{c_2 + 8}{11} \left(P_{ij} - \frac{2}{3} \delta_{ij} P^k \right) \\
 &- \rho \frac{8c_2 - 2}{11} \left(\mathcal{D}_{ij} - \frac{2}{3} \delta_{ij} P^k \right) - \frac{60c_2 - 4}{55} \rho k \bar{s}_{ij}
 \end{aligned} \tag{11.89}$$

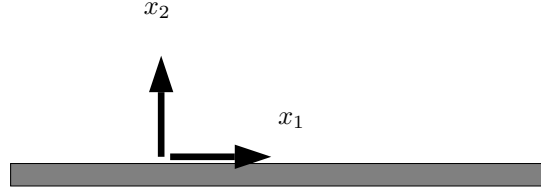
where $c_2 = 0.4$. Note that $\Phi_{ii} = 0$ as we required in Eq. 11.81. This pressure-strain model is called the LRR model and it was proposed in [32].

All three terms in Eq. 11.89 satisfy continuity and symmetry conditions. It might be possible to use a simpler pressure-strain model using one or any two terms. Since the first term is the most important one, a simpler model has been proposed [32, 33]

$$\Phi_{ij,2} = -c_2 \rho \left(P_{ij} - \frac{2}{3} \delta_{ij} P^k \right) \tag{11.90}$$

It can be noted that there is a close similarity between the Rotta model and Eq. 11.90: both models represent “return-to-isotropy”, the first expressed in $\overline{v'_i v'_j}$ and the second in P_{ij} . The model in Eq. 11.90 is commonly called the IP model (IP=Isotropization by Production). Since two terms are omitted we should expect that the best value of γ should be different than $(c_2 + 8)/11$; a value of $\gamma = 0.6$ ($c_2 = -1.4$) was found to give good agreement with experimental data. Since Eq. 11.90 is a truncated form of Eq. 11.89 it does not satisfy all requirements that Eq. 11.89 do. Equation 11.90 does satisfy symmetry condition and continuity but it does not satisfy the integral condition in Eq. 11.83. Although Eq. 11.90 is a simpler, truncated version of Eq. 11.89, it is often found to give more accurate results [34]. Since the IP model is both simpler and seems to be more accurate than Eq. 11.89, it is one of the most popular models of the rapid pressure-strain term. The coefficients for the slow and rapid terms in the LRR and LRR-IP models are summarized in Table 11.1

	LRR model	LRR-IP model
c_1 (Eq. 11.57)	1.5	1.5
c_2 (Eq. 11.89)	0.4	—
c_2 (Eq. 11.90)	—	0.6

Table 11.1: Constants in the LRR and LRR-IP pressure-strain models.**Figure 11.4:** Modeling of wall correction in pressure-strain terms.

11.7.6 Wall model of the pressure-strain term

When we derived the rapid pressure-strain model using Green's function in Eq. 11.68 we neglected the influence of any boundaries. In wall-bounded domains it turns out that the effect of the walls must be taken into account. Both the rapid term in the LRR model and the IP model must be modified to include wall modeling.

The effect of the wall is to dampen turbulence. There are two main effects whose underlying physics are entirely different.

1. **Viscosity.** Close to the wall the viscous processes (viscous diffusion and dissipation) dominate over the turbulent ones (production and turbulent diffusion).
2. **Pressure.** When a fluid particle approaches a wall, the presence of the wall is felt by the fluid particle over a long distance. This is true for a fluid particle carried by the wind approaching a building as well as for a fluid particle carried by a fluctuating velocity approaching the wall in a turbulent boundary layer. In both cases it is the pressure that informs the fluid particle of the presence of the wall.

Since the pressure-strain term includes the fluctuating pressure, it is obviously the second of these two processes that we want to include in the wall model. Up to now we have introduced two terms for modeling the pressure-strain term, the slow and the fast term. It is suitable to include a slow and a fast **wall model term**, i.e.

$$\Phi_{ij} = \Phi_{ij,1} + \Phi_{ij,2} + \Phi_{ij,1w} + \Phi_{ij,2w} \quad (11.91)$$

where subscript w denotes wall modeling.

Consider a wall, see Fig. 11.4. The pressure fluctuations dampens the wall-normal fluctuations. Furthermore, the damping effect of the wall should decrease for increasing wall distance. We need to scale the wall-normal distance with a relevant quantity and the turbulent length scale, $k^{3/2}/\varepsilon$, seems to be a good candidate. For the wall-normal

fluctuations, the IP wall model reads [35]

$$\begin{aligned}\Phi_{22,1w} &= -2c_{1w} \frac{\varepsilon}{k} \overline{v_2'^2} f \\ f &= \min \left\{ \frac{k^{\frac{3}{2}}}{2.55 |n_{i,w}(x_i - x_{i,w})| \varepsilon}, 1.0 \right\}\end{aligned}\quad (11.92)$$

where $n_{i,w}(x_i - x_{i,w})$ denotes the distance to the wall. f may exceed one near the wall and that's why we put an upper limit on it. As explained above, this damping is inviscid (due to pressure) and affects the turbulent fluctuations well into the log-region. It has nothing to do with viscous damping. Away from the wall, in the fully turbulent region, the damping function goes to zero since the distance to the wall, $|n_{i,w}(x_i - x_{i,w})|$, increases faster than the turbulence length scale, $k^{3/2}/\varepsilon$. Moreover, function f should not exceed one.

The IP wall model for the wall-parallel fluctuations reads

$$\Phi_{11,1w} = \Phi_{33,1w} = c_{1w} \frac{\varepsilon}{k} \overline{v_2'^2} f \quad (11.93)$$

The requirement that the sum of the pressure strain term should be zero. i.e. $\Phi_{ii,1w} = 0$, is now satisfied since $\Phi_{11,1w} + \Phi_{22,1w} + \Phi_{33,1w} = 0$.

The wall model for the shear stress is set as

$$\Phi_{12,1w} = -\frac{3}{2} c_{1w} \frac{\varepsilon}{k} \overline{v_1' v_2'} f \quad (11.94)$$

The factor $3/2$ is needed to ensure that $\Phi_{ii,1w} = 0$ is satisfied when the coordinate system is rotated. You can prove this by rotating the matrix $[\Phi_{11,1w}, \Phi_{12,1w}; \Phi_{21,1w}, \Phi_{22,1w}]$ and taking the trace of Φ in the principal coordinates system (i.e. taking the sum of the eigenvalues).

The general formula for a wall that is not aligned with a Cartesian coordinate axis reads [35]

$$\Phi_{ij,1w} = c_{1w} \frac{\varepsilon}{k} \left(\overline{v_k' v_m'} n_{k,w} n_{m,w} \delta_{ij} - \frac{3}{2} \overline{v_k' v_i'} n_{k,w} n_{j,w} - \frac{3}{2} \overline{v_k' v_j'} n_{i,w} n_{k,w} \right) f \quad (11.95)$$

An analogous wall model is used for the rapid part which reads

$$\Phi_{ij,2w} = c_{2w} \left(\Phi_{km,2w} n_{k,w} n_{m,w} \delta_{ij} - \frac{3}{2} \Phi_{ki,2w} n_{k,w} n_{j,w} - \frac{3}{2} \Phi_{kj,2w} n_{i,w} n_{k,w} \right) f \quad (11.96)$$

In Section 61, you find some detail on how to compute one of the terms, $\overline{v_k' v_m'} n_{k,w} n_{m,w}$.

11.8 The $k - \varepsilon$ model

The exact k equation is given by Eq. 11.23. By inserting the model assumptions for the turbulent diffusion (Eq. 11.40), the production (Eq. 11.39) and the buoyancy term (Eqs. 11.35 and 11.36) we get the *modeled* equation for k

$$\begin{aligned}\frac{\partial k}{\partial t} + \bar{v}_j \frac{\partial k}{\partial x_j} &= \nu_t \left(\frac{\partial \bar{v}_i}{\partial x_j} + \frac{\partial \bar{v}_j}{\partial x_i} \right) \frac{\partial \bar{v}_i}{\partial x_j} + g_i \beta \frac{\nu_t}{\sigma_\theta} \frac{\partial \bar{\theta}}{\partial x_i} \\ &\quad - \varepsilon + \frac{\partial}{\partial x_j} \left[\left(\nu + \frac{\nu_t}{\sigma_k} \right) \frac{\partial k}{\partial x_j} \right]\end{aligned}\quad (11.97)$$

In the same way, the modeled ε equation is obtained from Eq. 11.29

$$\begin{aligned} \frac{\partial \varepsilon}{\partial t} + \bar{v}_j \frac{\partial \varepsilon}{\partial x_j} = & \frac{\varepsilon}{k} c_{\varepsilon 1} \nu_t \left(\frac{\partial \bar{v}_i}{\partial x_j} + \frac{\partial \bar{v}_j}{\partial x_i} \right) \frac{\partial \bar{v}_i}{\partial x_j} \\ & + c_{\varepsilon 1} g_i \frac{\varepsilon}{k} \frac{\nu_t}{\sigma_\theta} \frac{\partial \bar{\theta}}{\partial x_i} - c_{\varepsilon 2} \frac{\varepsilon^2}{k} + \frac{\partial}{\partial x_j} \left[\left(\nu + \frac{\nu_t}{\sigma_\varepsilon} \right) \frac{\partial \varepsilon}{\partial x_j} \right] \end{aligned} \quad (11.98)$$

The turbulent viscosity is computed as

$$\nu_t = c_\mu \frac{k^2}{\varepsilon} \quad (11.99)$$

The standard values for the coefficients read

$$(c_\mu, c_{\varepsilon 1}, c_{\varepsilon 2}, \sigma_k, \sigma_\varepsilon) = (0.09, 1.44, 1.92, 1, 1.3) \quad (11.100)$$

For details on how to obtain these constants are obtained, see Section 11.14.2 and Section 3 in [Introduction to turbulence models](#). In that report, details on wall-functions and low-Reynolds number models can be found in Sections 3 and 4, respectively.

11.9 The modeled $\overline{v'_i v'_j}$ equation with IP model

With the models for diffusion, pressure-strain and dissipation we get the Reynolds Stress Model [RSM]

$$\begin{aligned}
& \frac{\partial \overline{v'_i v'_j}}{\partial t} + \quad (\text{unsteady term}) \\
& \bar{v}_k \frac{\partial \overline{v'_i v'_j}}{\partial x_k} = \quad (\text{convection}) \\
& -\overline{v'_i v'_k} \frac{\partial \bar{v}_j}{\partial x_k} - \overline{v'_j v'_k} \frac{\partial \bar{v}_i}{\partial x_k} \quad (\text{production}) \\
& -c_1 \frac{\varepsilon}{k} \left(\overline{v'_i v'_j} - \frac{2}{3} \delta_{ij} k \right) \quad (\text{pressure strain, slow part}) \\
& -c_2 \left(P_{ij} - \frac{2}{3} \delta_{ij} P^k \right) \quad (\text{pressure strain, rapid part, IP model}) \\
& + c_{1w} \rho \frac{\varepsilon}{k} \left[\overline{v'_k v'_m} n_k n_m \delta_{ij} - \frac{3}{2} \overline{v'_i v'_k} n_k n_j \right. \\
& \quad \left. - \frac{3}{2} \overline{v'_j v'_k} n_k n_i \right] f \quad (\text{pressure strain, wall, slow part}) \\
& + c_{2w} \left[\Phi_{km,2} n_k n_m \delta_{ij} - \frac{3}{2} \Phi_{ik,2} n_k n_j \right. \\
& \quad \left. - \frac{3}{2} \Phi_{jk,2} n_k n_i \right] f \quad (\text{pressure strain, wall, rapid part, IP model}) \\
& + \nu \frac{\partial^2 \overline{v'_i v'_j}}{\partial x_k \partial x_k} \quad (\text{viscous diffusion}) \\
& + \frac{\partial}{\partial x_m} \left[\frac{\nu_t}{\sigma_k} \frac{\partial \overline{v'_i v'_j}}{\partial x_m} \right] \quad (\text{turbulent diffusion}) \\
& - g_i \beta \overline{v'_j \theta'} - g_j \beta \overline{v'_i \theta'} \quad (\text{buoyancy production}) \\
& - \frac{2}{3} \varepsilon \delta_{ij} \quad (\text{dissipation})
\end{aligned} \tag{11.101}$$

11.10 Algebraic Reynolds Stress Model (ASM)

The Algebraic Reynolds Stress Model is a simplified Reynolds Stress Model. The RSM and $k - \varepsilon$ models are written in symbolic form (see p. 130 & 133) as:

$$\begin{aligned}
\text{RSM} : C_{ij} - D_{ij} &= P_{ij} + \Phi_{ij} - \varepsilon_{ij} \\
k - \varepsilon : C^k - D^k &= P^k - \varepsilon
\end{aligned} \tag{11.102}$$

In ASM we assume that the transport (convective and diffusive) of $\overline{v'_i v'_j}$ is related to that of k , i.e.

$$C_{ij} - D_{ij} = \frac{\overline{v'_i v'_j}}{k} (C^k - D^k)$$

Inserting Eq. 11.102 into the equation above gives

$$P_{ij} + \Phi_{ij} - \varepsilon_{ij} = \frac{\overline{v'_i v'_j}}{k} (P^k - \varepsilon) \quad (11.103)$$

Thus the transport equation (PDE) for $\overline{v'_i v'_j}$ has been transformed into an *algebraic* equation based on the assumption in Eq. 11.102.

Now we want to re-write this equation as an equation for $\overline{v'_i v'_j}$. Insert the IP models for $\Phi_{ij,1}$ (Eq. 11.57) and $\Phi_{ij,2}$ (Eq. 11.90) and the isotropic model for ε_{ij} (Eq. 11.49) in Eq. 11.103 and multiply by k/ε so that

$$\begin{aligned} \frac{k}{\varepsilon} P_{ij} - c_1 \left(\overline{v'_i v'_j} - \frac{2}{3} \delta_{ij} k \right) - c_2 \frac{k}{\varepsilon} \left(P_{ij} - \frac{2}{3} \delta_{ij} P^k \right) - \frac{2}{3} \delta_{ij} k \\ + \frac{k}{\varepsilon} (\Phi_{ij,1w} + \Phi_{ij,2w}) = \frac{\overline{v'_i v'_j}}{\varepsilon} (P^k - \varepsilon) \end{aligned}$$

Collect all $\overline{v'_i v'_j}$ terms so that

$$\begin{aligned} \overline{v'_i v'_j} \left(\frac{P^k}{\varepsilon} - 1 + c_1 \right) = \\ \frac{k}{\varepsilon} \left[P_{ij} - c_2 \left(P_{ij} - \frac{2}{3} \delta_{ij} P^k \right) + \Phi_{ij,1w} + \Phi_{ij,2w} \right] + \frac{2}{3} \delta_{ij} k (-1 + c_1) \\ = \frac{k}{\varepsilon} \left[P_{ij} \boxed{-\delta_{ij} \frac{2}{3} P^k} - c_2 \left(P_{ij} - \frac{2}{3} \delta_{ij} P^k \right) + \Phi_{ij,1w} + \Phi_{ij,2w} \right] + \boxed{\frac{2}{3} \delta_{ij} k (P^k/\varepsilon)} (-1 + c_1) \end{aligned}$$

where $(2/3)\delta_{ij}P^k k/\varepsilon$ was added and subtracted at the last line (shown in boxes). Dividing both sides by $P^k/\varepsilon - 1 + c_1$ gives finally

$$\overline{v'_i v'_j} = \frac{2}{3} \delta_{ij} k + \frac{k(1 - c_2) \left(P_{ij} - \frac{2}{3} \delta_{ij} P^k \right) + \Phi_{ij,1w} + \Phi_{ij,2w}}{c_1 + P^k/\varepsilon - 1} \quad (11.104)$$

In boundary layer flow Eq. 11.104 reads (without any wall terms, i.e. $\Phi_{ij,1w} = \Phi_{ij,2w} = 0$)

$$-\overline{v'_1 v'_2} = \frac{2}{3} (1 - c_2) \underbrace{\frac{c_1 - 1 + c_2 P^k/\varepsilon}{(c_1 - 1 + P^k/\varepsilon)}}_{c_\mu} \frac{k^2}{\varepsilon} \frac{\partial \bar{v}_1}{\partial y}$$

As can be seen, this model can be seen as an extension of an eddy-viscosity model where the c_μ constant is made a function of the ratio P^k/ε .

11.11 Explicit ASM (EASM or EARSM)

Equation 11.104 is an *implicit* equation for $\overline{v'_i v'_j}$, i.e. the Reynolds stresses appear both on the left and the right side of the equation. It would of course be advantageous to be able to get an *explicit* expression for the Reynolds stresses. Pope [36] managed to derive an explicit expression for ASM in two dimensions. He assumed that the Reynolds stress tensor can be expressed in the strain-rate tensor, \bar{s}_{ij} , and the vorticity tensor, $\bar{\Omega}_{ij}$. Furthermore, he showed that the coefficients, $G^{(n)}$, in that expression can be a function of not more than the following five invariants

$$\begin{aligned} (k^2/\varepsilon^2) \bar{s}_{ij} \bar{s}_{ji}, \quad (k^2/\varepsilon^2) \bar{\Omega}_{ij} \bar{\Omega}_{ji}, \quad (k^3/\varepsilon^3) \bar{s}_{ij} \bar{s}_{jk} \bar{s}_{ki} \\ (k^3/\varepsilon^3) \bar{\Omega}_{ij} \bar{\Omega}_{jk} \bar{s}_{ki}, \quad (k^4/\varepsilon^4) \bar{\Omega}_{ij} \bar{\Omega}_{jk} \bar{s}_{km} \bar{s}_{mi} \end{aligned} \quad (11.105)$$

There are five invariants because when \bar{s}_{ij} and $\bar{\Omega}_{ij}$ are transformed to principal coordinates, there are three eigenvalue for each of them. Furthermore, $\bar{s}_{ii} = 0$ which means there are only five independent invariants.

In two dimension the expression reads

$$\overline{v'_i v'_j} = \frac{2}{3} k \delta_{ij} + G^{(1)} \frac{k^2}{\varepsilon} \bar{s}_{ij} + G^{(2)} \frac{k^3}{\varepsilon^2} (\bar{s}_{ik} \bar{\Omega}_{kj} - \bar{\Omega}_{ik} \bar{s}_{kj}) \quad (11.106)$$

In general three-dimensional flow, the Reynolds stress tensor depends on 10 tensors, T_{ij}^n [36], i.e.

$$\begin{aligned} \overline{v'_i v'_j} - \frac{2}{3} k \delta_{ij} &= \sum_{n=1}^{10} G^{(n)} T_{ij}^n \\ T_{ij}^1 &= \bar{s}_{ij}, \quad T_{ij}^2 = \bar{s}_{ik} \bar{\Omega}_{kj} - \bar{s}_{jk} \bar{\Omega}_{ki}, \quad T_{ij}^3 = \bar{s}_{ik} \bar{s}_{kj} - \frac{1}{3} \delta_{ij} \bar{s}_{mk} \bar{s}_{km} \\ T_{ij}^4 &= \bar{\Omega}_{ik} \bar{\Omega}_{kj} - \frac{1}{3} \delta_{ij} \bar{\Omega}_{ik} \bar{\Omega}_{ki}, \quad T_{ij}^5 = \bar{\Omega}_{ik} \bar{s}_{km} \bar{s}_{mj} - \bar{s}_{im} \bar{s}_{mk} \bar{\Omega}_{kj} \\ T_{ij}^6 &= \bar{\Omega}_{im} \bar{\Omega}_{mk} \bar{s}_{kj} + \bar{s}_{ik} \bar{\Omega}_{km} \bar{\Omega}_{mj} - \frac{2}{3} \delta_{ij} \bar{\Omega}_{pm} \bar{\Omega}_{mk} \bar{s}_{kp} \\ T_{ij}^7 &= \bar{\Omega}_{im} \bar{s}_{mk} \bar{\Omega}_{kn} \bar{\Omega}_{nj} - \bar{\Omega}_{im} \bar{\Omega}_{mk} \bar{s}_{kn} \bar{\Omega}_{nj}, \quad T_{ij}^8 = \bar{s}_{im} \bar{\Omega}_{mk} \bar{s}_{kn} \bar{s}_{nj} - \bar{s}_{im} \bar{s}_{mk} \bar{\Omega}_{kn} \bar{s}_{nj} \\ T_{ij}^9 &= \bar{\Omega}_{im} \bar{\Omega}_{mk} \bar{s}_{kn} \bar{s}_{nj} - \bar{s}_{im} \bar{s}_{mk} \bar{\Omega}_{kn} \bar{\Omega}_{nj} - \frac{2}{3} \delta_{ij} \bar{\Omega}_{pm} \bar{\Omega}_{mk} \bar{s}_{kn} \bar{s}_{np} \\ T_{ij}^{10} &= \bar{\Omega}_{im} \bar{s}_{mk} \bar{s}_{kn} \bar{\Omega}_{np} \bar{\Omega}_{pj} - \bar{\Omega}_{im} \bar{\Omega}_{mk} \bar{s}_{kn} \bar{s}_{np} \bar{\Omega}_{pj} \end{aligned} \quad (11.107)$$

where $G^{(n)}$ may depend on the five invariants in Eq. 11.105. Equation 11.107 is a general form of a non-linear eddy-viscosity model. Any ASM may be written on the form of Eq. 11.107.

It may be noted that Eq. 11.107 includes only linear and quadratic terms of \bar{s}_{ij} and $\bar{\Omega}_{ij}$. That is because of Cayley-Hamilton theorem which states that a second-order tensor satisfies its own characteristic equation (see Section 60.1 and Section 1.20 in [30]); hence cubic terms or higher can recursively be expressed in linear (\bar{s}_{ij}) and quadratic tensors ($\bar{s}_{ik} \bar{s}_{kj}$). Furthermore, note that all terms in Eq. 11.107 are symmetric and traceless as required by the left side, $\overline{v'_i v'_j} - 2\delta_{ij}k/3$.

11.12 Derivation of the Explicit Algebraic Reynolds Stress Model (EARSM)

The algebraic stress model (ASM) is given by Eq. 11.104. This equation is *implicit*, since the Reynolds stresses appear on the right side (in the production and the rapid pressure-strain terms). In this section we will derive an *explicit* algebraic Reynolds stress model (EARSM). The derivation presented here is based on [37]. Whereas the ASM employs the IP model (Eq. 11.90) for the rapid pressure-strain term, the EARSM is based on the LRR model (Eq. 11.89). Thus we start with Eq. 11.103 using the Rotta model for the slow part (Eq. 11.57) and the LRR model (Eq. 11.89) for the rapid part.

$$\begin{aligned}
(a_{ij} + \frac{2}{3}\delta_{ij})(P^k - \varepsilon) &= P_{ij} - c_1\varepsilon a_{ij} - \frac{c_2 + 8}{11} \left(P_{ij} - \frac{2}{3}\delta_{ij}P^k \right) \\
&\quad - \frac{8c_2 - 2}{11} \left(\mathcal{D}_{ij} - \frac{2}{3}\delta_{ij}P^k \right) - \frac{60c_2 - 4}{55} k\bar{s}_{ij} - \frac{2}{3}\delta_{ij}\varepsilon
\end{aligned} \tag{11.108}$$

where the anisotropy tensor, a_{ij} , in Eq. 11.59 is used on the left side. The wall correction terms are neglected (as they usually are in the LRR model). Equation 11.108 is re-arranged as

$$\begin{aligned}
a_{ij}(P^k + c_1\varepsilon - \varepsilon) &= P_{ij} - \frac{2}{3}\delta_{ij}P^k - \frac{c_2 + 8}{11} \left(P_{ij} - \frac{2}{3}\delta_{ij}P^k \right) \\
&\quad - \frac{8c_2 - 2}{11} \left(\mathcal{D}_{ij} - \frac{2}{3}\delta_{ij}P^k \right) - \frac{60c_2 - 4}{55} k\bar{s}_{ij}
\end{aligned} \tag{11.109}$$

Now we introduce the anisotropy tensor, a_{ij} , also on the right side. Start by expressing the production term, P_{ij} (see Eq. 11.11) in a_{ij} , \bar{s}_{ij} and $\bar{\Omega}_{ij}$ (see Eq. 9.12)

$$\begin{aligned}
P_{ij} &= -k(a_{ik} + \frac{2}{3}\delta_{ik})(\bar{s}_{jk} + \bar{\Omega}_{jk}) - k(a_{jk} + \frac{2}{3}\delta_{jk})(\bar{s}_{ik} + \bar{\Omega}_{ik}) \\
&= -\frac{4}{3}k\bar{s}_{ij} - ka_{ik}(\bar{s}_{jk} + \bar{\Omega}_{jk}) - ka_{jk}(\bar{s}_{ik} + \bar{\Omega}_{ik}) \\
&= -\frac{4}{3}k\bar{s}_{ij} - k(\bar{s}_{jk}a_{ik} + a_{jk}\bar{s}_{ki}) + k(a_{ik}\bar{\Omega}_{kj} - \bar{\Omega}_{ik}a_{kj})
\end{aligned} \tag{11.110}$$

The production term, P^k , is equal to $0.5P_{ii}$, and Eq. 11.110 gives

$$P^k = -k\bar{s}_{ik}a_{ik} \tag{11.111}$$

so that we can express the P^k terms on the right side in Eq. 11.109 as

$$\frac{2}{3}\delta_{ij}P^k \left(-1 + \frac{c_2 + 8}{11} + \frac{8c_2 - 2}{11} \right) = -\frac{2}{3}\delta_{ij}k\bar{s}_{ik}a_{ik} \frac{9c_2 - 5}{11} \tag{11.112}$$

\mathcal{D}_{ij} is the same thing as P_{ij} except that the indices on the velocity gradients (i.e. the tensors a and $\bar{\Omega}$ in Eq. 11.110 are switched), see Eq. 11.88. Hence we get (cf. Eq. 11.110)

$$\mathcal{D}_{ij} = -\frac{4}{3}k\bar{s}_{ij} - k(\bar{s}_{jk}a_{ki} + a_{jk}\bar{s}_{ki}) - k(a_{ik}\bar{\Omega}_{kj} - \bar{\Omega}_{ik}a_{kj}) \tag{11.113}$$

Collect all terms including P_{ij} , \bar{s}_{ij} and \mathcal{D}_{ij} in Eq. 11.109

$$P_{ij} \left(1 - \frac{c_2 + 8}{11} \right) - \frac{8c_2 - 2}{11} \mathcal{D}_{ij} - \frac{60c_2 - 4}{55} k\bar{s}_{ij} - \frac{2}{3}\delta_{ij}k\bar{s}_{mn}a_{nm} \frac{9c_2 - 5}{11}$$

Inserting Eqs. 11.110 and 11.113 gives

$$\begin{aligned}
&k \left(1 - \frac{c_2 + 8}{11} \right) \left(-\frac{4}{3}\bar{s}_{ij} - (\bar{s}_{jk}a_{ik} + a_{jk}\bar{s}_{ki}) + (a_{ik}\bar{\Omega}_{kj} - \bar{\Omega}_{ik}a_{kj}) \right) \\
&\quad - k \frac{8c_2 - 2}{11} \left(-\frac{4}{3}\bar{s}_{ij} - (\bar{s}_{jk}a_{ki} + a_{jk}\bar{s}_{ki}) - (a_{ik}\bar{\Omega}_{kj} - \bar{\Omega}_{ik}a_{kj}) \right) \\
&\quad \quad \quad - \frac{2}{3}\delta_{ij}k\bar{s}_{mn}a_{nm} \frac{9c_2 - 5}{11} - \frac{60c_2 - 4}{55} k\bar{s}_{ij}
\end{aligned} \tag{11.114}$$

Gathering all terms including \bar{s}_{ij} gives

$$-\frac{4}{3}k\bar{s}_{ij} \left(1 - \frac{c_2 + 8}{11} + \frac{8c_2 - 2}{11} - \frac{3}{4} \frac{60c_2 - 4}{55} \right) = -\frac{8}{15}k\bar{s}_{ij} \quad (11.115)$$

The terms including the product of the tensors a and s in Eq. 11.114 read

$$-k \left(1 - \frac{c_2 + 8}{11} \right) (\bar{s}_{jk}a_{ik} + a_{jk}\bar{s}_{ki}) + \frac{8c_2 - 2}{11}k(\bar{s}_{jk}a_{ki} + a_{jk}\bar{s}_{ki}) = \frac{k}{11}(\bar{s}_{jk}a_{ki} + a_{jk}\bar{s}_{ki})(9c_2 - 5) \quad (11.116)$$

and the product of the tensors a and $\bar{\Omega}$ in Eq. 11.114 read

$$k \left(1 - \frac{c_2 + 8}{11} \right) (a_{ik}\bar{\Omega}_{kj} - \bar{\Omega}_{ik}a_{kj}) + k \frac{8c_2 - 2}{11} (a_{ik}\bar{\Omega}_{kj} - \bar{\Omega}_{ik}a_{kj}) = \frac{k}{11}(a_{ik}\bar{\Omega}_{kj} - \bar{\Omega}_{ik}a_{kj})(1 + 7c_2) \quad (11.117)$$

Using Eqs. 11.115, 11.116, 11.117 and the underlined term in Eq. 11.114, Eq. 11.114 can now be written

$$-k \frac{8}{15} \bar{s}_{ij} + k \frac{1 + 7c_2}{11} (a_{ik}\bar{\Omega}_{kj} - \bar{\Omega}_{ik}a_{kj}) + k \frac{9c_2 - 5}{11} \left(\bar{s}_{jk}a_{ki} + a_{jk}\bar{s}_{ki} - \frac{2}{3} \delta_{ij} k \bar{s}_{mn} a_{nm} \right) \quad (11.118)$$

Equation 11.118 is the right side of Eq. 11.109. Insert Eq. 11.118 into Eq. 11.109 and divide by ε

$$a_{ij} \left(\frac{P^k}{\varepsilon} + c_1 - 1 \right) = -\frac{k}{\varepsilon} \frac{8}{15} \bar{s}_{ij} + \frac{k}{\varepsilon} \frac{1 + 7c_2}{11} (a_{ik}\bar{\Omega}_{kj} - \bar{\Omega}_{ik}a_{kj}) + \frac{k}{\varepsilon} \frac{9c_2 - 5}{11} \left(\bar{s}_{jk}a_{ki} + a_{jk}\bar{s}_{ki} - \frac{2}{3} \delta_{ij} k \bar{s}_{mn} a_{nm} \right) \quad (11.119)$$

The coefficient, c_2 , in the LRR model is usually set to $c_2 = 0.4$, see Table 11.1. In [38–40], they noted that the relation in Eq. 11.119 is substantially simplified if $c_2 = 5/9$. This assumption is made in EARSM [37], which gives

$$a_{ij} \left(\frac{P^k}{\varepsilon} + c_1 - 1 \right) = -\frac{8}{15} \bar{s}_{ij}^* + \frac{4}{9} (a_{ik}\bar{\Omega}_{kj}^* - \bar{\Omega}_{ik}^* a_{kj}) \quad (11.120)$$

where the strain-rate and vorticity tensors are made non-dimensional

$$\bar{s}_{ij}^* = \frac{k}{\varepsilon} \bar{s}_{ij}, \quad \bar{\Omega}_{ij}^* = \frac{k}{\varepsilon} \Omega_{ij} \quad (11.121)$$

Equation 11.120 can now be written as

$$Na_{ij} = -\frac{6}{5} \bar{s}_{ij}^* + (a_{ik}\bar{\Omega}_{kj}^* - \bar{\Omega}_{ik}^* a_{kj}) \quad (11.122)$$

$$N = \frac{9P^k}{4\varepsilon} + c'_1, \quad c'_1 = \frac{9}{4}(c_1 - 1) \quad (11.123)$$

The most general form of a_{ij} is given by Eq. 11.107. In two-dimensional flow, it is sufficient to include only the two first terms (see Eq. 60.2), i.e.

$$a_{ij} = \beta_1 \bar{s}_{ij}^* + \beta_4 (\bar{s}_{im}^* \bar{\Omega}_{mj}^* - \bar{\Omega}_{im}^* \bar{s}_{mj}^*) \quad (11.124)$$

where we now denote the coefficients by β_1 and β_4 as in [37]. In order to solve Eq. 11.122, insert Eq. 11.124 which gives

$$\begin{aligned} N(\beta_1 \bar{s}_{ij}^* + \beta_4 (\bar{s}_{ik}^* \bar{\Omega}_{kj}^* - \bar{\Omega}_{ik}^* \bar{s}_{kj}^*)) &= -\frac{6}{5} \bar{s}_{ij}^* + (\beta_1 \bar{s}_{ik}^* + \beta_4 (\bar{s}_{im}^* \bar{\Omega}_{mk}^* - \bar{\Omega}_{im}^* \bar{s}_{mk}^*)) \bar{\Omega}_{kj}^* \\ &\quad - \bar{\Omega}_{ik}^* (\beta_1 \bar{s}_{kj}^* + \beta_4 (\bar{s}_{km}^* \bar{\Omega}_{mj}^* - \bar{\Omega}_{km}^* \bar{s}_{mj}^*)) \\ &= -\frac{6}{5} \bar{s}_{ij}^* + \beta_1 (\bar{s}_{ik}^* \bar{\Omega}_{kj}^* - \bar{\Omega}_{ik}^* \bar{s}_{kj}^*) + \beta_4 (\bar{s}_{im}^* \bar{\Omega}_{mk}^* \bar{\Omega}_{kj}^* - 2 \bar{\Omega}_{im}^* \bar{s}_{mk}^* \bar{\Omega}_{kj}^* + \bar{\Omega}_{ik}^* \bar{\Omega}_{km}^* \bar{s}_{mj}^*) \end{aligned} \quad (11.125)$$

The last term including β_4 can be considerably simplified. Recall that $\bar{\Omega}_{11}^* = \bar{\Omega}_{22}^* = 0$ and $\bar{\Omega}_{12}^* = -\bar{\Omega}_{21}^*$, see Eq. 1.11. We get for the 11 component of Eq. 11.125

$$\begin{aligned} &\bar{s}_{1m}^* \bar{\Omega}_{mk}^* \bar{\Omega}_{k1}^* - 2 \bar{\Omega}_{1m}^* \bar{s}_{mk}^* \bar{\Omega}_{k1}^* + \bar{\Omega}_{1k}^* \bar{\Omega}_{km}^* \bar{s}_{m1}^* \\ &= \bar{s}_{11}^* \bar{\Omega}_{12}^* \bar{\Omega}_{21}^* - 2 \bar{\Omega}_{12}^* \bar{s}_{22}^* \bar{\Omega}_{21}^* + \bar{\Omega}_{12}^* \bar{\Omega}_{21}^* \bar{s}_{11}^* = 4 \bar{s}_{11}^* \bar{\Omega}_{12}^* \bar{\Omega}_{21}^* \end{aligned} \quad (11.126)$$

since $\bar{s}_{11}^* = -\bar{s}_{22}^*$ ($\bar{s}_{ii}^* = 0$ due to continuity). In the same way we get $4 \bar{s}_{22}^* \bar{\Omega}_{12}^* \bar{\Omega}_{21}^*$ for the 22 component. The 12 component (and the 21 component) read

$$\begin{aligned} &\bar{s}_{1m}^* \bar{\Omega}_{mk}^* \bar{\Omega}_{k2}^* - 2 \bar{\Omega}_{1m}^* \bar{s}_{mk}^* \bar{\Omega}_{k2}^* + \bar{\Omega}_{1k}^* \bar{\Omega}_{km}^* \bar{s}_{m2}^* \\ &= \bar{s}_{12}^* \bar{\Omega}_{21}^* \bar{\Omega}_{12}^* - 2 \bar{\Omega}_{12}^* \bar{s}_{21}^* \bar{\Omega}_{12}^* + \bar{\Omega}_{12}^* \bar{\Omega}_{21}^* \bar{s}_{12}^* \\ &= \bar{s}_{12}^* \bar{\Omega}_{21}^* \bar{\Omega}_{12}^* + 2 \bar{\Omega}_{12}^* \bar{s}_{21}^* \bar{\Omega}_{21}^* + \bar{\Omega}_{12}^* \bar{\Omega}_{21}^* \bar{s}_{12}^* = 4 \bar{\Omega}_{12}^* \bar{\Omega}_{21}^* \bar{s}_{12}^* \end{aligned} \quad (11.127)$$

We find that the last term including β_4 in Eq. 11.125 can be written as $2II_\Omega \bar{s}_{ij}^*$ where $II_\Omega = \bar{\Omega}_{km}^* \bar{\Omega}_{mk}^* = \bar{\Omega}_{12}^* \bar{\Omega}_{21}^* + \bar{\Omega}_{21}^* \bar{\Omega}_{12}^* = 2 \bar{\Omega}_{12}^* \bar{\Omega}_{21}^*$. Equation 11.125 can now be re-written as

$$N(\beta_1 \bar{s}_{ij}^* + \beta_4 (\bar{s}_{ik}^* \bar{\Omega}_{kj}^* - \bar{\Omega}_{ik}^* \bar{s}_{kj}^*)) = -\frac{6}{5} \bar{s}_{ij}^* + \beta_1 (\bar{s}_{ik}^* \bar{\Omega}_{kj}^* - \bar{\Omega}_{ik}^* \bar{s}_{kj}^*) + 2\beta_4 II_\Omega \bar{s}_{ij}^* \quad (11.128)$$

Separating \bar{s}_{ij}^* and $(\bar{s}_{ik}^* \bar{\Omega}_{kj}^* - \bar{\Omega}_{ik}^* \bar{s}_{kj}^*)$ we get two equations for β_1 and β_4

$$\begin{aligned} N\beta_1 &= -\frac{6}{5} + 2\beta_4 II_\Omega \\ N\beta_4 &= \beta_1 \end{aligned} \quad (11.129)$$

so that

$$\begin{aligned} \beta_4 &= -\frac{6}{5} \frac{1}{N^2 - 2II_\Omega} \\ \beta_1 &= -\frac{6}{5} \frac{N}{N^2 - 2II_\Omega} \end{aligned} \quad (11.130)$$

In order to get the final equation for N , multiply Eq. 11.124 by \bar{s}_{jk}^* and then take the trace (which is equal to the production $P^k/\varepsilon = a_{ij} \bar{s}_{ji}^*$, see Eq. 11.111), i.e.

$$\frac{P^k}{\varepsilon} \equiv -a_{ij} \bar{s}_{ji}^* = -\beta_1 II_S + \beta_4 (\bar{s}_{im}^* \bar{\Omega}_{mj}^* - \bar{\Omega}_{im}^* \bar{s}_{mj}^*) \bar{s}_{ji}^* \quad (11.131)$$

where $II_S = \bar{s}_{ij}^* \bar{s}_{ji}^*$. The β_4 term reads

$$\begin{aligned} & (\bar{s}_{12}^* \bar{\Omega}_{21}^* - \bar{\Omega}_{12}^* \bar{s}_{21}^*) \bar{s}_{11}^* \\ & + (\bar{s}_{11}^* \bar{\Omega}_{12}^* - \bar{\Omega}_{12}^* \bar{s}_{22}^*) \bar{s}_{21}^* \\ & + (\bar{s}_{22}^* \bar{\Omega}_{21}^* - \bar{\Omega}_{21}^* \bar{s}_{11}^*) \bar{s}_{12}^* \\ & + (\bar{s}_{21}^* \bar{\Omega}_{12}^* - \bar{\Omega}_{21}^* \bar{s}_{12}^*) \bar{s}_{22}^* = 0 \end{aligned} \quad (11.132)$$

since line 2 and 3 are zero and line 1 and 4 cancel each other ($\bar{\Omega}_{12}^* = -\bar{\Omega}_{21}^*$, $\bar{s}_{12}^* = \bar{s}_{21}^*$ and $\bar{s}_{11}^* = -\bar{s}_{22}^*$). β_1 is now obtained from Eq. 11.131 as

$$\beta_1 = -\frac{P^k}{II_S \varepsilon} \quad (11.133)$$

Inserting β_1 in Eq. 11.130 gives

$$\frac{P^k}{\varepsilon} = \frac{6}{5} \frac{N}{N^2 - 2II_\Omega} II_S \quad (11.134)$$

Equations 11.123 and 11.134 gives finally an equation for N

$$N = \frac{9}{4} \frac{6}{5} \frac{N}{N^2 - 2II_\Omega} II_S + c'_1 \quad (11.135)$$

which is re-written as

$$N(N^2 - 2II_\Omega) - \frac{27}{10} II_S N - c'_1(N^2 - 2II_\Omega) = 0$$

so that

$$N^3 - c'_1 N^2 - \left(\frac{27}{10} II_S + 2II_\Omega \right) N + 2c'_1 II_\Omega = 0.$$

The analytical solution for the positive root reads [37]

$$\begin{aligned} N &= \frac{c'_1}{3} + \left(P_1 + \sqrt{P_2} \right)^{1/3} + \text{sign} \left(P_1 - \sqrt{P_2} \right) \left| P_1 - \sqrt{P_2} \right|^{1/3}, P_2 \geq 0 \\ N &= \frac{c'_1}{3} + 2 \left(P_1^2 - P_2 \right)^{1/6} \cos \left[\frac{1}{3} \arccos \left(\frac{P_1}{\sqrt{P_1^2 - P_2}} \right) \right], P_2 < 0 \end{aligned} \quad (11.136)$$

where $0 \leq \xi \leq \pi$ in $\arccos(\xi)$ and

$$\begin{aligned} P_1 &= \left(\frac{1}{27} c_1'^2 + \frac{9}{20} II_S - \frac{2}{3} II_\Omega \right) c'_1 \\ P_2 &= P_1^2 - \left(\frac{1}{9} c_1'^2 + \frac{9}{10} II_S + \frac{2}{3} II_\Omega \right)^3 \end{aligned} \quad (11.137)$$

Equation 11.137 is valid for two-dimensional flow. For three-dimensional flow, Eq. 11.124 includes more (six) of the terms in 11.107. This derivation is given in [37]. It results in a 6th -order equation for N which must be solved numerically.

In the original LRR model, $c_1 = 1.5$ and $c_2 = 0.4$ (see Table 11.1). In the EARS model, $c_1 = 1.8$ and $c_2 = 5/9$; recall that this choice of c_2 simplifies the rapid pressure-strain model (cf. Eqs. 11.119 and 11.120).

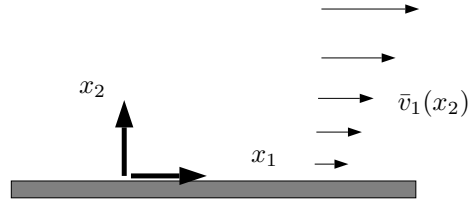


Figure 11.5: Boundary layer flow.

11.13 Boundary layer flow

In order to better understand the Reynolds stress equation, Eq. 11.101, it is useful to look at its source terms which to a large degree govern the magnitude of $\overline{v'_i v'_j}$. A large source term in the equation for the $\overline{v_1'^2}$ equation, for example, will increase $\overline{v_1'^2}$ and vice versa, see Section 9.1. Let us study boundary layer flow (Fig. 11.5) where $\bar{v}_2 \simeq 0$, $\partial \bar{v}_1 / \partial x_2 \gg \partial \bar{v}_1 / \partial x_1$. The production P_{ij} has the form:

$$P_{ij} = -\overline{v'_i v'_k} \frac{\partial \bar{v}_j}{\partial x_k} - \overline{v'_j v'_k} \frac{\partial \bar{v}_i}{\partial x_k}$$

In this special case we get:

$$P_{11} = -2\overline{v'_1 v'_2} \frac{\partial \bar{v}_1}{\partial x_2}$$

$$P_{12} = -\overline{v_2'^2} \frac{\partial \bar{v}_1}{\partial x_2}$$

$$P_{22} = 0$$

Is $\overline{v_2'^2}$ zero because its production term P_{22} is zero? No! The sympathetic term Φ_{ij} , which takes from the rich (i.e. $\overline{v_1'^2}$) and gives to the poor (i.e. $\overline{v_2'^2}$), saves the unfair situation! The IP model for $\Phi_{ij,1}$ and $\Phi_{ij,2}$ (Eq. 11.57) and $\Phi_{ij,2}$ (Eq. 11.90) gives

$$\begin{aligned} \Phi_{22,1} &= c_1 \frac{\varepsilon}{k} \left(\frac{2}{3} k - \overline{v_2'^2} \right) > 0 \\ \Phi_{22,2} &= c_2 \frac{1}{3} P_{11} = -c_2 \frac{2}{3} \overline{v'_1 v'_2} \frac{\partial \bar{v}_1}{\partial x_2} > 0 \end{aligned}$$

Note also that the dissipation term for the $\overline{v'_1 v'_2}$ is zero, but it takes the value $\frac{2}{3}\varepsilon$ for the $\overline{v_1'^2}$ and $\overline{v_2'^2}$ equations (see p. 139). Since the modeled $\overline{v'_1 v'_2}$ does not have any dissipation term, the question arises: what is the main sink term in the $\overline{v'_1 v'_2}$ equation? The answer is, again, the pressure strain term $\Phi_{12,1}$ and $\Phi_{12,2}$.

11.14 Wall boundary conditions

There are two options for treating the wall boundary conditions.

- Use a coarse mesh near the walls and assume that the logarithmic law applies. This is called *wall functions*

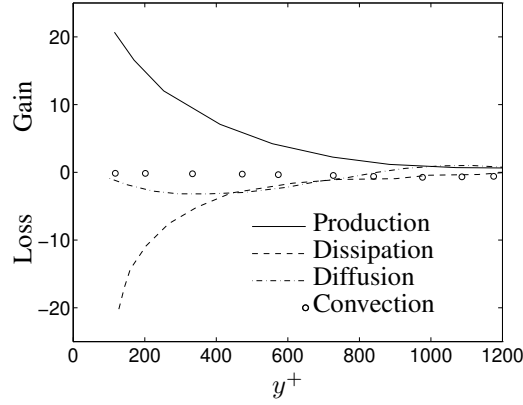


Figure 11.6: Boundary along a flat plate. Energy balance in k equation [41]. $Re_\delta \simeq 4400$, $u_*/U_0 \simeq 0.043$.

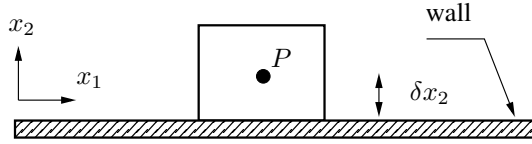


Figure 11.7: Wall-adjacent cell. Cell-centered finite volume grid.

- Use a fine mesh near the walls and modify the turbulence models to account for the viscous effects. This is called *Low-Reynolds number models*

11.14.1 Wall Functions

The natural way to treat wall boundaries is to make the grid sufficiently fine so that the sharp gradients prevailing there are resolved. Often, when computing complex three-dimensional flow, that requires too much computer resources. An alternative is to *assume* that the flow near the wall behaves like a turbulent boundary layer (see Fig. 6.2) and prescribe boundary conditions employing wall functions. The assumption that the flow near the wall has the characteristics of a that in a boundary layer if often not true at all. However, given a maximum number of nodes that we can afford to use in a computation, it is often preferable to use wall functions which allows us to use fine grid in other regions where the gradients of the flow variables are large.

The log-law we use can be written as

$$\frac{\bar{v}_1}{u_\tau} = \frac{1}{\kappa} \ln \left(\frac{Eu_\tau x_2}{\nu} \right) \quad (11.138)$$

$$E = 9.0$$

Comparing this with the standard form of the log-law (see Eq. 6.33)

$$\frac{\bar{v}_1}{u_\tau} = \frac{1}{\kappa} \ln \left(\frac{u_\tau x_2}{\nu} \right) + B. \quad (11.139)$$

We find that

$$B = \frac{1}{\kappa} \ln E.$$

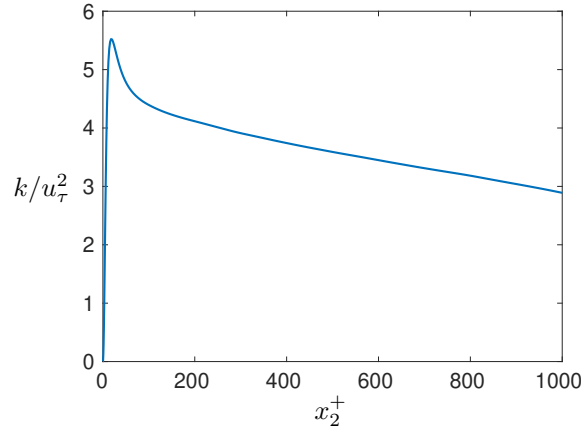


Figure 11.8: Turbulent kinetic energy in a boundary layer predicted by Large Eddy Simulations at $Re_\theta = 8\,200$ [42].

We compute the friction velocity from Equation 11.138 as

$$u_\tau = \frac{\kappa \bar{v}_{1,P}}{\ln(E u_\tau \delta x_2 / \nu)} \quad (11.140)$$

where $\bar{v}_{1,P}$ is the velocity in the wall-adjacent cell and δx_2 is the distance from the cell center, P , to the wall, see Fig. 11.7. Equation 11.140 is solved by iterating (the newest value of u_τ is inserted at the right-hand side at every iteration). The equation converges very quickly. The wall shear stress, $\tau_w = \rho u_\tau^2$ (see Eq. 6.16) is then used as a force wall boundary condition for the \bar{v}_1 equation.

For the wall-normal velocity, \bar{v}_2 , it is much easier. The convective velocity is zero at the wall and hence $\bar{v}_2 = 0$. It is the diffusion term in the \bar{v}_1 equation which causes the problems: then we must estimate the gradient, $\partial \bar{v}_1 / \partial x_2$ at the wall, and that's why we need to use the log law.

In a turbulent boundary layer the production term and the dissipation term in the log-law region ($30 < x_2^+ < 400$) are much larger than the other terms, see Figs. 8.3 and 11.6. Hence, we can approximate the modelled k equation (see Eq. 11.97) as

$$0 = P^k - \rho \varepsilon = \mu_t \left(\frac{\partial \bar{v}_1}{\partial x_2} \right)^2 - \rho \varepsilon. \quad (11.141)$$

where we have assumed that the buoyancy term is zero. In the log-law region the shear stress $-\rho \overline{v'_1 v'_2}$ is equal to the wall shear stress τ_w , see Eq. 6.26 and Fig. 6.3. The Boussinesq assumption for the shear stress reads (see Eqs. 6.29 and 11.33)

$$\tau_w = -\rho \overline{v'_1 v'_2} = \mu_t \frac{\partial \bar{v}_1}{\partial x_2} \quad (11.142)$$

Inserting Eq. 11.142 into Eq. 11.141 gives

$$0 = \frac{\overline{v'_1 v'_2}^2}{\nu_t} - \varepsilon = \frac{u_\tau^4}{\nu_t} - \varepsilon \quad (11.143)$$

which with Eq. 11.99 gives

$$C_\mu = \left(\frac{u_\tau^2}{k} \right)^2 \quad (11.144)$$

From experiments and DNS we have that in the log-law region of a boundary layer $u_\tau^2/k \simeq 0.3$ so that $C_\mu = 0.09$, see Figs. 6.8 and 11.8 (it may be noted that the DNS/LES data give a slightly larger values of k/u_τ^2 than $1/0.3$).

C_μ constant

When we are using wall functions k and ε are not solved at the nodes adjacent to the walls. Instead they are fixed according to the theory presented above. The turbulent kinetic energy is set from Eq. 11.144, i.e.

b.c. for k

$$k_P = C_\mu^{-1/2} u_\tau^2 \quad (11.145)$$

where the friction velocity u_τ is obtained, iteratively, from the log-law (Eq. 11.138). Index P denotes the first interior node (adjacent to the wall).

The dissipation ε is obtained from Eq. 11.141. The dissipation can thus be written as

b.c. for ε

$$\varepsilon_P = P^k = \frac{u_\tau^3}{\kappa \delta x_2} \quad (11.146)$$

where the velocity gradient in the production term $P^k = -\overline{v_1' v_2'} \partial \bar{v}_1 / \partial x_2 \simeq u_\tau^2 \partial \bar{v}_1 / \partial x_2$ is computed from the log-law (see Eqs. 6.28 and 11.138), i.e.

$$\frac{\partial \bar{v}_1}{\partial x_2} = \frac{u_\tau}{\kappa \delta x_2}. \quad (11.147)$$

For the velocity component parallel to the wall the wall shear stress is used as a force boundary condition (cf. prescribing heat flux in the temperature equation). When the wall is not parallel to any velocity component, it is more convenient to prescribe the turbulent viscosity [27].

b.c. for velocity

The log-law is valid for $30 < x_2^+ < 400$. If x_2^+ for some wall-adjacent cells is small, the friction velocity, u_τ , is obtained from the linear law (see Eq. 6.22), i.e.

$$u_\tau = \left(\nu \frac{\bar{v}_{1,P}}{\delta x_2} \right)^{1/2} \quad (11.148)$$

The point at which we switch from the log-law to the linear law is taken at $x_2^+ = 11$ which is the intersection point of the two laws. For $x_2^+ < 11$, \bar{v}_1 is set to zero at the wall and k and ε are set from Eqs. 11.145 and 11.146 taking u_τ from Eq. 11.148. For $11 < x_2^+ < 30$, a combination of the linear law and the log-law is sometimes used. In many commercial codes they interpolate between the linear law and the log-law for the velocity, k and ε . In STAR-CCM+ this is called *All y+ Wall Treatment*.

11.14.2 Low-Re Number Turbulence Models

In the previous section we discussed wall functions which are used in order to reduce the number of cells. However, we must be aware that this is an approximation which, if the flow near the boundary is important, can be rather crude. In many internal flows – where all boundaries are either walls, symmetry planes, inlet or outlets – the boundary layer may not be that important, as the flow field is often pressure-determined. For external flows (for example flow around cars, ships, aeroplanes etc.), however, the flow conditions in the boundaries are almost invariably important. When we are predicting heat transfer it is in general no good idea to use wall functions, because the heat transfer at the walls are very important for the temperature field in the whole domain.

When we chose not to use wall functions we thus insert sufficiently many grid lines near solid boundaries so that the boundary layer can be adequately resolved. However, when the wall is approached the viscous effects become more important and for

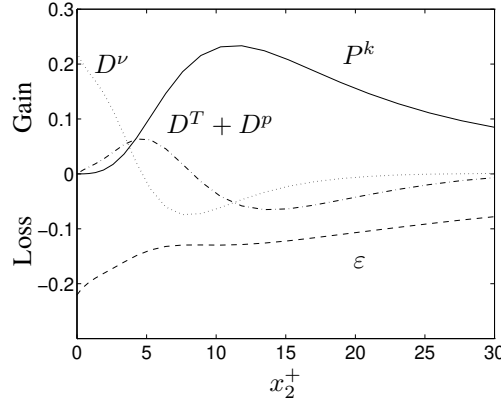


Figure 11.9: Direct numerical simulations [43]. $Re = \bar{v}_{1,C}\delta/\nu = 7890$ (subscript C denotes the center of the channel). $u_\tau/\bar{v}_{1,C} = 0.050$. Energy balance in k equation. Production P^k , dissipation ε , turbulent diffusion (by velocity triple correlations and pressure) $D^T + D^p$, and viscous diffusion D^ν . All terms have been scaled with u_τ^4/ν .

$x_2^+ < 5$ the flow is viscous dominating, i.e. the viscous diffusion is much larger than the turbulent one (see Fig. 11.9). Thus, the turbulence models presented so far may not be correct since fully turbulent conditions have been assumed; this type of models are often referred to as high- Re number models. In this section we will discuss modifications of high- Re number models so that they can be used all the way down to the wall. These modified models are called *low Reynolds number models*. Note that “high Reynolds number” and “low Reynolds number” do *not* refer to the global Reynolds number (for example Re_L , Re_x , Re_δ etc.) but here we are talking about the local turbulent Reynolds number $Re_\ell = \mathcal{U}\ell/\nu$ formed by a turbulent fluctuation and turbulent length scale, see Eq. 5.16. This Reynolds number varies throughout the computational domain and is proportional to the ratio of the turbulent and physical viscosity ν_t/ν , i.e. $Re_\ell \propto \nu_t/\nu$. This ratio is of the order of 100 or larger in fully turbulent flow and it goes to zero when a wall is approached.

We start by studying how various quantities behave close to the wall when $x_2 \rightarrow 0$. Taylor expansion of the fluctuating velocities v'_i (also valid for the mean velocities \bar{v}_i) gives

$$\begin{aligned} v'_1 &= a_0 + a_1x_2 + a_2x_2^2 + \dots \\ v'_2 &= b_0 + b_1x_2 + b_2x_2^2 + \dots \\ v'_3 &= c_0 + c_1x_2 + c_2x_2^2 + \dots \end{aligned} \quad (11.149)$$

where $a_0 \dots c_2$ are functions of x_1 , x_3 and t . At the wall we have no-slip conditions, i.e. $v'_1 = v'_2 = v'_3 = 0$ which gives $a_0 = b_0 = c_0$. Furthermore, at the wall $\partial v'_1/\partial x_1 = \partial v'_3/\partial x_3 = 0$ so that the continuity equation gives $\partial v'_2/\partial x_2 = 0$. This means that $b_1 = 0$. Equation 11.149 can now be written

$$\begin{aligned} v'_1 &= a_1x_2 + a_2x_2^2 + \dots \\ v'_2 &= b_2x_2^2 + \dots \\ v'_3 &= c_1x_2 + c_2x_2^2 + \dots \end{aligned} \quad (11.150)$$

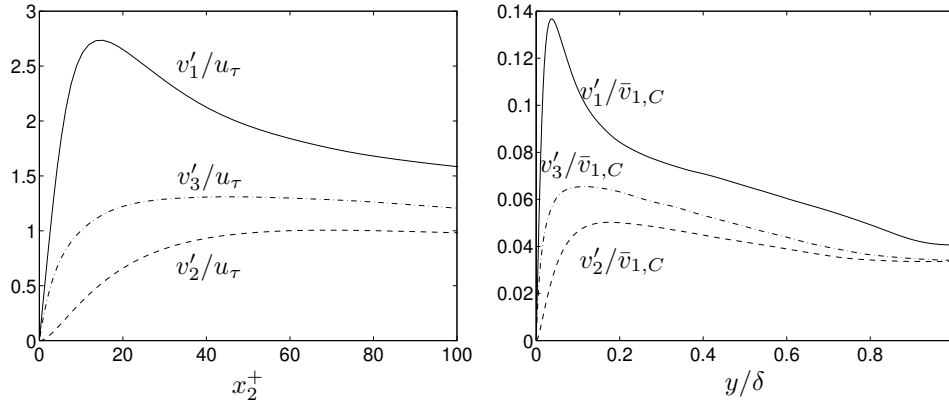


Figure 11.10: Flow between two parallel plates. Direct numerical simulations [43]. $Re = \bar{v}_{1,C}\delta/\nu = 7890$. $u_\tau/\bar{v}_{1,C} = 0.050$. Fluctuating velocity components $v'_i = \sqrt{v'^2_{1,i}}$.

From Eq. 11.150 we immediately get

$$\begin{aligned}
 \overline{v'^2_1} &= \overline{a_1^2 x_2^2} + \dots &= \mathcal{O}(x_2^2) \\
 \overline{v'^2_2} &= \overline{b_2^2 x_2^4} + \dots &= \mathcal{O}(x_2^4) \\
 \overline{v'^2_3} &= \overline{c_1^2 x_2^2} + \dots &= \mathcal{O}(x_2^2) \\
 \overline{v'_1 v'_2} &= \overline{a_1 b_2 x_2^3} + \dots &= \mathcal{O}(x_2^3) \\
 k &= \overline{(a_1^2 + c_1^2) x_2^2} + \dots &= \mathcal{O}(x_2^2) \\
 \partial \bar{v}_1 / \partial x_2 &= \overline{a_1} + \dots &= \mathcal{O}(x_2^0) \\
 \partial v'_1 / \partial x_2 &= \overline{a_1} + \dots &= \mathcal{O}(x_2^0) \\
 \partial v'_2 / \partial x_2 &= \overline{2b_2 x_2} + \dots &= \mathcal{O}(x_2^1) \\
 \partial v'_3 / \partial x_2 &= \overline{a_1} + \dots &= \mathcal{O}(x_2^0)
 \end{aligned} \tag{11.151}$$

In Fig. 11.10 DNS data of velocity fluctuations for the fully developed flow in a channel are presented.

11.14.3 Low-Re $k - \varepsilon$ Models

There exist a number of Low-Re number $k - \varepsilon$ models [44–48]. When deriving low-Re models it is common to study the behavior of the terms when $x_2 \rightarrow 0$ in the exact equations and require that the corresponding terms in the modelled equations behave in the same way. Let us study the exact k equation near the wall (see Eq. 8.26).

$$\begin{aligned}
 \rho \bar{v}_1 \frac{\partial k}{\partial x_1} + \rho \bar{v}_2 \frac{\partial k}{\partial x_2} &= \underbrace{-\overline{\rho v'_1 v'_2} \frac{\partial \bar{v}_1}{\partial x_2}}_{\mathcal{O}(x_2^3)} - \underbrace{\frac{\partial \overline{p' v'_2}}{\partial x_2}}_{\mathcal{O}(x_2^3)} - \underbrace{\frac{\partial}{\partial x_2} \left(\frac{1}{2} \overline{\rho v'_2 v'_i v'_i} \right)}_{\mathcal{O}(x_2^3)} \\
 &\quad + \underbrace{\mu \frac{\partial^2 k}{\partial x_2^2}}_{\mathcal{O}(x_2^0)} - \underbrace{\mu \frac{\partial v'_i}{\partial x_j} \frac{\partial v'_i}{\partial x_j}}_{\mathcal{O}(x_2^0)}
 \end{aligned} \tag{11.152}$$

The dissipation term includes all velocity gradients but most of them go to zero close to the wall, see Eq. 11.151. The only velocity gradients that do not go to zero are $\partial v'_1 / \partial x_2$ and $\partial v'_3 / \partial x_2$ and hence $\varepsilon \propto \mathcal{O}(x_2^0)$. The pressure diffusion $\partial \overline{p' v'_2} / \partial x_2$ term

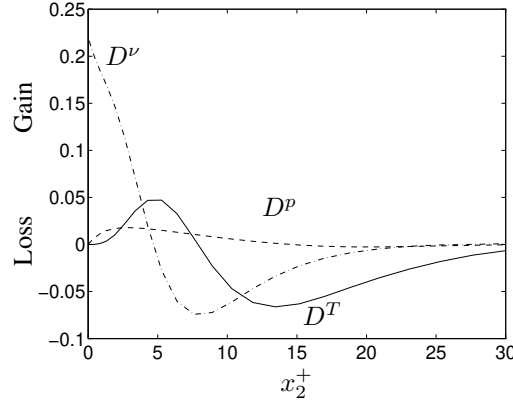


Figure 11.11: Flow between two parallel plates. Direct numerical simulations [43]. $Re = \bar{v}_{1,C} \delta / \nu = 7890$. $u_\tau / \bar{v}_{1,C} = 0.050$. Energy balance in k equation. Turbulent diffusion by velocity triple correlations D^T , Turbulent diffusion by pressure D^p , and viscous diffusion D^ν . All terms have been scaled with u_τ^4 / ν .

is usually neglected, partly because it is not measurable, and partly because close to the wall it is not important, see Fig. 11.11 (see also [49]). The modelled equation reads (see Eq. 11.97)

$$\begin{aligned} \rho \bar{v}_1 \frac{\partial k}{\partial x_1} + \rho \bar{v}_2 \frac{\partial k}{\partial x_2} &= \underbrace{\mu_t \left(\frac{\partial \bar{v}_1}{\partial x_2} \right)^2}_{\mathcal{O}(x_2^4)} + \underbrace{\frac{\partial}{\partial x_2} \left(\frac{\mu_t}{\sigma_k} \frac{\partial k}{\partial x_2} \right)}_{\mathcal{O}(x_2^4)} \\ &\quad + \underbrace{\mu \frac{\partial^2 k}{\partial x_2^2}}_{\mathcal{O}(x_2^0)} - \underbrace{\rho \varepsilon}_{\mathcal{O}(x_2^0)} \end{aligned} \quad (11.153)$$

When arriving at that the production term is $\mathcal{O}(x_2^4)$ we have used

$$\nu_t = C_\mu \frac{k^2}{\varepsilon} = \frac{\mathcal{O}(x_2^4)}{\mathcal{O}(x_2^0)} = \mathcal{O}(x_2^4) \quad (11.154)$$

Comparing Eqs. 11.152 and 11.153 we find that the dissipation term in the modelled equation behaves in the same way as in the exact equation when $x_2 \rightarrow 0$. However, both the modelled production and the diffusion term are of $\mathcal{O}(x_2^4)$ whereas the exact terms are of $\mathcal{O}(x_2^3)$. This inconsistency of the modelled terms can be removed by replacing the C_μ constant by $C_\mu f_\mu$ where f_μ is a damping function f_μ so that

$$f_\mu = \mathcal{O}(x_2^{-1}) \quad (11.155)$$

when $x_2 \rightarrow 0$ and $f_\mu \rightarrow 1$ when $x_2^+ \geq 50$. Now we get $\nu_t = \mathcal{O}(x_2^3)$. Please note that the term “damping term” in this case is not correct since f_μ actually is increasing μ_t when $x_2 \rightarrow 0$ rather than damping it. However, it is common to call all low-Re number functions for “damping functions”.

Instead of introducing a damping function f_μ , we can choose to solve for a modified dissipation which is denoted $\tilde{\varepsilon}$, see Refs. [27, 50]

It is possible to compare the exact and the modeled ε equation when deriving damping functions for the ε equation [51]. An alternative way is to study the modelled

ε equation near the wall and keep only the terms which do not tend to zero. From Eq. 11.29 we get (note that $\partial\varepsilon/\partial x_2 = \mathcal{O}(x_2^0)$, $\partial\varepsilon/\partial x_1 = \mathcal{O}(x_2^0)$)

$$\underbrace{\rho\bar{v}_1 \frac{\partial\varepsilon}{\partial x_1}}_{\mathcal{O}(x_2^1)} + \underbrace{\rho\bar{v}_2 \frac{\partial\varepsilon}{\partial x_2}}_{\mathcal{O}(x_2^2)} = \underbrace{C_{\varepsilon 1} \frac{\varepsilon}{k} P^k}_{\mathcal{O}(x_2^1)} + \underbrace{\frac{\partial}{\partial x_2} \left(\frac{\mu_t}{\sigma_\varepsilon} \frac{\partial\varepsilon}{\partial x_2} \right)}_{\mathcal{O}(x_2^2)} + \underbrace{\mu \frac{\partial^2 \varepsilon}{\partial x_2^2}}_{\mathcal{O}(x_2^0)} - \underbrace{C_{\varepsilon 2} \rho \frac{\varepsilon^2}{k}}_{\mathcal{O}(x_2^{-2})} \quad (11.156)$$

The left-side has been written on non-conservative form (see Section 2.4) which makes it easier to see that the term goes to zero at the wall. Furthermore, it has been assumed that the turbulent viscosity has been suitable modified so that $\nu_t = \mathcal{O}(x_2^3)$. We find that the only terms which do not vanish at the wall are the viscous diffusion term and the dissipation term so that close to the wall the dissipation equation reads

$$0 = \mu \frac{\partial^2 \varepsilon}{\partial x_2^2} - C_{\varepsilon 2} \rho \frac{\varepsilon^2}{k}. \quad (11.157)$$

This equation needs to be modified since the diffusion term cannot balance the destruction term when $x_2 \rightarrow 0$. We multiply the destruction term by $f_2 \propto \mathcal{O}(x_2^2)$. For more details, see [27].

11.14.4 Wall boundary Condition for k

The wall boundary condition of k is simple. Since the first cell is in the viscous sublayer ($x_2^+ \simeq 1$) and the turbulent fluctuations are zero at the wall we set

$$k = 0 \quad (11.158)$$

11.14.5 Different ways of prescribing ε at or near the wall

When setting wall boundary condition for ε we look at the k equation. The largest term in the k equation (see Eq. 11.152) close to the wall, are the dissipation term and the viscous diffusion term which both are of $\mathcal{O}(x_2^0)$ so that

$$0 = \mu \frac{\partial^2 k}{\partial x_2^2} - \rho \varepsilon. \quad (11.159)$$

From this equation we get immediately a boundary condition for ε as

$$\varepsilon_{wall} = \nu \frac{\partial^2 k}{\partial x_2^2}. \quad (11.160)$$

From Eq. 11.159 we can derive alternative boundary conditions. The exact form of the dissipation term close to the wall reads (see Eq. 8.26)

$$\varepsilon = \nu \left\{ \left(\frac{\partial v'_1}{\partial x_2} \right)^2 + \left(\frac{\partial v'_3}{\partial x_2} \right)^2 \right\} \quad (11.161)$$

where $\partial/\partial x_2 \gg \partial/\partial x_1 \simeq \partial/\partial x_3$ and $\partial v'_1/\partial x_2 \simeq \partial v'_3/\partial x_2 \gg \partial v'_2/\partial x_2$ have been assumed. Using Taylor expansion gives (see Eq. 11.150)

$$\varepsilon = \nu \left(\overline{a_1^2} + \overline{c_1^2} \right) + \dots \quad (11.162)$$

In the same way we get an expression for the turbulent kinetic energy (see Eq. 11.150)

$$k = \frac{1}{2} \left(\overline{a_1^2} + \overline{c_1^2} \right) x_2^2 + \dots \quad (11.163)$$

so that

$$\left(\frac{\partial \sqrt{k}}{\partial x_2} \right)^2 = \frac{1}{2} \left(\overline{a_1^2} + \overline{c_1^2} \right) + \dots \quad (11.164)$$

Comparing Eqs. 11.162 and 11.164 we find

$$\varepsilon_{wall} = 2\nu \left(\frac{\partial \sqrt{k}}{\partial x_2} \right)^2. \quad (11.165)$$

In many $k - \varepsilon$ models the following form is used

$$\varepsilon_P = 2\nu \frac{k}{x_2^2} \quad (11.166)$$

where subscript P denotes wall-adjacent cells, see Fig. 11.7. This is not really a boundary condition; instead we prescribe ε at the wall-adjacent cells. This is obtained by assuming $a_1 = c_1$ in Eqs. 11.162 and 11.163 so that

$$\begin{aligned} \varepsilon &= 2\nu \overline{a_1^2} \\ k &= \overline{a_1^2} x_2^2 \end{aligned} \quad (11.167)$$

which gives Eq. 11.166.

A Introduction to tensor notation

The convection-diffusion equation for temperature reads

$$\begin{aligned} \frac{\partial}{\partial x_1} (\rho v_1 T) + \frac{\partial}{\partial x_2} (\rho v_2 T) + \frac{\partial}{\partial x_3} (\rho v_3 T) = \\ \frac{\partial}{\partial x_1} \left(\Gamma \frac{\partial T}{\partial x_1} \right) + \frac{\partial}{\partial x_2} \left(\Gamma \frac{\partial T}{\partial x_2} \right) + \frac{\partial}{\partial x_3} \left(\Gamma \frac{\partial T}{\partial x_3} \right) \end{aligned}$$

Using tensor notation it can be written as

$$\boxed{\frac{\partial}{\partial x_j} (\rho v_j T) = \frac{\partial}{\partial x_j} \left(\Gamma \frac{\partial T}{\partial x_j} \right)}$$

The Navier-Stokes equation reads (incompressible and $\mu = \text{const.}$)

$$\begin{aligned} \frac{\partial}{\partial x_1} (v_1 v_1) + \frac{\partial}{\partial x_2} (v_2 v_1) + \frac{\partial}{\partial x_3} (v_3 v_1) = \\ - \frac{1}{\rho} \frac{\partial p}{\partial x_1} + \nu \left(\frac{\partial^2 v_1}{\partial x_1^2} + \frac{\partial^2 v_1}{\partial x_2^2} + \frac{\partial^2 v_1}{\partial x_3^2} \right) \end{aligned}$$

$$\begin{aligned} \frac{\partial}{\partial x_1} (v_1 v_2) + \frac{\partial}{\partial x_2} (v_2 v_2) + \frac{\partial}{\partial x_3} (v_3 v_2) = \\ - \frac{1}{\rho} \frac{\partial p}{\partial x_2} + \nu \left(\frac{\partial^2 v_2}{\partial x_1^2} + \frac{\partial^2 v_2}{\partial x_2^2} + \frac{\partial^2 v_2}{\partial x_3^2} \right) \end{aligned}$$

$$\begin{aligned} \frac{\partial}{\partial x_1} (v_1 v_3) + \frac{\partial}{\partial x_2} (v_2 v_3) + \frac{\partial}{\partial x_3} (v_3 v_3) = \\ - \frac{1}{\rho} \frac{\partial p}{\partial x_3} + \nu \left(\frac{\partial^2 v_3}{\partial x_1^2} + \frac{\partial^2 v_3}{\partial x_2^2} + \frac{\partial^2 v_3}{\partial x_3^2} \right) \end{aligned}$$

Using tensor notation it can be written as

$$\boxed{\frac{\partial}{\partial x_j} (v_j v_i) = - \frac{1}{\rho} \frac{\partial p}{\partial x_i} + \nu \frac{\partial^2 v_i}{\partial x_j \partial x_j}}$$

a : A tensor of zeroth rank (scalar)

a_i : A tensor of first rank (vector) $\nearrow a_i = (2, 1, 0)$

a_{ij} : A tensor of second rank (tensor)

A common tensor in fluid mechanics (and solid mechanics) is the stress tensor σ_{ij}

$$\sigma_{ij} = \begin{pmatrix} \sigma_{11} & \sigma_{12} & \sigma_{13} \\ \sigma_{21} & \sigma_{22} & \sigma_{23} \\ \sigma_{31} & \sigma_{32} & \sigma_{33} \end{pmatrix}$$

It is symmetric, i.e. $\sigma_{ij} = \sigma_{ji}$. For fully, developed flow in a 2D channel (flow between infinite plates) σ_{ij} has the form:

$$\sigma_{12} = \sigma_{21} = \mu \frac{dv_1}{dx_2}$$

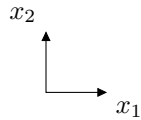
and the other components are zero. As indicated above, the coordinate directions (x_1, x_2, x_3) correspond to (x, y, z) , and the velocity vector (v_1, v_2, v_3) corresponds to (u, v, w) .

A.1 What is a tensor?

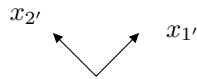
A tensor is a *physical* quantity. Consequently it is independent of which coordinate system. The tensor of rank one (vector) b_i below



is physically the same expressed in the coordinate system (x_1, x_2)



where $b_i = (1/\sqrt{2}, 1/\sqrt{2}, 0)^T$ and in the coordinate system $(x_{1'}, x_{2'})$



where $b_{i'} = (1, 0, 0)^T$. The tensor is the same even if its *components* are different.

The stress tensor σ_{ij} is a physical quantity which expresses the stress experienced by the fluid (or the solid); this stress is the same irrespective of coordinate system.

A.2 Examples of equations using tensor notation

A.2.1 Newton's second law

$$m \frac{d^2 \mathbf{x}}{dt^2} = \mathbf{F}$$

which on component form reads

$$\begin{aligned} m \frac{d^2 x_1}{dt^2} &= F_1 \\ m \frac{d^2 x_2}{dt^2} &= F_2 \\ m \frac{d^2 x_3}{dt^2} &= F_3. \end{aligned} \tag{A.1}$$

On tensor notation:

$$m \frac{d^2 x_i}{dt^2} = F_i$$

When an index appears once in each term (a free index) it indicates that the whole equation should be applied in each coordinate direction, cf. Eq. A.1.

A.2.2 Divergence $\nabla \cdot \mathbf{v} = 0$

The equation above reads

$$\frac{\partial v_1}{\partial x_1} + \frac{\partial v_2}{\partial x_2} + \frac{\partial v_3}{\partial x_3} = 0 \Leftrightarrow \sum_{i=1}^3 \frac{\partial v_i}{\partial x_i} = 0 \tag{A.2}$$

In tensor notation the following rule is introduced: if an index appears twice (a dummy index) within a term, we should apply summation over this index. Normally the summation is taken from 1 to 3 (the three coordinate directions). If our coordinate system is 2D, the summation goes, of course, only from 1 to 2.

Equation A.2 is thus written as

$$\frac{\partial v_i}{\partial x_i} = 0. \tag{A.3}$$

Note that, since the dummy index implies a summation over each term, it can be interchanged against any index, i.e.

$$\frac{\partial v_k}{\partial x_k} = 0.$$

is exactly the same equation as Eq. A.3. Equation A can, for example, be written as

$$\frac{\partial}{\partial x_\ell} (v_\ell v_m) = -\frac{1}{\rho} \frac{\partial p}{\partial x_m} + \nu \frac{\partial v_m^2}{\partial x_k \partial x_k}$$

where different dummy indices have been used (ℓ and k); this is perfectly correct, because the summation is carried out for each term separately. What is not allowed, however, it to choose the dummy index same as the free index, i.e. for the equation above we are not allowed to use m as a dummy index.

A.2.3 The left-hand side of Navier-Stokes $v_\ell \partial v_m / \partial x_\ell$

For simplicity, let's assume 2D. The left-hand side of the equation above includes both a free index (m) and a dummy index (ℓ). Let's first write out the summation on component form so that

$$v_1 \frac{\partial v_m}{\partial x_1} + v_2 \frac{\partial v_m}{\partial x_2}.$$

The free index indicates that the equation should be written in each coordinate direction (x_1 and x_2 in this case, since we have assumed 2D flow), cf. Eq. A.1, i.e.

$$\begin{aligned} v_1 \frac{\partial v_1}{\partial x_1} + v_2 \frac{\partial v_1}{\partial x_2} \\ v_1 \frac{\partial v_2}{\partial x_1} + v_2 \frac{\partial v_2}{\partial x_2} \end{aligned}$$

A.3 Contraction

If two free indices are set equal, they are turned into dummy indices, and the rank of the tensor is decreased by two. This is called *contraction*. If the tensor equation

$$a_{ij} = b_j c d_i - f_{ij}$$

is contracted, the result is

$$a_{ii} = b_i c d_i - f_{ii}.$$

For a tensor of rank two, a_{ij} , contraction is simply summation of the diagonal elements, i.e. $a_{11} + a_{22} + a_{33}$.

A.4 Two Tensor Rules

A.4.1 The summation rule

A summation over a dummy index corresponds to a scalar product or a divergence; it should not appear more than twice. The following expressions are not valid:

$$a_{kkk} = 0, \quad a_{iik} b_{ij} = d_{kj}, \quad a_i b_i c_i = d$$

A.4.2 Free Index

In an expression the free index (indices) must be the same in all terms. The following expressions are not valid:

$$a_{ikk} = b_j, \quad c_i a_i b_j = d_k, \quad a_{ij} d_{jk} = c_{im}$$

A.5 Special Tensors

A.5.1 Kronecker's δ (identity tensor)

It is defined as

$$\delta_{ij} = \begin{cases} 1 & i = j \\ 0 & i \neq j \end{cases}$$

Contraction of δ_{ij} yields

$$\delta_{ii} = \delta_{11} + \delta_{22} + \delta_{33} = 3$$

Another example of contraction can now be given. We have the expression for the turbulent stress tensor based on the Boussinesq hypothesis (see Eq. 11.33)

$$\overline{\rho v_i' v_j'} = -\mu_t \left(\frac{\partial \bar{v}_i}{\partial x_j} + \frac{\partial \bar{v}_j}{\partial x_i} \right) + \frac{2}{3} \delta_{ij} \rho k. \quad (\text{A.4})$$

Contraction gives

$$\rho \overline{u_i u_i} = -2\mu_t \frac{\partial \bar{v}_i}{\partial x_i} + \frac{2}{3} \delta_{ii} \rho k = -2\mu_t \frac{\partial \bar{v}_i}{\partial x_i} + 2\rho k.$$

For incompressible flow the first term on the right-hand side is zero (due to continuity) so that

$$\overline{u_i u_i} = 2k,$$

which actually is the definition of k . Thus Eq. A.4 is valid upon contraction; this should always be the case. As can be seen, contraction of Eq. A.4 corresponds simply to the sum of the diagonal components (elements 11, 22 & 33).

A.5.2 Levi-Civita's ε_{ijk} (permutation tensor)

It is defined as

$$\varepsilon_{ij} = \begin{cases} 1 & \text{if } (i, j, k) \text{ are cyclic permutations of } (1, 2, 3) \\ 0 & \text{if at least two indices are equal} \\ -1 & \text{otherwise} \end{cases} \quad (\text{A.5})$$

Examples:

$$\begin{aligned} \varepsilon_{123} &= 1, \quad \varepsilon_{132} = -1, \quad \varepsilon_{113} = 0 \\ \varepsilon_{312} &= 1, \quad \varepsilon_{321} = -1, \quad \varepsilon_{233} = 0 \end{aligned}$$

A.6 Symmetric and antisymmetric tensors

A tensor a_{ij} is symmetric if $a_{ij} = a_{ji}$.

A tensor b_{ij} is antisymmetric if $b_{ij} = -b_{ji}$. It follows that for an antisymmetric tensor all diagonal components must be zero (for example, $b_{11} = -b_{11} \Rightarrow b_{11} = 0$).

The (inner) product of a symmetric and antisymmetric tensor is always zero. This can be shown as follows:

$$a_{ij} b_{ij} = a_{ji} b_{ij} = -a_{ji} b_{ji} = -a_{ij} b_{ij},$$

where we first used the fact that $a_{ij} = a_{ji}$ (symmetric), then that $b_{ij} = -b_{ji}$ (antisymmetric), and finally we interchanged the indices i and j , since they are dummy indices. Thus the product must be zero.

This can of course also be shown by writing out $a_{ij} b_{ij}$ on component form, i.e.

$$a_{ij} b_{ij} = a_{11} b_{11} + a_{12} b_{12} + a_{13} b_{13} + \dots + a_{32} b_{32} + a_{33} b_{33} = 0$$

By inserting

$$\begin{aligned} a_{12} &= a_{21}, & a_{13} &= a_{31}, & a_{23} &= a_{32} \\ b_{11} &= b_{22} = b_{33} = 0 \\ b_{12} &= -b_{21}, & b_{13} &= -b_{31}, & b_{23} &= -b_{32} \end{aligned}$$

the relation above, i.e. $a_{ij}b_{ij} = 0$, is verified.

A.7 Vector Product

The vector cross product

$$\mathbf{c} = \mathbf{a} \times \mathbf{b}$$

is on tensor notation written

$$c_i = \varepsilon_{ijk} a_j b_k. \quad (\text{A.6})$$

This is easily shown by writing it on component form. Using Sarrus' rule we get

$$\mathbf{c} = \begin{pmatrix} \mathbf{x} & \mathbf{y} & \mathbf{z} \\ a_1 & a_2 & a_3 \\ b_1 & b_2 & b_3 \end{pmatrix} = (a_2 b_3 - a_3 b_2, a_3 b_1 - a_1 b_3, a_1 b_2 - a_2 b_1)^T$$

We find that the first component of Eq. A.6 is

$$\begin{aligned} c_1 &= \varepsilon_{1jk} a_j b_k = \\ &= \varepsilon_{111} a_1 b_1 + \varepsilon_{112} a_1 b_2 + \varepsilon_{113} a_1 b_3 \\ &\quad + \varepsilon_{121} a_2 b_1 + \varepsilon_{122} a_2 b_2 + \varepsilon_{123} a_2 b_3 \\ &\quad + \varepsilon_{131} a_3 b_1 + \varepsilon_{132} a_3 b_2 + \varepsilon_{133} a_3 b_3 \\ &= \varepsilon_{123} a_2 b_3 + \varepsilon_{132} a_3 b_2 = a_2 b_3 - a_3 b_2. \end{aligned}$$

Recall that ε_{ijk} is zero if any two indices are equal (see Eq. A.5, p. 283).

A.8 Derivative Operations

A.8.1 The derivative of a vector \mathbf{B} :

Tensor notation	Vector notation
$\frac{\partial B_i}{\partial x_j}$	$\text{grad}(\mathbf{B})$ or $\nabla \mathbf{B}$

The result is a tensor of rank two (rank of B_i plus one)

A.8.2 The gradient of a scalar a :

Tensor notation	Vector notation
$\frac{\partial a}{\partial x_j}$	$\text{grad}(a)$ or ∇a

The result is a *vector*.

A.8.3 The divergence of a vector \mathbf{B} :

Tensor notation	Vector notation
$\frac{\partial B_j}{\partial x_j}$	$\text{div}(\mathbf{B})$ or $\nabla \cdot \mathbf{B}$

The result is a *scalar*.

A.8.4 The curl of a vector \mathbf{B} :

Tensor notation	Vector notation
$\varepsilon_{ijk} \frac{\partial B_k}{\partial x_j}$	$\text{curl}(\mathbf{B})$ or $\nabla \times \mathbf{B}$

The result is a *vector*.

A.8.5 The Laplace operator on a scalar a :

Tensor notation	Vector notation
$\frac{\partial^2 a}{\partial x_j \partial x_j}$	$\nabla \cdot (\nabla a) = \nabla^2 a$

The result is a *scalar*.

A.9 Integral Formulas

Stokes theorem

$$\oint_C \mathbf{B} \cdot d\mathbf{x} = \int_S (\nabla \times \mathbf{B}) \cdot d\mathbf{S},$$

where the surface S is bounded by the line C . On tensor notation:

$$\oint_C B_i dx_i \quad \text{or} \quad \int_S \varepsilon_{ijk} \frac{\partial B_k}{\partial x_j} dS_i.$$

Gauss theorem

$$\int_S \mathbf{B} \cdot d\mathbf{S} = \int_V \nabla \cdot \mathbf{B} dV,$$

where the volume V is bounded by the surface S . On tensor notation:

$$\int_S B_i dS_i \quad \text{or} \quad \int_V \frac{\partial B_i}{\partial x_i} dV$$

A.10 Multiplication of tensors

Two tensors can be multiplied in two ways: either the number of free indices is reduced by two (inner product), or it is unchanged (outer product). The product

$$a_{ijk} b_{k\ell} = c_{ij\ell}$$

represents an inner product; the rank of the product is the sum of the rank of the two tensors ($3 + 2 = 5$) on the left-hand side minus two ($5 - 3 = 2$). An outer product between the two tensors reads

$$a_{ijk} b_{m\ell} = d_{ijk\ell m}.$$

Now the rank of the resulting tensor d_{ijklm} (rank 5) is the sum of the rank of the two tensors ($3 + 2 = 5$).

B TME226: $\epsilon - \delta$ identity

THE $\epsilon - \delta$ identity reads

$$\epsilon_{inm}\epsilon_{mjk} = \epsilon_{min}\epsilon_{mjk} = \epsilon_{nmi}\epsilon_{mjk} = \delta_{ij}\delta_{nk} - \delta_{ik}\delta_{nj}$$

In Table B.1 the components of the $\epsilon - \delta$ identity are given.

i	n	j	k	$\epsilon_{inm}\epsilon_{mjk}$	$\delta_{ij}\delta_{nk} - \delta_{ik}\delta_{nj}$
1	2	1	2	$\epsilon_{12m}\epsilon_{m12} = \epsilon_{123}\epsilon_{312} = 1 \cdot 1 = 1$	$1 - 0 = 1$
2	1	1	2	$\epsilon_{21m}\epsilon_{m12} = \epsilon_{213}\epsilon_{312} = -1 \cdot 1 = -1$	$0 - 1 = -1$
1	2	2	1	$\epsilon_{12m}\epsilon_{m21} = \epsilon_{123}\epsilon_{321} = 1 \cdot -1 = -1$	$0 - 1 = -1$
1	3	1	3	$\epsilon_{13m}\epsilon_{m13} = \epsilon_{132}\epsilon_{213} = -1 \cdot -1 = 1$	$1 - 0 = 1$
3	1	1	3	$\epsilon_{31m}\epsilon_{m13} = \epsilon_{312}\epsilon_{213} = 1 \cdot -1 = -1$	$0 - 1 = -1$
1	3	3	1	$\epsilon_{13m}\epsilon_{m31} = \epsilon_{132}\epsilon_{231} = -1 \cdot 1 = -1$	$0 - 1 = -1$
2	3	2	3	$\epsilon_{23m}\epsilon_{m23} = \epsilon_{231}\epsilon_{123} = 1 \cdot 1 = 1$	$1 - 0 = 1$
3	2	2	3	$\epsilon_{32m}\epsilon_{m23} = \epsilon_{321}\epsilon_{123} = -1 \cdot 1 = -1$	$0 - 1 = -1$
2	3	3	2	$\epsilon_{23m}\epsilon_{m32} = \epsilon_{231}\epsilon_{132} = 1 \cdot -1 = -1$	$0 - 1 = -1$

Table B.1: The components of the $\epsilon - \delta$ identity which are non-zero.

C TME226 Assignment 1 in 2024: laminar flow in a channel

YOU will get results of a developing two-dimensional channel flow (i.e. flow between two parallel plates), see Fig. C.1. The flow is steady and incompressible. The simulations have been done with Calc-BFC [199]. The inlet boundary condition (left boundary) is $v_1 = V_{in} = 0.9$. The height of the channel is $h = 0.01m$ and $L = 0.6385m$; the fluid is air of $20^\circ C$.

You'll use data from a coarse DNS. Although some of the data are probably not fully accurate, in this exercise we consider the data to be exact. You can use [Matlab](#), [Octave](#) or [Python](#). Both Octave and Python are open-source software. Octave is a Matlab clone. Many large Swedish industries prefer engineers to use Python instead of Matlab due to Matlab's high license fees

- First, find out and write down the governing equations (N.B.: you cannot assume that the flow is fully developed).

From the course www page <https://www.tfd.chalmers.se/~lada/MoF/>, download the data file `channel_flow_data.dat` and the m-file `channel_flow.m` which reads the data and plot some results. Open Python or Matlab/Octave and execute `channel_flow`.

Open `channel_flow.m` in an editor and make sure that you understand it. There are three field variables, v_1 , v_2 and p ; the corresponding Python/Matlab/Octave arrays are `v1_2d`, `v2_2d` and `p_2d`. The grid is 199×28 , i.e. $n_i = 199$ grid points in the x_1 direction and $n_j = 28$ grid points in the x_2 direction. The field variables are stored at these grid points. We denote the first index as i and the second index as j , i.e. `v1_2d(i, j)`. Hence in Python

`v1_2d[:, 0]` are the v_1 values at the lower wall;

`v1_2d[:, nj-1]` are the v_1 values at the upper wall;

`v1_2d[0, :]` are the v_1 values at the inlet;

`v1_2d[ni-1, :]` are the v_1 values at the outlet;

and in Matlab/Octave

`v1_2d(:, 1)` are the v_1 values at the lower wall;

`v1_2d(:, nj)` are the v_1 values at the upper wall;

`v1_2d(1, :)` are the v_1 values at the inlet;

`v1_2d(ni, :)` are the v_1 values at the outlet;

The work should be carried out in groups of two (you may also do it on your own, but we don't recommend it). At the end of this Assignment the group should write and submit a report (in English). Divide the report into sections corresponding to the sections C.1 – C.9. In some sections you need to make derivations; these should clearly be described and presented. Present the results in each section with a figure (or a numerical value). The results should also be discussed and – as far as you can – explained.

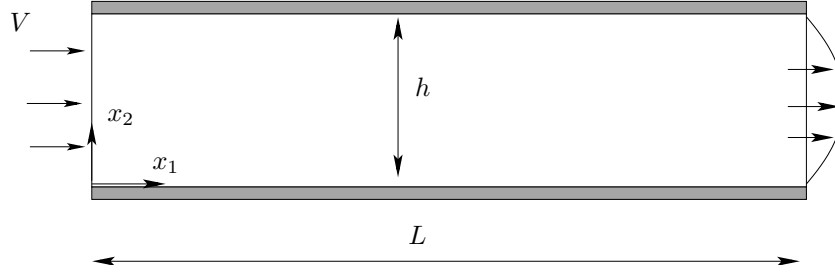


Figure C.1: Flow between two plates (not to scale).

It is recommended (but not required) that you use \LaTeX (an example of how to write in \LaTeX is available on the course [www](#) page). You find \LaTeX [here](#). You can also use \LaTeX [on-line](#).

C.1 Fully developed region

Fully developed conditions mean that the flow does not change in the streamwise direction, i.e. $\partial v_1 / \partial x_1 = 0$. If we define “fully developed” as the location where the velocity gradient in the center becomes smaller than 0.01, i.e. $|\partial v_1 / \partial x_1| < 0.01$, how long distance from the inlet does the flow become fully developed?

Another way to define fully developed conditions can be the x_1 position where the centerline velocity has reached, for example, 99% of its final value. What x_1 value do you get?

In Section 3.2.2, a distance taken from the literature is given. How well does this agree with your values?

In the fully developed region, compare the velocity profile with the analytical profile (see Section 3.2.2).

Look at the vertical velocity component, v_2 . What value should it take in the fully developed region (see Section 3.2.2)? What value does it take (at $x_2 = h/4$, for example)?

C.2 Wall shear stress

On the lower wall, the wall shear stress, $\tau_{w,L}$ (index L denotes Lower), is computed as

$$\tau_{w,L} \equiv \tau_{21,w,L} = \mu \left. \frac{\partial v_1}{\partial x_2} \right|_L \quad (\text{C.1})$$

Recall that $\tau_{12} = \mu(\partial v_1 / \partial x_2 + \partial v_2 / \partial x_1)$ (see Eqs. 2.10) but at the wall $\partial v_2 / \partial x_1 = 0$; Plot $\tau_{w,L}$ versus x_1 . Why does it behave as it does?

Now we will compute the wall shear stress at the upper wall, $\tau_{w,U}$. If you use Eq. C.1, you get the incorrect sign. Instead, use Cauchy’s formula (see Fig. 1.3 and [3], Chapt. 4.2)

$$t_i^{(\hat{n})} = \tau_{ji} n_j \quad (\text{C.2})$$

which is a general way to compute the stress vector on a surface whose (outward pointing) normal vector is $\hat{n} = n_j$. The expression for τ_{ij} can be found in Eqs. 1.9 and 2.4; recall that the flow is incompressible. On the top wall, the normal vector points *out* from the surface (i.e. $n_j = (0, -1, 0)$). Use Eq. C.2 to compute the wall shear

stress at the upper wall. Plot the two wall shear stresses in the same figure. How do they compare? In the fully developed region, compare with the analytical value (see Eq. 3.30).

C.3 Inlet region

In the inlet region the flow is developing from its inlet profile ($v_1 = V = 0.9$) to the fully developed profile somewhere downstream. The v_1 velocity is decelerated in the near-wall regions, and hence the v_1 velocity in the center must increase due to continuity. Plot v_1 in the center and near the wall as a function of x_1 . Plot also $\partial v_1 / \partial x_1$. If you, for a fixed x_1 , integrate v_1 , i.e.

$$\xi(x_1) = \int_0^h v_1(x_1, x_2) dx_2$$

what do you get? How does $\xi(x_1)$ vary in the x_1 direction? How should it vary?

C.4 Wall-normal velocity in the developing region

In Section C.3 we found that, in the developing region, v_1 near the walls decreases for increasing x_1 . What about v_2 ? How do you explain the behaviour of v_2 ?

C.5 Vorticity

Do you expect the flow to be *irrotational* anywhere? Let's find out by computing the vorticity vector ω_i , see Section 1.4 (note that only one component of ω_i is non-zero). Plot it in the fully developed region as ω_3 vs. x_2 . Where is it largest? Plot the vorticity also in the inlet and developing regions; what happens with the vorticity in the inlet region? Now, *is* the flow rotational anywhere? Why? Why not?

C.6 Deformation

In Section 1.6, we divided the velocity gradient into a strain-rate tensor, S_{ij} , and a vorticity tensor, Ω_{ij} . Since the flow is two-dimensional, we have only two off-diagonal terms (which ones?). Plot and compare one of the off-diagonal term of S_{ij} and Ω_{ij} . Where are they largest? Why? What is the physical meaning of S_{ij} and Ω_{ij} , respectively? Compare Ω_{ij} with the vorticity, ω_i , you plotted in Section C.5. Are they similar? Any comment?

C.7 Dissipation

Compute and plot the dissipation, $\Phi = \tau_{ji} \partial v_i / \partial x_j$, see Eq. 2.15. What is the physical meaning of the dissipation? Where do you expect it to be largest? Where is it largest? Any difference in its behaviour in the inlet region compared to in the fully developed region?

The dissipation appears as a source term in the equation for internal energy, see Eq. 2.15. This means that dissipation increases the internal energy, i.e. the temperature. This is discussed in some detail at p. 34.

Use Eq. 2.17 to compute the temperature increase that is created by the flow (i.e. by dissipation). Start by integrating the dissipation over the entire computational domain. Next, re-write the left side on conservative form (see Section 2.4) and then apply the

Gauss divergence theorem, See Section 3.2.3. Assume that the upper and the lower wall are adiabatic; furthermore we can neglect the heat flux by conduction, q_1 , (see Eq. 2.14) at the inlet and outlet.

Compute the increase in bulk temperature, T_b , from inlet to outlet. The bulk temperature is defined as

$$T_b = \frac{\int_0^h v_1 T dx_2}{\int_0^h v_1 dx_2} \quad (\text{C.3})$$

When you compute the convective flux in Eq. 2.12 at the outlet, for example, you get

$$\int_0^h v_1 T dx_2$$

which indeed is very similar to the bulk temperature in Eq. C.3.

C.8 Eigenvalues

Compute and plot the eigenvalues of the viscous stress tensor, τ_{ij} . Use the Python command `np.linalg.eig` or the Matlab/Octave command `eig`. If you have computed the four elements of the τ_{ij} matrix you can use the following commands in Python

```
tau=[tau_11 tau_12; tau_21 tau_22]
lambda,n=np.linalg.eig(tau)
```

and in Matlab/Octave

```
tau=[tau_11 tau_12; tau_21 tau_22];
[n,lambda]=eig(tau);
```

where `n` and `lambda` denote eigenvalues and eigenvectors, respectively. Note that `tau_11`, `tau_12`, `tau_21`, `tau_22` are scalars and hence the coding above must be inserted in `for` loops.

What is the physical meaning of the eigenvalues (see Chapter 1.8)? Pick an x_1 location where the flow is fully developed. Plot one eigenvalue as a $x-y$ graph (eigenvalue versus x_2). Plot also the four stress components, τ_{ij} , versus x_2 . Is (Are) anyone(s) negligible? How does the largest component of τ_{ij} compare with the largest eigenvalue? Any thoughts? And again: *what is the physical meaning of the eigenvalues?*

C.9 Eigenvectors

Compute and plot the eigenvectors of τ_{ij} . Recall that at each point you will get two eigenvectors, perpendicular to each other. It is enough to plot one of them. An eigenvector is, of course, a vector. Use the Python command `plt.quiver` or the Matlab/Octave command `quiver` to plot the field of the eigenvectors. Recall that the sign of the eigenvector is not defined (for example, both \hat{v}_1 and $-\hat{v}_1$ in Fig. 1.11 at p. 30 are eigenvectors).

Recall that the stress vector, $t_i^{(\hat{n})}$, (see Eq. C.2 and Fig. 1.3) can be computed as the product of the eigenvalues and eigenvectors. Do that as a vector plot⁷. In regions where the eigenvalues are close to zero, the eigenvectors have no meaning.

Try to analyze why the eigenvectors behave as they do. ‘

⁷If you plot it over the entire region, you’ll see nothing; make a zoom

AH TME226, Assignment 2: Turbulent flow using STAR-CCM+

IN this task, a commercial CFD software (STAR-CCM+ 2402) will be used. The task is to do simulation of a two-dimensional hill flow. Several turbulence models will be used and the results will be compared with experimental data. Before doing the task, it is recommended to first do one of the tutorials in the User Guide (Version 2402) of STAR-CCM+. The tutorial which is similar to this task is the "Steady Flow: Backward Facing Step".

You can do the assignment on your own or in a group of two. It is recommended (but not required) that you use \LaTeX (an example of how to write in \LaTeX is available on the course [www](#) page). You find \LaTeX [here](#). You can also use \LaTeX [on-line](#).

AH.1 Backward Facing Step Tutorial (Optional)

This tutorial is a good bridge before doing different cases. Here are some steps to access the tutorial:

1. Open a terminal window. In the terminal window, type starccm+
2. To start a new simulation, click **File** → **New**
3. Tick the Power-On-Demand box and fill the license box with the POD Key.
4. Download the tutorial instruction and data from the course homepage

AH.2 2D Hill Flow

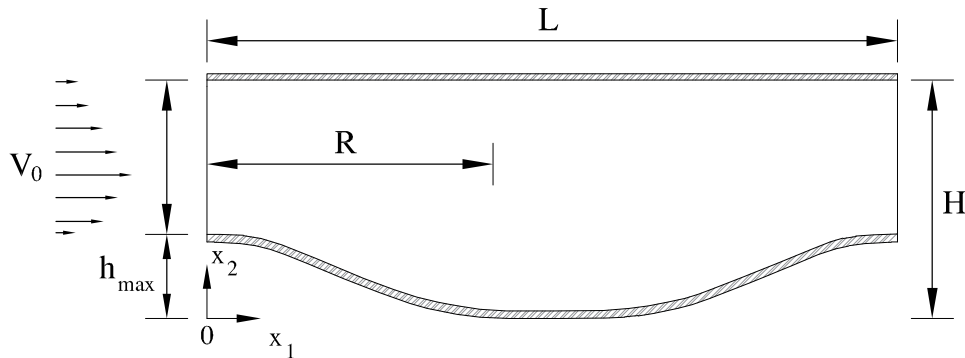


Figure AH.1: flow over two consecutive hills

In this case, a two-dimensional, steady and incompressible flow over two consecutive hills mounted on the bottom of the channel will be studied. The height of the channel is $H = 151.75 \text{ mm}$. The maximum height and length of each hill are $h_{max} = 50 \text{ mm}$ and $R = 192.8 \text{ mm}$, respectively. The space between each of the consecutive hills is $9.0h_{max}$. The fluid is water of 20° Celsius and the Reynolds number ($Re = 37000$) is based on the mean centerline velocity at inlet and the inlet channel height. The inlet boundary condition (left boundary) is imposed as the velocity profile of the

fully-developed channel flow in the absence of the hills. The case is built based on the paper [201]. Please read this paper.

AH.3 Steady Flow: 2D Hill Flow Tutorial

1. Start the STAR-CCM+
 - Open a terminal window → type `starccm+`
2. Create a new simulation
 - Click the new simulation icon (left icon of the system toolbar) → tick the Power-On-Demand (POD) box.
 - In the **Process Options** section, choose **Serial** (default option) mode. DO NOT change it to any other options.
 - Fill the POD box with the POD Key and then press OK button.
3. Importing the Geometry and Mesh
 - Select **File** → **Import** → **Import Volume Mesh** from the menu bar.
 - In the *Open* window, navigate to the stored location and select the file *2dHill.ccm*
 - Click the **Open** button to import the mesh file.
 - Save the new simulation as *2dHill.sim*
4. Visualizing the Imported Mesh
 - Right-click the node **Scenes** in the explorer pane (to the left) and then select **New Scene** → **Mesh**. The mesh can be seen in a scene in the graphics window.
 - The edges of the square are boundaries. By clicking on each edge in the graphics window, a label with its name appears on the graphics window. The node corresponding to the selected edge (boundary) is also highlighted in the explorer pane, **Regions** → **Fluid** → **Boundaries**.
5. Setting Up the Physics Models
 - Expand the node **Continua**.
 - Edit the default continuum (**Physics 1**) including appropriate physical models for the simulation. Right-click the node **Physics 1** and then in the new window, click **Select models**:
 - In the left-bottom of the window **Physics 1 Model Selection**, untick the Auto-select recommended models. Choose the required models as:
 - Time box: Steady
 - Material box: Liquid
 - Flow box: Segregated flow
 - Equation of State box: Constant Density
 - Viscous Regime box: Turbulent
 - Turbulence box: Reynolds-Averaged Navier-Stokes*

- Reynolds-Averaged Turbulence box: K-Epsilon Turbulence model
- K-Epsilon Turbulence Models box: Standard K-Epsilon Low-Re
- Choose desired sub-model(s) for the selected turbulence model in the K-Epsilon Damped Low Re Wall Treatment box: Low y+ Wall Treatment
- Close the window **Physics 1 Model Selection**
- Turning the color of the node **Physics 1**, from gray to blue, indicates that sufficient models have been activated.
- Expand the node **Physics 1**, go to **Initial Conditions** → **Turbulence Specification**.
- In the properties window, set the *Method* to be the same as the selected turbulence model (K-Epsilon).
- Save the simulation.

6. Setting Fluid Properties

- Go to the node **Continua** → **Physics 1** → **Models** → **Liquid** → **Water** → **Material Properties** → **Density** → **Constant** → *Value* = 998.29 kg/m^3 .
- Go to the node **Continua** → **Physics 1** → **Models** → **Liquid** → **Water** → **Material Properties** → **Dynamic Viscosity** → **Constant** → *Value* = $0.001003 \text{ Pa} \cdot \text{s}$.

7. Importing Inlet and Measurement Data

- Go to the node **Tools** → **Tables**.
- Right click on **Tables** and select **New Table** → **File Table**.
- In the *Open* window, navigate to the stored location and select all *.xy files.
- Click the **Open** button to import all data.

8. Setting Boundary Conditions and Values

- Expand the node **Regions** and go to **Fluid** → **Boundaries**.
- Inlet
 - Click on the node **Inlet**. In the properties window, change the *Type* from *Wall* to *Velocity Inlet*.
 - Expand the node **Inlet** and go to **Physics Conditions** → **Turbulence Specification**.
 - In the properties window, set the *Method* to be the same as the selected turbulence model, e.g. K+Epsilon.
 - Under the node **Inlet**, go to **Physics Conditions** → **Velocity Specification**.
 - In the properties window, set the *Method* to be *Components*.
 - In case of choosing K+Epsilon turbulence model, in the node **Inlet**, go to **Physics Values** and select **Turbulent Dissipation Rate**.
 - In the properties window, set the *Method* to be *Table (x, y, z)*.
 - **Table(x,y,z)** is created under **Turbulent Dissipation Rate**.

- Click on **Table(x,y,z)**. In the properties window, set the *Table* to be `inletProfile` and *Table:Data* to be `Epsilon`.
- In the node **Inlet**, go to **Physics Values** and select **Turbulent Kinetic Energy**.
- In the properties window, set the *Method* to be `Table(x, y, z)`.
- **Table(x,y,z)** is created under **Turbulent Kinetic Energy**.
- Click on **Table(x,y,z)**. In the properties window, set the *Table* to be `inletProfile.xy` and *Table:Data* to be `K`.
- In the node **Inlet**, go to **Physics Values** and select **Velocity**.
- In the properties window, set the *Method* to be `Table(x, y, z)`.
- **Table(x,y,z)** is created under **Velocity**.
- Click on **Table(x,y,z)**. In the properties window, set the *Table* to be `inletProfile.xy`. Similarly, set *Table: X-Data*, *Table: Y-Data* and *Table: Z-Data* to be `U`, `V` and `W`, respectively.
- **Outlet**
 - Click on the node **Outlet**. In the properties window, change the *Type* from `Wall` to `Pressure Outlet`.
- Save the simulation.

9. Setting the Solver Parameters and Stopping Criteria

- **Solvers**
 - Expand the node **Solvers** and keep the default settings.
 - To Extract more variables from the simulation (e.g., Kolmogorov Length Scale), expand the node related to the selected turbulence model (e.g., K-Epsilon Turbulence).
 - In the properties window, tick *Temporary Storage Retained*.
 - By enabling *Temporary Storage Retained*, additional scalar, vector and tensor variables are appeared in the node **Tools** → **Field Functions**.
- **Stopping Criteria**
 - Expand the node **Stopping Criteria** and select **Maximum Steps**.
 - In the properties window, set *Maximum Steps* to 2000.
 - Again, go to the node **Solvers** → **Steady** → **Stopping Criteria**, create **Maximum Steps** by clicking right. Check that in the properties window, the value of **Maximum Steps** must be greater than or equal to the value of **Maximum Steps** in the node **Stopping Criteria**.
 - Change *Logical Rule* to `And` in the Stopping Criteria Maximum Steps.
 - A new stopping criterion should also be created as:
 - (a) Right click on the node **Stopping Criteria** and select **New Monitor Criterion**.
 - (b) In the Select Monitor window, Choose your interested Monitor(s) (e.g., X-Momentum) and press the **OK** button. A new sub-node, **X-Momentum Criterion** is created.
 - (c) Go to **X-Momentum Criterion**. In the properties window, set *Criterion Option* to `Minimum` and change *Logical Rule* to `And`.

- (d) Go to **X-Momentum Criterion** → **Minimum Limit**. In the properties window, set *Minimum Value* equal to $1 \cdot 0\text{E}-4$.

10. Initializing and Running the Simulation

- Go to the menu bar and click **Solution** → **Initialize Solution**. Generally, you may specify initial conditions through the node **Continua** → **Physics 1** → **Initial Conditions**. (Disregard eventual warnings on turbulent viscosity.)
- Again, go to the menu bar and click **Solution** → **Run** to execute the simulation.
- After running, the Residuals plot is shown automatically in the graphics Window.
- You may stop the simulation process (before the stopping criteria are satisfied) by clicking **Solution** → **Stop Iterating** in the menu bar. By clicking **Solution** → **Run**, the simulation will be run again.
- If all the previous steps were correct, the simulation should stop after about 4500 iterations.

11. Visualizing the Solution. This is optional. You can do all plotting in Python or Matlab/Octave (see Item 14)

- Right click on the node **Scenes**, and select **New Scene** → **Scalar**.
- A new sub-node **Scalar Scene 1** is created under the node **Scenes**.
- Expand **Scalar Scene 1** and go to **Displayers** → **Scalar 1**.
- Expand the sub-node **Scalar 1** and then click **Scalar Field**.
- In the properties window in front of *Function*, click <Select Function> to open Scalar Field-Function window.
- Scroll down, expand the node *Velocity* and select *Magnitude*.

12. Creating Parts (Plane, Line or Probe) to Extract Simulation Data

- Right click on the node **Derived Parts** and select **New Part** → **Probe** → **Line**.
- In Create Line Probe window, set the parameters as:

Property	Value
Input Parts	[Fluid]
Point 1	[0.10, 0.0, 0.0]
Point 2	[0.10, 0.16, 0.0]
Resolution	200
Display	No Displayer

- Click on **Create** button and then **Close**.
- In the node **Derived Parts**, a new sub-node, **Line Probe** is created.
- Right-click on **Line Probe** and rename it to $x/h=2$.
- $x/h=a$ means the streamwise station at $x=h_{max} \cdot a$ ($h_{max}=50$ mm). For instance, $x/h=2$ indicates the streamwise station at $x=2 \cdot 50 \text{ mm}=0.1 \text{ m}$ (See the *Point 1* and *Point 2* in the above table).

- Do the same procedure for other streamwise stations (same as the measurement locations), i.e. $xh1.xy$, $xh2.xy$, ... and $xh8.xy$.

13. Plotting Simulation Data.

- Right-click on the node **Plot** and select **New Plot** → **XY Plot**.
- In the node **Plot**, a new sub-node displayed as **XY Plot 1** is created.
- Rename it to $U@x/h=2$
- Set the parameters as:

Node	Property	Value
U@x/h=2	Parts	[x/h=2]
X Type	X-Axis	Bottom Axis
	Data Type	Scalar
Scalar Function	Field Function	Velocity[i]
Y Types	Y-Axis	Left Axis
	Data Type	Direction
	Smooth Values	✓
	Value	[0, 1, 0]
	Line Style	Style
Symbol Style	Shape	○

- To add the measurement data to compare with the simulation results, go to the node **Plots** → **U@x/h=2** → **Data Series**.
- Right-click on **Data Series** and then click **Add Data**.
- In the **Add Data Providers to Plot** window, select the measurement file corresponds to the location you have chosen for the simulation. As an example, we choose **xh2**.
- A new sub-node, **xh2** is created. Click on it.
- In the properties window, set *X Column*, *X-Axis*, *Y Column* and *Y-Axis* equal to *U*, *Bottom Axis*, *y* and *Left Axis*, respectively.
- You may change line and symbol style for the measurement plot different than the ones for simulation.
- To extract the plot data as a table (in *.csv format), right-click on the node **Plot** → **U@x/h=2** and then click **Export**.
- Choose an appropriate file name and storage location, then press Save button.

14. Extracting Simulation Field Data as Table for Python/Matlab/Octave

- Go to the node **Tools** → **Tables**.
- Right click on the node **New Table**, and select **XYZ Internal Table**.
- The sub-node **XYZ Internal Table** is created under the node **Table**.
- Set the parameters as the table below.

Node	Property	Value
XYZ Internal Table	Scalars	Cell Index
		Velocity[i]
		Velocity[j]
		Pressure
		Turbulent Kinetic Energy
		Turbulent Dissipation Rate
		Turbulent Viscosity
	Parts	[Fluid]
	Data on Vertices	
	Update	
	Enabled	✓
	Auto Extract	✓
	Trigger	None

- Right-click on **XYZ Internal Table**, then click on **Extract** and **Export...**, respectively.
- Specify an appropriate file name and storage location, then press Save button.

15. Loading data in Python/Matlab/Octave

- Use Python/Matlab/Octave to read the extracted data from STAR-CCM+.
- Download the experimental data from the course homepage.
- At the course homepage, you can download a file (`pl_vect`) which reads the simulation and experimental data and plot some results.
- Change the `open('output_standard-keps-low-re.csv')` in the Python script `pl_vect.py` or in the `fileName=sprintf('*.csv')` in the Matlab/Octave script (`pl_vect.m`) according to the name of ".csv" file which you have generated from the STAR-CCM+ simulation.
- Make sure you put all files (extracted table in *.csv format from STAR-CCM+ and the measurement data in *.xy format), in the directory where you execute `pl_vect`.

Open Python or Matlab/Octave in an editor and execute `pl_vect`. There are six field variables, \bar{v}_1 , \bar{v}_2 , p , k , ϵ , and ν_t ; the corresponding Python/Matlab/Octave arrays are `v1_2d`, `v2_2d`, `p_2d`, `k_2d`, `e_2d` and `mut_2d`, respectively. The grid is 200×202 , i.e. $ni = 200$ cells in the x_1 direction and $nj = 202$ cells in the x_2 direction. The field variables are stored at the center of these cells. We denote the first index as i and the second index as j , i.e. `v1_2d(i, j)`.

Hence in Python

```
v1_2d[:, 0] are the  $\bar{v}_1$  values at the lower wall;
v1_2d[:, nj-1] or v1_2d[:, -1] are the  $\bar{v}_1$  values at the upper wall;
v1_2d[0, :] are the  $\bar{v}_1$  values at the inlet;
v1_2d[ni-1, :] or v1_2d[-1, :] are the  $\bar{v}_1$  values at the outlet;
```

and in Matlab/Octave

```
v1_2d(:, 1) are the  $\bar{v}_1$  values at the lower wall;
v1_2d(:, nj) are the  $\bar{v}_1$  values at the upper wall;
v1_2d(1, :) are the  $\bar{v}_1$  values at the inlet;
v1_2d(ni, :) are the  $\bar{v}_1$  values at the outlet;
```

AH.3.1 Pressure

Execute the `pl_vect` file with Python/Matlab/Octave. It plots the contours of \bar{v}_1 , the velocity vector field and the \bar{v}_1 profile along x_2 at $x_1 = 1$ comparing with experiments. As you can see, there is a large recirculation region where the flow goes backwards.

- Plot a contour plot of the pressure. Where is it high and low and why? (think of the Bernoulli equation, see Eq. 4.35)

The Bernoulli equation describes one-dimensional flow (inviscid, without friction). Let's compare the pressure from STAR-CCM+ and the Bernoulli equation. Since the 2D hill geometry is horizontal, then the gravity term does not contribute in the Bernoulli equation. Then you must make the velocity from STAR-CCM+ one-dimensional.

- Compute the bulk velocity (at each x_1 station)

$$V_b = \frac{1}{h(x_1)} \int_{x_{2,min}}^{x_{2,max}} \bar{v}_1 dx_2 \quad (\text{AH.1})$$

where $h(x_1) = x_{2,max} - x_{2,min}$ is the local height of the channel. Then compute the pressure from Bernoulli equation (Eq. 4.35). Compare it with the bulk STAR-CCM+ pressure computed similar to the bulk velocity in Eq. AH.1. Compare the pressure drop from inlet to outlet for STAR-CCM+ and the Bernoulli equation. Why do they differ? How large is the pressure drop from the Bernoulli equation? How large should it be?

hint: the domain is symmetric in the x_1 direction.

How large is the pressure drop in terms of dynamic pressure, i.e. $\rho V_{b,inlet}^2/2$? How large is it compared to [pipe flow](#) pressure drop? In [pipe flow](#), you may compute the friction factor (f_D) either from **Turbulent regime/Smooth-pipe regime** equation or from Figure 2. Then you can compute the pressure drop (Δp) from the first equation (Darcy-Weisbach equation) in [pipe flow](#).

The pressure drop is usually an important engineering quantity. A large pressure drop means a large, expensive pump. You have used the AKN K-Epsilon turbulence model. How dependent are your results on the choice of turbulence model?

- Try some other turbulence models. Does the flow change a lot? And, more important, how much does the pressure drop change? This part is **optional**.

AH.3.2 Skinfriction

The skinfriction, C_f , is an important concept in fluid dynamics. It is a non-dimensional wall shear stress which is defined as

$$C_f = \frac{\tau_w}{0.5\rho V_b^2} \quad (\text{AH.2})$$

where V_b is the bulk velocity (which is the same at all x_1 planes due to continuity). The bulk velocity at any x_1 plane is defined in Eq. AH.1. The wall shear stress is defined in Eq. 6.16.

- We must first extract data for the bottom wall

- Go to the node **Tools** → **Tables**.
- Right-click on the node **New Table**, and select **XYZ Internal Table**.
- The sub-node **XYZ Internal Table** is created under the node **Table**.
- Set the parameters as the table below.

Node	Property	Value
XYZ Internal Table	Scalars	Ustar
		Wall Y+
		Wall Shear Stress Magnitude
	Parts	[Fluid Bottom]
	Data on Vertices	
Update	Enabled	✓
	Auto Extract	✓
	Trigger	None

- Right-click on **XYZ Internal Table**, then click on **Extract** and **Export...**, respectively.
- Specify an appropriate file name and storage location, then press Save button.

Now create another **XYZ Internal Table** table for the top wall.

- First, load the two exported files from STAR-CCM+ (bottom and top wall). Then plot the skinfriction along the top and bottom walls.

AH.3.3 Vorticity

In the first assignment you computed the vorticity in laminar flow. Now you will do it for turbulent flow. The velocity gradients are computed in `pl_vect` using the function `dphidx_dy`.

- Compute $\bar{\omega}_3$, see Eq. 1.12. Where is it largest? (cf. Fig 8.4). In the first assignment we could identify a region of inviscid flow (no vorticity). What about this case?

AH.3.4 Turbulent viscosity

You have computed a turbulent flow with a turbulence model. We have said that the turbulent viscosity is much larger than the viscous one.

- Plot the ratio μ_t/μ as a contour plot. What is the maximum turbulent viscosity? Where?
- When you use another turbulence model, does the maximum value change? This part is **optional**.
- Plot μ_t/μ versus x_2 also as x-y graphs at a couple of x_1 stations. Plot μ_t/μ also versus $x_2^+ = u_\tau x_2/\nu$ for the bottom wall (you have exported u_τ (Ustar) at the bottom wall in Section AH.3.2). Please note that in $x_2^+ = u_\tau x_2/\nu$, x_2 is the wall distance. Zoom also in near the wall. Does the turbulent viscosity go to zero at the wall as it should?

AH.3.5 Diffusion

You have computed a turbulent flow with a turbulence model. You have learnt – hopefully – that the turbulent diffusion in channel flow is much larger than the usual physical (viscous) diffusion (except very close to the wall), see Fig. 6.6. Channel flow is essentially two attached boundary layer whereas the hill flow includes recirculation regions.

- Compute the viscous and turbulent diffusion terms in the \bar{v}_1 equation (see the expression for both viscous and turbulent diffusions in Eq. 11.31). Plot them in x-y graphs at a couple of x_1 stations (choose one x_1 station at the top of a hill). Plot them also versus x_2^+ for the bottom wall. Compare with Fig. 6.6. Do you see the same behaviour as in in channel flow?

Hint: Use the function `dphidx_dy` when computing the derivative of $\partial \bar{v}_1 / \partial x_2$ and $\mu_t \partial \bar{v}_1 / \partial x_2$.

AH.3.6 Production

The production term, P^k , in the k equation is usually a large term (see Figs. 8.3 and 11.6). When a source is large, it usually also means that the variable in question is large (see Section 9.1), i.e. when P^k is large so is k . If this is not the case, it means simply that other terms are larger. Now let's see how strong the relation between k and P^k is.

- Plot k and P^k as contour plots. (The k exists in the *csv* file extracted from your STAR-CCM+ simulation. You only need to compute P^k according to Eq. 11.39). Is there any strong relation?

The turbulent viscosity is computed as $\mu_t = \rho C_\mu k^2 / \varepsilon$. There is a fair chance that μ_t is large where P^k is large.

- Plot μ_t as a contour plot. Is there any strong relation between μ_t and P^k ?

AH.3.7 Wall boundary conditions for ε

The wall boundary conditions for ε are discussed in Section 11.14.5. The boundary condition for the turbulent kinetic energy is simply $k = 0$. The boundary condition for ε is given by Eq. 11.166 which means that ε is set to that value at the wall-adjacent cells. Please note that x_2 in Eq. 11.166 is the wall distance and k is the value at the wall-adjacent cells.

- Compare ε from STAR-CCM+ at the wall-adjacent cells with Eq. 11.166 (both upper and lower wall). Do they agree?

AH.3.8 Near-wall behaviour of f_μ

In Section 11.14.3 we show that the f_μ damping function near the wall actually must be an augmentation function, see Eq. 11.155. The f_μ damping function in the AKN model reads (see Eq. 1798 in Section *Damping Functions* in the STAR-CCM+ User guide)

$$f_\mu = \left[1 - \exp\left(-\frac{x_2^*}{14}\right) \right]^2 \left\{ 1 + \frac{5}{R_t^{3/4}} \exp\left[-\left(\frac{R_t}{200}\right)^2\right] \right\} \quad (\text{AH.3})$$

where $R_t = k^2/(\nu\varepsilon)$ and $x_2^* = (\varepsilon\nu)^{1/4}x_2/\nu$. Show mathematically that $f_\mu = \mathcal{O}(x_2^{-1})$.

Hint: Taylor expansion gives $1 - \exp(-x) = x - x^2 \dots$

AH.3.9 Compare with experiments

The measurement data at seven x_1 locations can be download from the course home-page. Each file consists of seven columns that are x_2 , \bar{v}_1 , \bar{v}_2 , $\overline{v_1'^2}$, $\overline{v_2'^2}$, $\overline{v_1'v_2'}$ and x_3 , respectively. Since it is a 2D case, the x_3 values are zero. The predicted \bar{v}_1 velocity is compared with experiments at $x_1 = h_{max}$ (*xh1.xy*) in `pl_vect`.

- ▶ Compare \bar{v}_1 with experiment and the other six locations.

The agreement between predictions and experiments is not good. The main reason is that you are simulating the flow over only one hill. The inlet boundary conditions are taken from another CFD simulation of an infinite long channel (periodic boundary conditions were used).

In the experiments they use ten hills. The object is to achieve a periodic flow where the time-averaged flow is identical between two hills. In the CFD simulations one can then use *periodic* boundary conditions.

- ▶ Change the boundary conditions at the inlet and outlet boundaries to *periodic* boundary conditions. Compare the \bar{v}_1 velocities with experiments. This part is **optional**.
- Change **Inlet-Outlet** boundary conditions to **Periodic** boundary conditions
 - Expand **Regions/Fluid/Boundaries**
 - Press Ctrl key and choose **Inlet** and **Outlet**. Right-click and select **Create Interface**
 - You have now created an interface and need to change type and topology
 - Expand **Interface**
 - Right-click on **Interface 1** and select **Edit**
 - Change **Type** to **Fully-Developed Interface**
 - Change **Topology** to **Periodic**
 - Expand **Interface 1/Physics Condition** and click on **Fully Developed Condition** and select **Mass Flow Rate**
 - Expand **Interface 1/Physics Values** and click on **Mass Flow Rate** and set an appropriate value. To get the mass flow rate you can integrate the inlet velocity profile in `pl_vect`.

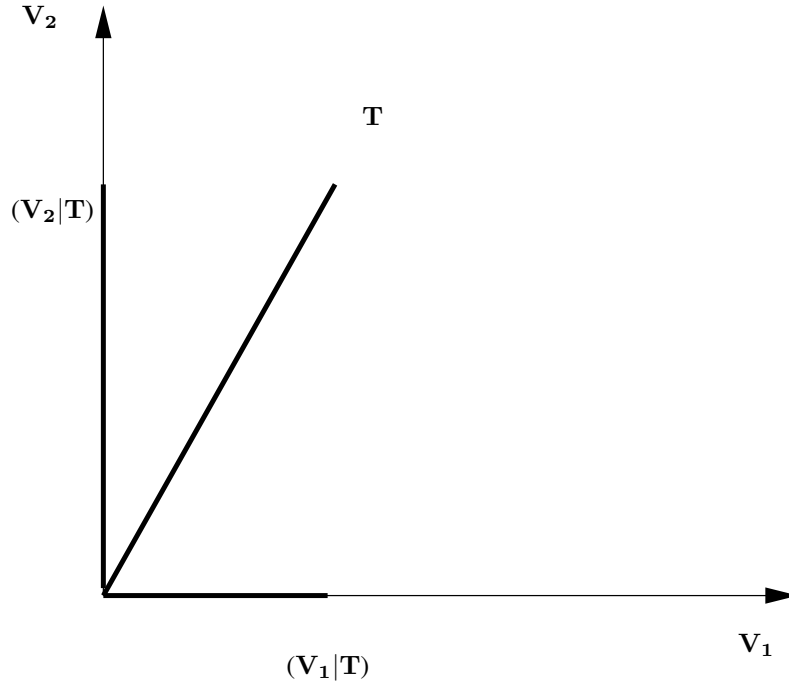


Figure AI.1: Scalar product.

AI TME226: Fourier series

HERE a brief introduction to Fourier series extracted from [202] is given.

AI.1 Orthogonal functions

Consider three vectors, \mathbf{V}_1 , \mathbf{V}_2 , \mathbf{V}_3 , in physical space which form an orthogonal base in \mathbf{R}^3 (i.e. their scalar products are zero). Let us call them *basis functions*. Any vector, \mathbf{T} , in \mathbf{R}^3 can now be expressed in these three vectors, i.e.

$$\mathbf{T} = c_1 \mathbf{V}_1 + c_2 \mathbf{V}_2 + c_3 \mathbf{V}_3 \quad (\text{AI.1})$$

see Fig. AI.1. Now define the scalar product of two vectors, \mathbf{a} and \mathbf{b} , as $\mathbf{a} \cdot \mathbf{b} = (\mathbf{a}|\mathbf{b})$. The coordinates, c_i , can be determined by making a scalar product of Eq. AI.1 and \mathbf{V}_i which gives

$$\begin{aligned} (\mathbf{T}|\mathbf{V}_i) &= (c_1 \mathbf{V}_1|\mathbf{V}_i) + (c_2 \mathbf{V}_2|\mathbf{V}_i) + (c_3 \mathbf{V}_3|\mathbf{V}_i) \\ &= (c_1 \mathbf{V}_1|\mathbf{V}_1) + (c_2 \mathbf{V}_2|\mathbf{V}_2) + (c_3 \mathbf{V}_3|\mathbf{V}_3) \\ &= c_1 |\mathbf{V}_1|^2 + c_2 |\mathbf{V}_2|^2 + c_3 |\mathbf{V}_3|^2 = c_i |\mathbf{V}_i|^2 \end{aligned} \quad (\text{AI.2})$$

where $|\mathbf{V}_i|$ denotes the length of \mathbf{V}_i ; the second line follows because of the orthogonality of \mathbf{V}_i . Hence the coordinates, c_i , are determined by

$$c_i = (\mathbf{T}|\mathbf{V}_i) / |\mathbf{V}_i|^2 \quad (\text{AI.3})$$

Now let us define an infinite (∞ -dimensional) functional space, \mathbf{B} , with orthogonal basis functions $\{g\}_1^\infty$. The “scalar product” of two functions, f and g_n , is defined as

$$(f|g_n) = \int_a^b f(x)g_n(x)dx \quad (\text{AI.4})$$

Then, in a similar way to Eq. AI.1, any function can, over the interval $[a, b]$, be expressed as

$$f = \sum_{n=1}^{\infty} c_n g_n \quad (\text{AI.5})$$

As above, we must now find the “coordinates”, c_n (cf. the coordinates, c_i , in Eq. AI.1). Multiply, as in Eq. AI.2, f with the basis functions, g_i , i.e.

$$(f|g_i) = \sum_{n=1}^{\infty} c_n (g_n|g_i) \quad (\text{AI.6})$$

Since we know that all g_n are orthogonal, Eq. AI.6 is non-zero only if $i = n$, i.e.

$$\begin{aligned} (f|g_i) &= (c_1 g_1|g_i) + (c_2 g_2|g_i) \dots c_i (g_i|g_i) \dots c_{i+1} (g_{i+1}|g_i) \dots = \\ &= c_i (g_i|g_i) = c_i \|g_i\|^2 \end{aligned} \quad (\text{AI.7})$$

Similar to Eq. AI.3, the “coordinates” can be found from (switch from index i to n)

$$c_n = (f|g_n) / \|g_n\|^2 \quad (\text{AI.8})$$

The “coordinates”, c_n , are called the *Fourier* coefficients to f in system $\{g\}_1^\infty$ and $\|g_n\|$ is the “length” of g_n (cf. $|\mathbf{V}_i|$ which is the length of \mathbf{V}_i in Eq. AI.3), i.e.

$$\|g_n\| = (g_n|g_n)^{1/2} = \left(\int_a^b g_n(x)g_n(x)dx \right)^{1/2} \quad (\text{AI.9})$$

Let us now summarize and compare the basis functions in physical space and the basis functions in functional space.

- | | |
|---|--|
| 1. Any vector in \mathbf{R}^3 can be expressed in the orthogonal basis vectors \mathbf{V}_i | 1. Any function in $[a, b]$ can be expressed in the orthogonal basis functions g_n |
| 2. The length of the basis vector, \mathbf{V}_i , is $ \mathbf{V}_i $ | 2. The length of the basis function, g_n , is $\ g_n\ $ |
| 3. The coordinates of \mathbf{V}_i are computed as $c_i = (\mathbf{T} \mathbf{V}_i) / \mathbf{V}_i ^2$ | 3. The coordinates of g_n are computed as $c_n = (f g_n) / \ g_n\ ^2$ |

AI.2 Trigonometric functions

Here we choose g_n as trigonometric functions which are periodic in $[-\pi, \pi]$. The question is now how to choose the orthogonal function system $\{g\}_1^\infty$ on the interval $[-\pi, \pi]$. In mathematics, we usually start by doing an intelligent “guess”, and then we prove that it is correct. So let us “guess” that the trigonometric series

$$[1, \sin x, \cos x, \sin(2x), \dots, \sin(nx), \cos(nx), \dots] \quad (\text{AI.10})$$

is an orthogonal system. The function system in Eq. AI.10 can be defined as

$$g_n(x) = \begin{cases} \phi_k(x), & \text{for } n = 2k = 2, 4, \dots \\ \psi_k(x), & \text{for } n = 2k + 1 = 1, 3, \dots \end{cases} \quad (\text{AI.11})$$

where $\phi_k(x) = \sin(kx)$ ($k = 1, 2, \dots$) and $\psi_k(x) = \cos(kx)$ ($k = 0, 1, \dots$). Now we need to show that they are orthogonal, i.e. that the integral of the product of any two functions ϕ_k and ψ_k is zero on $\mathbf{B}[-\pi, \pi]$ and we need to compute their “length” (i.e. their norm).

Orthogonality of ψ_n and ψ_k

$$\begin{aligned} (\psi_n | \psi_k) &= \int_{-\pi}^{\pi} \cos(nx) \cos(kx) dx = \frac{1}{2} \int_{-\pi}^{\pi} [\cos((n+k)x) + \cos((n-k)x)] dx \\ &= \frac{1}{2} \left[\frac{1}{n+k} \sin((n+k)x) + \frac{1}{n-k} \sin((n-k)x) \right]_{-\pi}^{\pi} = 0 \quad \text{for } k \neq n \end{aligned} \quad (\text{AI.12})$$

AI.2.1 “Length” of ψ_k

$$\begin{aligned} (\psi_k | \psi_k) &= \|\psi_k\|^2 = \int_{-\pi}^{\pi} \cos^2(kx) dx = \left[\frac{x}{2} + \frac{1}{4k} \sin(2kx) \right]_{-\pi}^{\pi} = \pi \quad \text{for } k > 0 \\ (\psi_0 | \psi_0) &= \|\psi_0\|^2 = \int_{-\pi}^{\pi} 1 \cdot dx = 2\pi \end{aligned} \quad (\text{AI.13})$$

AI.2.2 Orthogonality of ϕ_n and ψ_k

$$\begin{aligned} (\phi_n | \psi_k) &= \int_{-\pi}^{\pi} \sin(nx) \cos(kx) dx = \frac{1}{2} \int_{-\pi}^{\pi} [\sin((n+k)x) + \sin((n-k)x)] dx \\ &= -\frac{1}{2} \left[\frac{1}{n+k} \cos((n+k)x) + \frac{1}{n-k} \cos((n-k)x) \right]_{-\pi}^{\pi} = 0 \end{aligned} \quad (\text{AI.14})$$

because $\cos((n+k)\pi) = \cos(-(n+k)\pi)$ and $\cos((n-k)\pi) = \cos(-(n-k)\pi)$.

AI.2.3 Orthogonality of ϕ_n and ϕ_k

$$\begin{aligned} (\phi_n | \phi_k) &= \int_{-\pi}^{\pi} \sin(nx) \sin(kx) dx = \frac{1}{2} \int_{-\pi}^{\pi} [\cos((n-k)x) - \cos((n+k)x)] dx \\ &= \frac{1}{2} \left[\frac{1}{n-k} \sin((n-k)x) - \frac{1}{n+k} \sin((n+k)x) \right]_{-\pi}^{\pi} = 0 \quad \text{for } k \neq n \end{aligned} \quad (\text{AI.15})$$

AI.2.4 “Length” of ϕ_k

$$(\phi_k | \phi_k) = \|\phi_k\|^2 = \int_{-\pi}^{\pi} \sin^2(kx) dx = \left[\frac{x}{2} - \frac{1}{4k} \sin(2kx) \right]_{-\pi}^{\pi} = \pi \quad \text{for } k \geq 1 \quad (\text{AI.16})$$

AI.3 Fourier series of a function

Now that we have proved that $\{g\}_1^\infty$ in Eq. AI.11 forms an orthogonal system of functions, we know that we can express any periodic function, f (with a period of 2π) in $\{g\}_1^\infty$ as

$$f(x) = c + \sum_{n=1}^{\infty} (a_n \cos(nx) + b_n \sin(nx)) \quad (\text{AI.17})$$

where x is a spatial coordinate. The Fourier coefficients are given by

$$b_n = (f|\phi_n)/\|\phi_n\|^2 = \frac{1}{\pi} \int_{-\pi}^{\pi} f(x) \sin(nx) dx \quad (\text{AI.18a})$$

$$a_n = (f|\psi_n)/\|\psi_n\|^2 = \frac{1}{\pi} \int_{-\pi}^{\pi} f(x) \cos(nx) dx \quad (\text{AI.18b})$$

$$c = (f|\psi_0)/\|\psi_0\|^2 = \frac{1}{2\pi} \int_{-\pi}^{\pi} f(x) dx \quad (\text{AI.18c})$$

where $n > 0$. If we set $c = a_0/2$, then a_0 is obtained from Eq. AI.18b, i.e.

$$f(x) = \frac{a_0}{2} + \sum_{n=1}^{\infty} (a_n \cos(nx) + b_n \sin(nx)) \quad (\text{AI.19a})$$

$$b_n = (f|\phi_n)/\|\phi_n\|^2 = \frac{1}{\pi} \int_{-\pi}^{\pi} f(x) \sin(nx) dx \quad (\text{AI.19b})$$

$$a_n = (f|\psi_n)/\|\psi_n\|^2 = \frac{1}{\pi} \int_{-\pi}^{\pi} f(x) \cos(nx) dx \quad (\text{AI.19c})$$

Note that $a_0/2$ corresponds to the average of f . Taking the average of f (i.e. integrating f from $-\pi$ to π) and dividing with the integration length, 2π , gives (see Eq. AI.19a)

$$\bar{f} = \frac{1}{2\pi} \int_{-\pi}^{\pi} f(x) dx = \frac{1}{2\pi} \frac{a_0}{2} \cdot 2\pi = \frac{a_0}{2} \quad (\text{AI.20})$$

Hence, if $\bar{f} = 0$ then $a_0 = 0$.

AI.4 Derivation of Parseval's formula

Parseval's formula reads

$$\int_{-\pi}^{\pi} (f(x))^2 dx = \frac{\pi}{2} a_0^2 + \pi \sum_{n=1}^{\infty} (a_n^2 + b_n^2) \quad (\text{AI.21})$$

We will try to prove this formula. Assume that we want to approximate the function f as well as possible with an orthogonal series

$$\sum_{n=1}^{\infty} a_n g_n \quad (\text{AI.22})$$

Now we want to prove that the Fourier coefficients are the best choice to minimize the difference

$$\|f - \sum_{n=1}^N a_n g_n\| \quad (\text{AI.23})$$

Later we will let $N \rightarrow \infty$. Using the definition of the norm and the laws of scalar product we can write

$$\begin{aligned} \|f - \sum_{n=1}^N a_n g_n\|^2 &= \left(f - \sum_{n=1}^N a_n g_n \left| f - \sum_{k=1}^N a_k g_k \right. \right) \\ &= (f|f) - \sum_{n=1}^N a_n (f|g_n) - \sum_{k=1}^N a_k (f|g_k) + \sum_{n=1}^N \sum_{k=1}^N a_n a_k (g_n|g_k) = \quad (\text{AI.24}) \\ &= (f|f) - 2 \sum_{n=1}^N a_n (f|g_n) + \sum_{n=1}^N a_n^2 (g_n|g_n) \end{aligned}$$

because of the orthogonality of the function system, $\{g\}_1^N$. Expressing f in the second term using the Fourier coefficients c_n (see Eqs. AI.5 and AI.8) gives

$$\begin{aligned} (f|f) - 2 \sum_{n=1}^N a_n c_n (g_n|g_n) + \sum_{n=1}^N a_n^2 (g_n|g_n) \\ = \|f\|^2 + \sum_{n=1}^N \|g_n\|^2 (a_n^2 - 2a_n c_n) \quad (\text{AI.25}) \\ = \|f\|^2 + \sum_{n=1}^N \|g_n\|^2 (a_n - c_n)^2 - \sum_{n=1}^N \|g_n\|^2 c_n^2 \end{aligned}$$

The left side of Eq. AI.24 is thus minimized if the coefficients a_n are chosen as the Fourier coefficients, c_n so that

$$\|f - \sum_{n=1}^N a_n g_n\|^2 = \|f\|^2 - \sum_{n=1}^N \|g_n\|^2 c_n^2 \quad (\text{AI.26})$$

The left side must always be positive and hence

$$\sum_{n=1}^N \|g_n\|^2 c_n^2 \leq \|f\|^2 = \int_{-\pi}^{\pi} (f(x))^2 dx \quad \text{for all } N \quad (\text{AI.27})$$

As N is made larger, the magnitude of the left side increases, and its magnitude gets closer and closer to that of the right side, but it will always stay smaller than $\|f\|^2$. This means that the series on the left side is *convergent*. Using the Fourier coefficients in Eq. AI.19 and letting $N \rightarrow \infty$ it can be shown that we get equality of the left and right side, which gives Parseval's formula,

$$\begin{aligned} \|f\|^2 &\equiv \int_{-\pi}^{\pi} (f(x))^2 dx = \sum_{n=1}^N \|g_n\|^2 c_n^2 = \|\psi_0\| \left(\frac{a_0^2}{2} \right) + \sum_{n=1}^N \|\psi_n\| a_n^2 + \|\phi_n\| b_n^2 \\ &= 2\pi \left(\frac{a_0^2}{2} \right) + \pi \sum_{n=1}^N a_n^2 + b_n^2 = \frac{\pi}{2} a_0^2 + \pi \sum_{n=1}^{\infty} (a_n^2 + b_n^2) \end{aligned}$$

Note that 2π and π on the second line are the “length” of $\|g_n\|$, i.e. the length of $\|\psi_0\|$, $\|\psi_n\|$ and $\|\phi_n\|$ (see Sections AI.2.1 and AI.2.4).

Appendix 46 describes in detail how to create energy spectra from two-point correlations.

AI.5 Complex Fourier series

Equation AI.19 gives the Fourier series of a real function. It is more convenient to express a Fourier series in complex variables even if the function f itself is real. On complex form it reads

$$f(x) = \sum_{n=-\infty}^{\infty} c_n \exp(\imath nx) \quad (\text{AI.28a})$$

$$c_n = \frac{1}{2\pi} \int_{-\pi}^{\pi} f(x) \exp(-\imath nx) dx \quad (\text{AI.28b})$$

where the Fourier coefficients, c_n , are complex. Below we verify that if f is real, then Eq. AI.28 is equivalent to Eq. AI.19. The Fourier coefficients, c_n , read – assuming that f is real – according to Eq. AI.28

$$c_n = \frac{1}{2\pi} \int_{-\pi}^{\pi} f(x) (\cos(nx) - \imath \sin(nx)) dx = \frac{1}{2} (a_n - \imath b_n), \quad n > 0 \quad (\text{AI.29})$$

where a_n and b_n are given by Eq. AI.19. For negative n in Eq. AI.28 we get

$$c_{-n} = c_n^* = \frac{1}{2\pi} \int_{-\pi}^{\pi} f(x) (\cos(nx) + \imath \sin(nx)) dx = \frac{1}{2} (a_n + \imath b_n), \quad n > 0 \quad (\text{AI.30})$$

where c_n^* denotes the complex conjugate. For $n = 0$, Eq. AI.28 reads

$$c_0 = \frac{1}{2\pi} \int_{-\pi}^{\pi} f(x) dx = \frac{1}{2} a_0 \quad (\text{AI.31})$$

see Eq. AI.19. Inserting Eqs. AI.29, AI.30 and AI.31 into Eq. AI.28 gives

$$\begin{aligned} f(x) &= \frac{1}{2} a_0 + \frac{1}{2} \sum_{n=1}^{\infty} (a_n - \imath b_n) \exp(\imath nx) + (a_n + \imath b_n) \exp(-\imath nx) \\ &= \frac{1}{2} a_0 + \frac{1}{2} \sum_{n=1}^{\infty} (a_n - \imath b_n) (\cos(nx) + \imath \sin(nx)) + (a_n + \imath b_n) (\cos(nx) - \imath \sin(nx)) \\ &= \frac{1}{2} a_0 + \sum_{n=1}^{\infty} a_n \cos(nx) - \imath^2 b_n \sin(nx) = \frac{1}{2} a_0 + \sum_{n=1}^{\infty} a_n \cos(nx) + b_n \sin(nx) \end{aligned} \quad (\text{AI.32})$$

which verifies that the complex Fourier series for a real function f is indeed identical to the usual formulation in Eq. AI.19 although the Fourier coefficients, c_n , are complex. One advantage of Eq. AI.28 over the formulation in Eq. AI.19 is that we don't need any special definition for the first Fourier coefficient, a_0 . The trick in the formulation in Eq. AI.28 is that the imaginary coefficients for negative and positive n cancel whereas the real coefficients add. This means that the real coefficients are multiplied by a factor two except the first coefficient, a_0 , which makes up for the factor $\frac{1}{2}$ in front of a_0 in Eq. AI.19.

AL TME226 Discussion seminars

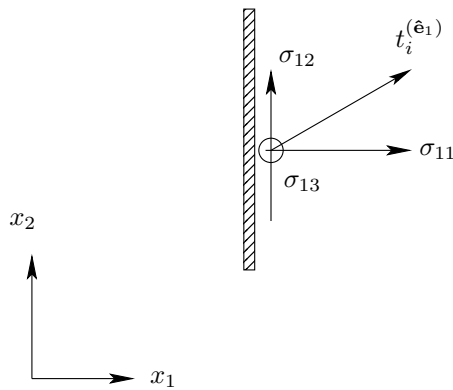
Discussion seminar 1

Course material. Recorded Lecture 1; eBook: Section 1.1, 1.2, Appendix B, Section 1.3-1.7

Lecture 1

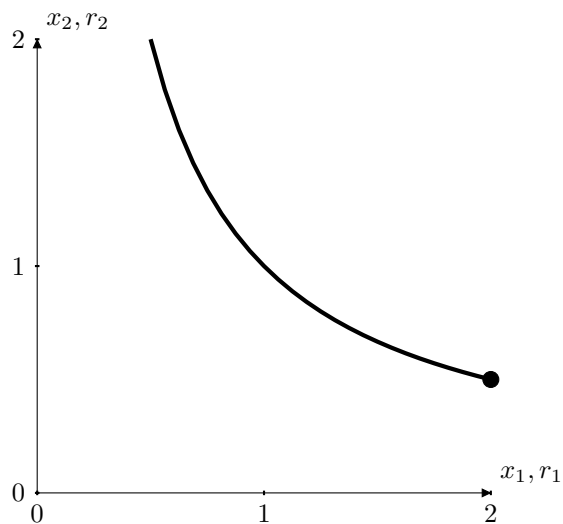
1. Show which stress components, σ_{ij} (see figure below), that act on a Cartesian surface whose normal vector is $n_i = (0, 1, 0)$. Show also the stress vector, $t_i^{\hat{n}}$.

Hint: $t_i^{(\hat{n})} = \tau_{ji}n_j$



Stress components and stress vector on a surface.

2. $\frac{\partial v_i}{\partial x_j} = \frac{1}{2} \left(\frac{\partial v_i}{\partial x_j} + \frac{\partial v_j}{\partial x_i} \right) + \frac{1}{2} \left(\frac{\partial v_i}{\partial x_j} - \frac{\partial v_j}{\partial x_i} \right) = S_{ij} + \Omega_{ij}$.
Explain the physical meaning of diagonal and off-diagonal components of S_{ij} .
3. Consider the stagnation flow in the figure below at time $t = \ln(2)$.



Flow path $x_2 = 1/x_1$. The filled circle shows the point at time $t = \ln(2)$ (Lagrangian) and at $(x_1, x_2) = (2, 1/2)$ (Eulerian). $r_1 = x_1 = \exp(t)$, $r_2 = x_2 = \exp(-t)$.

- (a) Compute the Lagrangian and Eulerian velocities at this location.
 - (b) Compute the Lagrangian and Eulerian time derivative, $\frac{dv_2^L}{dt}$
 - (c) Compute the local Eulerian time derivative, $\frac{\partial v_2^E}{\partial t}$
 - (d) Compute the vorticity and the strain-rate using the Eulerian velocities. Try to explain why the vorticity is zero by looking at Fig. 1.4.
4. What is the definition of irrotational flow?
 5. Consider 2D flow ($x_1 - x_2$ direction)
 - (a) The definition of the vorticity vector is $\omega_i = \epsilon_{ijk} \frac{\partial v_k}{\partial x_j}$. Give ω_1 , ω_2 and ω_3 .
 - (b) The definition of the strain-rate tensor is $S_{ij} = \frac{1}{2} \left(\frac{\partial v_i}{\partial x_j} + \frac{\partial v_j}{\partial x_i} \right)$. Give S_{11} and S_{12} .
 - (c) The definition of the vorticity tensor is $\Omega_{ij} = \frac{1}{2} \left(\frac{\partial v_i}{\partial x_j} - \frac{\partial v_j}{\partial x_i} \right)$. Give Ω_{11} and Ω_{12} .

Discussion seminar 2

Course material. Recorded Lectures 1 and 2; eBook: Sections 1.8, 2.1-2.4, 3.1

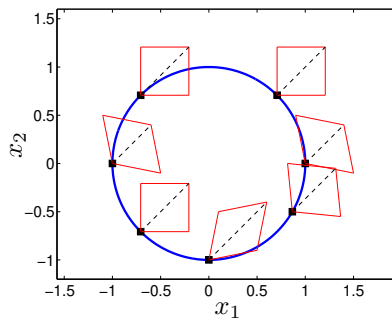
1. Explain the physical meaning of the eigenvectors and the eigenvalues of the stress tensor (see Section 1.8 and the Lecture notes of Ekh [4])
2. Explain – in words – how to show that the vorticity is zero in an ideal vortex (see Item 13vi above)

Hint:

$$v_1 = -v_\theta \frac{x_2}{(x_1^2 + x_2^2)^{1/2}}$$

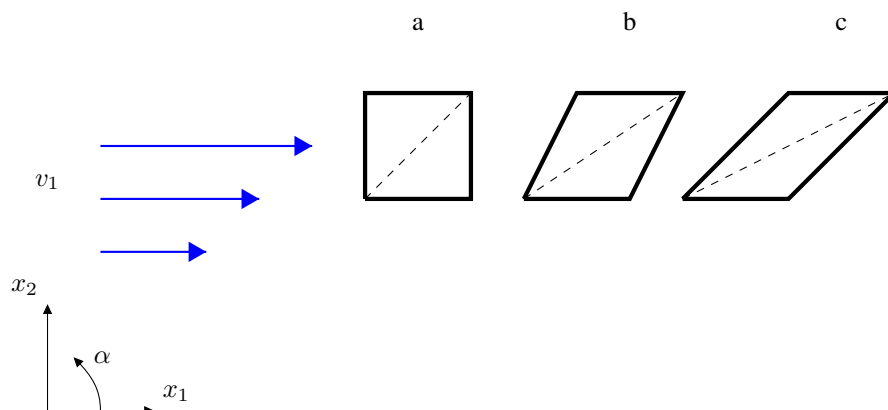
$$v_2 = v_\theta \frac{x_1}{(x_1^2 + x_2^2)^{1/2}}$$

3. Consider an ideal vortex. Discuss the difference between a vortex and vorticity.



Ideal vortex.

4. Consider the two-dimensional shear flow below (e.g. a boundary-layer flow). Compute the three vorticity components ($\omega_i = \epsilon_{ijk} \frac{\partial v_k}{\partial x_j}$).



A shear flow. A fluid particle with vorticity. $v_1 = cx_2^2$.

5. Watch the on-line lecture *Vorticity, part 1* at
http://www.tfd.chalmers.se/~lada/MoF/flow_viz.html
After 4:20 minutes, the teacher shows the figure of a boundary layer. He says that one of the “vorticity legs” is parallel to the wall and the other leg rotates in the counter-clockwise direction (positive α); hence there is vorticity.

Lecture 2

1. The Navier-Stokes equations read

$$\rho \frac{dv_i}{dt} = -\frac{\partial P}{\partial x_i} + \frac{\partial \tau_{ji}}{\partial x_j} + \rho f_i = -\frac{\partial P}{\partial x_i} + \frac{\partial}{\partial x_j} \left(2\mu S_{ij} - \frac{2}{3}\mu \frac{\partial v_k}{\partial x_k} \delta_{ij} \right) + \rho f_i$$

Describe – in words – how to simplify the Navier-Stokes equation for incompressible flow and constant viscosity (Eq. 2.9)

- (a) The transport equation for the internal energy, u , reads

$$\rho \frac{du}{dt} = -P \frac{\partial v_i}{\partial x_i} + \underbrace{2\mu S_{ij} S_{ij} - \frac{2}{3}\mu S_{kk} S_{ii}}_{\Phi} + \frac{\partial}{\partial x_i} \left(k \frac{\partial T}{\partial x_i} \right)$$

What is the physical meaning of the different terms? Simplify the transport equation for internal energy, u , to the case when the flow is incompressible (Eq. 2.18).

- (b) The basic form (without inserting the constitution law) of the transport equation for the kinetic energy, $k = v_i v_i / 2$, reads

$$\rho \frac{dk}{dt} = \frac{\partial v_i \sigma_{ji}}{\partial x_j} - \sigma_{ji} \frac{\partial v_i}{\partial x_j} + \rho v_i f_i \quad (\text{AL.1})$$

Describe (in words) how to derive the transport equation above. What is the physical meaning of the different terms?

- (c) The basic form (without inserting the constitution laws) of the transport equation for internal energy, u , reads

$$\rho \frac{du}{dt} = \sigma_{ji} \frac{\partial v_i}{\partial x_j} - \frac{\partial q_i}{\partial x_i} \quad (\text{AL.2})$$

Explain the energy transfer between kinetic energy, k , and internal energy, u (Eqs. AL.1 and AL.2).

2. The left side of the temperature equation and the Navier-Stokes, for example, can be written in three different ways

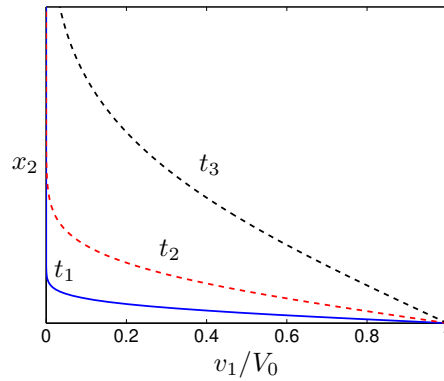
$$\begin{aligned} \rho \frac{dv_i}{dt} &= \underbrace{\rho \frac{\partial v_i}{\partial t} + \rho v_j \frac{\partial v_i}{\partial x_j}}_{(a)} = \underbrace{\frac{\partial \rho v_i}{\partial t} + \frac{\partial \rho v_j v_i}{\partial x_j}}_{(b)} \\ \rho \frac{dT}{dt} &= \underbrace{\rho \frac{\partial T}{\partial t} + \rho v_j \frac{\partial T}{\partial x_j}}_{(a)} = \underbrace{\frac{\partial \rho T}{\partial t} + \frac{\partial \rho v_j T}{\partial x_j}}_{(b)} \end{aligned}$$

Explain how the expressions (a) and (b) are obtained.

3. Consider the Rayleigh problem below



The plate moves to the right with speed V_0 for $t > 0$.



The v_1 velocity at three different times. $t_3 > t_2 > t_1$.

- (a) How is the Navier-Stokes equation

$$\frac{\partial v_i}{\partial x_i} = 0$$

$$\rho \frac{dv_i}{dt} \equiv \rho \frac{\partial v_i}{\partial t} + \rho v_j \frac{\partial v_i}{\partial x_j} = -\frac{\partial P}{\partial x_i} + \mu \frac{\partial^2 v_i}{\partial x_j \partial x_j} + \rho f_i$$

simplified for the Rayleigh problem?

- (b) What are the boundary conditions?
 (c) We introduce a similarity variable, η , related to x_2 and t as

$$\eta = \frac{x_2}{2\sqrt{\nu t}} \quad (\text{AL.3})$$

Explain how the Navier-Stokes is transformed from the independent variables x_i and t to η .

- (d) The transformed Navier-Stokes reads

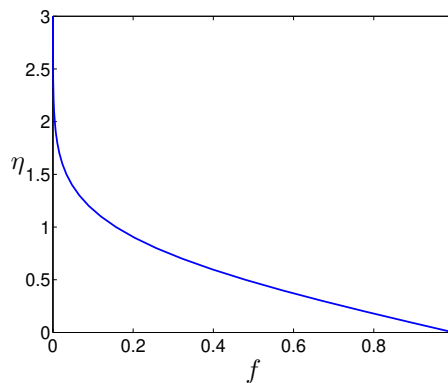
$$\frac{d^2 f}{d\eta^2} + 2\eta \frac{df}{d\eta} = 0, \quad f = \frac{v_1}{V_0} \quad (\text{AL.4})$$

What are the boundary conditions expressed in η ?

- (e) The final solution to Eq. AL.4 is

$$f(\eta) = 1 - \text{erf}(\eta)$$

Why is there only one curve in the figure below but three (or many more) in the figure above?



The velocity, $f = v_1/V_0$, given by Eq. 3.11.

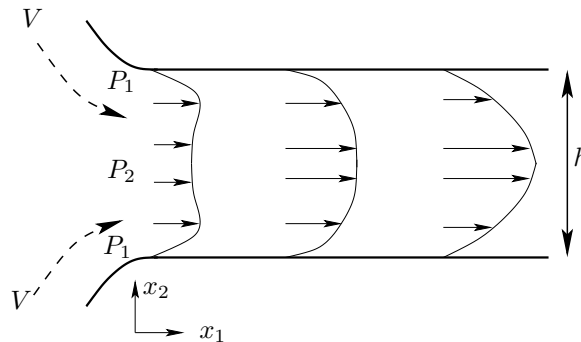
- (f) Given ν and t , show how the boundary layer thickness can be estimated from the Rayleigh problem using f and η and the figure above.

Discussion seminar 3

Course material. Recorded Lectures 3 and 4; eBook: Sections 3.2-3.3, 4.1-4.2

Lecture 3

1. Explain the pressure levels at points 1, 2 and 3 at the entrance (smooth curved walls) to a plane channel (see the figure below).

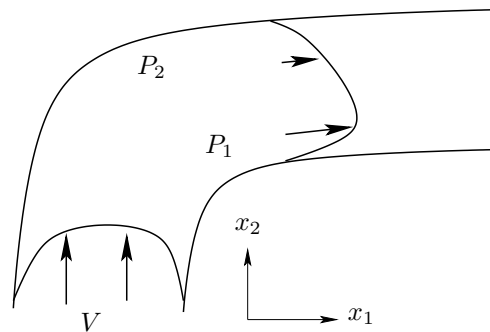


Flow in a horizontal channel. The inlet part of the channel is shown.

Explain the flow physics in a channel bend (Fig. 3.6). Watch also the on-line lecture *Pressure field and acceleration*

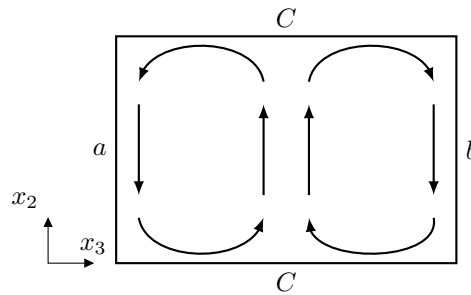
http://www.tfd.chalmers.se/~lada/MoF/flow_viz.html.

- (a) at 28 minutes into the movie the teacher discusses how the pressure varies in a fixed-body rotation flow
- (b) at 18 minutes into the movie the teacher discusses how the pressure varies for the flow in a bend.



Flow in a channel bend.

Explain the flow physics in a channel bend (see figure above) and in a duct bend (see figure below).



Secondary flow in a duct bend.

2. Consider steady, fully developed flow between two parallel plates, i.e. fully developed channel flow

- (a) What is the main flow criterion of fully developed flow between two parallel plates?
- (b) The incompressible, Navier-Stokes equation reads

$$\frac{\partial v_i}{\partial x_i} = 0$$

$$\rho \frac{dv_i}{dt} \equiv \rho \frac{\partial v_i}{\partial t} + \rho v_j \frac{\partial v_i}{\partial x_j} = -\frac{\partial P}{\partial x_i} + \mu \frac{\partial^2 v_i}{\partial x_j \partial x_j} + \rho f_i$$

- i. Simplify the v_1 equation for this flow (i.e. which terms are zero?)
 - ii. Do the same thing for the v_2
 - iii. How large is $\partial v_1 / \partial x_1$?
 - iv. How large is $\partial v_2 / \partial x_2$? Why?
3. The Blasius equation.

- (a) The stream function is defined as

$$v_1 = \frac{\partial \Psi}{\partial x_2}, \quad v_2 = -\frac{\partial \Psi}{\partial x_1}$$

Show that the continuity equation is automatically satisfied in 2D when the velocity is expressed in the streamfunction, Ψ

- (b) Explain in words how the v_1 component of the Navier-Stokes (see above) is transformed into an equation for ψ . For a flat-plate boundary layer we get the following equation

$$\frac{\partial \Psi}{\partial x_2} \frac{\partial^2 \Psi}{\partial x_1 \partial x_2} - \frac{\partial \Psi}{\partial x_1} \frac{\partial^2 \Psi}{\partial x_2^2} = \nu \frac{\partial^3 \Psi}{\partial x_2^3} \quad (\text{AL.5})$$

- (c) The final Blasius equation reads

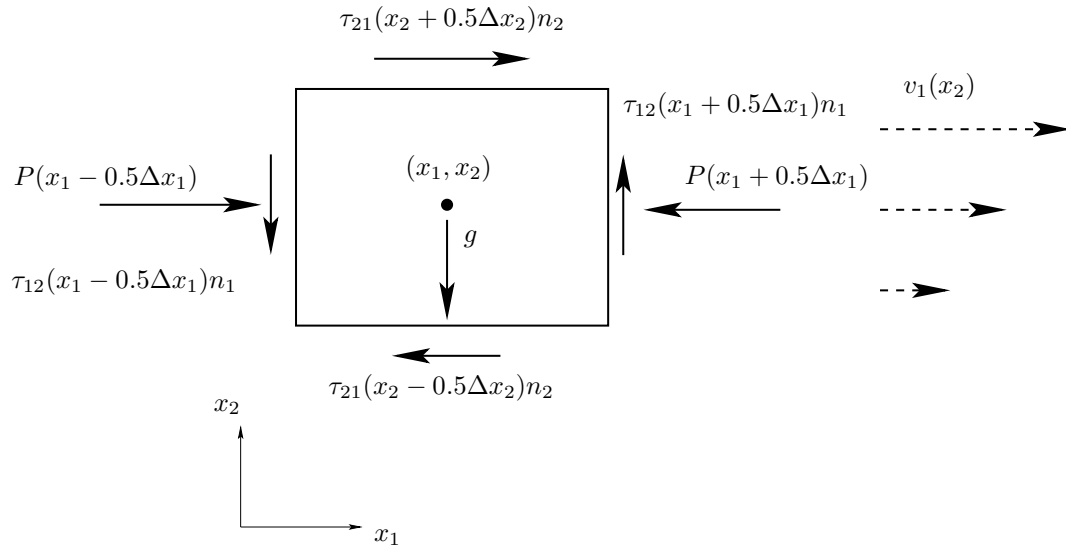
$$\frac{1}{2} g \frac{d^2 g}{d\xi^2} + \frac{d^3 g}{d\xi^3} \equiv \frac{1}{2} g g'' + g''' = 0$$

Explain why this equation is expressed in g and ξ whereas Eq. AL.5 is expressed in v_1 , x_1 and x_2 .

Hint: compare with Eq. AL.3

Lecture 4

1. Explain (using words) why vorticity can be created only by an imbalance (i.e. a gradient) of shear stresses, see the figure below. Explain why pressure and the gravity force cannot create vorticity.



Surface forces acting on a fluid particle. The fluid particle is located in the lower half of fully developed channel flow. The v_1 velocity is given by Eq. 3.28 and $v_2 = 0$. Hence $\tau_{11} = \tau_{22} = \partial\tau_{12}/\partial x_1 = 0$ and $-\partial\tau_{21}/\partial x_2 > 0$. The v_1 velocity field is indicated by dashed vectors.

1. The incompressible Navier-Stokes equation can be re-written on the form

$$\frac{\partial v_p}{\partial t} + \underbrace{\frac{\partial k}{\partial x_p}}_{\text{no rotation}} - \underbrace{\varepsilon_{pjk} v_j \omega_k}_{\text{rotation}} = -\frac{1}{\rho} \frac{\partial p}{\partial x_p} + \nu \frac{\partial^2 v_p}{\partial x_j \partial x_j} + f_p$$

- (a) Describe the first step in deriving the transport equation (3D) for the vorticity vector, Eq. 4.21

Hint: $\omega_i = \varepsilon_{pqi} \partial v_p / \partial x_q$

- (b) Which terms are zero?

Hint: the product of a symmetric tensor and a non-symmetric tensor is zero.

- (c) Show that the divergence of the vorticity vector, ω_i , is zero

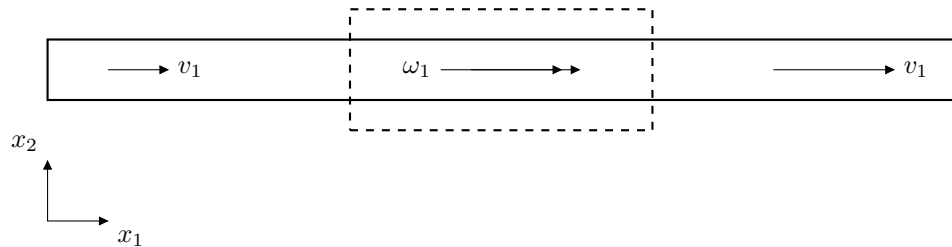
Discussion seminar 4

Course material. Recorded Lectures 4 and 5; eBook: Sections 4.2– 4.4

1. Explain vortex stretching, see figure below.

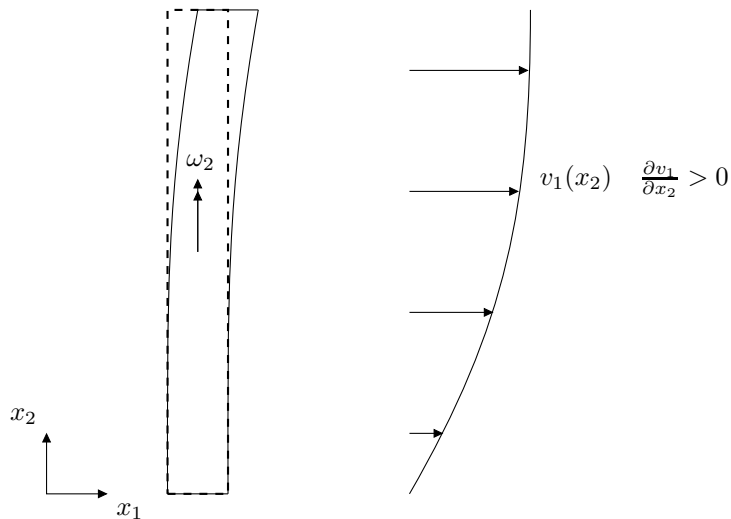
Hint: The vortex stretching/tilting terms reads

$$\omega_k \frac{\partial v_p}{\partial x_k} = \begin{cases} \omega_1 \frac{\partial v_1}{\partial x_1} + \omega_2 \frac{\partial v_1}{\partial x_2} + \omega_3 \frac{\partial v_1}{\partial x_3}, & p = 1 \\ \omega_1 \frac{\partial v_2}{\partial x_1} + \omega_2 \frac{\partial v_2}{\partial x_2} + \omega_3 \frac{\partial v_2}{\partial x_3}, & p = 2 \\ \omega_1 \frac{\partial v_3}{\partial x_1} + \omega_2 \frac{\partial v_3}{\partial x_2} + \omega_3 \frac{\partial v_3}{\partial x_3}, & p = 3 \end{cases}$$



Vortex stretching. Dashed lines denote fluid element before stretching. $\frac{\partial v_1}{\partial x_1} > 0$. Angular momentum, $r^2 \omega_1$, is constant.

2. Explain vortex tilting, see figure below.



Vortex tilting. Dashed lines denote fluid element before bending or tilting.

3. Watch the on-line lecture *Vorticity, part 2* (11 minutes into the movie) at http://www.tfd.chalmers.se/~lada/MoF/flow_viz.html It presents interesting discussions on vorticity.

4. Show that the vortex stretching/tilting term is zero in two-dimensional flow

Hint: The vortex-stretching term reads $\omega_k \partial v_p / \partial x_k = 0$.

The 3D transport equation for the vorticity vector reads

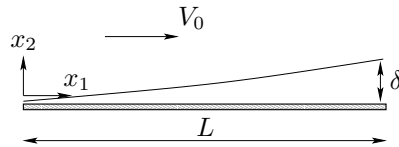
$$\frac{d\omega_p}{dt} \equiv \frac{\partial \omega_p}{\partial t} + v_k \frac{\partial \omega_p}{\partial x_k} = \omega_k \frac{\partial v_p}{\partial x_k} + \nu \frac{\partial^2 \omega_p}{\partial x_j \partial x_j}$$

Describe – in words – the form of the corresponding equation in 2D.

5. Show the similarities between the vorticity and temperature transport equations in fully developed flow between two parallel plates.

Use the diffusion of vorticity to show that $\frac{\delta}{\ell} \propto \sqrt{\frac{\nu}{U\ell}} = \sqrt{\frac{1}{Re}}$, see figure below and the expressions from the Rayleigh flow.

Hint: $\eta = 1.8 = \frac{x_2}{2\sqrt{\nu t}} \Rightarrow \delta = 3.6\sqrt{\nu t}$. Furthermore, recall that vorticity is created along the wall only near the leading edge: why?



Boundary layer. The boundary layer thickness, δ , increases for increasing streamwise distance from leading edge ($x_1 = 0$).

Lecture 5

1. Consider the derivative of the complex function $(f(z + z_0) - f(z))/z_0$ where $z = x + iy$ and $f = u + iv$. The derivative of f must be independent in which coordinate direction the derivative is taken (either along the real or the imaginary axis), i.e.

$$\frac{df}{dz} = \lim_{\Delta z \rightarrow 0} \frac{f(z_0 + \Delta z) - f(z_0)}{\Delta z}$$

$$= \lim_{\Delta x \rightarrow 0} \frac{f(x_0 + \Delta x, iy_0) - f(x_0, iy_0)}{\Delta x} = \lim_{\Delta y \rightarrow 0} \frac{f(x_0, iy_0 + i\Delta y) - f(x_0, iy_0)}{i\Delta y}.$$

The second line can be written as

$$\frac{\partial f}{\partial x} = \frac{1}{i} \frac{\partial f}{\partial y} = \frac{i}{i^2} \frac{\partial f}{\partial y} = -i \frac{\partial f}{\partial y}$$

Show that this leads to the *Cauchy-Riemann* equations

$$\frac{\partial u}{\partial x} = \frac{\partial v}{\partial y}, \quad \frac{\partial u}{\partial y} = -\frac{\partial v}{\partial x}$$

2. Explain – in words – why in potential flow both the velocity potential

$$v_1 = \partial\Phi/\partial x_1, v_2 = \partial\Phi/\partial x_2$$

and the stream function

$$v_1 = \partial\Psi/\partial x_2, v_2 = -\partial\Psi/\partial x_1$$

satisfy the Laplace equation.

3. Introduction: above, we formulated the complex function in a generic way, $f = u + iv$. Now we move to fluid mechanics.
 - (a) We formulate a “fluid mechanics” complex function $f = \Phi + i\Psi$ which is a potential function since both the real and imaginary part satisfy the Laplace equation.
 - (b) We guess a complex function $f = C_1 z^n$, $z = x + iy$
 - (c) It turns out that it is sometimes more convenient to express f in polar coordinates, i.e. $f = C_1 r e^{i\theta} = C_1 r^n (\cos(n\theta) + i \sin(n\theta))$
 - (d) Describe – in words – how to prove that $f = C_1 z^n$ satisfy the Laplace equation.
How are the velocity components for $n = 1$ and $n = 2$ obtained. What physical flow do these two cases correspond to?
4. Describe how to derive the polar velocity components for the complex potential $f = -i\Gamma \ln z / (2\pi)$ (Γ denotes circulation).
Tip: express z in polar coordinates (Euler form), i.e. $z = r e^{i\theta}$
How do you show that the complex potential satisfy the Laplace equation? What does the physical flow look like?

Discussion seminar 5

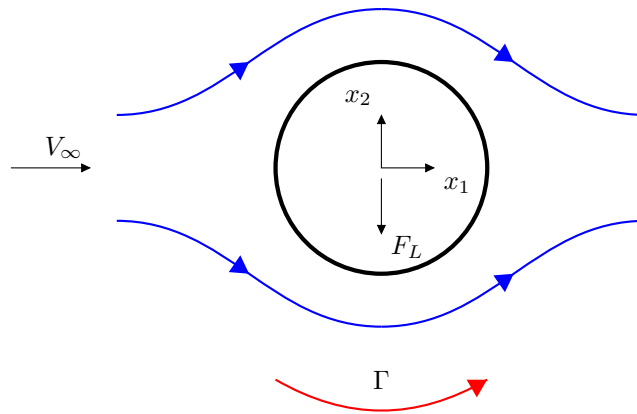
Course material. Recorded Lectures 5 and 6; eBook: Section 4.4, 5.1–5.3, 6.1

1. Consider the potential flow around a cylinder.

$$\begin{aligned} f &= \frac{V_\infty r_0^2}{r e^{i\theta}} + V_\infty r e^{i\theta} = V_\infty \left(\frac{r_0^2}{r} e^{-i\theta} + r e^{i\theta} \right) \\ &= V_\infty \left(\frac{r_0^2}{r} (\cos \theta - i \sin \theta) + r (\cos \theta + i \sin \theta) \right) \end{aligned}$$

It is a super-position of two “elementary” flow cases: which ones? Describe – in words – how to show that the radial velocity is zero at the surface. How can you get the surface pressure? Describe how you would then get the drag and lift. How large do you expect drag and lift to be? Why?

2. Consider the potential flow around a rotating cylinder.

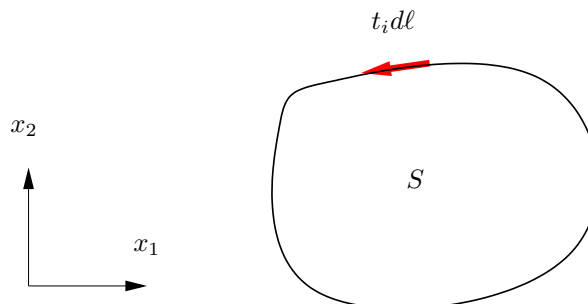


$$\begin{aligned} f &= \frac{V_\infty r_0^2}{z} + V_\infty z - i \frac{\Gamma}{2\pi} \ln z \\ &= V_\infty \left(\frac{r_0^2}{r} (\cos \theta - i \sin \theta) + r (\cos \theta + i \sin \theta) \right) - \frac{\Gamma}{2\pi} (i \ln r - \theta) \end{aligned}$$

in polar coordinates

The circulation is defined as

$$\Gamma = \oint v_i t_i d\ell$$



The surface, S , is enclosing by the line ℓ . The vector, t_i , denotes the unit tangential vector of the enclosing line, ℓ .

Where are the stagnation points located? How is the lift of the cylinder computed? (which applies for any body).

- What is the Magnus effect? Explain the three applications below: why is it efficient to use loops in table tennis? Why does the Magnus effect help a football player get the ball around the wall (of players) when making a free-kick? How does the Magnus effect help propulsing a ship using Flettner rotors. To look at old and new installations of Flettner rotors, see [Wikipedia](#).

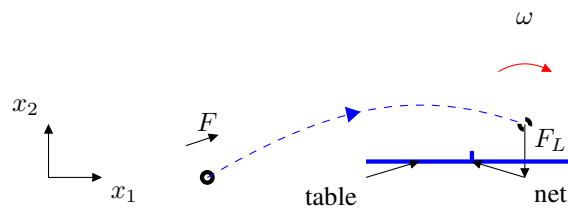
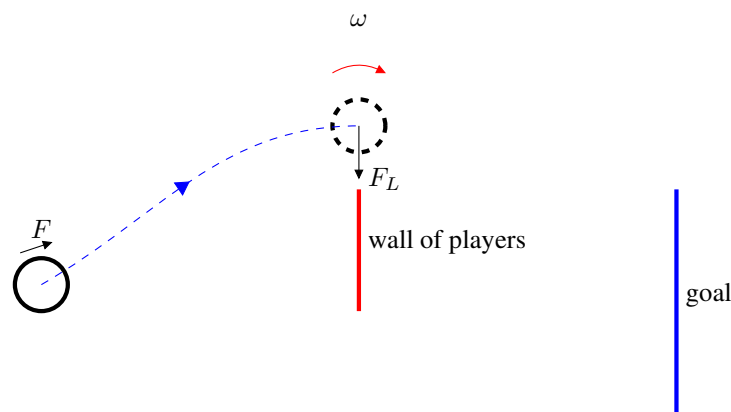
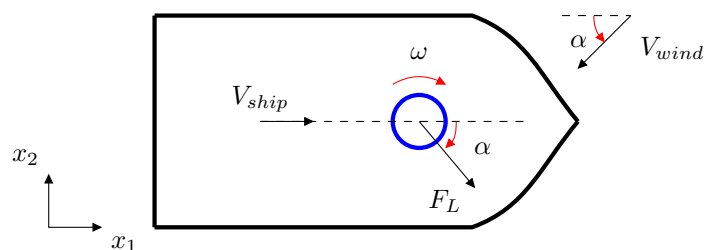


Table tennis. The loop uses the Magnus effect. Side view.



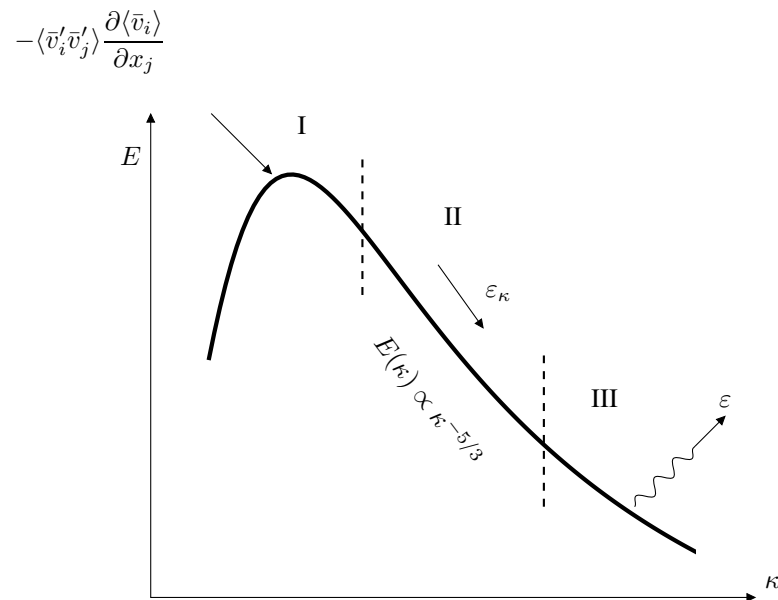
Football. A free-kick uses the Magnus effect. Top view



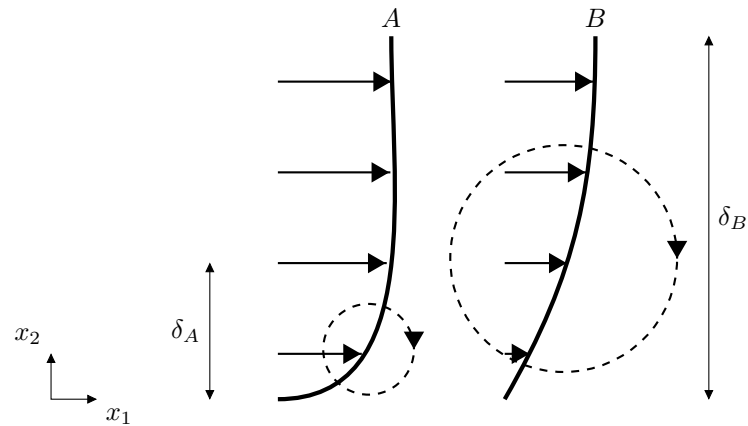
Flettner rotor (in blue) on a ship. The relative velocity between the ship and the wind is $V_{wind} + V_{ship}$. The ship moves with speed V_{ship} . Top view.

Lecture 6

1. What characterizes turbulence? Explain the characteristics. What is the life time of a turbulent eddy?
2. Explain the cascade process. How large are the largest scales? What is dissipation? Which eddies extract energy from the mean flow? Why are these these eddies “best” at extracting energy from the mean flow?
Hint: Look at the figure with two velocity profiles below.
3. The energy spectrum consists of three subregions: which? Describe their characteristics. Show the flow of turbulent kinetic energy in the energy spectrum. Given the energy spectrum, $E(\kappa)$, how is the turbulent kinetic energy, k , computed? Describe – in words – how to use dimensional analysis to derive the $-5/3$ Kolmogorov law.



Spectrum for turbulent kinetic energy, k . The wavenumber, κ , is proportional to the inverse of the length scale of a turbulent eddy, ℓ_κ , i.e. $\kappa \propto \ell_\kappa^{-1}$. For a discussion of ϵ_κ vs. ϵ , see Section 8.2.2.



The size of the largest eddies (dashed lines) for different velocity profiles.

4. What are the Kolmogorov dissipation scales? Describe – in words – how to use dimensional analysis to derive the expression for, for example, the length scale, ℓ_η .
5. What does isotropic turbulence mean? What about the shear stresses?
6. Describe how the ratio of the large eddies to the dissipative eddies depends on the Reynolds number.
Hint: $\frac{\ell_0}{\ell_\eta} = \left(\frac{\nu^3}{\varepsilon} \right)^{-1/4} \ell_0$
 Why is this expression useful for DNS (Direct Numerical Simulation)?
7. Draw a laminar and turbulent velocity profile for pipe flow. What is the main difference? In which flow is the wall shear stress $\tau_w = \mu \frac{\partial \bar{v}_1}{\partial x_2}$ largest, laminar or turbulent?

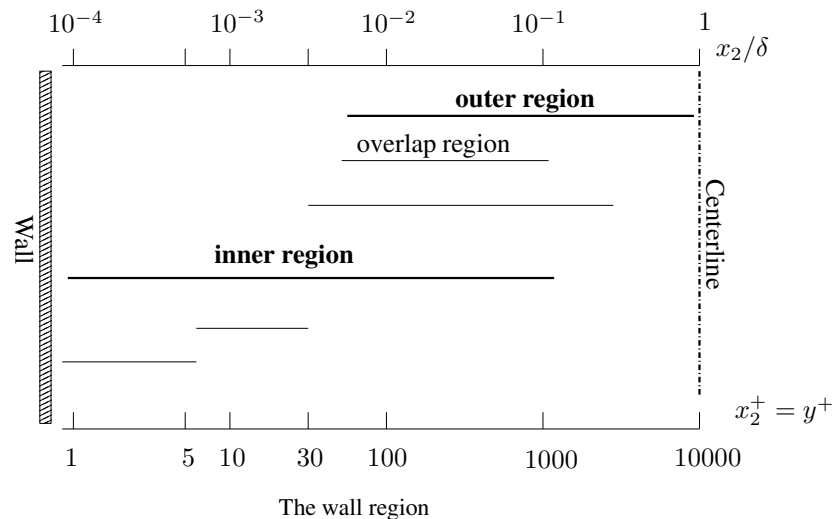
Lecture 7

1. Describe – in words – how to use the decomposition $v_i = \bar{v}_i + v'_i$ to derive the time-averaged Navier-Stokes equation. We start from the Navier-Stokes equation:

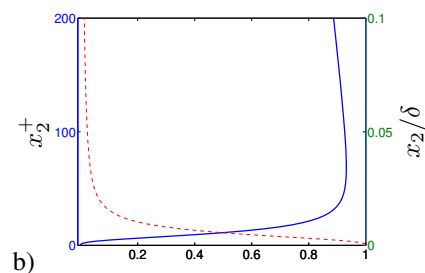
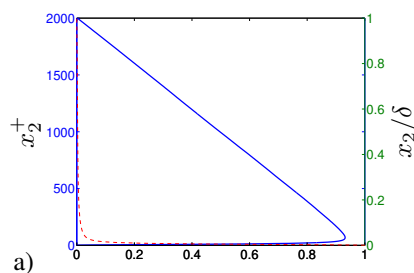
$$\rho \frac{\partial v_i}{\partial t} + \rho \frac{\partial v_i v_j}{\partial x_j} = -\frac{\partial p}{\partial x_i} + \mu \frac{\partial^2 v_i}{\partial x_j \partial x_j}$$

A new terms appears: what is it called? What is the physical meaning of the terms in the equation above?

2. How is the friction velocity, u_τ , defined? Define x_2^+ and \bar{v}_1^+ . The wall region is divided into an inner and outer region. The inner region is furthermore divided into a viscous sublayer, buffer layer and log-layer. Find those three regions in the figure below.

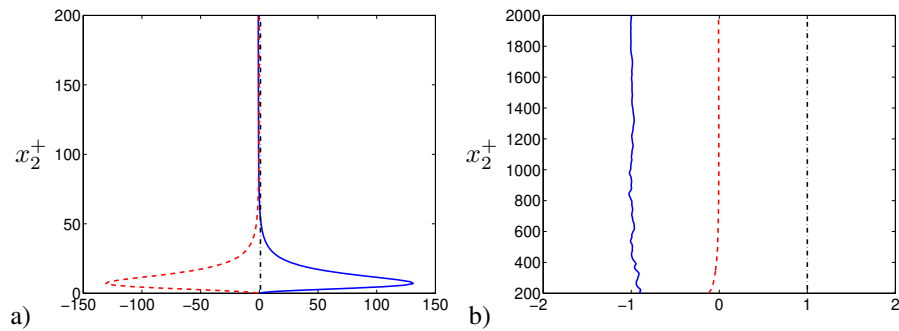


3. What are the relevant velocity and length scales in the viscous-dominated region ($x_2^+ \lesssim 5$)? What are the suitable velocity and length scales in the inertial region (the fully turbulent region)? When deriving the log-law for this region, we start by making an estimate of the velocity gradient: how is it estimated?
4. Consider fully developed turbulent channel flow. In which region (viscous sublayer, buffer layer or log-layer) does the viscous stress dominate? In which region is the turbulent shear stress large? The turbulent and the viscous shear stresses are shown in the figures below. Which is which?



Reynolds shear stress. $Re_\tau = 2000$. a) lower half of the channel; b) zoom near the wall.

5. In fully developed turbulent channel flow, the time-averaged Navier-Stokes consists only of three terms (which?). Identify them in the figures below and discuss their physical meaning.



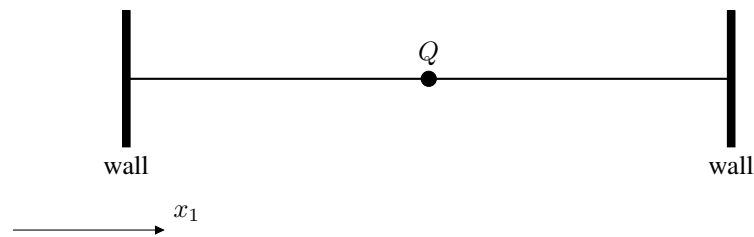
Fully developed channel flow. $Re_\tau = 2000$. Forces in the \bar{v}_1 equation. a) near the lower wall of the channel; b) lower half of the channel excluding the near-wall region.

Lecture 8

1. In order to analyze the k equation it is useful to look at the source terms. A positive source term in a transport equation, for example T , increases the value of T . A simple example is the one-dimensional unsteady heat conduction equation

$$\frac{\partial T}{\partial t} = \alpha \frac{\partial^2 T}{\partial x_1^2} + Q$$

where Q is a heat source, see figure below. Note that the source term(s) should always appear on the opposite side of the unsteady term (or the same side as the diffusion term).



One-dimensional unsteady heat conduction. In the middle there is a heat source, Q .

The exact equation for turbulent kinetic energy, $k = 0.5 \overline{v'_i v'_i}$ reads

$$\underbrace{\frac{\partial \bar{v}_j k}{\partial x_j}}_I = \underbrace{-\overline{v'_i v'_j} \frac{\partial \bar{v}_i}{\partial x_j}}_{II} - \underbrace{\frac{\partial}{\partial x_j} \left[\frac{1}{\rho} \overline{v'_j p'} + \frac{1}{2} \overline{v'_j v'_i v'_i} - \nu \frac{\partial k}{\partial x_j} \right]}_{III} - \underbrace{\nu \frac{\partial v'_i}{\partial x_j} \frac{\partial v'_i}{\partial x_j}}_{IV}$$

Discuss the physical meaning of the different terms in the k equation. Which terms are transport terms? Which is the main source term? Which is the main sink (i.e. negative source) term?

2. Rules for time-averaging, see Section 8.1. Assume that we have a time-series of four time instants with v'_1 and v'_2 as

$$v'_1 = [0.2, -0.3, 0.18, -0.08]$$

$$v'_2 = [0.15, -0.25, 0.04, 0.06]$$

$$\overline{v'_1} = \frac{1}{N} \sum_{n=1}^N v'_{1,n} = (0.2 - 0.3 + 0.18 - 0.08)/4 = 0$$

$$\overline{v'_2} = \frac{1}{N} \sum_{n=1}^N v'_{2,n} = (0.15 - 0.25 + 0.04 + 0.06)/4 = 0$$

so that

$$\overline{v'_1} \overline{v'_2} = \left(\frac{1}{N} \sum_{n=1}^N v'_{1,n} \right) \left(\frac{1}{N} \sum_{n=1}^N v'_{2,n} \right) = 0 \cdot 0 = 0$$

However, the time average of their product is not zero, i.e.

$$\overline{v'_1 v'_2} = \frac{1}{N} \sum_{n=1}^N v'_{1,n} v'_{2,n} = (0.2 \cdot 0.15 + 0.3 \cdot 0.25 + 0.18 \cdot 0.04 - 0.08 \cdot 0.06)/4 = 0.02685$$

Discussion seminar 6

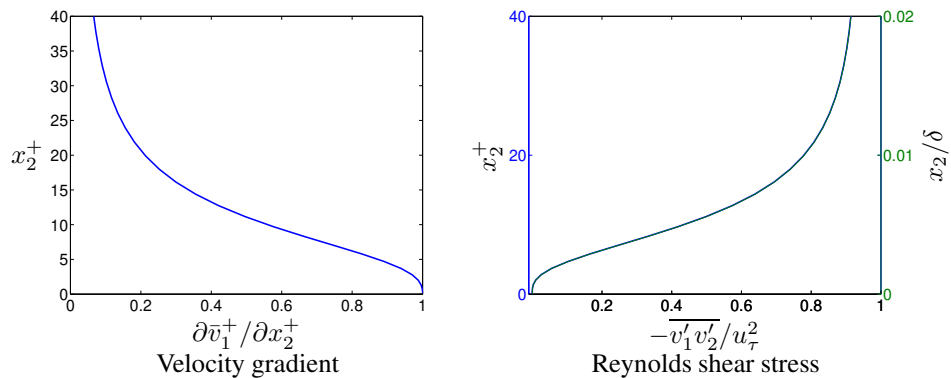
Course material. Recorded Lectures 8, 9 and 10; eBook: Section 6.2–6.3, 8.1, 11.6, 8.2, 8.3

1. The exact k equation for 2D Boundary Layers reads

$$\underbrace{\frac{\partial \bar{v}_1 k}{\partial x_1} + \frac{\partial \bar{v}_2 k}{\partial x_2}}_{\text{conservative form}} \equiv \underbrace{\bar{v}_1 \frac{\partial k}{\partial x_1} + \bar{v}_2 \frac{\partial k}{\partial x_2}}_{\text{non-conservative form}} = -\overline{v'_1 v'_2} \frac{\partial \bar{v}_1}{\partial x_2} - \frac{\partial}{\partial x_2} \left[\frac{1}{\rho} \overline{p' v'_2} + \frac{1}{2} \overline{v'_2 v'_i v'_i} - \nu \frac{\partial k}{\partial x_2} \right] - \nu \overline{\frac{\partial v'_i}{\partial x_j} \frac{\partial v'_i}{\partial x_j}}$$

All spatial derivatives are kept in the dissipation term: why? Which terms are non-zero at the wall? Note that it is easier to realize that the left-hand side is zero when it is formulated on the non-conservative form. Can you express the turbulent diffusive terms on non-conservative form?

2. Where is the production term, $P^k = -\overline{v'_1 v'_2} \partial \bar{v}_1 / \partial x_2$, largest? In order to explain this, look at the figures below.



Channel flow at $Re_\tau = 2000$.

Lecture 9

1. The exact transport equation for mean kinetic energy, $K = 0.5\bar{v}_i\bar{v}_i$ reads

$$\frac{\partial \bar{v}_j K}{\partial x_j} = \underbrace{\overline{v'_i v'_j} \frac{\partial \bar{v}_i}{\partial x_j}}_{-P^k, \text{ sink}} - \underbrace{\frac{\bar{v}_i}{\rho} \frac{\partial \bar{p}}{\partial x_i}}_{\text{source}} - \frac{\partial}{\partial x_j} \left(\bar{v}_i \overline{v'_i v'_j} - \nu \frac{\partial K}{\partial x_j} \right) - \underbrace{\nu \frac{\partial \bar{v}_i}{\partial x_j} \frac{\partial \bar{v}_i}{\partial x_j}}_{\varepsilon_{mean}, \text{ sink}}$$

Discuss the physical meaning of the different terms. One term appears in both the k and the K equations: which one? Consider the dissipation terms in the k and the K equations: which is largest near the wall and away from the wall, respectively?

2. Which terms in the k equation need to be modeled?

$$\bar{v}_1 \frac{\partial k}{\partial x_1} + \bar{v}_2 \frac{\partial k}{\partial x_2} = -\overline{v'_1 v'_2} \frac{\partial \bar{v}_1}{\partial x_2} - \frac{\partial}{\partial x_2} \left[\frac{1}{\rho} \overline{p' v'_2} + \frac{1}{2} \overline{v'_2 v'_i v'_i} - \nu \frac{\partial k}{\partial x_2} \right] - \nu \frac{\partial \overline{v'_i}}{\partial x_j} \frac{\partial \overline{v'_i}}{\partial x_j}$$

3. Which term is unknown in the time-averaged Navier-Stokes equations? (also called the RANS equations [RANS=Reynolds-Averaged Navier-Stokes])

$$\rho \frac{\partial \bar{v}_i \bar{v}_j}{\partial x_j} = -\frac{\partial \bar{p}}{\partial x_i} + \frac{\partial}{\partial x_j} \left(\mu \frac{\partial \bar{v}_i}{\partial x_j} - \rho \overline{v'_i v'_j} \right)$$

4. The Boussinesq approximation reads (almost)

$$-\overline{v'_i v'_j} = \nu_t \left(\frac{\partial \bar{v}_i}{\partial x_j} + \frac{\partial \bar{v}_j}{\partial x_i} \right)$$

Which term is missing?

5. Show how the modeled production term, $P^k = -\overline{v'_i v'_j} \frac{\partial \bar{v}_i}{\partial x_j}$, is modelled in the $k - \varepsilon$ model.
6. The modeled k equation can symbolically be written:

$$C^k = P^k + D^k + G^k - \varepsilon$$

Using this equation, describe how to derive the modeled ε equation.

Lecture 10

- Two options are used for treating the wall boundary conditions: which ones? Explain the main features.
- Consider wall functions. Describe how the expression

$$u_\tau = \frac{\kappa \bar{v}_{1,P}}{\ln(E u_\tau \delta x_2 / \nu)}$$

is obtained. What is the wall boundary condition for the velocity equation?

Hint: The log-law reads $\frac{\bar{v}_1}{u_\tau} = \frac{1}{\kappa} \ln \left(\frac{E u_\tau x_2}{\nu} \right)$

- How is the k equation simplified in the log-law region? Show how the boundary condition

$$k_P = C_\mu^{-1/2} u_\tau^2$$

for k is derived (wall functions).

Hint: Simplified k equation: $0 = P^k - \rho \varepsilon = \mu_t \left(\frac{\partial \bar{v}_1}{\partial x_2} \right)^2 - \rho \varepsilon$. The wall shear stress reads $\tau_w = -\rho \overline{v'_1 v'_2} = \mu_t \frac{\partial \bar{v}_1}{\partial x_2}$

- Show how the boundary condition for ε (used in wall functions)

$$\varepsilon_P = P^k = \frac{u_\tau^3}{\kappa \delta x_2}$$

is derived (wall functions).

Hint: $\varepsilon \simeq \mathcal{U}^3 / \mathcal{L}$.

- How fine should the grid be near the wall when using a low-Reynolds number model? Why must the turbulence model be modified?
- In the eBook we derive the following expressions using Taylor expansion:

$$\begin{array}{lll} \frac{\bar{v}_1}{v_1'^2} & = \frac{\overline{a_1} x_2}{a_1^2 x_2^2} + \dots & = \mathcal{O}(x_2^1) \\ \frac{\bar{v}_1}{v_2'^2} & = \frac{\overline{a_1^2} x_2^2}{b_2^2 x_2^4} + \dots & = \mathcal{O}(x_2^2) \\ \frac{\bar{v}_2}{v_2'^2} & = \frac{\overline{b_2^2} x_2^4}{c_1^2 x_2^2} + \dots & = \mathcal{O}(x_2^4) \\ \frac{v_3'^2}{v_1' v_2'} & = \frac{\overline{c_1^2} x_2^2}{a_1 b_2 x_2^3} + \dots & = \mathcal{O}(x_2^2) \\ \frac{v_1' v_2'}{v_1' v_2'} & = \frac{\overline{a_1 b_2} x_2^3}{(a_1^2 + c_1^2) x_2^2} + \dots & = \mathcal{O}(x_2^3) \\ k & = (\overline{a_1^2} + \overline{c_1^2}) x_2^2 + \dots & = \mathcal{O}(x_2^2) \\ \partial \bar{v}_1 / \partial x_2 & = \overline{a_1} + \dots & = \mathcal{O}(x_2^0) \\ \partial v_1' / \partial x_2 & = a_1 + \dots & = \mathcal{O}(x_2^0) \\ \partial v_2' / \partial x_2 & = 2 \overline{b_2} x_2 + \dots & = \mathcal{O}(x_2^1) \\ \partial v_3' / \partial x_2 & = a_1 + \dots & = \mathcal{O}(x_2^0) \end{array}$$

Describe how they are obtained.

- The exact k equation reads

$$\begin{aligned} \rho \bar{v}_1 \frac{\partial k}{\partial x_1} + \rho \bar{v}_2 \frac{\partial k}{\partial x_2} &= -\overline{\rho v_1' v_2'} \frac{\partial \bar{v}_1}{\partial x_2} - \frac{\partial \overline{p' v_2'}}{\partial x_2} - \frac{\partial}{\partial x_2} \left(\frac{1}{2} \overline{\rho v_2' v_i' v_i'} \right) \\ &+ \mu \frac{\partial^2 k}{\partial x_2^2} - \mu \frac{\overline{\partial v_i'}}{\partial x_j} \frac{\partial v_i'}{\partial x_j} \end{aligned}$$

Using the Taylor expansions above, show how the production term, the viscous and turbulent diffusion terms and the dissipation vary near the wall.

8. The modeled k eq. reads

$$\rho \bar{v}_1 \frac{\partial k}{\partial x_1} + \rho \bar{v}_2 \frac{\partial k}{\partial x_2} = \mu_t \left(\frac{\partial \bar{v}_1}{\partial x_2} \right)^2 + \frac{\partial}{\partial x_2} \left(\frac{\mu_t}{\sigma_k} \frac{\partial k}{\partial x_2} \right) + \mu \frac{\partial^2 k}{\partial x_2^2} - \rho \varepsilon$$

Using the Taylor expansions above, show how the production term, the turbulent diffusion term and the dissipation vary near the wall.

9. Looking at how the exact and the modelled terms in the k behave near walls, which terms need to be modified? How?
10. In low-Reynolds number models, what is the boundary condition for k ?
11. A boundary condition for ε can be derived by looking at the two terms in the k eq. (see above) that do not go to zero. Show this boundary condition.
12. In the eBook it is shown that Taylor expansion gives



$$\varepsilon = \nu \left(\overline{a_1^2} + \overline{c_1^2} \right) + \dots$$

and

$$k = \frac{1}{2} \left(\overline{a_1^2} + \overline{c_1^2} \right) x_2^2 + \dots$$

Show how the “third b.c.” for ε is obtained using these two expressions.

- [1] S. Perzon and L. Davidson. On CFD and transient flow in vehicle aerodynamics. In *SAE Technical Paper 2000-01-0873, Detroit*, 2000. ([document](#)), [19.1](#), [19.2](#), [19.6](#)
- [2] J. O. Hinze. *Turbulence*. McGraw-Hill, New York, 2nd edition, 1975. ([document](#)), [8.2.1](#), [18.7](#), [18.9](#), [21.1](#), [27.6](#), [42](#)
- [3] J. N. Reddy. *An Introduction to Continuum Mechanics*. Cambridge University Press, New York, 2008. [1.1](#), [1.3](#), [1.4](#), [1.6](#), [1.8](#), [2](#), [2.2](#), [2.5](#), [C.2](#)
- [4] M. Ekh. Mechanics of solids & fluids – introduction to continuum mechanics. Report, Div. of Material and Computational Mechanics, Dept. of Applied Mechanics, Chalmers University of Technology, Göteborg, Sweden, 2017. [1.3](#), [1.3](#), [1.4](#), [2.1.1](#), [2.1.2](#), [13](#), [2.2](#), [2.2](#), [2.2](#), [2.2](#), [2.5](#), [2.5](#), [3.2.3](#), [4](#), [12](#), [1](#)
- [5] H. Abedi. *Development of Vortex Filament Method for Wind Power Aerodynamics*. PhD thesis, Div. of Fluid Dynamics, Dept. of Applied Mechanics, Chalmers University of Technology, Göteborg, Sweden, 2016. [1.7](#), [4.4.8](#)
- [6] J. Wojtkowiak and C.O. Popiel. Inherently linear annular-duct-type laminar flowmeter. *Journal of Fluids Engineering*, 128(1):196–198, 2006. [3.2.2](#)
- [7] H. Blasius. *Grenzschichten in Flüssigkeiten mit kleiner Reibung*. PhD thesis, University of Göttingen, Göttingen, Germany, 1907. [3.3](#)
- [8] W. H. Hager. Blasius: A life in research and education. *Experiments in Fluids*, 34:566–571, 2003. [3.3](#)
- [9] L. Qu, Ch. Norberg, L. Davidson, S.-H. Peng, and F. Wang. Quantitative numerical analysis of flow past a circular cylinder at Reynolds number between 50 and 200. *Journal of Fluids and Structures*, 39:347–370, 2013. [13\(a\)](#), [4.4.6](#)
- [10] S. Hong and T. Asai. Effect of panel shape of soccer ball on its flight characteristics. *Scientific Reports*, 4(5068), 2014. [4.4.7.1](#)
- [11] W. Zhang, R. Bensow, M. Golubev, and V Chernoray. Flow past a rotating finite length cylinder: numerical and experimental study. In *51st AIAA Aerospace Sciences Meeting including the New Horizons Forum and Aerospace Exposition, AIAA 2013-0987*, 2012. [4.4.7.1](#)
- [12] H. Abedi. Development of vortex filament method for aerodynamic loads on rotor blades. Thesis for licentiate of engineering, Div. of Fluid Dynamics, Dept. of Applied Mechanics, Chalmers University of Technology, Göteborg, Sweden, 2013. [4.4.8](#)
- [13] S. B. Pope. *Turbulent Flow*. Cambridge University Press, Cambridge, UK, 2001. [5.1](#), [6.2](#), [60](#), [60](#), [60.2](#), [60.2](#)
- [14] H. Tennekes and J. L. Lumley. *A First Course in Turbulence*. The MIT Press, Cambridge, Massachusetts, 1972. [5.1](#)
- [15] P. Bradshaw. *Turbulence*. Springer-Verlag, Berlin, 1976. [5.4](#)

- [16] S. Hoyas and J. Jiménez. Scaling of the velocity fluctuations in turbulent channels up to $Re_\tau = 2003$. *Physics of Fluids A*, 18(011702), 2006. [6.3](#), [6.4](#), [6.6](#), [6.8](#), [8.3](#), [8.4](#), [8.5](#), [9.1](#), [9.4](#), [9.5](#), [9.6](#)
- [17] S. Hoyas and J. Jiménez. <http://torroja.dmt.upm.es/ftp/channels/data/statistics/>. 2006. [6.3](#), [6.4](#), [6.6](#), [6.8](#), [8.3](#), [8.4](#), [8.5](#), [9.1](#), [9.4](#), [9.5](#), [9.6](#)
- [18] Th. von Kármán. Mechanische ähnlichkeit und Turbulenz. *Nachrichten von der Gesellschaft der Wissenschaften zu Göttingen, Fachgruppe 1 (Mathematik)*, 5:58–76, 1930. [6.2](#)
- [19] J.M. Österlund. *Experimental Studies of Zero Pressure-Gradient Turbulent Boundary-Layer Flow*. PhD thesis, Department of Mechanics, Royal Institute of Technology, Stockholm, Sweden, 1999. [6.2](#)
- [20] M. Österlund, A.V. Johansson, H.M. Nagib, and M.H. Hites. Mean-flow characteristics of high Reynolds number turbulent boundary layers from two facilities. In *30th Fluid Dynamics Conference, 28 June-1 July, Norfolk, Virginia*, 1999. [6.2](#)
- [21] M. Österlund, A.V. Johansson, H.M. Nagib, and M.H. Hites. A note on the overlap region in turbulent boundary layers. *Physics of Fluids A*, 12(1):1–4, 2000. [6.2](#)
- [22] P. R. Spalart. Direct simulation of a turbulent boundary layer up to $R_\theta = 1410$. *Journal of Fluid Mechanics*, 187:61–98, 1988. [6.9](#)
- [23] A. A. Townsend. Equilibrium layers and wall turbulence. *Journal of Fluid Mechanics*, 11:97–120, 1961. [8.4](#)
- [24] L. Davidson. Transport equations in incompressible URANS and LES . Report 2006/01, Div. of Fluid Dynamics, Dept. of Applied Mechanics, Chalmers University of Technology, Göteborg, Sweden, 2006. [9.1](#), [11.2](#), [18.9](#), [18.14](#), [45.12](#), [45.12](#)
- [25] K. Hanjalic. Advanced turbulence closure models: A view of current status and future prospects. *Int. J. Heat and Fluid Flow*, 15:178–203, 1994. [11.3](#)
- [26] D. C. Wilcox. *Turbulence Modeling for CFD*. DCW Industries, Inc., 5354 Palm Drive, La Cañada, California 91011, 2 edition, 1998. [11.5](#)
- [27] L. Davidson. An introduction to turbulence models . Technical Report 97/2, Dept. of Thermo and Fluid Dynamics, Chalmers University of Technology, Gothenburg, 1997. [11.5](#), [11.14.1](#), [11.14.3](#), [11.14.3](#), [16](#), [24.1](#), [52.3](#)
- [28] K. Hanjalic and B. E. Launder. A Reynolds stress model of turbulence and its application to thin shear flows. *Journal of Fluid Mechanics*, 52:609–638, 1972. [11.7.2](#)
- [29] J. C. Rotta. Statistische theorie nichthomogener turbulenz. *Zeitschrift für Physik*, 129:547–572, 1951. [11.7.4](#), [60](#)
- [30] G. E. Mase. *Continuum Mechanics*. Schaum's Outline Series. McGraw-Hill, 1970. [11.7.4](#), [11.11](#), [13](#), [53.1](#)

- [31] S. Fu, B. E. Launder, and D. P. Tselepidakes. Accomodating the effects of high strain rates in modelling the pressure-starin correlation. Technical Report TFD/87/5, UMIST, Mechanical Engineering Dept., 1987. [11.7.4](#), [13.1](#)
- [32] B. E. Launder, G. J. Reece, and W. Rodi. Progress in the development of a Reynolds-stress turbulence closure. *Journal of Fluid Mechanics*, 68(3):537–566, 1975. [11.7.5](#), [60](#)
- [33] D. Naot, A. Shavit, and M. Wolfshtein. Interactions between components of the turbulent velocity correlation tensor. *Israel J. Techn.*, 8:259, 1970. [11.7.5](#)
- [34] B. E. Launder. An introduction to single-point closure methodology. In T. B. Gatski, M. Y. Hussaini, and J. L. Lumpley, editors, *Simulation and Modeling of Turbulent Flows*, New York, 1996. Oxford University Press. [11.7.5](#)
- [35] M. M. Gibson and B. E. Launder. Ground effects on pressure fluctuations in the atmospheric boundary layer. *Journal of Fluid Mechanics*, 86:491–511, 1978. [11.7.6](#), [11.7.6](#)
- [36] S. B. Pope. A more general effective-viscosity hypothesis. *Journal of Fluid Mechanics*, 472:331–340, 1975. [11.11](#), [11.11](#), [14](#), [60](#), [60](#)
- [37] S. Wallin and A. V. Johansson. A new explicit algebraic Reynolds stress model for incompressible and compressible turbulent flows. *Journal of Fluid Mechanics*, 403:89–132, 2000. [11.12](#), [11.12](#), [11.12](#), [11.12](#), [11.12](#), [14](#), [2](#), [60](#), [60](#), [60](#)
- [38] A. V. Johansson and S. Wallin. A new explicit algebraic Reynolds stress model. In *Advances in Turbulence VI*, pages 31–34, Netherlands, 1996. Kluwer Academic Publishers. [11.12](#)
- [39] S. S. Girimaji. Fully-explicit and self-consistent algebraic Reynolds stress model. *Theoretical and Computational Fluid Dynamics*, 8:387–402, 1996. [11.12](#), [60](#)
- [40] S. S. Girimaji. Improved algebraic Reynolds stress model for engineering flows. In W. Rodi and G. Bergeles, editors, *Engineering Turbulence Modelling and Measurements – ETMM3*, pages 121–129. Elsevier, 1996. [11.12](#)
- [41] A. A. Townsend. *The Structure of Turbulent Shear Flow*. Cambridge University Press, New York, second edition, 1976. [11.6](#)
- [42] G. Eitel-Amor, R. Orlu, and P. Schlatter. Simulation and validation of a spatially evolving turbulent boundary layers up to $Re_\theta = 8300$. *International Journal of Heat and Fluid Flow*, 47:57–69, 2014. [11.8](#), [59.1](#), [59.1](#)
- [43] J. Kim. The collaborative testing of turbulence models (organized by P. Bradshaw *et al.*). Data Disk No. 4 (also available at Ercoftac’s www-server <http://fluindigo.mech.surrey.ac.uk/database>), 1990. [11.9](#), [11.10](#), [11.11](#)
- [44] V. C. Patel, W. Rodi, and G. Scheuerer. Turbulence models for near-wall and low Reynolds number flows: A review. *AIAA Journal*, 23:1308–1319, 1985. [11.14.3](#)

- [45] H. C. Chen and V. C. Patel. Near-wall turbulence models for complex flows including separation. *AIAA Journal*, 26:641–648, 1988. [11.14.3](#)
- [46] L. Davidson. Calculation of the turbulent buoyancy-driven flow in a rectangular cavity using an efficient solver and two different low reynolds number $k - \varepsilon$ turbulence models. *Numer. Heat Transfer*, 18:129–147, 1990. [11.14.3](#)
- [47] K. Abe, T. Kondoh, and Y. Nagano. A new turbulence model for predicting fluid flow and heat transfer in separating and reattaching flows - 1. Flow field calculations. *Int. J. Heat Mass Transfer*, 37(1):139–151, 1994. [11.14.3](#), [20.1](#), [23](#), [45.6](#)
- [48] F. S. Lien and M. A. Leschziner. Low-Reynolds-number eddy-viscosity modelling based on non-linear stress-strain/vorticity relations. In W. Rodi and G. Bergeles, editors, *Engineering Turbulence Modelling and Experiments 3*, pages 91–100. Elsevier, 1996. [11.14.3](#)
- [49] N. N. Mansour, J. Kim, and P. Moin. Reynolds-stress and dissipation-rate budgets in a turbulent channel flow. *Journal of Fluid Mechanics*, 194:15–44, 1988. [11.14.3](#)
- [50] B. E. Launder and B. T. Sharma. Application of the energy dissipation model of turbulence to the calculation of flow near a spinning disc. *Lett. Heat and Mass Transfer*, 1:131–138, 1974. [11.14.3](#)
- [51] C. G. Speziale, R. Abid, and E. C. Anderson. Critical evaluation of two-equation models for near-wall turbulence. *AIAA Journal*, 30:324–331, 1992. [11.14.3](#)
- [52] P. Bradshaw. Effects of streamline curvature on turbulent flow. Agardograph progress no. 169, AGARD, 1973. [12.2](#)
- [53] W. Rodi and G. Scheuerer. Calculation of curved shear layers with two-equation turbulence models. *Physics of Fluids*, 26:1422–1435, 1983. [12.2](#)
- [54] B. E. Thompson and J. H. Whitelaw. Characteristics of a trailing-edge flow with turbulent boundary-layer separation. *Journal of Fluid Mechanics*, 157:305–326, 1985. [12.2](#)
- [55] L. Davidson. Prediction of the flow around an airfoil using a Reynolds stress transport model. *Journal of Fluids Engineering*, 117:50–57, 1995. [12.4](#)
- [56] P. A. Durbin. On the $k - 3$ stagnation point anomaly. *International Journal of Heat and Fluid Flow*, 17:89–90, 1996. [13](#), [13](#), [15](#)
- [57] J. Hult. *Cartesiska tensorer: Ett praktiskt fikonspråk*. Almqvist & Wiksell, 1972. [13](#)
- [58] J. L. Lumley. Computational modeling of turbulent flows. *Advances in Applied Mechanics*, 18:123–176, 1978. [13.1](#), [13.1](#)
- [59] T. J. Craft and B. E. Launder. A Reynolds stress closure designated for complex geometries. *International Journal of Heat and Fluid Flow*, 17(3):245–254, 1996. [13.1](#)

- [60] T. J. Craft, B. E. Launder, and K. Suga. Prediction of turbulent transitional phenomena with a nonlinear eddy-viscosity model. *International Journal of Heat and Fluid Flow*, 18:15–28, 1997. [14](#), [14](#), [14](#), [14](#), [59](#)
- [61] T. B. Gatski and C. G. Speziale. On explicit algebraic stress models for complex turbulent flows. *Journal of Fluid Mechanics*, 154:59–78, 1993. [14](#), [60](#)
- [62] T.-H. Shih, J. Zhu, and J. L. Lumley. A new Reynolds stress algebraic equation model. *Comput. Methods Appl. Engng.*, 125:287–302, 1995. [14](#)
- [63] P. A. Durbin. Near-wall turbulence closure modeling without damping functions. *Theoretical and Computational Fluid Dynamics*, 3:1–13, 1991. [15](#)
- [64] P. A. Durbin. Application of a near-wall turbulence model to boundary layers and heat transfer. *International Journal of Heat and Fluid Flow*, 14(4):316–323, 1993. [15](#)
- [65] A. Sveningsson. Analysis of the performance of different $\overline{v^2} - f$ turbulence models in a stator vane passage flow. Thesis for licentiate of engineering, Dept. of Thermo and Fluid Dynamics, Chalmers University of Technology, Göteborg, Sweden, 2003. [15](#), [15](#), [15.2](#)
- [66] K. Hanjalic, M. Popovacx, and M. Habziabdic. A robust near-wall elliptic relaxation eddy-viscosity turbulence model for CFD. *International Journal of Heat and Fluid Flow*, 2004. [15](#)
- [67] F-S Lien and G. Kalitzin. Computations of transonic flow with the v2f turbulence model. *International Journal of Heat and Fluid Flow*, 22(1):53–61, 2001. [15.1](#), [15.2](#)
- [68] A. Sveningsson and L. Davidson. Assessment of realizability constraints in $\overline{v^2} - f$ turbulence models. *International Journal of Heat and Fluid Flow*, 25(5):785–794, 2004. [15.2](#)
- [69] A. Sveningsson and L. Davidson. Computations of flow field and heat transfer in a stator vane passage using the $\overline{v^2} - f$ turbulence model. Paper GT2004-53586, ASME TURBO EXPO 2004, Vienna, 2004. [15.2](#)
- [70] A. Sveningsson and L. Davidson. Computations of flow field and heat transfer in a stator vane passage using the $\overline{v^2} - f$ turbulence model. *Journal of Turbomachinery*, 127(3):627–634, 2005. [15.2](#)
- [71] A. Sveningsson. *Turbulence Transport Modelling in Gas Turbine Related Applications*. PhD thesis, Div. of Fluid Dynamics, Dept. of Applied Mechanics, Chalmers University of Technology, Göteborg, Sweden, 2006. [15.2](#)
- [72] L. Davidson, P. V. Nielsen, and A. Sveningsson. Modifications of the $v^2 - f$ model for computing the flow in a 3D wall jet. In K. Hanjalic, Y. Nagano, and M. J. Tummers, editors, *Turbulence Heat and Mass Transfer 4*, pages 577–584, New York, Wallingford (UK), 2003. begell house, inc. [15.3](#), [15.3](#)
- [73] F. R. Menter. Two-equation eddy-viscosity turbulence models for engineering applications. *AIAA Journal*, 32:1598–1605, 1994. [16](#), [16](#), [16](#), [16](#), [20.2](#)

- [74] D. C. Wilcox. Reassessment of the scale-determining equation. *AIAA Journal*, 26(11):1299–1310, 1988. [16](#)
- [75] F. R. Menter. Influence of freestream values on $k - \omega$ turbulence model predictions. *AIAA Journal*, 30(6):1657–1659, 1992. [16](#)
- [76] A. Hellsten. New advanced $k - \omega$ turbulence model for high-lift aerodynamics. *AIAA Journal*, 43(9):1857–1869, 2005. [16](#)
- [77] J. Bredberg. On two-equation eddy-viscosity models. Report 01/8, can be downloaded from <http://www.tfd.chalmers.se/~lada/allpaper.html>, Dept. of Thermo and Fluid Dynamics, Chalmers University of Technology, 2001. [16](#)
- [78] P. Bradshaw, D. H. Ferriss, and N. P. Atwell. Calculation of boundary-layer development using the turbulent energy equation. *Journal of Fluid Mechanics*, 28:593–616, 1967. [16](#)
- [79] F. R. Menter, M. Kuntz, and R. Langtry. Ten years of industrial experience of the SST turbulence model. In K. Hanjalić, Y. Nagano, and M. J. Tummers, editors, *Turbulence Heat and Mass Transfer 4*, pages 624–632, New York, Wallingford (UK), 2003. begell house, inc. [16](#), [20.1](#), [20.2](#), [20.3](#), [47.6](#)
- [80] S. Ghosal and P. Moin. The basic equations for the large eddy simulation of turbulent flows in complex geometry. *J. Comp. Phys.*, 118:24–37, 1995. [18.1](#), [26](#)
- [81] J. Smagorinsky. General circulation experiments with the primitive equations. *Monthly Weather Review*, 91:99–165, 1963. [18.6](#)
- [82] P. Moin and J. Kim. Numerical investigation of turbulent channel flow. *Journal of Fluid Mechanics*, 118:341–377, 1982. [18.6](#)
- [83] W. P. Jones and M. Wille. Large eddy simulation of a jet in a cross-flow. In *10th Symp. on Turbulent Shear Flows*, pages 4:1 – 4:6, The Pennsylvania State University, 1995. [18.6](#)
- [84] H. Schlichting. *Boundary-Layer Theory*. McGraw-Hill, New York, 7 edition, 1979. [18.7](#)
- [85] M. Germano, U. Piomelli, P. Moin, and W. H. Cabot. A dynamic subgrid-scale eddy viscosity model. *Physics of Fluids A*, 3:1760–1765, 1991. [18.11](#), [18.23](#)
- [86] Y. Zang, R. L. Street, and J. R. Koseff. A dynamic mixed subgrid-scale model and its application to turbulent recirculating flows. *Physics of Fluids A*, 5:3186–3196, 1993. [18.12.2](#)
- [87] D. K. Lilly. A proposed modification of the Germano subgrid-scale closure method. *Physics of Fluids A*, 4:633–635, 1992. [18.13](#)
- [88] J. P. Boris, F. F. Grinstein, E. S. Oran, and R. L. Kolbe. New insights into large eddy simulation. *Fluid Dynamic Research*, 10:199–228, 1992. [18.14](#)
- [89] J. Bardina, J. H. Ferziger, and W. C. Reynolds. Improved subgrid scale models for large eddy simulation. AIAA 80-1357, Snomass, Colorado, 1980. [18.16](#), [18.18](#)

- [90] C. G. Speziale. Galilean invariance of subgrid-scale stress models in the large-eddy simulation of turbulence. *Journal of Fluid Mechanics*, 156:55–62, 1985. [18.16](#), [18.17](#), [40](#), [40](#)
- [91] M. Germano. A proposal for a redefinition of the turbulent stresses in the filtered Navier-Stokes equations. *Phys. Fluids A*, 7:2323–2324, 1986. [18.17](#)
- [92] L. Davidson. A dissipative scale-similarity model. In V. Armenio, B. Geurts, and J. Fröhlich, editors, *DLES7: Direct and Large-Eddy Simulations 7*, volume 13 of *ERCOTAC series*, pages 261–266, 2010. [18.18](#), [18.18](#)
- [93] C. Hirsch. *Numerical Computation of Internal and External Flows: Fundamentals of Numerical Discretization*, volume 1. John Wiley & Sons, Chichester, UK, 1988. [18.18](#)
- [94] L. Davidson. Hybrid LES-RANS: back scatter from a scale-similarity model used as forcing. *Phil. Trans. of the Royal Society A*, 367(1899):2905–2915, 2009. [18.19](#)
- [95] P. Emvin. *The Full Multigrid Method Applied to Turbulent Flow in Ventilated Enclosures Using Structured and Unstructured Grids*. PhD thesis, Dept. of Thermo and Fluid Dynamics, Chalmers University of Technology, Göteborg, 1997. [18.20](#), [4](#), [18.20](#)
- [96] L. Davidson and S.-H. Peng. Hybrid LES-RANS: A one-equation SGS model combined with a $k - \omega$ model for predicting recirculating flows. *International Journal for Numerical Methods in Fluids*, 43:1003–1018, 2003. [18.20](#), [19](#)
- [97] S. V. Patankar. *Numerical Heat Transfer and Fluid Flow*. McGraw-Hill, New York, 1980. [18.20.1](#)
- [98] H. K. Versteegh and W. Malalasekera. *An Introduction to Computational Fluid Dynamics - The Finite Volume Method*. Longman Scientific & Technical, Harlow, England, 1995. [18.20.1](#), [23.1.1](#)
- [99] L. Davidson and M. Billson. Hybrid LES/RANS using synthesized turbulent fluctuations for forcing in the interface region. *International Journal of Heat and Fluid Flow*, 27(6):1028–1042, 2006. [18.21](#), [20.1](#), [21.2](#), [21.2](#), [22.5](#), [27.1](#), [27.9](#), [28](#), [45.12](#), [46.1](#), [46.3](#), [46.4](#), [46.5](#), [50](#), [50.4](#)
- [100] L. Davidson. Large eddy simulation: A dynamic one-equation subgrid model for three-dimensional recirculating flow. In *11th Int. Symp. on Turbulent Shear Flow*, volume 3, pages 26.1–26.6, Grenoble, 1997. [18.23](#), [45.12](#)
- [101] L. Davidson. Large eddy simulations: A note on derivation of the equations for the subgrid turbulent kinetic energies. Technical Report 97/11, Dept. of Thermo and Fluid Dynamics, Chalmers University of Technology, Gothenburg, 1997. [18.23](#), [45.12](#)
- [102] A. Sohankar, L. Davidson, and C. Norberg. Large eddy simulation of flow past a square cylinder: Comparison of different subgrid scale models. *Journal of Fluids Engineering*, 122(1):39–47, 2000. [18.23](#)
- [103] A. Sohankar, L. Davidson, and C. Norberg. Erratum. *Journal of Fluids Engineering*, 122(3):643, 2000. [18.23](#)

- [104] S. Krajnović and L. Davidson. A mixed one-equation subgrid model for large-eddy simulation. *International Journal of Heat and Fluid Flow*, 23(4):413–425, 2002. [18.24](#)
- [105] S. Krajnović and L. Davidson. Large eddy simulation of the flow around a bluff body. *AIAA Journal*, 40(5):927–936, 2002. [18.25](#), [19.2](#)
- [106] S. Krajnović. *Large Eddy Simulations for Computing the Flow Around Vehicles*. PhD thesis, Dept. of Thermo and Fluid Dynamics, Chalmers University of Technology, Göteborg, Sweden, 2002. [18.25](#)
- [107] J. Pallares and L. Davidson. Large-eddy simulations of turbulent flow in a rotating square duct. *Physics of Fluids*, 12(11):2878–2894, 2000. [18.25](#)
- [108] J. Pallares and L. Davidson. Large-eddy simulations of turbulent heat transfer in stationary and rotating square duct. *Physics of Fluids*, 14(8):2804–2816, 2002. [18.25](#)
- [109] S. Krajnović and L. Davidson. Numerical study of the flow around the bus-shaped body. *Journal of Fluids Engineering*, 125:500–509, 2003. [18.25](#)
- [110] S. Krajnović and L. Davidson. Flow around a simplified car. part I: Large eddy simulations. *Journal of Fluids Engineering*, 127(5):907–918, 2005. [18.25](#)
- [111] S. Krajnović and L. Davidson. Flow around a simplified car. part II: Understanding the flow. *Journal of Fluids Engineering*, 127(5):919–928, 2005. [18.25](#)
- [112] S. Krajnović and L. Davidson. Influence of floor motions in wind tunnels on the aerodynamics of road vehicles. *Journal of Wind Engineering and Industrial Aerodynamics*, 92(5):677–696, 2005. [18.25](#)
- [113] S. Dahlström and L. Davidson. Large eddy simulation applied to a high-Reynolds flow around an airfoil close to stall. AIAA paper 2003-0776, 2003. [18.25](#)
- [114] S. Dahlström. *Large Eddy Simulation of the Flow Around a High-Lift Airfoil*. PhD thesis, Dept. of Thermo and Fluid Dynamics, Chalmers University of Technology, Göteborg, Sweden, 2003. [18.25](#), [48.1](#)
- [115] J. Ask and L. Davidson. Flow and dipole source evaluation of a generic SUV. *Journal of Fluids Engineering*, 132(051111), 2010. [18.25](#), [25.1.3](#)
- [116] H. Hemida and S. Krajnović. LES study of the impact of the wake structures on the aerodynamics of a simplified ICE2 train subjected to a side wind. In *Fourth International Conference on Computational Fluid Dynamics (ICCFD4)*, 10-14 July, Ghent, Belgium, 2006. [18.25](#)
- [117] H. Hemida and S. Krajnović. Numerical study of the unsteady flow structures around train-shaped body subjected to side winds. In *ECCOMAS CFD 2006*, 5-8 September, Egmond aan Zee, The Netherlands, 2006. [18.25](#)
- [118] S. Krajnović. Numerical simulation of the flow around an ICE2 train under the influence of a wind gust. In *International Conference on Railway Engineering 2008 (IET ICRE2008)*, 25-28 March, Hong Kong, China, 2008. [18.25](#)

- [119] S.-H. Peng and L. Davidson. On a subgrid-scale heat flux model for large eddy simulation of turbulent thermal flow. *International Journal of Heat and Mass Transfer*, 45:1393–1405, 2002. [18.25](#)
- [120] S.-H. Peng and L. Davidson. Large eddy simulation for turbulent buoyant flow in a confined cavity. *International Journal of Heat and Fluid Flow*, 22:323–331, 2001. [18.25](#)
- [121] S.-H. Peng. *Modeling of Turbulent flow and Heat Transfer for Building Ventilation*. PhD thesis, Dept. of Thermo and Fluid Dynamics, Chalmers University of Technology, Göteborg, 1998. [18.25](#)
- [122] D. G. Barhaghi and L. Davidson. Natural convection boundary layer in a 5:1 cavity. *Physics of Fluids*, 19(125106), 2007. [18.25](#)
- [123] D. Barhaghi. *A Study of Turbulent Natural Convection Boundary Layers Using Large-Eddy Simulation*. PhD thesis, Div. of Fluid Dynamics, Dept. of Applied Mechanics, Chalmers University of Technology, Göteborg, Sweden, 2007. [18.25](#)
- [124] D. G. Barhaghi, L. Davidson, and R. Karlsson. Large-eddy simulation of natural convection boundary layer on a vertical cylinder. *International Journal of Heat and Fluid Flow*, 27(5):811–820, 2006. [18.25](#)
- [125] D. G. Barhaghi and L. Davidson. Les of mixed convection boundary layer between radiating parallel plates. In *5th International Symposium on Turbulence, Heat and Mass Transfer*, September 25–29, 2006, Dubrovnik, Croatia, 2006. [18.25](#)
- [126] S. R. Robinson. Coherent motions in the turbulent boundary layer. *Annual Review of Fluid Mechanics*, 23:601–639, 1991. [18.26](#), [21](#)
- [127] L. Davidson. Large eddy simulations: how to evaluate resolution. *International Journal of Heat and Fluid Flow*, 30(5):1016–1025, 2009. [18.14](#), [18.26](#), [21.2](#), [45.5](#), [48.3](#), [48.7](#), [1](#), [2](#), [5](#), [48.7.2](#)
- [128] L. Davidson. How to estimate the resolution of an LES of recirculating flow. In M. V. Salvetti, B. Geurts, J. Meyers, and P. Sagaut, editors, *ERCOFTAC*, volume 16 of *Quality and Reliability of Large-Eddy Simulations II*, pages 269–286. Springer, 2010. [18.26](#), [45.5](#), [48.3](#), [48.7](#), [1](#), [2](#), [5](#), [48.7](#), [48.7.2](#)
- [129] L. Davidson. Inlet boundary conditions for embedded LES. In *First CEAS European Air and Space Conference*, 10–13 September, Berlin, 2007. [18.26](#), [27](#)
- [130] L. Davidson, D. Cokljat, J. Fröhlich, M. A. Leschziner, C. Mellen, and W. Rodi, editors. *LESFOIL: Large Eddy Simulation of Flow Around a High Lift Airfoil*, volume 83 of *Notes on Numerical Fluid Mechanics*. Springer Verlag, 2003. [18.26](#), [20](#), [21](#)
- [131] C. P. Mellen, J. Fröhlich, and W. Rodi. Lessons from LESFOIL project on large eddy simulation of flow around an airfoil. *AIAA Journal*, 41(4):573–581, 2003. [18.26](#), [21](#)

- [132] S. Johansson, L. Davidson, and E. Olsson. Numerical simulation of vortex shedding past triangular cylinders at high reynolds numbers using a $k - \varepsilon$ turbulence model. *International Journal for Numerical Methods in Fluids*, 16:859–878, 1993. [19](#), [19.3](#), [19.4](#)
- [133] S. Perzon and L. Davidson. On transient modeling of the flow around vehicles using the Reynolds equation. In J.-H. Wu, Z.-J. Zhu, F.-P. Jia, X.-B. Wen, and W. Hu, editors, *ACFD 2000*, Beijing, 2000. [19.1](#)
- [134] T. H. Shih, J. Zhu, and J. L. Lumley. A realizable Reynolds stress algebraic equation model. Technical memo 105993, NASA, 1993. [19.1](#)
- [135] P. Spalart and S. Allmaras. A one equation turbulence model for aerodynamic flows. AIAA paper 92-0439, Reno, NV, 1992. [20](#)
- [136] P. R. Spalart, W.-H. Jou, M. Strelets, and S. R. Allmaras. Comments on the feasibility of LES for wings and on a hybrid RANS/LES approach. In C. Liu and Z. Liu, editors, *Advances in LES/DNS, First Int. conf. on DNS/LES*, Louisiana Tech University, 1997. Greyden Press. [20](#), [21](#), [28](#)
- [137] F. R. Menter, M. Kuntz, and R. Bender. A scale-adaptive simulation model for turbulent flow prediction. AIAA paper 2003–0767, Reno, NV, 2003. [20](#)
- [138] A. K. Travin, M. Shur, , M. Strelets, and P. R. Spalart. Physical and numerical upgrades in the detached-eddy simulations of complex turbulent flows. In R. Friederich and W.Rodi, editors, *Fluid Mechanics and its Applications. Advances in LES of Complex Flows*, volume 65 of *Euromech Colloquium 412. Fluid Mechanics and its Applications. Advances in LES of Complex Flows*, pages 239–254. Academic Publishers, Dordrecht, 2002. [20.1](#), [20.1](#)
- [139] C. De Langhe, B. Merci, K. Lodefier, and E. Dick. Hybrid RANS-LES modelling with the renormalization group. In K. Hanjalić, Y. Nagano, and M. J. Tummers, editors, *Turbulence Heat and Mass Transfer 4*, pages 697–704, New York, Wallingford (UK), 2003. begell house, inc. [20.1](#)
- [140] J. C. Kok, H. S. Dol, B. Oskam, and H. van der Ven. Extra-large eddy simulation of massively separated flows. AIAA paper 2004-264, Reno, NV, 2004. [20.1](#), [23](#), [28](#)
- [141] J. Yan, C. Mocket, and F. Thiele. Investigation of alternative length scale substitutions in detached-eddy simulation. *Flow, Turbulence and Combustion*, 74:85–102, 2005. [20.1](#), [20.1](#)
- [142] S. S. Girimaji. Partially-averaged Navier-Stokes model for turbulence: A Reynolds-averaged Navier-Stokes to direct numerical simulation bridging method. *ASME Journal of Applied Mechanics*, 73(2):413–421, 2006. [20.1](#), [25.2](#), [28](#)
- [143] J. Ma, S.-H. Peng, L. Davidson, and F. Wang. A low Reynolds number variant of Partially-Averaged Navier-Stokes model for turbulence. *International Journal of Heat and Fluid Flow*, 32(3):652–669, 2011. 10.1016/j.ijheatfluidflow.2011.02.001. [20.1](#), [23](#), [25.2](#), [48.3](#)

- [144] R. Schiestel and A. Dejoan. Towards a new partially integrated transport model for coarse grid and unsteady turbulent flow simulations. *Theoretical and Computational Fluid Dynamics*, 18(6):443–468, 2005. [20.1](#), [23](#), [24](#), [24.2](#), [28](#)
- [145] L. Davidson. Zonal PANS: evaluation of different treatments of the RANS-LES interface. *Journal of Turbulence*, 17(3):274–307, 2016. [20.1](#), [23.2](#), [23.2.2.2](#), [23.2.2.3](#), [26](#), [52.3](#)
- [146] P. Batten, U. Goldberg, and S. Chakravarthy. Interfacing statistical turbulence closures with large-eddy simulation. *AIAA Journal*, 42(3):485–492, 2004. [20.1](#)
- [147] U. Piomelli, E. Balaras, H. Pasinato, K. D. Squire, and P. R. Spalart. The inner-outer layer interface in large-eddy simulations with wall-layer models. *International Journal of Heat and Fluid Flow*, 24:538–550, 2003. [20.1](#), [21](#), [21.2](#)
- [148] L. Davidson and S. Dahlström. Hybrid LES-RANS: An approach to make LES applicable at high Reynolds number. *International Journal of Computational Fluid Dynamics*, 19(6):415–427, 2005. [20.1](#), [21.2](#)
- [149] J. Larsson, F. S. Lien, and E. Yee. The artificial buffer layer and the effects of forcing in hybrid LES/RANS. *International Journal of Heat and Fluid Flow*, 28(6):1443–1459, 2007. [20.1](#)
- [150] P. Spalart, S. Deck, M. Shur, K. Squires, M. Strelets, and A. Travin. A new version of detached-eddy simulation, resistant to ambiguous grid densities. *Theoretical and Computational Fluid Dynamics*, 20:181–195, 2006. 10.1007/s00162-006-0015-0. [20.3](#)
- [151] F. Nicoud and F. Ducros. Subgrid-scale stress modelling based on the square of the velocity gradient tensor. *Flow, Turbulence and Combustion*, 62(3):183–200, 1999. [20.3](#), [45.11](#)
- [152] F. R. Menter and M. Kuntz. Adaption of eddy-viscosity turbulence models to unsteady separated flows behind vehicles. In Rose McCallen, Fred Browand, and James Ross, editors, *The Aerodynamics of Heavy Vehicles: Trucks, Buses, and Trains*, volume 19 of *Lecture Notes in Applied and Computational Mechanics*. Springer Verlag, 2004. [20.3](#)
- [153] M. Strelets. Detached eddy simulation of massively separated flows. AIAA paper 2001–0879, Reno, NV, 2001. [20.3](#), [21](#)
- [154] P. R. Spalart. Strategies for turbulence modelling and simulations. *International Journal of Heat and Fluid Flow*, 21:252–263, 2000. [21](#), [28](#)
- [155] N. V. Nikitin, F. Nicoud, B. Wasistho, K. D. Squires, and P. Spalart. An approach to wall modeling in large-eddy simulations. *Physics of Fluids*, 12(7):1629–1632, 2000. [21](#)
- [156] F. R. Menter and Y. Egorov. Revisiting the turbulent length scale equation. In *IUTAM Symposium: One Hundred Years of Boundary Layer Research*, Göttingen, 2004. [22.2](#), [22.2](#)
- [157] F. R. Menter, M. Kuntz, and R. Bender. A scale-adaptive simulation model for turbulent flow predictions. AIAA-2003-0767, Reno, 2003. [22.2](#)

- [158] J. C. Rotta. *Turbulente Strömungen*. Teubner Verlag, Stuttgart, 1972. [22.2](#)
- [159] F. R. Menter and Y. Egorov. A scale-adaptive simulation model using two-equation models. AIAA paper 2005–1095, Reno, NV, 2005. [22.2](#), [22.3](#), [22.3](#), [47.7](#)
- [160] F. R. Menter and Y. Egorov. The scale adaptive simulation method for unsteady turbulent flow predictions. Part 1: Theory and description. *Flow, Turbulence and Combustion*, 85:113–138, 2010. [22.2](#), [22.3](#), [22.3](#), [28](#), [47.7](#)
- [161] Y. Egorov, F. R. Menter, R. Lechner, and D. Cokljat. The scale adaptive simulation method for unsteady flow predictions. Part 2: Application to complex flows. *Flow, Turbulence and Combustion*, 85:139–165, 2010. [22.2](#), [22.3](#), [22.3](#), [28](#), [47.7](#)
- [162] L. Davidson. Evaluation of the SST-SAS model: Channel flow, asymmetric diffuser and axi-symmetric hill. In *ECCOMAS CFD 2006*, September 5–8, 2006, Egmond aan Zee, The Netherlands, 2006. [22.4](#), [22.5](#), [47.7](#)
- [163] S. S. Girimaji. Partially-averaged Navier-Stokes model for turbulence: A Reynolds-averaged Navier-Stokes to direct numerical simulation bridging method. *ASME Journal of Applied Mechanics*, 73(2):413–421, 2006. [23](#), [23](#)
- [164] S. S. Girimaji and K. S. Abdul-Hamid. Partially-Averaged Navier-Stokes model for turbulence: Implementation and Validation. AIAA paper 2005–0502, Reno, N.V., 2005. [23](#), [23.3](#)
- [165] M. L. Shur, P. R. Spalart, M. Kh. Strelets, and A. K. Travin. A hybrid RANS-LES approach with delayed-DES and wall-modelled LES capabilities. *International Journal of Heat and Fluid Flow*, 29:1638–1649, 2008. [23](#), [23.4.2](#), [26](#), [28](#), [48.4](#)
- [166] J. Ma, S.-H. Peng, L. Davidson, and F. Wang. A low Reynolds number partially-averaged Navier-Stokes model for turbulence. In *8th International ERCOFTAC Symposium on Engineering Turbulence, Modelling and Measurements*, Marseille, France, 9–11 June, 2010. [23](#)
- [167] L. Davidson. The PANS $k - \varepsilon$ model in a zonal hybrid RANS-LES formulation. *International Journal of Heat and Fluid Flow*, 46:112–126, 2014. [23.1](#), [23.1.1](#), [23.2.2.2](#), [23.2.2.4](#), [25.3.1](#), [25.3.2](#), [25.4.2](#), [47.4](#), [48](#)
- [168] S. S. Girimaji and S. Wallin. Closure modeling in bridging regions of variable-resolution (VR) turbulence computations. *Journal of Turbulence*, 14(1):72 – 98, 2013. [23.1.1](#), [23.2](#), [23.2.1](#), [23.2.1](#), [23.2.1](#), [23.2.2.1](#), [26](#)
- [169] S. Kenjeres and K. Hanjalic. LES, T-RANS and hybrid simulations of thermal convection at high ra numbers. *International Journal of Heat and Fluid Flow*, 27:800–810, 2006. [23.3](#)
- [170] H. Foroutan and S. Yavuzkurt. A partially-averaged Navier-Stokes model for the simulation of turbulent swirling flow with vortex breakdown. *International Journal of Heat and Fluid Flow*, 50:402–416, 2014. [23.3](#)
- [171] L. Davidson and C. Friess. A new formulation of f_k for the PANS model. *Journal of Turbulence*, pages 1–15, 2019. [23.3](#), [23.3.1](#), [23.4.3](#), [48.7.2](#)

- [172] C. Friess, R. Manceau, and T.B. Gatski. Toward an equivalence criterion for hybrid RANS/LES methods. *Computers & Fluids*, 122:233–246, 2015. [23.3.1](#), [23.4](#), [23.4.3](#), [23.4.3](#)
- [173] M. Gritskevich, A. Garbaruk, J. Schütze, and F. R. Menter. Development of DDES and IDDES formulations for the $k-\omega$ shear stress transport model. *Flow, Turbulence and Combustion*, 88:431–449, 2012. [23.4.2](#)
- [174] L. Davidson and C. Friess. The PANS and PITM model: a new formulation of f_k . In *Proceedings of 12th International ERCOFTAC Symposium on Engineering Turbulence Modelling and Measurements (ETMM12), Montpellier, France 26-28 September*, 2018. [23.4.3](#), [48.7.2](#)
- [175] C. Friess and L. Davidson. A formulation of PANS able to mimic IDDES. *International Journal of Heat and Fluid Flow*, 86(108666), 2020. [23.4.4](#), [47](#)
- [176] B. Chaouat and R. Schiestel. A new partially integrated transport model for subgrid-scale stresses and dissipation rate for turbulent developing flows. *Physics of Fluids*, 17(065106), 2005. [24](#), [28](#)
- [177] L. Davidson. Using isotropic synthetic fluctuations as inlet boundary conditions for unsteady simulations. *Advances and Applications in Fluid Mechanics*, 1(1):1–35, 2007. [25.4.1](#), [27.1](#), [27.4](#), [27.8](#)
- [178] L. Davidson and S.-H. Peng. Embedded large-eddy simulation using the partially averaged Navier-Stokes model. *AIAA Journal*, 51(5):1066–1079, 2013. [25.4.1](#), [27.9](#), [48](#), [48](#), [48.1](#), [48.3](#), [48.3](#), [48.3](#), [48.4](#), [49](#), [49.1](#)
- [179] A. Travin, M. Shur, M., Strelets, and P. Spalart. Detached-eddy simulations past a circular cylinder. *Flow, Turbulence and Combustion*, 63:293–313, 2000. [26](#)
- [180] F. Hamba. Analysis of filtered Navier-Stokes equation for hybrid RANS/LES simulation. *Physics of Fluids A*, 23(015108), 2011. [26](#), [26](#), [26](#)
- [181] S. Arvidson, L. Davidson, and S.-H. Peng. Hybrid RANS-LES modeling based on a low-Reynolds-number $k-\omega$ model. *AIAA Journal*, 54(12):4032–4037, 2016. [26](#)
- [182] S. Arvidson, L. Davidson, and S.-H. Peng. Interface methods for grey-area mitigation in turbulence-resolving hybrid RANS-LES. *International Journal of Heat and Fluid Flow*, 73:236–257, 2018. [26](#)
- [183] L. Davidson. Two-equation hybrid RANS-LES models: A novel way to treat k and ω at inlets and at embedded interfaces. *Journal of Turbulence*, 18(4):291–315, 2017. [26](#), [52.2](#)
- [184] S. Arvidson. *Methodologies for RANS-LES interfaces in turbulence-resolving simulations*. PhD thesis, Div. of Fluid Dynamics, Dept. of Mechanics and Maritime Sciences, Chalmers University of Technology, Göteborg, Sweden, 2017. [26](#)
- [185] L. Davidson. Hybrid LES-RANS: Inlet boundary conditions for flows including recirculation. In *5th International Symposium on Turbulence and Shear Flow Phenomena*, volume 2, pages 689–694, 27–29 August, Munich, Germany, 2007. [27](#), [27.8](#)

- [186] N. Jarrin, S. Benhamadouche, D. Laurence, and R. Prosser. A synthetic-eddy-method for generating inflow conditions for large-eddy simulations. *International Journal of Heat and Fluid Flow*, 27(4):585–593, 2006. [27](#)
- [187] M. Billson. *Computational Techniques for Turbulence Generated Noise*. PhD thesis, Dept. of Thermo and Fluid Dynamics, Chalmers University of Technology, Göteborg, Sweden, 2004. [27.1](#), [27.9](#), [27.9.2](#)
- [188] M. Billson, L.-E. Eriksson, and L. Davidson. Jet noise prediction using stochastic turbulence modeling. AIAA paper 2003-3282, 9th AIAA/CEAS Aeroacoustics Conference, 2003. [27.1](#)
- [189] L. Davidson. Hybrid LES-RANS: Inlet boundary conditions. In B. Skallerud and H. I. Andersson, editors, *3rd National Conference on Computational Mechanics – MekIT’05 (invited paper)*, pages 7–22, Trondheim, Norway, 2005. [27.1](#), [27.4](#)
- [190] L. Davidson. Hybrid LES-RANS: Inlet boundary conditions for flows with recirculation. In *Second Symposium on Hybrid RANS-LES Methods*, Corfu island, Greece, 2007. [27.1](#), [27.4](#)
- [191] J. R. Welty, C. E. Wicks, and R. E. Wilson. *Fundamentals of Momentum, Heat, and Mass Transfer*. John Wiley & Sons, New York, 3 edition, 1984. [27.8](#)
- [192] L. Davidson. HYBRID LES-RANS: Inlet boundary conditions for flows with recirculation. In *Advances in Hybrid RANS-LES Modelling*, volume 97 of *Notes on Numerical Fluid Mechanics and Multidisciplinary Design*, pages 55–66. Springer Verlag, 2008. [27.8](#), [48](#)
- [193] M. Billson, L.-E. Eriksson, and L. Davidson. Modeling of synthetic anisotropic turbulence and its sound emission. The 10th AIAA/CEAS Aeroacoustics Conference, AIAA 2004-2857, Manchester, United Kindom, 2004. [27.9](#), [27.9.2](#)
- [194] R. D. Moser, J. D. Kim, and N. N. Mansour. Direct numerical simulation of turbulent channel flow up to $Re_\tau = 590$. *Physics of Fluids*, 11(4):943–945, 1999. [1](#)
- [195] L. Davidson. Python and matlab scripts for synthetic fluctuations, 2014. [27.9](#)
- [196] Lars Davidson and Shia-Hui Peng. Hybrid LES-RANS: A one-equation SGS model combined with a $k - \omega$ for predicting recirculating flows. *International Journal for Numerical Methods in Fluids*, 43(9):1003–1018, 2003. [28](#)
- [197] J. Fröhlich and D. von Terzi. Hybrid LES/RANS methods for the simulation of turbulent flows. *Progress in Aerospace*, 44(5):349–377, 2008. [28](#)
- [198] A. Travin, M. Shur, M. Strelets, and P. Spalart. Detached-eddy simulations past a circular cylinder. *Flow Turbulence and Combustion*, 63(1/4):293–313, 2000. [28](#)
- [199] L. Davidson and B. Farhanieh. CALC-BFC: A finite-volume code employing collocated variable arrangement and cartesian velocity components for computation of fluid flow and heat transfer in complex three-dimensional geometries. Rept. 95/11, Dept. of Thermo and Fluid Dynamics, Chalmers University of Technology, Gothenburg, 1995. [C](#), [33](#)

- [200] B. P. Leonard. A stable and accurate convective modelling based on quadratic upstream interpolation. *Computational Methods in Applied Mechanical Engineering*, 19:59–98, 1979. [33](#)
- [201] M. Breuer, N. Peller, Ch. Rapp, and M. Manhart. Flow over periodic hills – numerical and experimental study in a wide range of Reynolds numbers. *Computers & Fluids*, 38:433–457, 2009. [AH.2](#)
- [202] F. Eriksson. *Flerdimensionell analys (in Swedish)*. Studentlitteratur, Lund, Sweden, 4 edition, 1977. [AI](#)
- [203] R. L. Panton. *Incompressible Flow*. John Wiley & Sons, New York, 1984. [40](#)
- [204] L. Davidson. [pyCALC-LES: A Python Code for DNS, LES and Hybrid LES-RANS](#). Division of Fluid Dynamics, Dept. of Mechanics and Maritime Sciences, Chalmers University of Technology, Gothenburg, 2021. [44.1](#)
- [205] B. J. Daly and F. H. Harlow. Transport equation in turbulence. *Physics of Fluids*, 13:2634–2649, 1970. [4](#)
- [206] L. Davidson. Using neural network for improving an explicit algebraic stress model in 2D flow (to appear). In J. C. Tyacke and N. R. Vadlamani, editors, *CUSF 2024, Proceedings of the Cambridge Unsteady Flow Symposium 2024*. Springer Nature Switzerland AG, 2024. [44.2](#), [44.2](#), [44.2](#)
- [207] L. Davidson. Large eddy simulation of heat transfer in boundary layer and backstep flow using PANS (corrected version can be downloaded at <http://www.tfd.chalmers.se/~lada/>). In *Turbulence, Heat and Mass Transfer, THMT-12*, Palermo, Sicily/Italy, 2012. [45.6](#)
- [208] L. Davidson and S.-H. Peng. Embedded LES with PANS. In *6th AIAA Theoretical Fluid Mechanics Conference, AIAA paper 2011-3108*, 27-30 June, Honolulu, Hawaii, 2011. [45.6](#), [48](#), [48.1](#), [48.3](#), [48.2](#), [48.3](#), [48.4](#), [49.1](#)
- [209] Siavash Toosi and Johan Larsson. Anisotropic grid-adaptation in large eddy simulations. *Computers & Fluids*, 156:146–161, 2017. [47.8](#), [47.8](#)
- [210] J. Larsson. private communication. Department of Mechanical Engineering, University of Maryland, 2019. [47.8](#)
- [211] D. Greenblatt, K. B. Paschal, C.-S. Yao, J. Harris, N. W. Schaeffler, and A. E. Washburn. A separation control CFD validation test case. Part 1: Baseline & steady suction. AIAA-2004-2220, 2004. [48](#)
- [212] D. Greenblatt, K. B. Paschal, C.-S. Yao, and J. Harris. A separation control CFD validation test case Part 1: Zero efflux oscillatory blowing. AIAA-2005-0485, 2005. [48](#)
- [213] B. van Leer. Towards the ultimate conservative difference scheme. Monotonicity and conservation combined in a second order scheme. *Journal of Computational Physics*, 14(4):361–370, 1974. [48.1](#)
- [214] S. Dahlström and L. Davidson. Large eddy simulation of the flow around an Aerospaiale A-aerofoil. In *ECCOMAS 2000, European Congress on Computational Methods in Applied Sciences and Engineering, 11-14 September*, Barcelona, Spain, 2000. [48.1](#)

- [215] L. Davidson and C. Friess. Detached eddy simulations: Analysis of a limit on the dissipation term for reducing spectral energy transfer at cut-off [\[4\]](#). In *13th International ERCOFTAC Symposium on Engineering Turbulence Modelling and Measurements (ETMM13), Rhodes/Digital, Greece 15-17 September, 2021*. 48.4
- [216] S.B. Pope. Ten questions concerning the large-eddy simulations of turbulent flows. *New Journal of Physics*, 6(35):1–24, 2004. 3, 48.7
- [217] L. Davidson. A new approach of zonal hybrid RANS-LES based on a two-equation $k - \varepsilon$ model. In *ETMM9: 9th International ERCOFTAC Symposium on Turbulence Modelling and Measurements*, Thessaloniki, Greece, 2012. 50
- [218] S-H Peng, L. Davidson, and S. Holmberg. A modified low-Reynolds-number $k - \omega$ model for recirculating flows. *Journal of Fluids Engineering*, 119:867–875, 1997. 52.1
- [219] A. Zarmehri. Aerodynamic analysis of wind turbine. MSc Thesis 2012:58, Division of Fluid Dynamics, Department of Applied Mechanics, Chalmers University of Technology, Göteborg, Sweden, 2012. 52.3
- [220] O. Brander. *Vektoranalys (in Swedish)*. Studentlitteratur, Lund, Sweden, 2007. 54
- [221] L. Davidson. Using machine learning for improving a non-linear $k - \varepsilon$ model: A first attempt [\[4\]](#). Technical report, Division of Fluid Dynamics, Dept. of Mechanics and Maritime Sciences, Chalmers University of Technology, Gothenburg, 2023. 59, 59, 59.2
- [222] G. Eitel-Amor, R. Orlu, and P. Schlatter. Simulation and validation of a spatially evolving turbulent boundary layers up to $Re_\theta = 8300$, DNS Data base. 2014. 59.1
- [223] S.S. Girimaji. Fully-explicit and self-consistent algebraic Reynolds stress model. ICASE Rep. 95-82, Institute for Computer Applications in Science and Engineering NASA Langley Research Center, Hampton, VA, USA, 1995. 60, 60, 60, 60